LIÈGE université
GIGA institute

Molecular Angiogenesis Laboratory
Faculty of Sciences
University of Liège

UNRAVELLING THE EXOSOMAL EXPORT OF MIR-503 AND ITS IMPLICATION IN TUMOR RESPONSE TO CHEMOTHERAPY

Amandine Boeckx

Thesis submitted in partial fulfilment of the requirements for the degree of Doctor in Sciences by the Univeristy of Liège

Supervisor: Dr. Ingrid Struman

Academic year 2021-2022

A mes grands-parents. Mamy, Papoutch, Nonna & Papy

Acknowledgments

Avant tout, je tiens à remercier ma promotrice, Ingrid Struman. Tout d'abord, pour m'avoir accueillie au sein de son laboratoire, mais surtout pour m'avoir toujours soutenue et accompagnée tout au long de ma thèse. Merci pour ton soutien, tes conseils mais surtout ta bienveillance. Merci aussi pour ces formidables moments que nous avons eu la chance de partager. Je citerai bien sûr notre voyage au Canada qui fût rempli d'ARN non codants, de détente, de neige (de chutes pour ma part), de bières à la châtaigne, de tequila, et bien d'autres. Pour tout cela, je te remercie.

Alors Steph, alias Stephouille (anciennement Vomito), sache que ton retour au laboratoire m'a rempli de joie. Tu as amené avec toi le soleil d'Italie avec ton enthousiasme, ton sourire, tes blagues et surtout tes gossips. Tu as vraiment été un pilier pour moi ! Merci d'avoir cru en moi, de m'avoir transmis ton savoir, tes protocoles et surtout tes conseils tant professionnels que personnels. Merci pour tout !

Maumau, alias dropi-dropa, ma voisine de bench, de thèse, bref mon amie. Même si je pense que mon ancien surnom te correspond également : le tyran. J'ai été heureuse de passer ces deux dernières années à tes côtés. Merci à toi pour nos chouettes discussions et nos rigolades. Tu es une personne formidable, n'en doute jamais ! Je te souhaite tout le meilleur dans ta vie et plein de merveilleux résultats !

Auré, mon petit tic, mon acolyte chez les rangers du risque, j'ai été contente de travailler à tes côtés, même si tu me piquais mes pipettes. Trêve de plaisanteries, merci pour les discussions, les fou-rires et ton aide durant ces derniers mois.

Florian (c'est étrange de t'appeler comme ça). Tout d'abord désolé d'avoir été à l'origine de tes innombrables surnoms : Bob, flofi, etc. Merci pour ta gentillesse et ta bonne humeur.

Eme, même si nous n'avons pas eu la chance de travailler beaucoup ensemble, je te remercie pour nos discussions sur un sujet que nous aimons particulièrement, Disney. Je te souhaite le meilleur pour la suite. Florine, Mic mic, Gaëlle et Claire, les derniers arrivés, merci pour votre gaieté. Gaëlle merci beaucoup pour ton aide avec la mise en page. J'espère que Mic mic et Florine se joindront définitivement à l'équipe du BMGG. Bonne route à tous !

Merci Mimi, pour ces belles années passées ensemble. Heureusement que tu n'es pas partie trop loin. Comment aurais-je survécu sans toi ? Tu as été plus qu'une collègue pour moi. Merci pour ton écoute et ta gentillesse. Je te souhaite le meilleur. Tu le mérites. J'espère que nos chemins se croiseront le plus souvent posssible.

Thom alias Minus, mon binôme du labo, mon ami. Lorsque je vois le chemin que tu as parcouru en si peu de temps je me dis que tu as bel et bien conquit le monde ! Merci d'avoir rendu mes journées plus belles. Merci pour tous ces beaux moments que nous avons eu la chance de partager. Team Salami !

Merci à Oli, pour ses protocoles, pour nos discussions, ses astuces. Merci pour ces journées remplies de manips souris, pour les quicks du midi. Merci de m'avoir souvent prêté ton bac à glace gravé avec ta devise « On n'est pas à une vache près ». Bref, on se sera souvent bien marré.

Stella, ma petite étoile, merci pour ta gentillesse, pour ces discussions si enrichissantes et tellement variées. Ton sourire, ta bonne humeur m'ont vite manqué mais, j'avoue, que c'était une délivrance de ne plus avoir à renifler les odeurs de tes fromages dans notre frigo. Je t'en veux tout de même de m'avoir abandonné si vite mais merci pour tout !

I also want to express my gratitude to Jennifer Perez-Boza. Thank you for sharing, our discussions and our paper. I wish you all the best.

Un tout grand merci à Séba et à Claire, avec qui j'ai passé de belles années pluvieuses. Bon, Claire tu étais habituée mais j'avoue que Seb, ça a dû être difficile. Claire, un grand merci pour ton aide avec les analyses bioinformatiques, et Séba, pour tes conseils.

Je tiens également à remercier du fond du cœur Anne-so, ma bestie, qui m'a aidé à maintes et maintes reprises à sortir la tête hors de l'eau. Tu as été une épaule sur laquelle je pouvais me reposer. Bien entendu, bestie, tu représentes beaucoup plus qu'une simple collègue à mes yeux. Saches que tu resteras ma plus belle rencontre au sein du BMGG. Merci pour ces merveilleux souvenirs partagés. Ces nouvelles expressions que tu m'as fait découvrir. Nos missions secrètes en tant que spices. Nos voyages avec ces innombrables signes magiques que nous seules, sorcières, étions à même de reconnaitre. Merci de m'avoir fait l'honneur d'être témoin du plus beau jour de votre vie. A nos aventures, aux salamis, aux mini-besties (Enfin, Alba aura une super amie pour la vie avec qui jouer !), bref, à notre amitié.

Arnaud alias sisto ou bestie de ma bestie. Je pense qu'il est grand temps de trouver un surnom plus court. Qu'en penses-tu ? D'accord, ça sera Jerry. Tout simplement merci d'être un ami sincère sur qui l'on peut toujours compter. On se retrouve tous dans 10 ans pour créer notre spin-off mais en attendant, merci d'être un super tonton hanneton et qui sera, j'en suis certaine, un super papa.

Ma petite Marie, française sur papier mais belge dans le cœur. Merci pour ces conversations, ces gossips, ces temps de midi et ces sorties. Spices forever (même si nous devons nous partager Sam). Tu es une de mes plus belles rencontres. Ma Marie, mon amie, je te souhaite le meilleur et encore plus ! Vivement ce run Disney !

Bien entendu, je tiens également à remercier tout le BMGG pour leur accueil et leur gentillesse. Depuis le début de cette folle aventure qu'est la thèse, j'ai pu compter sur votre bienveillance. Jojo merci pour ton sourire, ta joie de vivre et ta zen attitude. Vivi, merci pour ton savoir et ta bonne humeur. Claudia, guapa, merci d'avoir amené un peu de soleil dans la grisaille belge. Laura, Jerem, Renaud merci à vous trois. Patricia, merci pour ces chouettes discussions. Gustavo, merci pour ces cours d'espagnol entre deux PCR. Je vous souhaite le meilleur.

A mon amie de toujours, Margaud, ma collègue de thèse, je tiens à exprimer toute ma gratitude. Tout a commencé lors d'un TP histologie où une jeune femme pétillante et moi entamons une discussion. Depuis, plus jamais l'une sans l'autre. A nos temps de midi de blocus (les frites, les dino, nos salades, nos McDo, les repas chez la Nonna), à nos soirées mémorables, à notre amitié. Malgré un court entracte, je te compte parmi mes amies les plus chères. Une tata formidable qui a su dénicher un tonton formidable (juste parce qu'il aime chanter du Disney…).

Mes parents, qui ont toujours cru en moi. Merci pour tout ! Si j'en suis là c'est grâce à vous. Maman, merci de m'avoir toujours poussé à toujours vouloir aller plus loin lors de mes études. Papa, merci de m'avoir changé les idées lors des moments de doutes.

Ma belle-famille, et en particulier mes nièces. Les petits rayons de soleil qui illuminaient mes dimanches. Vos rires, vos jeux et votre douceur m'ont permis plus d'une fois d'oublier tous mes soucis.

Ce dernier paragraphe sera dédié aux deux êtres qui comptent le plus pour moi. Ma famille.

Damien, mon mari. Depuis le commencent, tu as toujours été présent. Merci de m'avoir remonté le moral lors des moments de doutes (et Dieu sait combien il y en a eu). Merci d'avoir été cette épaule si rassurante. Nous avons traversé beaucoup d'épreuves et tu as toujours été mon roc. Sans toi, je ne serais pas là en j'en suis actuellement. Enfin, octobre 2020, Alba, notre petit miracle pointe le bout de son nez avec quelques mois d'avance. Baba, saches que tu as été pour moi une bouffée d'oxygène. Tu es un rayon de soleil et une fille que tout le monde rêverait d'avoir. Le plus beau rôle de ma vie est d'être ta maman. Ton papa et toi êtes les humains les plus formidables du monde. A nous, à nos prochaines aventures. Je vous aime.

Résumé

Les tumeurs sont des systèmes hétérogènes interagissant constamment avec leur microenvironnement. La communication entre les cellules cancéreuses et les autres cellules, présentes dans cet environnement, pourrait aider au développement de nouvelles stratégies anti-cancéreuses. Les vésicules extracellulaires (VEs), impliquées dans la communication intercellulaire, sont des intervenants clés dans la progression tumorale. En effet, toutes les cellules génèrent ces vésicules. De par le transfert de leur cargo d'une cellule émettrice vers une cellule réceptrice, ces particules sont capables d'induire des changements au niveau cellulaire. En effet, ils transportent des microRNAs, de petits ARNs non-codants impliqués dans diverses voies. Dans le cadre du cancer, les VEs et les miRNAs participent grandement à la progression tumorale et modulent la réponse de la tumeur aux traitements.

Durant ce travail, nous avons démontré que l'épirubicine induisait l'export d'un miRNA anti-tumoral, miR-503, dans les VEs produites par les cellules endothéliales. Nous avons identifié quatre protéines impliquées dans ce mécanisme : ANXA2, hnRNPA2B1, TSP1 et VIM. Nous avons mis en évidence que l'épirubicine entraînait une dissociation du miR-EXO complexe (complexe formé par miR-503 et les protéines qui y sont attachées). hnRNPA2B1 retournait dans le noyau tandis qu'ANXA2 et miR-503 étaient exportés dans les VEs. Nous avons réprimé l'expression des protéines et observé qu'hnRNPA2B1 inhibait l'export de miR-503. Ensuite, nous avons réalisé des tests fonctionnels afin de déterminer les effets de cette répression endothéliale sur les cellules cancéreuses du sein. Les expériences de coculture ont montré que l'inhibition d'hnRNPA2B1 augmentait les niveaux de miR-503 dans les cellules de cancer du sein triple-négatif tandis que ses cibles, CCND2 et CCND3, voyaient leurs niveaux réduits. L'inhibition de ces cibles pro-tumorales a réduit les capacités prolifératives, migratoires et invasives des cellules tumorales. De plus, nous avons analysé les fonctions de miR-503 sur des cellules cancéreuses du sein résistant à l'épirubicine ou au paclitaxel. De façon intéressante, comparés aux cellules sensibles, les niveaux basaux du miRNA étaient réduits dans les cellules résistantes. Grâce à plusieurs tests fonctionnels, nous avons démontré que la surexpression de miR-503 réduisait la progression des cellules sensibles et résistantes. Ses cibles, CCND1 et CCND3, étaient également diminuées. De plus, nous avons traité les cellules cancéreuses avec des VEs enrichis avec miR-503 et le même phénotype a été observé. Les expériences *in vivo* ont montré que ces VEs enrichis étaient capables de réduire de façon drastique la croissance tumorale. Enfin, les données cliniques ont révélé que la délétion de miR-503 réduisait la survie des patientes atteintes d'un cancer du sein.

En conclusion, ces résultats suggèrent que les cellules endothéliales et cancéreuses interagissent par le transfert de miRNAs via les VEs. Leur incorporation réduit la progression des cellules de cancer du sein. De plus, les fonctions anti-tumorales de miR-503 sont conservées dans les cellules résistantes.

Abstract

Tumors are heterogeneous systems in constant interactions with their microenvironment. The communication between cancerous and other types of cells might help in the development of new anti-cancer strategies. Extracellular vesicles (EVs), involved in cell-to-cell communication, are key players in tumor progression. Indeed, all cell types generate EVs. By transferring their bioactive content from a donor to a recipient cell, these particles can induce cellular changes. Interestingly, EVs carry microRNAs, small non-coding RNAs involved in multiple pathways. In the context of malignancies, EVs and miRNAs highly participate in tumor progression and modulate the response to treatment.

In this work, we demonstrated that epirubicin induced the export of an anti-tumoral miRNA, miR-503, into EVs released from endothelial cells. We identified four proteins involved in the sorting mechanism: ANXA2, hnRNPA2B1, TSP1, and VIM. We showed that upon epirubicin treatment, the miR-EXO complex (complex formed by miR-503 and the proteins attached to it) disrupts. hnRNPA2B1 returned to the nucleus while ANXA2 and miR-503 were exported into EVs. We performed protein knockdown and observed that hnRNPA2B1 silencing mimicked epirubicin treatment. Therefore, we concluded that hnRNPA2B1 inhibited miR-503 sorting into EVs. Then, we performed functional assays to determine the effects of this endothelial silencing on breast cancer cells. Coculture experiments revealed that the endothelial knockdown of hnRNPA2B1 indeed increased the levels of miR-503 within triple-negative breast cancer cells while the levels of its targets, CCND2 and CCND3, were downregulated. The inhibition of these pro-tumoral targets reduced the proliferative, migratory and invasive capacities of tumor cells. Moreover, we analyzed the functions of miR-503 on epirubicin and paclitaxel-resistant breast cancer cells. Interestingly, the basal levels of the miRNA were downregulated in resistant cells compared to the sensitive ones. Using several functional assays, we demonstrated that miR-503 overexpression curtailed the tumorigenicity of both responding and non-responding cells. Its targets, CCND1 and CCND3, were also downregulated. Moreover, we treated cancer cells with miR-503-loaded EVs and the same phenotype was observed. *In vivo* experiments showed that EVs enriched in miR-503 could reduce tumor growth drastically. Finally, clinical data revealed that the deletion of miR-503 decreased the survival of breast cancer patients.

Taken together, these results suggest that endothelial and cancer cells interact through the transfer of miRNAs via EVs. Their incorporation curtails breast cancer cell progression. Moreover, the anti-tumoral functions of miR-503 are conserved in resistant cells.

List of abbreviations

3'-UTR	3' untranslated region
ABC	ATP-binding cassette
ABs	Apoptotic bodies
ACTB	β-Actin
ADARs	Adenosine deaminases acting on RNA
AGO/Ago	Argonaute
AKT3	AKT Serine/Threonine Kinase 3
ANXA2	Annexin A2
B2M	β2-microglobulin
BC	Breast cancer
Bcl-2	B cell lymphoma 2
BM	Basement membrane
BRCA1	Breast cancer associated gene 1
BRCA2	Breast cancer associated gene 2
BrdU	5-bromo-2-deoxyuridine
BSA	Bovine serum albumin
CAF	Cancer-associated fibroblast
CCDN2	Cyclin D2
CCND1	Cyclin D1
CCND3	Cyclin D3
ceRNAs	competing endogenous RNAs
CircRNAs	Circular RNAs
CircRNAs	circular RNAs
CNA	Copy number variation
CSCs	Cancer stem cells
CTLA-4	Cytotoxic T-Lymphocyte-Associated Antigen 4
Cyt c	Cytochrome c
DBS	Donor bovine serum
DCs	Dendritic cells
DGCR2	DiGeorge Syndrome Critical Region Gene 2
DGCR8	DiGeorge syndrome Critical Region gene 8
DLS	Dynamic light scattering

DNA	Deoxyribonucleic acid
DSB	DNA double-strand breaks
dsDNA	Double-stranded DNA
DTSSP	3,3'-dithiobis(sulfosuccinimidyl propionate)
ECM	Extracellular matrix
ECs	Endothelial cells
EDTA	Ethylenediaminetetraacetic acid
EEs	Early endosomes
EGF	Epidermal growth factor
EGFR	Epidermal Growth Factor Receptor
EGM2	Endothelial cell growth media 2
Epi	Epirubicin
Epi-R	Epirubicin-resistant
ER	Estrogen receptor
ESCRT	Endosomal Sorting Complex Required for Transport
EVs	Extracellular vesicles
Exos	Exosomes
FBS	Fetal Bovine Serum
FC	Fold change
FGF	Fibroblast growth factor
FGF2	Fibroblast growth factor 2
FGF7	Fibroblast growth factor 7
FN1	Fibronectin 1
FPKM	Fragments per kilo base of transcript per million mapped fragments
GADD45a	Growth arrest and DNA-damage-inducible protein 45a
GAPDH	Glyceraldehyde-3-phosphate dehydrogenase
GFP	Green fluorescent protein
GW182	Glycine-tryptophan protein of 182 kDa
HDL	High-density lipoprotein
HER2	Human epidermal growth factor receptor-2
HMVECs	Human microvascular endothelial cells
hnRNPA2B1	Heterogeneous nuclear ribonucleoprotein A2/B1
hnRNP-Q/SYNCRIP	Heterogeneous nuclear ribonucleoprotein Q

HRP	Horseradish peroxidase
Hsp	Heat shock proteins
HSPG2	Perlecan
HUVEC	Human umbilical cord endothelial cells
ILVs	Intraluminal vesicles
L1CAM	L1 Cell Adhesion Molecule
LECs	Lymphatic cells
LEs	Late endosomes
lncRNAs	Long non-coding RNA
LRs	Lipid rafts
MAPs	Microtubule-associated proteins
MDH2	Malate dehydrogenase 2
MDSCs	Myeloid-derived stem cells
MDR	Multi-drug resistance
MET	Mesenchymal-to-epithelial transition
METABRIC	Molecular Taxonomy of Breast Cancer International Consortium
miRNAs	MicroRNAs
MMPs	Matrix metalloproteinases
mRNA	messenger RNAs
MS	Mass spectrometry
mtDNA	mitochondrial DNA
MVBs	Multivesicular bodies
MVs	Microvesicles
MYB	Myeloblastosis proto-oncogene protein
NAC	Neoadjuvant chemotherapy
ncRNAs	non-coding RNAs
NGS	Next generation sequencing
NKs	Natural killers
NT	Non-treated
OncomiRs	Oncogenic miRNAs
PABPs	Poly(A)-binding proteins
Pacli-R	Paclitaxel-resistant
PACT	Protein Activator of PKR
PALM	Palmitoylation signal

PARP	Poly(ADP-ribose) polymerase
PAZ	PIWI-AGO-ZWILLE
P-bodies	Processing bodies
PBS	Phosphate buffered saline
PC	Pyruvate carboxylase
PCCA	Propionyl-CoA carboxylase
PD-1	programmed death 1
PD-L1	Programmed death ligand-1
P-gp	P-glycoprotein
PI	Propidium iodide
POR	Cytochrome P450 Oxidoreductase
PPIA	Peptidylprolyl isomerase
PR	Progesterone receptor
pre-miRNAs	precursor miRNAs
pri-miRNAs	primary miRNAs
PTGFR	Prostaglandin F Receptor
qPCR	Quantitative polymerase chain reaction
Ran	Ras-related nuclear protein
RIPA	Radioimmunoprecipitation assay buffer
RISC	RNA-induced silencing complex
RLC	RISC-loading complex
RNA	Ribonucleic acid
RNA Pol	RNA Polymerase
RBPs	RNA-binding proteins
ROS	Reactive oxygen species
rRNAs	Ribosomal RNAs
Scr	Scramble
SD	Standard deviation
SDCBP2	Syndecan Binding Protein 2
SDS	Sodium dodecyl sulfate
SEM	Standard error of the mean
shRNAs	small hairpin RNAs
siRNA	Small interfering RNA
SIRT6	Sirtuin 6

SNORD44/RNU44	Small Nucleolar RNA, C/D Box 44
SNORD48/RNU48	Small Nucleolar RNA, C/D Box 48
SNPs	Single nucleotide polymorphisms
ssDNA	single-stranded DNA
TAMs	Tumor-associated macrophages
TCGA	The Cancer Genome Atlas
TDEs	Tumor-derived exosomes
TECs	Tumor endothelial cells
TEM	Transmission electron microscopy
TGF-β	Transforming growth factor beta
TILs	Tumor-infiltrating lymphocytes (
TME	Tumor microenvironment
TNBC	Triple-negative breast cancer
TNF	Tumor necrosis factor
Top2α	Topoisomerase II α
Top2β	Topoisomerase II β
Tregs	Regulatory T lymphocytes
TRBP	Tar RNA Binding Protein
tRNAs	Transfer RNAs
TSP1	Thrombospondin-1
UP	Universal primer
VEGF	Vascular endothelial growth factor
VEGFR	Vascular endothelial growth factor receptor
VIM	Vimentine
VINC	Vinculin
Vps	Vacuolar protein sorting
XPO5	Exportin-5
YBX1	Y-box-binding protein 1

Table of contents

List of figures

List of tables

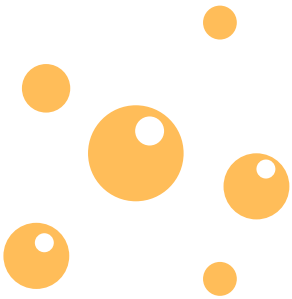

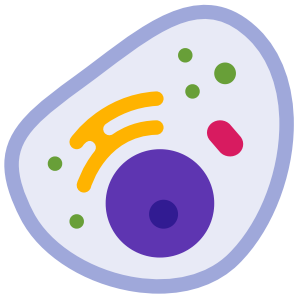
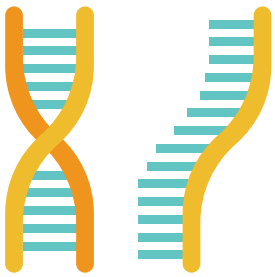

Introduction

Introduction

1. Breast cancer

In 2020, breast cancer was the most frequently diagnosed cancer in women, presenting a high mortality rate, with more than 2.260.000 new cases and 684.996 deaths worldwide (GLOBOCAN, 2020) (**Fig. I 1**). Nevertheless, there are tremendous differences between developed and developing countries. While the 5-year survival reaches 80% in developed countries, it is only 40% in developing countries because of the lack of prevention and belated diagnosis (Coleman *et al.*, 2008). Although breast cancer affects mostly women, with a rare incidence of 1%, this disease is also diagnosed in men (Gucalp *et al.*, 2019).

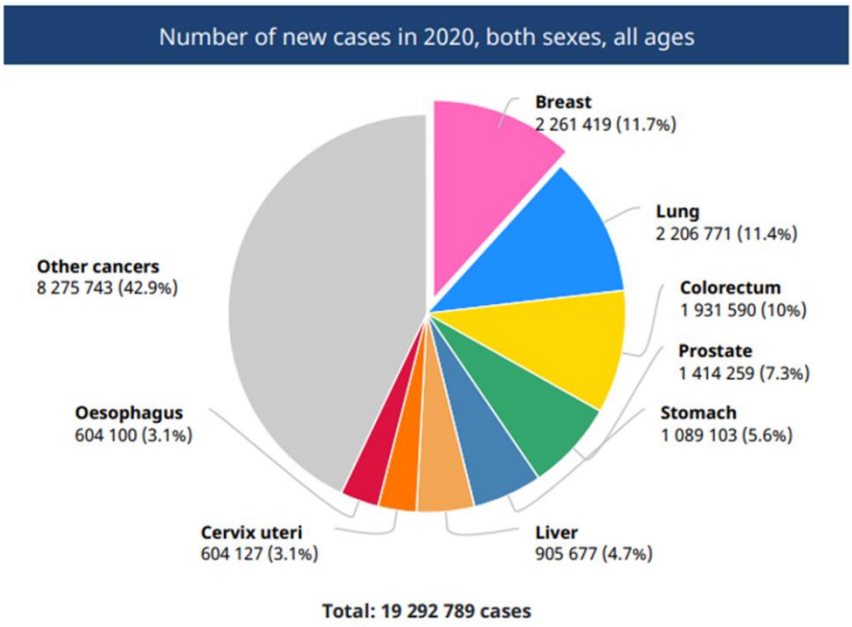

Figure I 1. Pie chart representing the number of new cases of cancers diagnosed worldwide.
In pink: new breast cancers diagnosed worldwide. Figure adapted from GLOBOCAN, 2020.

Breast cancer occurrence has many causes. This particular type of cancer is a heterogeneous disease. The prognosis and the adapted treatments depend on the subtypes and the nature of the tumor (Lüönd *et al.*, 2021). To improve the therapy efficiency, breast cancers were classified in multiple categories based on their histological features. Currently, the tumor classification depends on its molecular characteristics.

1.1. Risk factors

As for many other cancers, age is one of the preponderant risk factors for breast cancer. Indeed, the majority of mammary tumors are diagnosed in elderly women. For instance, eighty

percent of the new cases affect women older than 50 years (Kamińska *et al.*, 2015). Like other diseases, lifestyle, stress, obesity, tobacco, alcohol, and environmental exposures are well-established risk factors (Winters *et al.*, 2017). Among these environmental risk factors, exposure to pesticides, chemicals, radiation, and endocrine disruptive compounds correlated with a higher prevalence of breast cancer.

Breast carcinoma may also be hereditary. Women with a breast cancer family history show a higher frequency of developing the disease (Mahdavi *et al.*, 2019). Even if several genetic factors have been identified, almost 40% of hereditary breast cancers carry a mutation in the Breast cancer associated gene 1 and 2 (*BRCA1* and *BRCA2*) genes (Momenimovahed & Salehiniya, 2019). They both encode tumor suppressor proteins involved in the repair of double-strand breaks, regulation of genome integrity, and cell cycle (Roy *et al.* , 2012). Women carrying these mutations have a 70% risk of developing breast cancer (Casey & Bewtra, 2004). Nevertheless, compared to families carrying BRCA2 mutations, families with BRCA1 mutations face a higher risk of developing breast cancer (Graeser *et al.*, 2009). For instance, at the age of seventy, BRCA1 carriers have a 65% risk to develop breast cancer, whereas women with BRCA2 mutation face a risk of 45%.

Reproductive factors are predominant risks in cancers diagnosed in women. These factors comprise early age at menarche, later age of the first full-term pregnancy, later age of menopause, and breastfeeding (Dierssen-Sotos *et al.*, 2018). For instance, it has been reported that a pregnancy occurring at younger ages drastically reduces the risk of developing breast cancer up to 50%. Interestingly, it seems that this protection is mediated by the remodeling of the insulin-like growth factor system (Katz, 2016). Another reproductive risk factor is whether or not children were breastfed. Indeed, breastfeeding and lactation largely decrease the occurrence of breast cancer (Anstey *et al.*, 2017). Moreover, prolonged use of hormonal contraceptives has been linked to a slightly higher frequency of diagnosed breast cancer (Mørch *et al.*, 2017), even though Marchbanks et al. demonstrated that the prevalence was not affected by hormonal contraceptives (Marchbanks *et al.*, 2012).

1.2. Classification

Breast cancer is a heterogeneous disease comprising multiple subtypes that have different responses to treatment and clinical aspects. Nowadays, different methods of classification are used to characterize breast cancer.

1.2.1. Histological classification

Traditionally, breast cancers are classified according to their **histopathological criteria**. It relies on the analysis of a tumor biopsy by the pathologist. Most breast cancers are adenocarcinomas which are carcinomas with a glandular origin (Makki, 2015). Breast adenocarcinomas comprise two types: the ductal adenocarcinoma and the lobular adenocarcinoma, derived from the milk ducts or the milk-producing lobules. With up to 80% of breast cancer diagnosed, ductal carcinoma is the most common (Watkins, 2019). In situ breast tumors, including ductal carcinoma in situ and lobular carcinoma in situ, are non-invasive and are surrounded by a flawless basement membrane (Erbas *et al.*, 2006). On the other hand, invasive carcinoma can reach the neighboring stroma and facilitate metastasis formation. Invasive ductal carcinoma accounts for about 70% of all breast cancers (Makki, 2015). Moreover, other rare types of breast cancer exist, such as medullary, mucinous, Paget, tubular, cystic, and papillary (Carlson *et al.*, 2011).

Previously, the **grade** of the tumor was given by the Bloom & Richardson classification system. Nowadays, the Elston-Ellis system is used to classify cancer, analyzing three main criteria: the percentage of tubule formation, the degree of nuclear pleomorphism, and the mitotic count. A numerical score is applied to each characteristic, and their summation provides the cancer grade, from grade I to III (**Fig. I 2**). The tumor grading is correlated to the prognosis. Grade I represents well-differentiated tumors, while grade III are poorly differentiated tumors (Elston & Ellis, 1991; Phukan *et al.*, 2015).

Feature	Score
Tubule formation	
Majority of tumor (>75%)	1
Moderate degree (10-75%)	2
Little or none (<10%)	3
Nuclear pleomorphism	
Small, regular uniform cells	1
Moderate increase in size and variability	2
Marked variation	3
Mitotic counts (using Leitz Ortholux)	
0-9	1
10-19	2
>20	3

Figure I 2. Cancer grade determination using the Elston-Ellis classification system.

Another way to describe the tumor is to evaluate its **stage**. Breast cancer stages, from 0 to 4, depend on the tumor size and the degree of invasiveness of cancer cells. Stage 0 refers to the non-invasive form, whereas the 1, 2, 3, and 4 stages describe invasive carcinomas. Cancer aggressiveness is correlated to the higher stages. Currently, oncologists define the stage using TNM-based staging (Akram *et al.*, 2017). This system is based on the primary tumor size (T), the regional lymph node invasion (N), and the presence of metastasis (M). Nevertheless, as discussed previously, breast cancer is a highly heterogeneous disease in which subtypes are extremely different. For that purpose, this staging method was redesigned and is now called the European Institute of Oncology Dynamic TNM Classification (TNM_{EIO}) (Veronesi *et al.*, 2005). Cancer aggressiveness is correlated with the higher stages.

1.2.2. Molecular classification

High-throughput technologies such as microarray chips or next-generation sequencing (NGS) have contributed to a better understanding of breast cancer heterogeneity. Based on these methods, a new classification system has been developed which focuses on molecular features

of breast cancers, especially invasive ductal carcinomas. The breast cancer molecular profiles reflect the nature of the tumor but may also help to predict their response to treatment and clinical behavior (Yersal & Barutca, 2014). In 2000, Perou and colleagues developed, for the first time, a molecular classification for breast cancer based on the differences in gene expression (Perou *et al.*, 2000). Based on this classification, four clinically molecular subtypes were described: Luminal A, Luminal B, HER2+ and triple-negative breast cancer (TNBC). Nowadays, the classification used by oncologists is based on the expression of receptors such as estrogen receptors (ER), progesterone receptors (PR), and Human epidermal growth factor receptor 2 (HER2). Moreover, the expression of Ki-67, the cell proliferation regulator, is also used for this classification (Nascimento & Otoni, 2020).

1.2.2.1. Classification based on receptor expression

The most discriminating molecular factor relies on the expression status of the estrogen receptor (ER). Based on their ER profile, breast cancers are subdivided into two main groups: luminal (ER+ tumors) or basal (ER- tumors). Nevertheless, the expression status of other molecules such as progesterone receptor (PR) and human epidermal growth factor receptor-2 (HER2) is routinely used to classify breast cancer subtypes. The current molecular classification provides five different classes of breast cancer: luminal A, luminal B, HER-2, basal, and normal-like (Eliyatkin *et al.*, 2015) (**Fig. I 3**).

Luminal subtypes (ER+) account for approximately 75% of invasive breast carcinomas. Generally, these tumors are associated with a good prognosis. The characterization of these subtypes is mainly due to the assessment of hormone-receptor status and the expression of proteins produced by luminal cells such as cytokeratins 8, 18, and 19 (Mishra *et al.*, 2020). Within this subtype, two main groups are distinguished: **Luminal A** and **Luminal B**. The Luminal A carcinomas are characterized by a high expression of ER, PR, or both, and have a HER2 negative status. These tumors are frequently low grade and possess lower TP53 mutation and proliferation rate, and, therefore, are associated with the better prognosis. Type B carcinomas share common features with the luminal A subtype (ER+ and/or PR+). However, Luminal B, which are HER2+ or a HER2-, are more aggressive and are characterized by a higher Ki-67 rate(O'Brien *et al.*, 2010; Ades *et al.*, 2014; Yersal & Barutca, 2014).

HER2-positive tumors are basal carcinomas characterized by the overexpression of the oncogene HER2 and the lack of the hormone receptors (ER-, PR-). HER2+ subtype generally covers 7% of all the breast carcinomas and is associated with a poor prognosis and reduced

overall survival (O'Brien *et al.*, 2010; Voduc *et al.*, 2010; Yersal & Barutca, 2014). HER2+ subtype covers generally 15% to 20% of all the breast carcinomas. Historically, this particular cancer was associated with poor prognosis and a reduced overall survival. Nevertheless, the introduction of anti-HER2 treatment modified the outcomes of HER2+ patients, which currently present a better prognosis, similar to luminal tumors (Debusk *et al.*, 2021).

Basal-like subtypes are derived from basal and, myoepithelial cells, and express specific markers including cytokeratins 5, 6 and 17. It has also been reported that basal-like carcinomas also express the Epidermal Growth Factor Receptor (EGFR). This high grade breast cancer is often associated with a high proliferation index and a poor prognosis. Basal-like tumors lack the expression of hormone receptors (ER-, PR-) and the overexpression of HER2 (HER2-). Hence, these carcinomas are also termed **triple-negative breast cancer**. However, TNBC and basal-like cancers are not equal and overlap in approximately 70% of the cases (Sørlie *et al.*, 2001; Alluri & Newman, 2014). TNBC, accounting for about 15% of breast adenocarcinomas, is essentially diagnosed in young women (<40 years). In one quarter of the cases, TNBC appearance can be linked to hereditary mutations of *BRCA1*. Furthermore, TNBC is considered as the most aggressive type of breast cancer (higher recurrence, poor prognosis, metastasis dissemination, and lack of treatments) (Elias, 2010). TNBC can be divided into six subtypes: basal-like (BL1 and BL2), mesenchymal (M), mesenchymal stem-like (MSL), immunomodulatory (IM), and luminal androgen receptor (LAR) (Lehmann et al., 2011). BL1 subtype is characterized by amplified pro-tumor genes such as MYC and KRAS and deletion of tumor suppressors such as TP53. The BL2 and M subtypes show a higher activation of proliferative and migratory pathways, respectively. Interestingly, M-subtype patients are prone to acquire resistance to chemotherapy. The MSL group expresses high levels of stemness-related genes. Due to its higher levels of genes involved in immunity, immune checkpoints inhibitors might be delivered to patients with an IM subtype. Finally, compared to the other subtypes, LAR TNBC is characterized by the overexpression of the androgen receptor (AR) (Yin *et al.*, 2020).

Normal-like breast carcinomas are characterized by the similarity in gene expression profile with normal mammary glands. These subtypes, representing approximately 8% of all breast cancers, express both hormone receptors (ER+ and PR+) but do not show overexpression of HER2 (HER2-). Although similar to normal breast, normal-like tumors show a lower outcome than Luminal A subtypes (Dai *et al.*, 2015). A few other subtypes, less characterized, are also described, such as claudin-low breast cancers. Claudin-low tumors are characterized

by a lack of tight junctions proteins such as claudins and E-cadherin, which possess a high expression of mesenchymal markers (Sabatier *et al.*, 2014).

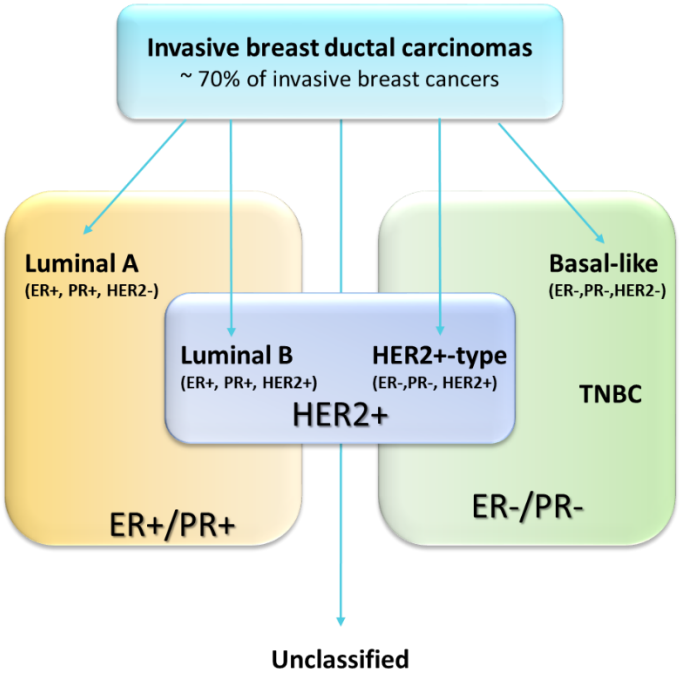

Figure I 3. Schematic illustration of breast cancer subtypes based on the molecular classification.
In orange and green: subtypes characterized by the expression status of ER/PR. In orange, the hormone receptor positive status (Luminal A and Luminal B subtypes) and in green, the negative status (HER2+, basal-like subtypes and TNBC). The central mauve zone represents the subtypes overexpressing HER2 (Luminal B and HER2+).

The patient's survival depends on breast cancer subtypes. Indeed, Luminal A patients represent the highest survival rate, followed by Luminal B tumors. Furthermore, triple-negative breast cancers show the poorest survival rate (Fallahpour *et al.*, 2017) (**Fig. I 4**).

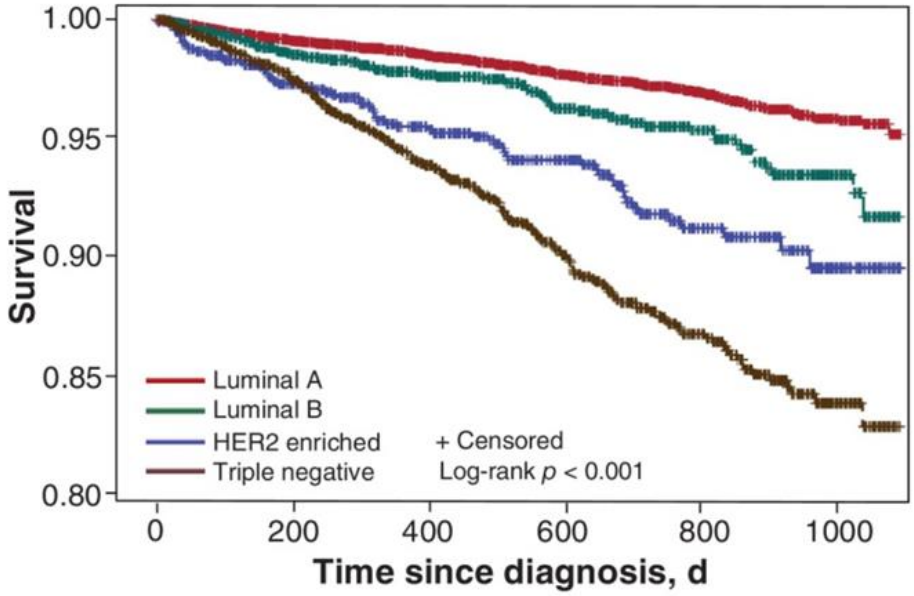

Figure I 4. Kaplan-Meier plot of overall breast cancer survival by molecular subtype.
Figure adapted from Fallahpour et al., 2017.

The classification methods, histological and molecular, are currently used by pathologists for breast cancer diagnosis. Moreover, these methods will help determine if the patient is likely to respond to a specific treatment.

1.3. Treatments

Breast cancer treatment is based on the tumor subtypes, stage and grade. For instance, in situ carcinomas are generally treated by a complete resection followed by radiotherapy or chemotherapy. In contrast, chemotherapy, targeted therapy, and radiotherapy are mainly required for higher grades of breast cancers.

1.3.1. Surgery

Surgical removal is traditionally the treatment of choice for breast cancer. Surgery treatments can be subdivided into two categories: breast-conservation surgery, a local excision followed by radiotherapy, and mastectomy, the removal of the entire breast. In Europe, the majority of newly diagnosed women undergoes breast-conservation surgery. However, this procedure is mainly limited by several factors such as the tumor size, and multicentricity, prior to radiotherapy treatment, extensive calcifications, and women with small breasts. Thereby, breast-conservation removal is aborted, and mastectomy is unavoidable (McDonald *et al.*, 2016). Nevertheless, if satisfactory cosmetic lumpectomies are conceivable, multicentric diseases might benefit from breast-conservation treatment (Rosenkranz *et al.*, 2018).

Mastectomy remains the prophylactic treatment for women who have undergone a prior chest radiation or carry hereditary *BRCA1/2* mutations. In some cases, surgery needs a prior treatment to reduce the tumor size and make it removable. This kind of treatment is termed neoadjuvant therapy. Neoadjuvant chemo- or radiotherapy can be administered to patients to facilitate breast-conservation surgery. Furthermore, clinicians perform a biopsy of the axillary lymph node to determine whether or not metastases are present. The status of the sentinel lymph node constitutes a robust predictor of breast cancer's long-term prognosis (Senkus *et al.*, 2015). When the regional lymph node is involved, the risk of recurrence can be reduced by post-mastectomy radiotherapy (Abe *et al.*, 2005).

1.3.2. Radiotherapy

Generally, breast-conservation surgery is followed by adjuvant radiotherapy. It involves the irradiation of the whole breast and the neighboring lymph nodes including the axillary and internal mammary nodes (Haussmann *et al.*, 2020). In 2011, the Early Breast Cancer Trialists' Collaborative Group (EBCTCG), through a meta-analysis of seventeen clinical trials, revealed that post-radiotherapy treatments reduced breast cancer risk recurrence but slightly ameliorated the survival (Abe *et al.*, 2005). Furthermore, the reduction in risk of recurrence can vary with age. For instance, radiotherapy might not be required for women older than seventy years with early-stage breast cancer (Hughes *et al.*, 2013). However, neoadjuvant radiotherapy might be considered to treat unresectable tumors to reduce their size and make them resectable (Senkus *et al.*, 2015).

1.3.3. Targeted therapy

Molecular classification of breast carcinomas allowed their characterization and the finding of new treatments. Targeted therapies use drugs that directly target proteins overexpressed in specific tumors (**Fig. I 5**). It is the case for breast cancer expressing hormone receptors (HR) and/or HER2. Endocrine therapy remains the treatment of choice for HR+/HER2- breast cancers. HR+ breast carcinomas are broadly guided by estrogens which promote their development by binding to their receptors. Thus, blocking the interaction hormone/receptor constitutes a considerable opportunity to treat these cancers. (Mohamed *et al.*, 2013). **Tamoxifen** is the most widely used ER blocker. This drug acts as a competitive estradiol inhibitor that binds directly to the estrogen receptors (Bentrem *et al.*, 2001). In post-menopausal patients, **aromatase inhibitors** such as anastrozole and letrozole are effective. Indeed, aromatases are responsible for the conversion of androgens to estrogens and, thus, for the endogenous production of estrogens. Nevertheless, in many cases, HR+ breast cancers become resistant to endocrine therapy (Waks & Winer, 2019). Aa new type of endocrine therapy was designed to overcome this phenomenon. **Fulvestrant** is a ER antagonist and modulates the ER avoiding agonist effects (Osborne *et al*., 2004).

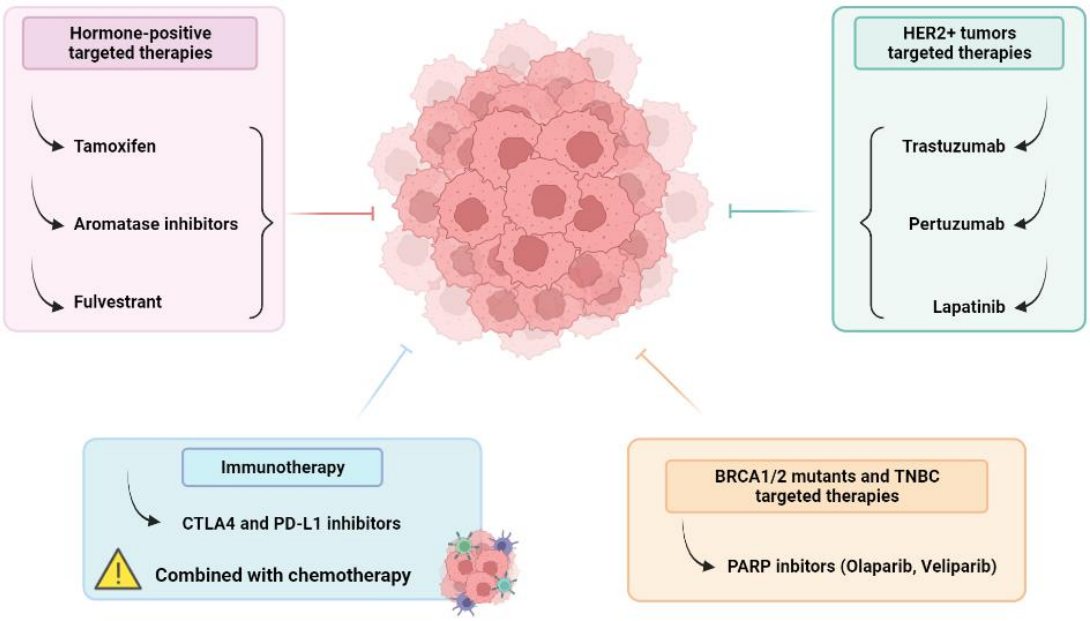

Figure I 5. Targeted therapies in breast cancer treatment.
The pink zone represents the efficient treatments for hormone-positive breast cancers: Tamoxifen, aromatase inhibitors, and fulvestrant. Treatments for HER2-overexpressing carcinomas (Trastuzumab, Pertuzumab and Laptinib) are represented in green. PARP inhibitors are treatments administered to TNBC or BRCA1/2 mutation carrying patients. Immunotherapy, also considered as a targeted therapy, is represented in blue and is always given in combination with chemotherapy. Figure created with BioRender.com.

Breast tumors might also overexpress the oncogene HER2. In the case of Luminal B tumors (HR+ and HER2+), HER2 signaling dominates the ER pathways leading to a resistance to endocrine therapy. To overcome this obstacle, anti-HER2 treatment might accompany hormone-based therapy. Among anti-HER2 therapies, **Trastuzumab**, a monoclonal antibody targeting HER2, was the first drug authorized for the treatment of HER2+ breast cancers and is, nowadays, routinely administered to patients in combination with chemotherapy. Since the commercialization of Trastuzumab, multiple anti-HER2 treatments have been developed such as Lapatinib, and Pertuzumab. Whereas Trastuzumab regulates the ligand-independent HER2 signaling, **Pertuzumab** inhibits the interaction between HER2 and HER3. Indeed, blocking the dimerization of both receptors inactivates Ras and PI3K pathways, involved in tumor growth (Higgins & Baselga, 2011). **Lapatinib**, on the other hand, is a tyrosine kinase inhibitor targeting HER2 and EGFR. Likewise, this inhibitor leads to resistance acquisition. Nevertheless, the combination between Lapatinib and Trastuzumab has been described to improve the clinical outcome (Scaltriti *et al.*, 2009).

As previously mentioned, some breast cancers patients might carry germline BRCA1 or BRCA2 mutations and can benefit from the synthetic lethality induced by the Poly(ADP-ribose) polymerase (PARP) inhibitors such as **Olaparib** and **Veliparib**. PARPs are enzymes involved

in DNA damage repair, especially in the detection of single-strand DNA breaks (Livraghi & Garber, 2015; Godet & Gilkes, 2017). Synthetic lethality arises from the combination of genetic and induced effects in which the alteration of both genes promotes cell death while the perturbation of a single gene is viable (O'Neil *et al.*, 2017). Interestingly, the addition of PARP inhibitors to a chemotherapy treatment provides a longer survival and reduces the recurrence (Tutt *et al.*, 2021).

Despite the numerous treatments developed for breast carcinomas, most of them lead to resistance phenomenon. Therefore, understanding how a tumor grows and evolves is crucial for developing new therapeutic strategies. Furthermore, the tumor microenvironment, a key player in cancer development, should not be neglected when studying cancer progression.

1.3.4. Immunotherapy

Although advances in treatment have improved the survival of breast cancer patients, metastatic breast carcinoma remains a significant threat. Therefore, improved therapies are urgently needed. For the past few years, accumulating evidences suggested a potential role for the immune system in either promoting or reducing cancer progression. The current understanding of the immune surveillance, by which immune cells eradicate cancer cells, constitutes the major breakthrough in the immunotherapy field (Yang, 2015).

Immune surveillance is modulated by immune checkpoints which are immune-cell membrane receptors that stimulate or inhibit immune responses (Esfahani *et al.*, 2020). Even though multiple immune checkpoints inhibitors have been approved for several cancers, none has yet been authorized for breast cancer. However, some clinical trials indicate the potential of several immune cell receptors such as Cytotoxic T-Lymphocyte-Associated Antigen 4 (CTLA-4). **Tremelimumab**, an antibody targeting CTLA4, prevents the interaction between the immune checkpoint and its ligands, improving T-cell activation. Tremelimumab benefit, in combination with an aromatase inhibitor, has been reported in patients with hormone-positive metastatic breast carcinomas (Vonderheide *et al.*, 2010). The therapeutic potential of other immune checkpoint inhibitors is currently studied in breast cancer. Among them, molecules targeting the programmed death ligand-1 (PD-L1), such as **Avelumab** and **Atezolizumab**, are promising. Interestingly, aggressive breast carcinomas are more likely to express a specific immune checkpoint, PD-L1, and respond strongly to avelumab and atezolizumab treatments (Emens, 2018). Nowadays, immunotherapy treatments are systematically combined with neoadjuvant chemotherapy. For instance, the combination of taxanes and anthracyclines

treatment with **Pembrolizumab**, an anti-programmed death 1 (PD-1) monoclonal antibody, showed anti-cancerous effects on early triple-negative breast cancers. Moreover, compared to patients who received neoadjuvant chemotherapy and the placebo, the immunotherapy treatments revealed a higher percentage of complete response (Schmid *et al.*, 2020). Interestingly, the immune checkpoint inhibitors, Atezolizumab and Pembrolizumab, are currently used for breast cancer treatment (Soare & Soare, 2019; Kwapisz, 2021).

Harnessing the immune responses through implementing immune checkpoint inhibitors will provide new therapeutic strategies for breast cancer treatments.

1.3.5. Chemotherapy

For many cancer types, chemotherapy remains one of the main treatments, along with surgery and radiotherapy. Adjuvant chemotherapy is given to patients after the tumor resection or radiotherapy to reduce the risks of metastasis appearance. On the other hand, neoadjuvant chemotherapy (NAC) was, initially, prescribed for inoperable breast cancers to reduce their size and facilitate the surgery. Nowadays, NAC has been extended to patients with smaller tumors, not only to lower their size, but likewise to control the tumor response to the agents, and, if necessary, accommodate better treatments. Furthermore, preoperative chemotherapy provides opportunities for individualized therapies (Montemurro *et al*., 2020). Chemotherapeutic agents are indicated for the treatment of high-grade breast carcinomas such as TNBC, Basal-like and HER2+ (Masood, 2016).

Over the past decades, novel drugs were discovered. Nevertheless, few are truly approved for patient healthcare. Thus, scientists keep trying to discover new efficient drugs or new methods to improve preexisting ones. Currently, a multitude of chemotherapeutic agents are available. Depending on their mechanism of action, drugs can be classified into five categories: antimetabolites, alkylating agents, mitotic spindle inhibitors such as taxanes, topoisomerase I/II inhibitors such as anthracyclines and others (Bukowski *et al*., 2020). Some are given as single agents, or combined with other molecules. They might be restricted to only one type of cancer, or treat several type of tumors. In the case of breast tumors, treatments depends essentially on a combination between taxanes and anthracyclines (Masoud and Pagès, 2017).

This work will focus on the effects of two chemotherapeutic agents: epirubicin, an anthracycline, and paclitaxel, a drug derived from the taxane family. Nowadays, these drugs are used for breast cancer treatment.

1.3.5.1. Epirubicin

Epirubicin is a member of the anthracycline family inhibiting the action of the topoisomerase II. The first anthracycline discovered, doxorubicin, has been isolated from *Streptomyces* bacterium *Streptomyces peucetius* (Grein, 1987). This antibiotics family was, for the first time, introduced for the treatment of aggressive breast cancer in the 1970's. Nowadays, two major drugs are used: epirubicin and doxorubicin (Conte *et al.*, 2000).

1.3.5.1.1. Mechanisms of action

Anthracyclines are cytotoxic drugs that might impair cell behavior at different levels. The main mechanism of action of these molecules is based on their intercalation between DNA base pairs (Carvalho *et al.*, 2009). Therefore, they are referred as DNA intercalating agents and will interfere with DNA and RNA synthesis (**Fig. I 6**). Anthracyclines are Topoisomerase II inhibitors through the stabilization of the covalent link between the DNA strand and the enzyme, which triggers DNA double-strand breaks (DSB). Two isoforms of Topoisomerase II are found in mammals: Topoisomerase IIα (Top2α) and IIβ (Top2β). Nevertheless, they are differentially expressed and involved in distinct mechanisms. For instance, Top2α is mainly found in high-proliferative tissues while Top2β is expressed in almost all tissues. The intercalating agent preferentially targets the IIα isoform, which is involved in the replication and cell division processes. However, Top2β might also be targeted by anthracyclines in a long-term process (Marinello *et al.*, 2018). Moreover, the generation of the TopII-DNA-drug complex leads to the appearance of irreversible DSB, which activates a p53-mediated apoptosis. Another cytotoxic mechanism is the production of reactive oxygen species (ROS) that causes DNA damages and membrane deterioration by lipid peroxidation (Beretta & Zunino, 2007). Interestingly, anthracyclines are also key players in the tumor immunity by promoting immune surveillance and reducing immunosuppression (Zhang *et al.*, 2015). Indeed, chemotherapeutic agents induce DNA damages causing the release of damage-associated molecular patterns (DAMPs) from dying cancer cells which assure an anti -tumor immunity. Moreover, due to its off-target effects, chemotherapy leads to the activation of immune cells such as natural killer (NK), dendritic cells (DCs, and CD8+ T cells. On the opposite, the treatment reduces the amount of immunosuppressive cells including M2 macrophages and myeloid-derived suppressor cells (MDSCs) (Zhang *et al.*, 2022). Together, these mechanisms contribute to cell death and support the inhibition of cancer progression.

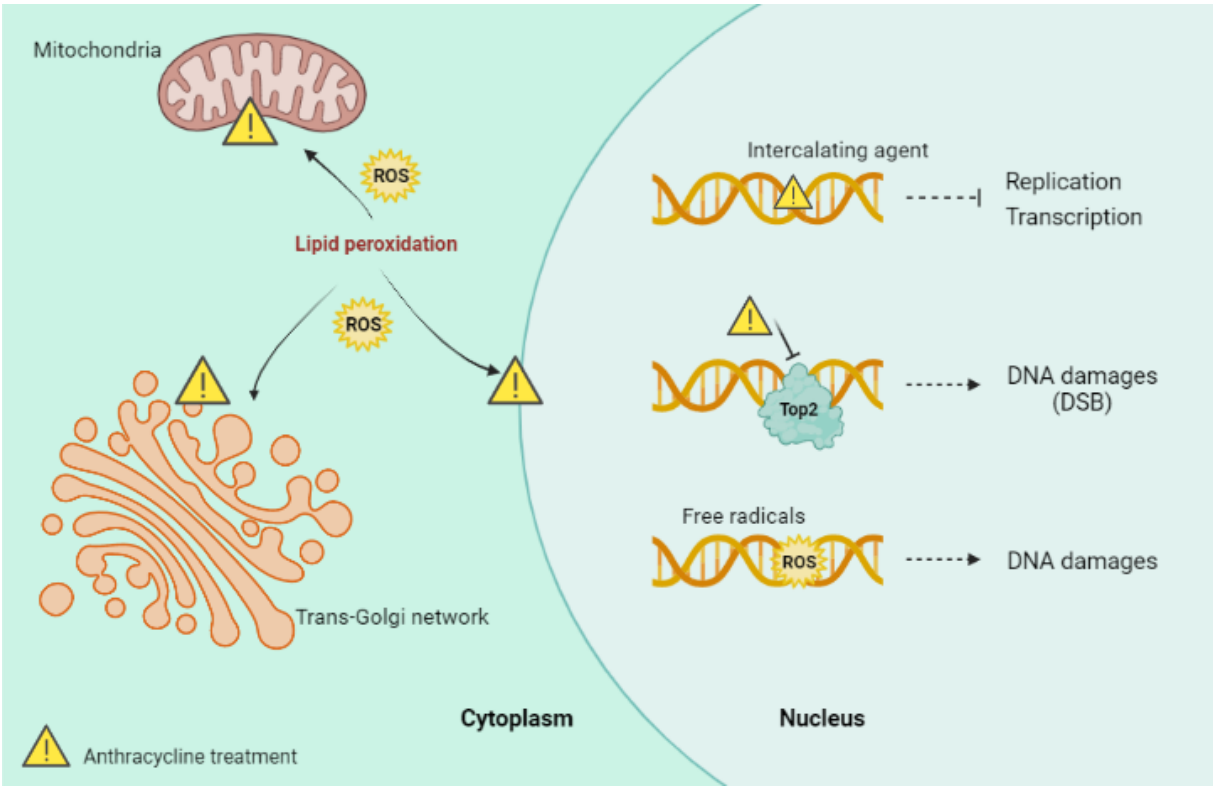

Figure I 6. Mechanisms of action of anthracyclines.
Anthracyclines cytotoxicity is mainly caused by its intercalating properties which interfere with replication and transcription processes. These drugs provoke also the generation of reactive oxygen species (ROS) leading to DNA damages and membrane lipid peroxidation. Finally, anthracyclines target the Topoisomerase II (Top2) and cause irreversible double-strand breaks (DSB). Figure created with BioRender.com

1.3.5.1.2. Doxorubicin to Epirubicin

The first anthracyclines were discovered in the late 1960s and called doxorubicin or daunorubicin. Rapidly, doxorubicin was used to treat solid and hematological cancers (Paul Launchbury & Habboubi, 1993). Nevertheless, the treatment with these molecules induced adverse side effects such as cardiotoxicity. Consequently, scientists were determined to isolate, or produce, new anthracycline analogs possessing a lower toxicity. Epirubicin is one of the two thousand analogs produced (Carvalho *et al.*, 2009). This molecule is a 4'-epimer of doxorubicin due to the invert configuration of the hydroxyl group (**Fig. I 7**). Interestingly, similar tumor responses and survival rate are observed between both anthracyclines, at equal concentrations. As for other anthracyclines, the major side effects of anthracyclines are cardiotoxicity and myelosuppression. However, epirubicin significantly reduces immunosuppression, cardiotoxicity and non-hematologic toxicities (Khasraw *et al.*, 2012). Moreover, the next generation drug and its metabolites are eliminated faster than its analog, reducing the time of exposure.

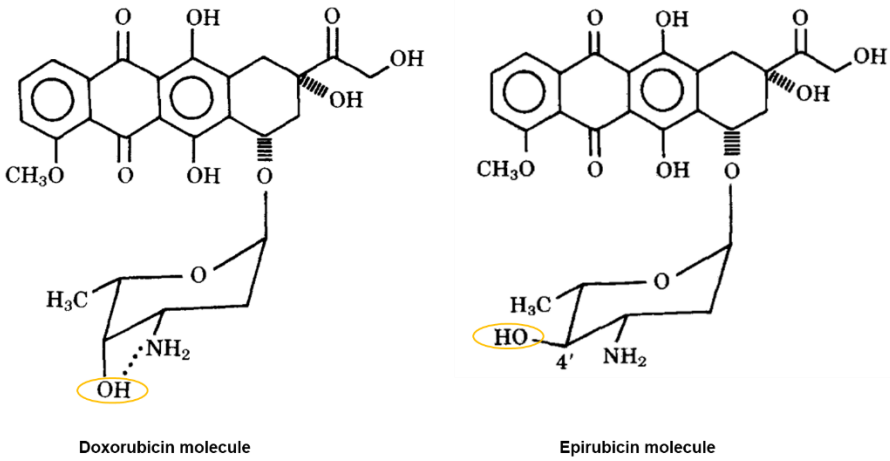

Figure I 7. Differences in the molecular structure of doxorubicin and epirubicin
In comparison with doxorubicin (left), epirubicin, on the right, results in the epimerization of the 4'-hydroxyl (OH) group (represented in orange). Figure adapted from Paul Launchbury & Habboubi, 1993.

1.3.5.2. Paclitaxel

Paclitaxel is a member of the taxanes family, a class of mitotic spindle inhibitors. Taxol was first isolated in 1967, from the Pacific Yew tree (*Taxus brevifolia*) (Wani *et al.*, 1971). It was only in 1992 that taxol became paclitaxel. Nevertheless, the drug did not, at first, arouse the interest of the scientific community. Due to the limited accessibility of paclitaxel and its promising anti-cancer properties, multiple laboratories worked on its synthesis. Regarding the structure complexity of paclitaxel, its total synthesis was not achieved until 1994 (Holton *et al.*, 1994). Interestingly, paclitaxel is effective for the treatment of several carcinomas such as breast, ovarian, lung and head and neck cancers.

1.3.5.2.1. Mechanisms of action

The main mechanism of action of taxanes is their role in mitosis. Indeed, these drugs are anti-mitotic molecules which stabilize microtubules and, thus, perturb the microtubules spindle system (**Fig. I 8**). Their interaction, through the N-terminal part of the beta-tubulin, with the filaments promote their polymerization, precludes their disassembly and, consequently, leads to the mitotic interruption in metaphase-anaphase (Fitzpatrick & De Wit, 2014). Moreover, the cell-cycle arrest induced by paclitaxel takes place owing to the activation of the spindle assembly checkpoints. Nevertheless, other cytotoxic modes of action exist. Another mechanism is the induction of apoptosis through different manners. For instance, in response to a lower calcium concentration within the mitochondria, the anti-cancer drug can induce the release of a pro-apoptotic factor, cytochrome C (Cyt C) from the mitochondria to the cytoplasm (Abu Samaan *et al.*, 2019). It has also been demonstrated to induce the expression of TNFα.

Interestingly, the process is specific to paclitaxel and does not occur with other taxanes (Burkhart *et al*., 1994).

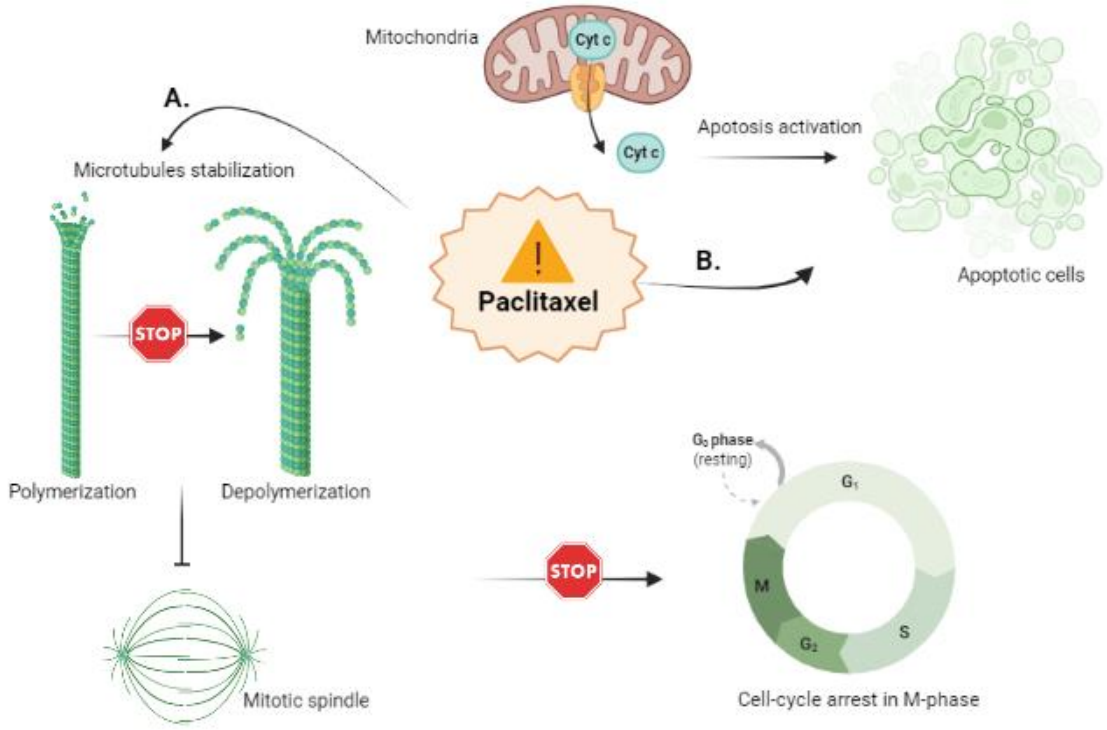

Figure I 8. Principal mechanisms of action of paclitaxel.
*Taxane toxicity is principally caused by a stabilization of the microtubules leading to cell-cycle arrest (**A**). Paclitaxel also induces apoptosis through the release of the cytochrome c (Cyt c) from the mitochondria to the cytosol (**B**). Figure created with BioRender.com.*

1.3.5.2.2. Taxanes toxicity

Paclitaxel is currently used for the treatment of several cancers such as breast, lung, ovarian and brain. Nevertheless, significant dose-limiting toxicities are observed. The major one is hematologic toxicity associated with neutropenia and leukopenia. Interestingly, these side effects are dose dependent and are promptly reversible. Moreover, it seems that longer period of treatment affects and stimulates the appearance of those symptoms (Eisenhauer *et al*., 1994). Upon paclitaxel treatment, neurotoxicity might also be observed which includes demyelination and axonopathy. Peripheral neuropathy represents the most common, non-hematologic, dose-limiting toxicity (Velasco & Bruna, 2010). Hypersensitivity is another encountered problem upon taxanes treatment and is, mainly, induced by the drug, itself, or its castor oil vehicle (Wang *et al.*, 2013). Other undesirable effects, less common, might appear. This is the case for cardiac and gastrointestinal toxicities (Al-Mahayri *et al*., 2021).

To bypass and reduce paclitaxel-induced toxicities, several strategies have been developed. For instance, new delivery methods significantly reduce the appearance of hypersensitivity (Marupudi *et al.*, 2007). On the other hand, to improve the clinical benefits of taxanes, paclitaxel derivatives have been synthetized: docetaxel and cabazitaxel. Both molecules are semi-synthetic analogs of paclitaxel. Whereas paclitaxel and docetaxel possess similar mechanisms of action, their toxicities are different (Verweij *et al.*, 1994). Unlike the first taxanes, cabazitaxel possesses a poor affinity for P-glycoprotein (P-gp), a drug efflux pump, reducing the risk of taxanes resistance development (Paller & Antonarakis, 2011). Paclitaxel protein-bound particles, also referred as *nab* paclitaxel, is a recent formulation of paclitaxel delivered without the castor oil vehicle system. It uses albumin and its receptor to enhance its delivery to cancer cells (Hennenfent & Govindan, 2006).

1.3.5.2.3. Combined epirubicin and paclitaxel in breast cancer treatment

Chemotherapy is usually recommended for the treatment of aggressive breast cancers such as TNBC, HER2+ and metastatic carcinomas. In such types of tumors, epirubicin and paclitaxel are often administered to patients as first-line therapy (Gennari *et al.*, 2004). Rather than being used alone, the association of both chemotherapeutic agents, with different mechanisms of action, offers a higher efficiency and reduces the development of multi-drug resistance (MDR). The most applied treatment is based on epirubicin in combination with fluorouracil and cyclophosphamide, followed by paclitaxel (Buzdar *et al.*, 2013). The addition of taxanes has been reported to improve the efficiency of chemotherapy, but increases non-cardiac toxicities. However, many evidences suggest that the utilization of anthracyclines and taxanes reduces breast cancer mortality (Senkus *et al.*, 2015).

1.3.5.2.4. Resistance to chemotherapy

Unfortunately, multi-drug resistance often occurs after chemotherapy treatment. This allows cancer cells to survive to a multitude of drugs via several processes (**Fig. I 9**). One of the most studied mechanisms is the implication of **drug-efflux pumps** which involve ABC (ATP-binding cassette) transporters. These phosphoglycoproteins reduce the accumulation of drugs within their cytoplasm by releasing it in the outer compartment. The most described molecule of this family is P-gp, a protein encoded by *MDR1*, aka ABCB1 (Ambudkar *et al.*, 2006). P-gp is able to bind to several chemotherapeutic agents, including anthracyclines and taxanes, and allow their release outside the cell. Within a tumor, cells might be either sensitive or resistant to chemotherapy. However, resistant cancer cells are able to transfer resistance

features to sensitive cells via extracellular vesicles. For instance, the transfer of P-gp, via exosomes, to breast cancer cells mediates the acquisition of resistance (Lv *et al.*, 2014).

Another mechanism is the **lower absorption** rate of the drugs due to the presence of mutations in membrane transporters such as SLC transporters (Girardi *et al.*, 2020).

The majority of cancer cells find a way to escape cell death by **inhibiting apoptosis pathways**. It has been reported that resistance to chemotherapy can be linked to the up-regulation of anti-apoptotic genes, for instance Bcl-2 and AKT, or the down-regulation of genes favoring apoptosis such as Bax. Moreover, mutations in p53 genes, implicated in the recognition of DNA damages, are also involved in the resistance acquisition (Hientz *et al.*, 2017).

Less known MDR mechanisms might also occur. Changes in the **drug metabolism** can cause such phenomenon. For instance, the detoxification of docetaxel by cytochrome P450 reduces the resistance via the inactivation of the drug (Bruno & Njar, 2007). Furthermore, the alterations in the **DNA repair** machinery within cancer cells impairs their sensitivity to the agents. Indeed, the enhancement of DNA repair increases the resistance of breast cancer cells to doxorubicin (Stefanski *et al.*, 2019).

Nevertheless, some resistance mechanisms are specific for taxanes or anthracyclines.

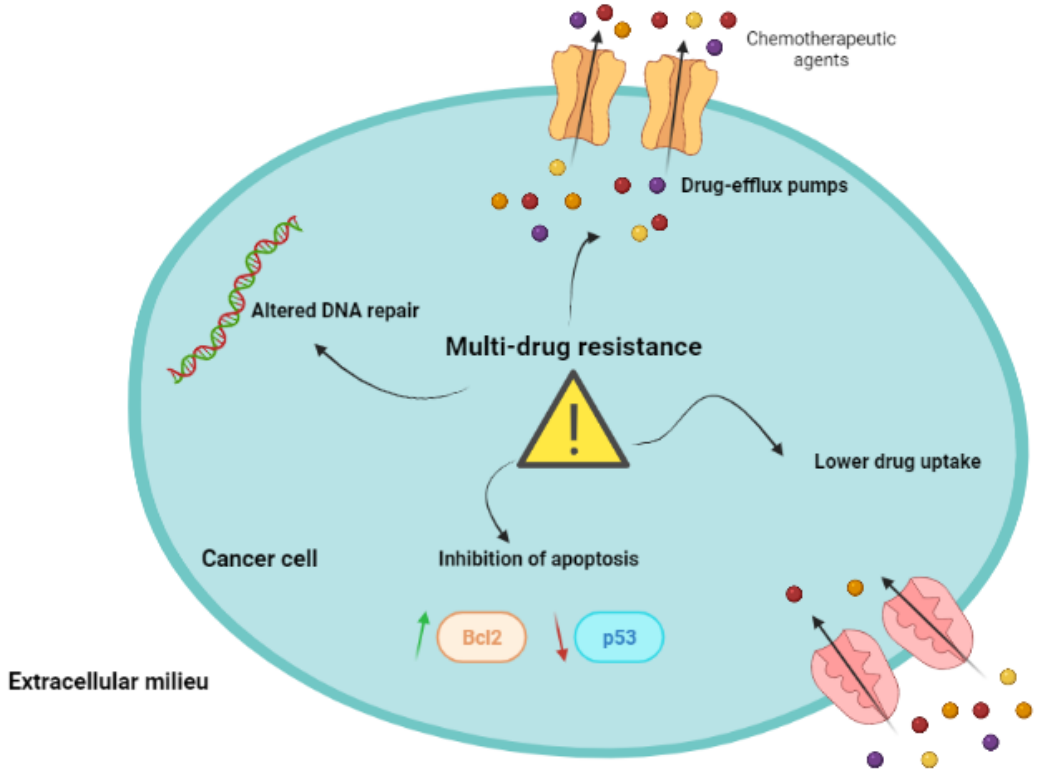

Figure I 9. Multi-drug resistance upon chemotherapy.
The common mechanisms of drug resistance comprise the up-regulation of proteins implicated in drug efflux, the lower drug absorption by cancer cells, the inhibition of apoptosis pathways (via an up-regulation of anti-apoptotic signals such as Bcl-2 or a down-regulation of p53) and altered DNA repair systems. Figure created with BioRender.com.

1.3.5.3. Resistance to anthracyclines

As discussed previously, anthracyclines inhibit the activity of Top2a. Alterations in both gene expression and activity of Top2a impact the sensitivity of cancer cells to anthracyclines (Beretta & Zunino, 2007). For instance, a multitude of studies have reported that decreased levels of Top2a induce chemoresistance to doxorubicin. Furthermore, post-translational modifications (phosphorylation and sumoylation) of this protein seem to contribute to the acquisition of resistance (Ganapathi & Ganapathi, 2013).

1.3.5.4. Resistance to taxanes

Besides MDR mechanisms, cells have diverse other ways to avoid the cytotoxic effects of taxanes. These drugs bind, with various affinities, different isoforms of tubulins. For instance, βIII-tubulin shows a lower affinity for taxanes and has been associated with resistance in many types of cancers (Kavallaris, 2010). Microtubule-associated proteins (MAPs) have also been shown to play a role in taxanes resistance. For instance, MAP4 expression, which stabilizes microtubules, is inversely correlated with p53 levels, and favors resistance to taxanes (Maloney *et al.*, 2020).

2. Tumor microenvironment

For many years, cancer was described as an autonomous disease, in which epigenetic modifications and gene mutations were sufficient to promote its progression. However, tumor pathogenesis is now recognized by the oncology field as a heterogeneous process, in which extracellular matrix (ECM), non-cancerous cells and tumor cells are closely related. Indeed, cancer progression requires the dynamic crosstalk between cancer cells and the surrounding microenvironment, also called tumor microenvironment (TME). The TME is now considered as an important contributor to tumor progression and metastasis formation. Interestingly, unraveling the interactions between cancer cells and the surrounding environment may provide therapeutic strategies to predict and reduce cancer progression (Baghban *et al.*, 2020).

The major components of the TME are the ECM, the stromal cells, and immune cells (**Figure I 10**). Moreover, **extracellular vesicles** play important roles within the microenvironment. These membrane-derived vesicles will be described in the next chapter.

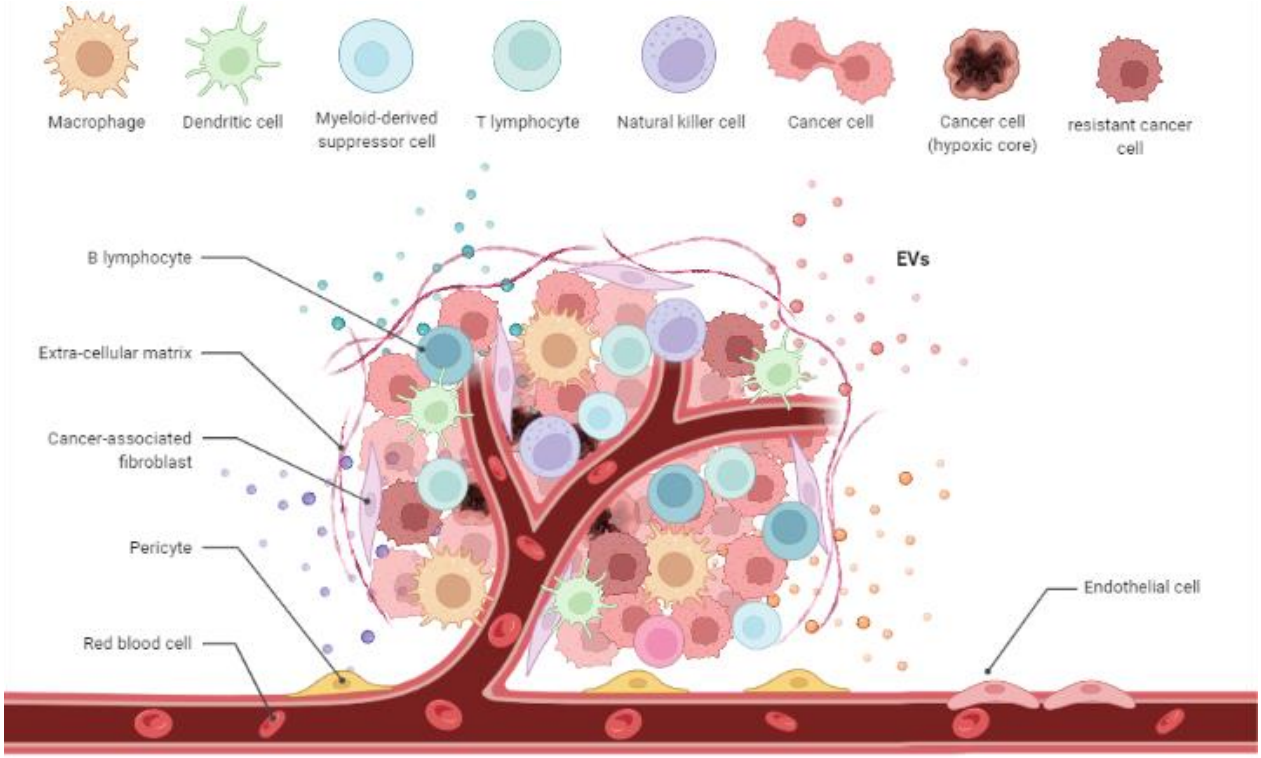

Figure I 10. Schematic representation of the tumor microenvironment composition.
Cancers are not homogenous diseases. Indeed, tumor cells are surrounded by other cell types and the extracellular matrix which together constitutes the tumor microenvironment (TME). A tumor requires constant crosstalk with cells composing TME such as endothelial cells, assuring the delivery of oxygen and nutrients, immune cells, promoting or reducing its growth, cancer-associated fibroblasts and many others. Moreover, cancer cells are also divided in multiple categories: sensitive, resistant to chemotherapy and hypoxic cancer cells. Finally, extracellular vehicles (EVs), released from all cell types, are major components of TME and assure the communication between cells within the microenvironment. Figure created with BioRender.com.

2.1. Extracellular matrix

Extracellular matrix, the non-cellular component of the TME, is a dynamic network which constitutes the scaffold of cellular constituents in all tissues (Frantz *et al.*, 2010). The assembly of ECM macromolecules in three-dimensional structures contributes to the cellular integrity and the efficiency of paracrine signals (Theocharis *et al.*, 2016). In addition, ECM also controls cellular pathways such as proliferation, differentiation, migration, adhesion and intercellular communication and, therefore, is able to regulate the hallmarks of cancer (Pickup *et al*., 2014). ECM is composed of an interstitial and a pericellular matrix. Cells are surrounded by the interstitial matrix, while the pericellular is associated with cells (Laurila & Leivo, 1993). The basement membrane (BM) is an example of a pericellular matrix. BM is a barrier which plays multiple roles within tissues, especially in cell adhesion and migration (Jayadev and Sherwood, 2017). Interestingly, the components of ECM vary between tissues or organs. In fact, every tissue displays a singular ECM composition that may help to develop tissue-specific therapies (Bonnans *et al*., 2014). ECM is a highly dynamic structure that steadily undergoes remodeling processes; synthesis and degradation. Among the proteinases that degrade ECM, the main group is composed of matrix metalloproteinases (Jabłońska-Trypuć *et al*., 2016).

Proteins such as collagen, fibronectin, laminins and elastins; and polysaccharides including proteoglycans are the major ECM components.

Collagen, the most abundant protein in mammals, is the main fibrous protein found within the ECM (Tanzer, 2006). Collagen superfamily includes 28 members referenced as Collagen-I to –XXVIII (Ricard-Blum, 2011), each with a triple helix characteristic structure (Bella & Hulmes, 2017). The alterations in the abundancy or the types of collagens are associated to most of cancer hallmarks such as chemoresistance, survival, invasion and metastasis formation (Voutouri *et al.*, 2016; Badaoui *et al.*, 2018; Xu *et al.*, 2018).

Fibronectin (FN) is a dimeric glycoprotein which allows interactions between ECM and cells. This protein can interact with ligands such as integrins and collagens (Pankov & Yamada, 2002). Numerous studies have reported the implication of FN in cancer progression. For instance, FN can promote metastasis (Cheng *et al.*, 2003; Wang *et al.*, 2017) and induce angiogenesis (Lugano *et al.*, 2018). The roles of this protein will be discussed in the results of the first chapter.

Laminins are heterotrimeric glycoproteins constituted by three chains of polypeptides (α, β and γ). These glycoproteins are major components of the basement membrane (Aumailley,

2013). Interestingly, in a tumor context, laminins are also present in the interstitial matrix. This aberrant distribution tallies with the degree of invasiveness of tumor cells. For instance, several studies have reported that laminin-5 promotes tumor invasion (Imura *et al.*, 2012; Troughton *et al*., 2020).

Elastic fibers are integral components of the ECM. They result from the assembly of proteins termed **elastins** (Vindin *et al*., 2019)**.** In concert with collagen fibers, elastins provide stretching and maintain the resilience of many tissues and organs (Ushiki, 2002). Overexpression of a protein responsible for the interactions between those two fibers, lysyl oxidase, has been observed in many cancers and promotes angiogenesis and invasion processes (Moon *et al.*, 2013; Peng *et al.*, 2017).

Finally, ECM is also composed of **proteoglycans**. These glycosylated proteins, covalently attached to glycosaminoglycan chains, constitute key components of the interstitial matrices (Yanagishita, 1993). Proteoglycans bind a large range of molecules such as growth factors, extracellular proteins and other ECM components. Their ability to bind bioactive molecules make proteoglycans key regulators of signal transduction (Lander & Selleck, 2000). Moreover, they are also involved in the migration, proliferation and cell adhesion processes (Wight *et al*., 1992), and consequently, proteoglycans play crucial roles in cancer progression. For instance, perlecan, a major component of the vascular ECM, is able to induce angiogenesis (Segev *et al.*, 2004).

2.2. Cellular components

2.2.1. Blood and lymphatic vessels

To grow, a tumor requires blood vessel to assure the delivery of nutrients, oxygen, and the release of molecules. **Angiogenesis**, mostly a quiescent mechanism, is defined by the formation of blood vessels from pre-existing ones. In diseases such as cancer, angiogenesis is reactivated through an angiogenic switch (Carmeliet & Jain, 2011) (**Fig. I 11**). Once a tumor reaches a certain size, hypoxia and nutrients deprivation induce angiogenesis to allow the tumor to expand. The main macromolecules responsible for blood vessels sprouting are VEGF-A, platelet-derived growth factor (PDGF), fibroblast growth factor (FGF) and angiopoietin-1. VEGF-A, the most described, binds to the receptor tyrosine kinase, also called VEGFR2, exhibited on endothelial cells and, therefore, promotes angiogenesis (Zecchin *et al.*, 2017). The components of tumor vasculature comprise pericytes, endothelial and lymphatic cells.

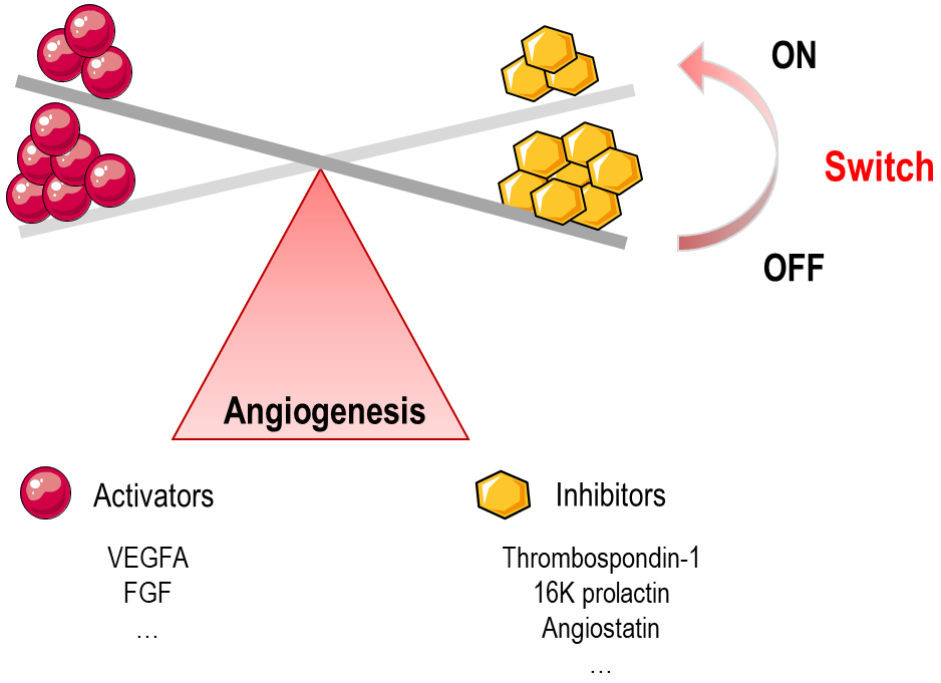

Figure I 11. Angiogenic switch.
Angiogenesis is defined by the creation of new blood vessels from pre-existing ones. This mechanism occurs mostly during embryogenesis and, then, remains quiescent. Nevertheless, multiple diseases can induce a stimulation of angiogenesis, also called angiogenic switch. This process is based on the balance between pro-angiogenic (activators; in red) and anti-angiogenic (inhibitors; in orange) molecules. When, the balance tilts towards the activators such as VEGFA, angiogenic switch occurs.

Endothelial cells (ECs) form the endothelium, the surrounding layer of blood vessels that isolates the tissue from the circulation. Tumor angiogenesis is mediated by the recruitment of endothelial cells transformed into tumor endothelial cells (TECs) (Nagl *et al.*, 2020). Unlike the normal endothelium, the architecture of tumor vasculature is completely disorganized. Blood vessels are extremely dilated and show a higher permeability. Unfortunately, the entry of therapeutic agents is impaired by the chaotic nature of the tumor vasculature (Joyce, 2005; Nagy *et al.*, 2010). However, numerous therapies have been developed to inhibit angiogenesis. For instance, the blocking of circulating VEGF-A through the administration of Bevacizumab has been reported to increase the survival of colorectal cancer (Hurwitz *et al.*, 2004). Nevertheless, endothelial cells play also a role in reducing cancer progression by, for example, secreting macromolecules such as miRNAs within extracellular vesicles (Bovy *et al.*, 2015).

Along with endothelial cells, **pericytes** are also required for angiogenesis. Pericytes are contractile cells that are present at the interface between the endothelium and the neighboring tissue and assure the maintenance of the blood barrier (Attwell *et al.*, 2016). Abnormal pericytes coverage has been reported to impact cancer progression. On another hand, a low coverage

affects blood vessels integrity and leads to dissemination of tumor cells (Cooke *et al.*, 2012; Barlow *et al.*, 2013).

Lymphatic cells (LECs) are endothelial cells lining the inner wall of the lymphatic vessels. Lymphangiogenesis, the formation of lymphatic vessels, is promoted by another subtype of VEGF molecules, VEGF-C (Karkkainen *et al.*, 2004). Interestingly, LECs show a lack of pericytes which confers a higher permeability to the vessels. Hence, tumor lymphatic vasculature enables the dissemination of circulating cancer cells and enhances the dissemination of metastasis (Alitalo, 2011; Alitalo & Detmar, 2012).

2.2.2. Cancer-associated fibroblasts

Cancer-associated fibroblasts (CAFs) are fibroblasts within the TME that are responsible for cancer progression and metastasis. The normal cell-CAF transition is a process barely understood which can be promoted by growth factors, stress and cytokines (Sahai *et al.*, 2020). CAFs are involved in most of the hallmarks of cancer. For instance, activated fibroblasts increase the secretion of Vascular Endothelial Growth Factor (VEGF) and, consequently, promote angiogenesis (Pula *et al.*, 2013; Hayashi *et al.*, 2016). Considering that CAFs strengthen tumor growth, numerous therapies have been developed to inhibit the CAFs maturation. Indeed, by producing matrix components, CAFs confer a fibrotic aspect of the tumor which decreases the immune cells infiltration. To circumvent this phenomenon, multiple strategies have been assessed. For instance, the repression of the chemokine receptor, CXCR4, inhibits the maturation of normal cells into CAFs resulting in the regression of breast cancer progression (Chen *et al.*, 2019).

2.2.3. Immune cells

For many years, the oncology community has focused its attention on the role of the immune system on tumor growth. Nowadays, immunotherapy has revolutionized cancer treatment. For that purpose, antibodies against immune checkpoints, regulators of immune evasion, have been developed. In melanoma, for instance, the cytotoxic T-lymphocyte-associated antigen 4 (CTLA-4) and programmed death 1 (PD-1) checkpoints have been described to promote cancer progression (Buchbinder & Desai, 2016). Immune cells are key players within the TME. Indeed, depending on the situation, immunity can either repress (also termed immunosurveillance) or promote tumorigenesis (immune evasion) and both innate and adaptive immune responses can participate in this phenomenon (Vesely *et al.*, 2011; Shalapour & Karin, 2015; Tang *et al.*, 2021).

The innate immune response within the TME comprises several types of immune cells such as macrophages, dendritic cells (DCs), natural killers (NKs) and neutrophils. Macrophages, also called **tumor-associated macrophages** (TAMs) in the context of tumor, represent the major infiltrating innate immune cells within the TME. TAMs participate in tumorigenesis (Ngambenjawong *et al.*, 2017) by playing crucial roles in inflammation, widely established to enhance cancer progression (Coussens & Werb, 2002). Within the tumor immune microenvironment, macrophages are classified into two categories: M1 and M2 phenotypes. The polarization of M1 macrophages confer pro-inflammatory and cytotoxic capacities that correlate with anti-tumor effects. In contrast, the M2 polarized macrophages, through their anti-inflammatory properties, contribute to tumor progression by promoting metastasis and angiogenesis. Broadly, in cancer, the M2/M1 ratio is upregulated (Dan *et al.*, 2020; Oshi *et al.*, 2020). **Dendritic cells**, required for the antigen presentation, are involved in, both, innate and adaptive immunity. DCs, which can activate naïve T cells or NKs, constitute a promising path for cancer therapy (Palucka *et al.*, 2010; Shang *et al.*, 2017). **Natural killers** are highly cytotoxic cells that can initiate apoptosis in cancer cells through the release of granules and, moreover, induce T cell immune response (Zingoni *et al.*, 2017). Currently, combined treatments with NKs are developed for several cancer types (Xie *et al.*, 2017; Minetto *et al.*, 2019). Similar to macrophages, **neutrophils** can also be classified in pro-inflammatory (N1) or anti-inflammatory cells (N2) which, respectively, suppress or induce tumor development (Fridlender & Albelda, 2012; Patel *et al.*, 2018). Therapies based on infiltrating innate immune cells are nowadays investigated for their therapeutic potential in cancer treatment. **Myeloid-derived suppressor cells** (MDSCs) are immature myeloid cells with an immunosuppressive action. MDSCs are divided into two groups: polymorphonuclear and monocytic MDSCs, which share the morphology and the phenotype of neutrophils and monocytes, respectively. In the context of cancer, MDSCs participate to tumor progression by promoting immune evasion and angiogenesis (Marvel & Gabrilovich, 2015; Yuhui Yang *et al.*, 2020).

T and B lymphocytes, also called **tumor-infiltrating lymphocytes** (TILs) in the context of cancer, are the adaptive immune cells found within the tumor microenvironment. Along with the type 1 CD4+ T helper (Th1), the cytotoxic CD8+ T cells are involved in the eradication of the tumor and are associated with a better prognosis for patients (Fridman *et al.*, 2012). Whereas, the Th2 subset generates pro-tumoral effects through the suppression of the anti-tumor immunity response (Chraa *et al.*, 2019). Through the inhibition of helper and cytotoxic T cells activation, regulatory T cells (Tregs) prevent immune surveillance and, thereby, promote tumor progression. However, Tregs are also essential players of the immune tolerance

mechanisms (Li *et al.*, 2020). Infiltrating B lymphocytes can either reduce cancer progression by inducing tumor cells death by NKs, the priming of CD4+ or CD8+ lymphocytes, and phagocytosis by macrophages, or promote tumor growth via the secretion of growth factors or auto-antibodies (Yuen *et al*., 2016).

3. Exosomes and other extracellular vesicles

Cell-to-cell communication is an essential process occurring between every cell type. This mechanism includes cell junctions, extracellular factors, such as hormones, growth factors, and, finally, vesicles. Extracellular vesicles (EVs) constitute a main mode of communication by transferring biological content to a recipient cell. Interestingly, all cells, eukaryotes and prokaryotes alike, appear to produce small membrane-bound vesicles.

EVs are small particles surrounded by a lipid bilayer similar to the plasma membrane of the producing cell. Among EVs, three classes are described: exosomes, microvesicles (MVs) and apoptotic bodies (ABs) (**Fig. I 12**). EVs classification is essentially based on their biogenesis, size and composition. However, cells may also release other non-characterized vesicles such as nanovesicles and large plasma membrane particles (Sedgwick & D'Souza-Schorey, 2018). For the aim of this work, we will focus on exosomes.

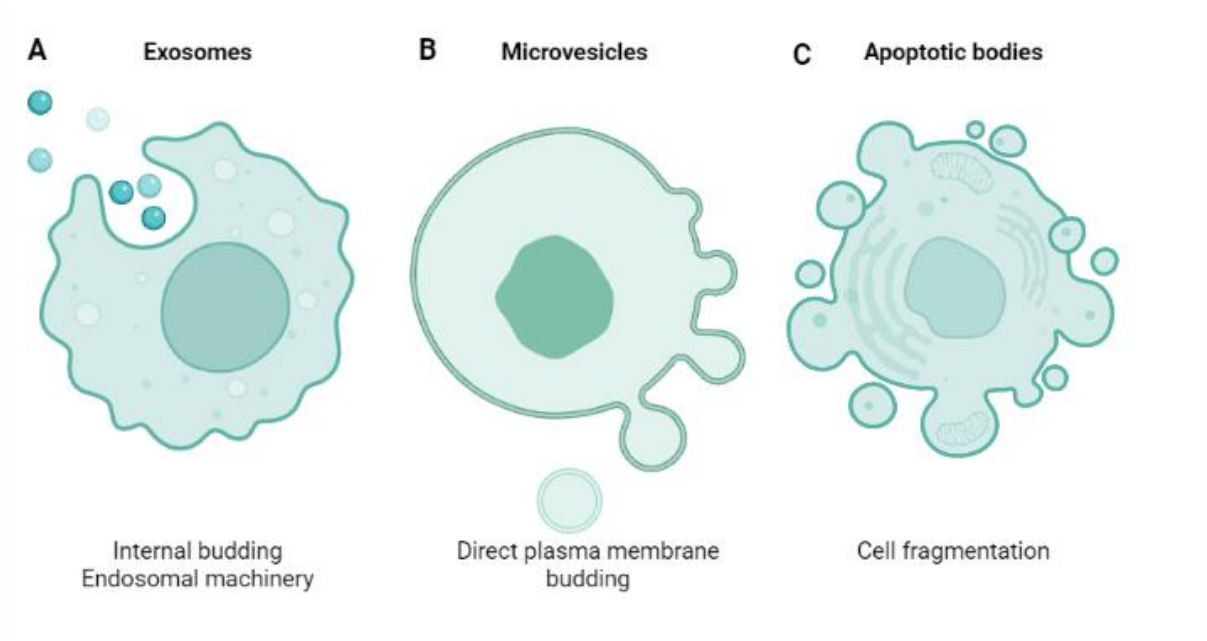

Figure I 12. Types of extracellular vesicles.
*EVs are classified in three categories based on their size and their biogenesis. (**A**) Exosomes are generated, by the endosomal machinery, through an inward budding of endosomes and then secreted in the extracellular milieu. (**B**) Microvesicles are produced by the direct budding of the plasma membrane. (**C**) Apoptotic bodies are released by cells undergoing apoptosis. Figure created with BioRender.com*

3.1. Types of EVs

3.1.1. Microvesicles

MVs, also referred as microparticles or ectosomes, result from the budding of the plasma membrane and are directly secreted in the extracellular milieu. Their biogenesis relies mainly on the redistribution of proteins and lipids from the plasma membrane. These modifications lead to a vertical trafficking of cargo to the membrane (D'Souza-Schorey & Clancy, 2012). Although MVs are produced by direct blebbing of the plasma membrane, their biogenesis requires some of the endosomal machinery components. For instance, the GTPase ADP-ribosylation factor (ARF6) and members of the endosomal sorting complexes required for transport (ESCRT) are required for cargo trafficking (Tricarico *et al*., 2017). The size of microparticles is between 50 to 1000 nm (Lee *et al.*, 2012). When cancer cells secrete MVs, they are named oncosomes (Minciacchi *et al*., 2015). The composition of MVs reflects the cell of origin. However, an enrichment of polyunsaturated glycerophosphoserine has been observed in MVs. Those particles are mostly studied for their protein content. Nevertheless, MVs also carry nucleic acids such as microRNAs (miRNAs) (Zaborowski *et al.*, 2015).

3.1.2. Apoptotic bodies

Whilst exosomes and microvesicles are secreted by healthy cells, ABs are only produced by dying cells. Indeed, when a cell undergoes apoptosis, several modifications occur such as plasma membrane blebbing, formation of protrusion and production of ABs (Caruso & Poon, 2018). Generally, ABs are larger than other EVs with a size range between 500 to 4000 nm (Akers *et al*., 2013). They contain chromatin, proteins, DNA fragments, and even entire organelles. Interestingly, RNA molecules, such as miRNAs, were also found in these vesicles (Crescitelli *et al.*, 2013; Battistelli & Falcieri, 2020).

3.1.3. Exosomes

In 1983, Pan & Johnstone described for the first time the secretion of nano-vesicles by sheep reticulocytes (Pan & Johnstone, 1983). Even though the term "exosomes" was used for the first time in 1981 but adopted only eight years later. However, they were considered as a way to eliminate macromolecules and cell debris (Trams *et al.*, 1981; Johnstone *et al.*, 1987). Now, the crucial roles of exosomes are well established.

Exosomes are cup-shaped small vesicles surrounded by a lipid bilayer. Their size varies between 40 to 120 nm. They are secreted by several cell types and their presence has been reported in many body fluids (Kharaziha *et al.*, 2012).

3.1.3.1. Exosomes biogenesis

The biogenesis of exosomes differs from the other EVs. Indeed, those nano-vesicles are generated by the endosomal machinery (**Fig. I 13**) (Van Niel *et al.*, 2018).

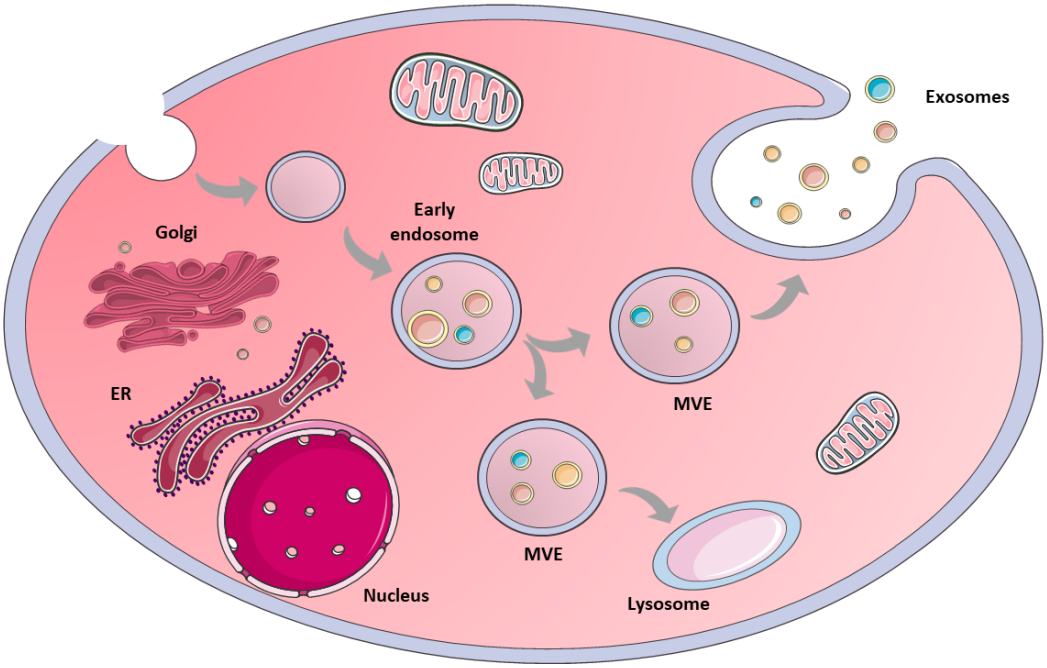

Figure I 13. Biogenesis of exosomes.
Exosome generation requires the endosomal machinery. Endosomes derived from the plasma membrane and will fuse to form early endosomes which will mature in late endosomes. These intracellular vesicles underwent an inward budding forming intraluminal vesicles (ILVs). Endosomes are now named multivesicular bodies (MVBs). MVBs can either fuse to lysosomes leading to their degradation or either fuse to the plasma membrane releasing exosomes in the extracellular milieu. Figure created with smart.servier.com.

The endocytic pathway involves two types of endosomes: early endosomes (EEs) and late endosomes (LEs). First, endocytic vesicles, produced by the plasma membrane, fuse within the cytoplasm forming EEs. EEs undergo acidification and mature to LEs (Huotari & Helenius, 2011; Hu *et al.*, 2015). An inward budding of the LEs generates intra-luminal vesicles (ILVs) and LEs are called multivesicular bodies (MVBs). The MVBs can pursue two different ways. First, fusion with lysosomes, acidic organelles, leads to their degradation. Moreover, MVBs may also fuse with the plasma membrane and release, in the extracellular space, the ILVs which are now referred as exosomes (Raposo & Stoorvogel, 2013; Zhang *et al.*, 2019).

Several mechanisms are implicated in the formation of MVBs. The most described is the one involving the ESCRT pathway (Colombo *et al.*, 2014). This machinery is composed of four different complexes, ESCRT-0, -I, -II and –III, associated with proteins such as ALIX, VTA1 and VPS34. The ESCRT-0 initiates the MVBs generation. This heterodimer, composed by the proteins Vps27 (vacuolar protein sorting) and HRS (HGF-regulated tyrosine kinase substrate) binds to ubiquitinated membrane proteins on the surface of the endosome and is responsible for ESCRT-I recruitment. The latter comprises four subunits: TSG101, Vps28, Vps37 and Mvb12. TSG101 and Vps28 are, respectively, responsible for ESCRT-0 and ESCRT-II binding. This interaction between ESCRT-I and -II induces the budding of the endosomal membrane. Then, they recruit ESCRT-III, which triggers membrane scission. Another complex is likewise required: Vps4 complex. Vps4, by hydrolyzing ATP, induces the dissociation and the recycling of ESCRT complexes (**Fig. I 14**) (Raiborg & Stenmark, 2009; Schmidt & Teis, 2012).

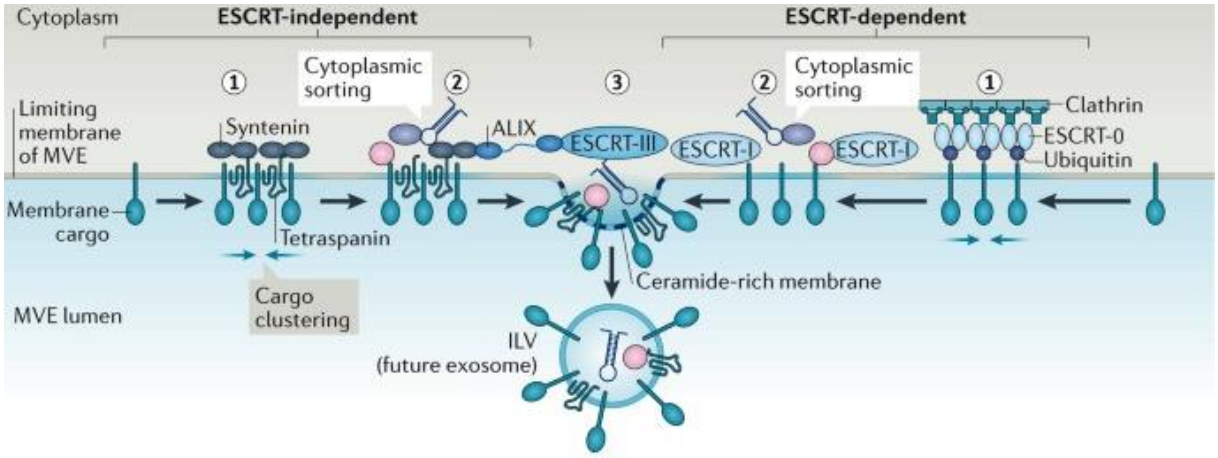

Figure I 14. ESCRT-dependent or –independent exosome sorting mechanisms.
Multiple pathways are efficient for exosome sorting. The most known requires the ESCRT machinery but ESCRT-independent mechanisms also occur. Figure adapted from Van Niel et al., 2018.

Another mechanism of ILVs formation implicating ALIX, an accessory protein of the ESCRT, has been described. It consists of the interaction between syndecan, syntenin and ALIX. Syndecans, molecules implicated in cell signaling, interact with their cytosolic adaptor, syntenin and recruits ALIX which leads to the budding of the endosomal membrane (Baietti *et al.*, 2012).

Studies suggest that exosomes can also be produced in an ESCRT-independent manner. It has been shown that protein composition is involved in the biogenesis of ILVs. Proteins such as tetraspanins, membrane proteins enriched in exosomes, were described to play a role in this

process. For instance, CD9 and CD63 downregulation reduce the amount of exosomes produced (Pettersen Hessvik & Llorente, 2018). Likewise, the lipid composition influences ILVs appearance. This ESCRT-independent process involves the formation of ceramides microdomains responsible for the membrane budding (Trajkovic *et al.*, 2008).

Once produced, MVBs fuse with the plasma membrane to release exosomes. This mechanism involves members of the Rab family and SNARE proteins (Bobrie *et al.*, 2011). For instance, it has been shown that Rab11, which plays typically a role in the endosomal recycling, could influence exosome secretion (Savina *et al.*, 2002). The fusion itself is coordinated by SNARE proteins. Nevertheless, the mechanism behind MVBs fusion remains not fully understood (Van Niel *et al.*, 2018).

3.1.3.2. Exosomes composition

The composition of exosomes depends on the content of the cell of origin. However, the nature and the amount of cargo molecules are generally influenced by the state of the secreting cell. Exosomes are composed by proteins, lipids and nucleic acids (**Fig. I 15)**. Two databases (ExoCarta and Vesiclepodia) list the nature of all lipids, proteins and RNA identified within exosomes. The current version of ExoCarta regroups 41,860 proteins, more than 9,000 RNA molecules and 1,116 lipids from several EVs studies (Keerthikumar *et al.*, 2016). Vesiclepodia comprises data obtained from more than one thousand studies and describe >300,000 proteins, >38,000 RNA and 639 metabolites (Pathan *et al.*, 2019).

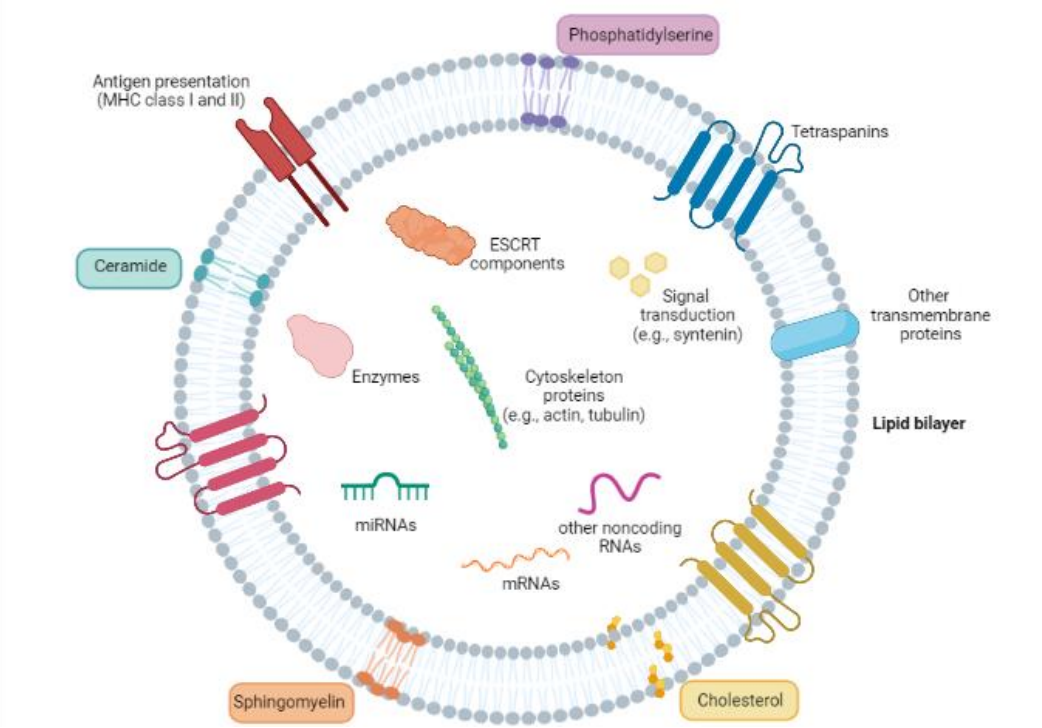

Figure I 15. Exosome composition.
Exosomes are composed of proteins, lipids and nucleic acids. Some proteins are found in all exosomes such as tetraspanins, ESCRT components, enzymes, signal transduction, etc. Exosomes are surrounded by a lipid bilayer enriched in various types of lipids: sphingomyelin, cholesterol, ceramide and phosphatidylserine. miRNAs (and other non-coding RNAs), DNA fragments and mRNAs can also be found within the exosomes. MHC: major histocompatibility complex. Figure created with BioRender.com.

3.1.3.2.1. Proteins

Proteins constitute the major part of the exosomes components. Some are specific to the donor cells but others depend on the physiological or pathological state of the cell. Nevertheless, no matter the cell type, some proteins are enriched in exosomes. Those particles are characterized by the presence of proteins implicated in the formation of MVBs (TSG101, ALIX), tetraspanins (CD9, CD63, CD81 and CD82), heat shock proteins (Hsp90, Hsc70) and other proteins such as GTPases, flotillin and annexins (Zhang *et al.*, 2019). Among those proteins, some are considered as exosomes markers. However, the presence of some exosomal markers are also reported in other types of extacellular vesicles. For instance, CD9 and CD63 are found on the surface of all extracellular vesicles while the other tetraspanin, CD81, is enriched in exosomes (Kowal *et al.*, 2016). Interestingly, protein markers from the nucleus, mitochondria, endoplasmic reticulum and the Golgi apparatus are generally absent within exosomes (Théry *et al.* , 2002). Nevertheless, a recent study highlighted a crosstalk between mitochondria and the endolysomal machinery. This inter-organelles communication implies that the presence of mitochondrial proteins in exosomes is, now, expected (Soto-Heredero *et al.*, 2017).

3.1.3.2.2. Lipids

The lipidic composition of exosomes reflects the membrane of the secreting cell (Théry *et al*., 2002). Nevertheless, regarding the lipid composition of the cell of origin, an enrichment of lipids such as glycosphingolipids, sphingomyelin, cholesterol and phosphatidylserine, was observed in exosomes (Llorente *et al.*, 2013). Interestingly, this exosomal enrichment is mainly due to the lipids parameters: their head group charge, length of the fatty acids and their lipidic saturation degree. These features can induce a curvature of the exosome membrane (Haraszti *et al.*, 2016). Furthermore, this specific composition presents similarities with lipid-rafts (LRs). For instance, these dynamic lipid microdomains are enriched in cholesterol, sphingolipids, as well as proteins involved in lipid-lipid or lipid-protein interactions. Among the lipids found in LRs, ceramides, by triggering the endosome membrane invagination, play an important role in the ILVs formation (Trajkovic *et al*., 2008; Skotland *et al*., 2017; Skryabin *et al.*, 2020). This may corroborate the implication of the lipid composition to the exosomes biogenesis. Likewise, exosomal lipids are also involved in the interactions with the recipient cell (Donoso-Quezada *et al*., 2021). The components of exosomes make them an excellent source of biomarkers. Indeed, a great amount of studies have highlighted nucleic acids and proteins as biomarkers. Although few studies demonstrated the potential role of lipids as biomarkers, they can induce changes in the recipient cells. For instance, it has been shown that sphingomyelinase, within the exosomes, catalyzes the conversion of sphingomyeline to ceramide and, therefore, induces cell growth in the recipient cell (Hsu *et al*., 2022).

3.1.3.2.3. Nucleic acids

The presence of genetic material in exosomes was first described by Valadi's team. They demonstrated that mRNAs were transferred to recipient cells and translated within them (Valadi *et al.*, 2007). Since this discovery, numerous studies have demonstrated that exosomes are capable of protecting nucleic acids from degradation and allow its transfer within the recipient cell to exert their biological properties.

i DNA

Only a handful of studies described the presence of DNA in extracellular vesicles. For instance, mitochondrial DNA (mtDNA) has been detected in exosomes. The packaging of mtDNA in exosomes and its horizontal transfer to cell induce the chemoresistance to endocrine therapy in breast cancer cells (Sansone *et al.*, 2017). Exosomes may also carry dsDNA that could be transferred within the recipient cell and modify its phenotype. Moreover, the dsDNA-

loaded EVs are also considered as biomarkers and, therefore, useful for the diagnosis of several diseases (Y. Wang *et al.*, 2019). Although ssDNA was also detected in small vesicles, the main part of exosomal DNA consists of dsDNA, but fragmented (Cai *et al.*, 2013; Kahlert *et al.*, 2014).

ii RNA

The most widely studied classes of molecules in exosomes are RNAs, especially miRNAs. Exosomal RNA reflects the physiological or pathological state of the producing cell but can also vary in terms of the RNA nature and concentration (O'Brien *et al.*, 2020). Exosomes carry a wide repertoire of coding and non-coding RNAs such as mRNAs, ribosomal RNAs (rRNAs), transfer RNAs (tRNAs), miRNAs, lncRNAs, and others (Kumar *et al.*, 2020). Interestingly, in rare cases, full-length mRNAs can be present. However, the majority of protein-coding RNAs is composed of fragments enriched in 3'-UTR regions (Batagov & Kurochkin, 2013). Those fragments are rich in miRNA complementary sequences and seem to be sorted in exosomes to reduce the effect of miRNAs by sequestering the sequence (Pérez-Boza *et al.*, 2018).

miRNAs are small non-coding RNAs implicated in the regulation of gene expression. By a base-pairing mechanism, miRNAs target complementary sequences within mRNAs leading to their repression. The functions, biogenesis and modes of action of miRNAs are described in the next chapter. MiRNAs are packaged in exosomes and transferred into recipient cells, where targets repression occurs. This horizontal transfer mechanism is quite studied in the case of cancer. For instance, macrophages produce miR-365-loaded exosomes which are incorporated in pancreatic cancer cells inducing the chemoresistance (Binenbaum *et al.*, 2018). Nevertheless, exosomes not only carry miRNAs but a wide range of small non-coding RNAs such as piwiRNAs, snRNAs, snoRNAs, yRNAs and vaultRNAs (Pérez-Boza *et al.*, 2018).

3.1.3.3. Exosomes transfer

Once released in the extracellular milieu, exosomes and their content will be incorporated in neighboring recipient cells, or transported in the circulation and taken up by distant recipient cells (**Fig. I 16**). However, the interaction between exosomes and cells is not fully unraveled. It seems that the specificity of the recipient cell is controlled by the interactions between proteins enriched on the exosomes surface and receptors at the plasma membrane. For instance, major histocompatibility complex class II-presenting exosomes released from dendritic cells can target, specifically, activated lymphocytes. The presence of the protein LFA-

1 on T cells was sufficient to promote the uptake of dendritic exosomes (Nolte-'t Hoen *et al.*, 2009). The exosome-recipient cell interaction is mainly due to mediators such as integrins, tetraspanins, lipids, proteoglycans and extracellular matrix components. For example, it has been shown that integrins present on the surface of tumor-derived exosomes can prepare the pre-metastatic niche. Moreover, the patterns of exosomal integrins can predict organ-specific metastasis formation (Hoshino *et al.*, 2015). Tetraspanins also play a role in the incorporation of exosomes within recipient cells. The association between those molecules and integrins contributes to the selection of the target cells (Rana *et al.*, 2012).

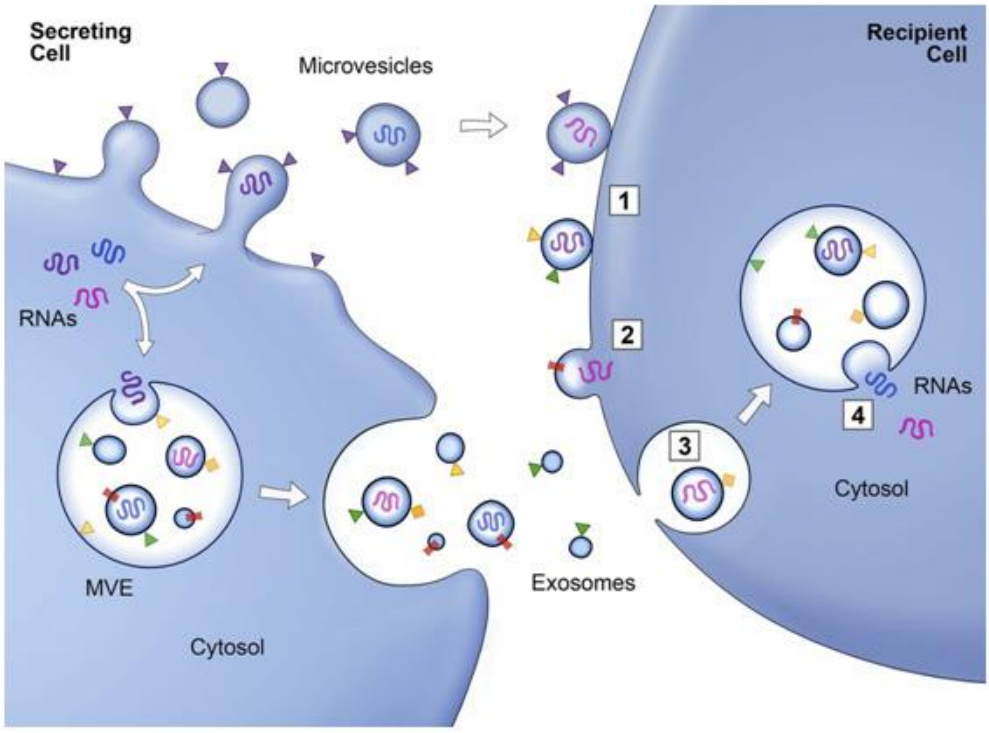

Figure I 16. Exosomes secretion and internalization by recipient cells.
EVs are released in the extracellular milieu by secreting cells through different sorting mechanisms. Once in the circulation, EVs can be internalized within recipient cells through several pathways: (1) Docking (2) Direct fusion (3) Endocytosis or (4) Endosomes integrates endosomal machinery. All mechanisms lead to the transfer of information (miRNA, proteins, lipids…) from a secreting to a recipient cell. Figure adapted from Raposo and Stoorvogel, 2013.

Once docked at the plasma membrane of the recipient cells, exosomes can follow different fates. The small vesicles can remain attached to the cell membrane and induce molecular changes in the target cell by a direct interaction. For instance, the expression of the tumor necrosis factor (TNF) on the surface of dendritic cells-derived exosomes leads to an activation of apoptosis in tumor cells. This activation is due to the interaction between the exosomal TNF and the cellular receptors of TNF on the target cell surface (Munich *et al.*, 2012). However, exosomes can also be internalized within the recipient cell. They can fuse with the

plasma membrane or be incorporated by several endocytic pathways (Raposo & Stoorvogel, 2013). The uptake of exosomes through phagocytosis is often used by phagocytic cells (Feng *et al.*, 2010). Macropinocytosis, an endocytic mechanism inducing the cell surface invagination, is also a common process for cellular incorporation of exosomes (Fitzner *et al.*, 2011). Several studies have described the internalization of exosomes through a clathrin-mediated endocytosis. For that purpose, a clathrin coating will be applied to the vesicles and they will undergo fusion with early endosomes (Tian *et al.*, 2014). The lipid composition of the recipient cell impacts the exosome uptake mechanism chosen by the cell. Indeed, the presence of lipid-rafts seem to influence the exosomes entry. Finally, the caveolin-dependent endocytosis contributes also to the internalization of exosomes (Svensson *et al.*, 2013; Delenclos *et al.*, 2017). Despite some cells use preferentially one mode to internalize exosomes, these different mechanisms co-exist and can be used concomitantly.

3.1.3.4. Exosomes in cancer

Their bioactive content and their presence in every biofluid make the exosomes major players in intercellular communication. Depending on the secreting cells, these nano-vesicles might promote or reduce the progression of many diseases, especially cancer. In malignancies, exosomes are also called oncosomes (**Fig. I 17**).

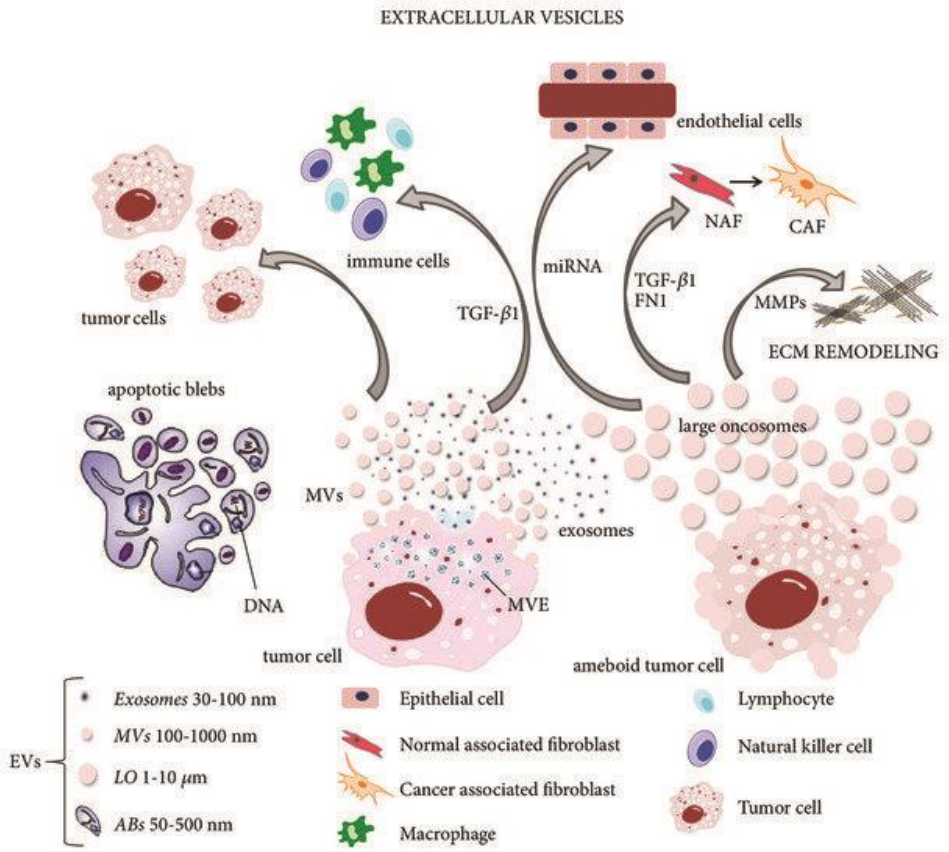

Figure I 17. EVs show multiple roles in cancer progression.
EVs are key actors of tumor growth. Indeed, these vesicles can either promote or reduce cancer progression by releasing their content within recipient cells. EVs are secreted by almost all cell types with the tumor microenvironment and can change the phenotype of other cells. Cancer cells are able to produce exosomes to favor their growth through the activation of endothelial cells, the inhibition of immune surveillance, etc. When tumor cells secrete EVs, they will be referred as oncosomes. On the other hand, TME cells have the ability to increase tumor growth of to curtail it. Figure adapted from Cufaro et al., 2019

3.1.3.4.1. Exosomes and the tumor microenvironment

As discussed previously, cancer cells are surrounded by other cells from the **tumor microenvironment**. Exosomes allow the transfer of molecules between cells within the tumor making them important actors in the TME. Cancer-associated fibroblasts are the principal components of TME (Zhao *et al.*, 2016). For instance, it has been shown that CAF-derived exosomes promote the progression of breast cancer by carrying the oncogene miR-92. The transfer of this miRNA to tumor cells increases tumor growth and suppresses the immune response (Dou *et al.*, 2020). The maintenance of cancer stem cells homeostasis can be regulated by exosomes. These little messengers induce the transformation of cancer cells to CSCs (Xu *et al.*, 2018). In liver carcinoma, CSCs-derived exosomes mediate the transfer of miR-19b promoting metastasis formation (L. Wang *et al.*, 2019). Exosomes seem to participate in

immune response, and, mainly, to immune evasion. TME is composed of different types of cells: macrophages, dendritic cells, lymphocytes and others. Tumor-derived exosomes (TDEs) suppress the differentiation and the maturation of DCs. This inhibition induces immunosuppression in the tumor-bearing host (Liu *et al.*, 2015). Within the tumor, TDEs may also induce apoptosis in activated cytotoxic T lymphocytes, and, therefore, reduce the immune response (Wieckowski *et al.*, 2009). Two categories of macrophages coexist: M1 and M2 macrophages. M2 cells induce angiogenesis and promote tumor growth. For example, through the transfer of miR-21 and miR-155, the exosomes derived from M2 macrophages increase colon cancer progression (Lan *et al.*, 2019).

Angiogenesis, by supplying oxygen and nutrition to cancer cells, is a crucial process required for cancer progression. The activation of endothelial cells is, therefore, necessary and can be controlled by exosomes. For instance, metastatic cancer cells released miR-210-loaded exosomes which are incorporated in endothelial cells enhancing angiogenesis (Kosaka *et al.*, 2013). Interestingly, CSCs produce exosomes expressing specific markers such as CD90. The incorporation of CD90+ vesicles within ECs stimulate tube formation and cell to cell adhesion (Conigliaro *et al.*, 2015). Retinoblastoma produced exosomes stimulating endothelial cells migration by the transfer of miR-92a (Chen *et al.*, 2021). However, exosomes can also decrease tumor growth by inhibiting angiogenesis (Ribeiro *et al.*, 2013). For instance, in head and neck cancer, mesenchymal stem cells can produce exosomes which elicit anti-angiogenic and anti-cancerous effects (Rosenberger *et al.*, 2019).

Metastasis formation appears also to be regulated by exosomes. The appearance of a pre-metastatic niche is required for the colonization of cancer cells in a specific organ. Hoshino et al., reported that exosomes presented features of integrins inducing the establishment of the niche in the specific organ (Hoshino *et al.*, 2015). Non-metastatic breast cancer cells might become metastatic when they incorporate miR-200-loaded exosomes released by non-metastatic cells (Le *et al.*, 2014). Nevertheless, it has been shown that exosomes derived from poorly metastatic melanoma cells may inhibit the formation of lung metastasis. These vesicles stimulate the production of monocytes which, at the end, will lead to the cancer cells destruction (Plebanek *et al.*, 2017).

3.1.3.4.2. Exosomes in drug resistance

Drug resistance constitutes a major obstacle in cancer therapy. Considering that exosomes participate in the regulation of cancer progression, scientists tried to elucidate their

roles in the chemoresistance (**Fig. I 18**). Several mechanisms are responsible for the acquisition of multidrug resistance (Szakács *et al.*, 2006). First, exosomes are implicated in the efflux of chemotherapeutic agents. For instance, the ovarian cancer cells used the secretion of exosomes to get rid of cisplatin (Safaei *et al.*, 2005). Then, exosomes are also responsible for the transfer of drug efflux pumps to sensitive cells. The best known molecule is P-glycoprotein (P-gp), encoded by *ABCB1*. Exosomes released by osteosarcoma or prostate cancer cells expressed P-gp at their surface. The internalization of those vesicles lead to the expression of the pump within the sensitive cancer cells and, therefore, to the acquisition of chemoresistance (Corcoran *et al.*, 2012; Torreggiani *et al.*, 2016). Finally, the last and also the most studied mechanism involve the transfer of cargo via exosomes. For instance, exosomal miR-210 derived from pancreatic CSCs resistant to gemcitabine increase the resistance of sensitive cancerous cells (Zhiyong Yang, Zhao, *et al.*, 2020). In the same way, ER-positive BC cells may acquire tamoxifen resistance through the transmission of miR-221/222 (Wei *et al.*, 2014). On the other hand, exosomes can also resensitize resistant cells. Recently our lab has demonstrated that upon epirubicin treatment, endothelial cells produced exosomes with higher levels of miR-503. Through its anti-tumor properties, miR-503 would act as a tumor-suppressor in TNBC cells (Bovy *et al.*, 2015). Likewise, miR-128-loaded exosomes enhance the sensitivity to oxaliplatin of colon cancer cells (Liu *et al.*, 2019).

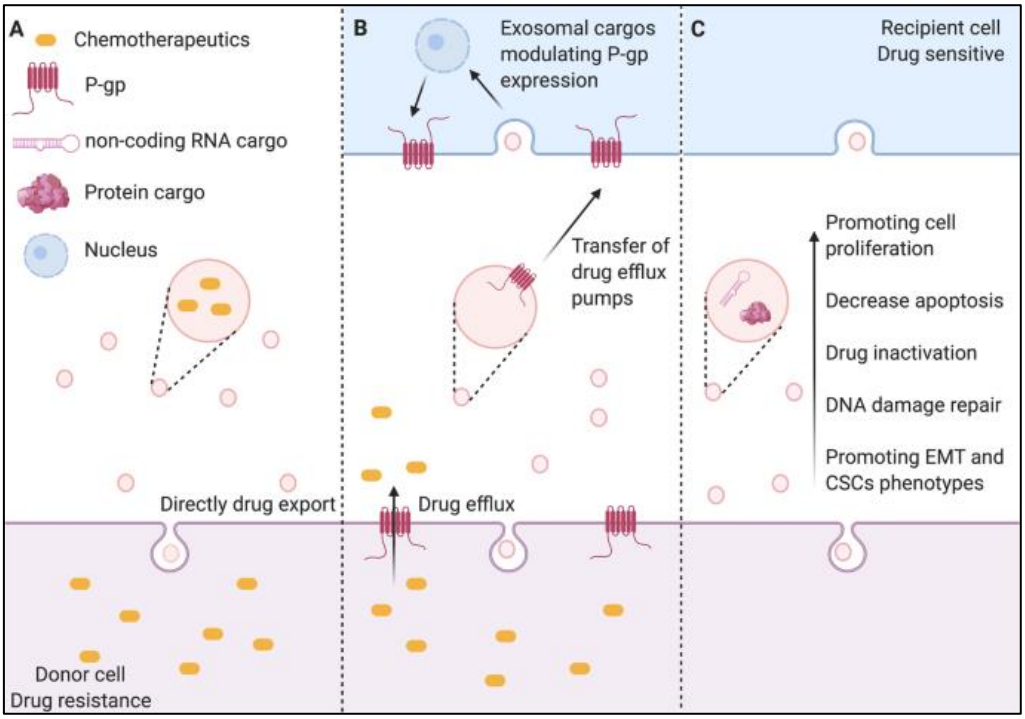

Figure I 18. EVs are involved in the acquisition of drug resistance in breast cancer.
*(A) Chemotherapeutic agents can be directy secreted by the donor cells and confer drug resistance to other cells. (**B**) Drug efflux pumps (such as P-gp) might also be transferred to recipient cells to induce resistance phenomenon. (**C**) The last mechanism involved the transfer of bioactive molecules such as nucleic acids (e.g., miRNAs) or proteins which will promote proliferation, reduce apoptosis, and multiple other pathways within recipient cells. Figure adapted from Dong et al., 2020.*

3.1.3.4.3. Exosomes as therapeutic tools

Currently, scientists are also studying exosomes for their potential in cancer therapy. The main application is to use these vesicles as vehicles for bioactive molecules (Kalluri & LeBleu, 2020). Interestingly, exosomes can be engineered to express and deliver specific molecules. For instance, Sterzenbach and colleagues demonstrated that the ubiquitination of Cre recombinase induces its loading within the MVBs and allows its transfer across the blood-brain barrier (Sterzenbach *et al.*, 2017). To reduce cell toxicity, exosomes could also be used for drug delivery. For instance, doxorubicin, a cardiotoxic chemotherapeutic agent, can be encapsulated in EVs and then incorporated in recipient cells (Schindler *et al.*, 2019). Many scientists are interested in the loading of non-coding RNAs in exosomes. For instance, the siRNA targeting the oncogene *KRAS* has been loaded in fibroblast-derived exosomes, delivered to pancreatic cancer and, therefore, inhibits cancer progression (Kamerkar *et al.*, 2017). Non coding RNAs and especially microRNAs are bioactive molecules often used for cancer therapy. The implications of miRNAs are described in the next chapter.

3.1.3.4.4. Exosomes in diagnosis

Exosomes are secreted by virtually every cell type and are present in all biological fluids. Moreover, they are highly stable, may be detected by a non-invasive method and carry bioactive cargo molecules. All of these characteristics make exosomes attractive for cancer diagnosis as biomarkers. In breast cancer diagnosis, cargo proteins are considered as good candidates. For instance, exosomes containing survivin, a protein inhibiting apoptosis, may offer a chance to detect early stages of breast cancer (Khan *et al.*, 2014). Several studies have demonstrated that the exosomal miRNAs act as biomarkers. Glioblastoma patients produce exosomes expressing higher levels of a seven miRNAs pattern compared to healthy patients (Ebrahimkhani *et al.*, 2018). Exosomal miRNAs secreted in bronchoalveolar lavage can serve for the detection of lung cancer (Kim *et al.*, 2018). These vesicles are also used to measure the treatment efficiency. Osteosarcoma patients associated with poor response to chemotherapy, for instance, presented various levels of specific miRNAs compared to those who respond to the chemotherapeutic agent (J. F. Xu *et al.*, 2017). Plasma is an excellent source of exosomal biomarkers. In colorectal cancer, it has been shown that plasmatic miR-125b-loaded exosomes could predict the acquisition of chemoresistance (Yagi *et al.*, 2019).

4. miRNAs

MicroRNAs (miRNAs) are small non-coding RNAs of ~22 nucleotides that have emerged to play a major role in numerous biological processes. miRNAs regulate genes expression by binding specifically to complementary regions of their target messenger RNAs (mRNAs) transcripts leading to their degradation or the inhibition of their translation. However, under specific conditions, miRNAs can lead to a posttranscriptional upregulation of their target genes.

In 1993, Lee et al. discovered a small non-coding RNA in the nematode *Caenorhabditis elegans* (*C.elegans*) that was able to regulate the expression of a specific mRNA. The miRNAs discovery revolutionized the molecular biology field (Lee et al. 1993). Even tough, non-coding regions were considered as "junk DNA, 98.5% of human genome consists of non-protein-coding DNA sequences. There are at least 2000 miRNAs that play important roles in the regulation of biological pathways. In mammals, MiRNAs are predicted to modulate the expression of ~50% of mRNAs, and have been described to participate in almost all physiological processes, but also in diseases. Depending on their location, abundancy and the affinity to mRNA targets, miRNAs can play various cellular roles. Some are secreted in biofluids or incorporated in extracellular vesicles. Nevertheless, since the structure and the biogenesis of miRNAs are distinct in animals, plants and viruses, we will focus only on animal's miRNAs in this work (Vasudevan, 2012; Boland, 2017; O'brien *et al.*, 2018; Dexheimer & Cochella, 2020).

4.1. Nomenclature

Essentially, miRNAs nomenclature includes several elements:

- The prefix designates the organism. For instance, *hsa* for humans, *mmu* for mice and *cel* for *C.elegans*.
- The terms *miR* or *mir* are given depending on the sequences. *miR* is used for the mature sequence whilst the hairpin precursor form is recorded *mir*.
- The number of miRNAs is allocated sequentially following their discovery (miR-503, miR-16). Furthermore, the same identifier is given for homologous sequences in different species (hsa-miR-503 and mmu-miR-503).
- The suffix -3p or -5p is added for sequences derived from the 3' or 5' arms of the hairpin precursor.

A letter suffix is assigned to miRNAs which are part of the same family, but present differences in their sequences, such as hsa-miR-148a and has-miR-148b.

An additional numerical suffix can be added to paralogous sequences, when the hairpin loci is different but the mature sequences are identical, such as hsa-miR-103a-1 and hsa-miR-103a-2.

Previously, miRNAs received another denomination. An asterisk mark was assigned to the passenger arm; the non-expressed sequence; while the guide sequence wasn't tagged, as in miR-100* and miR-100. However, it has been shown that mature sequences derived from both strands are biologically functional, thus, miRNAs were wrongly annotated and the -3p or -5p suffix has been adopted (Griffiths-Jones *et al.*, 2006, 2008; Kozomara & Griffiths-Jones, 2011, 2014).

4.2. Biogenesis

The biogenesis of miRNAs is a canonical process, including 5 compartmentalized steps (**Fig. I 19**).

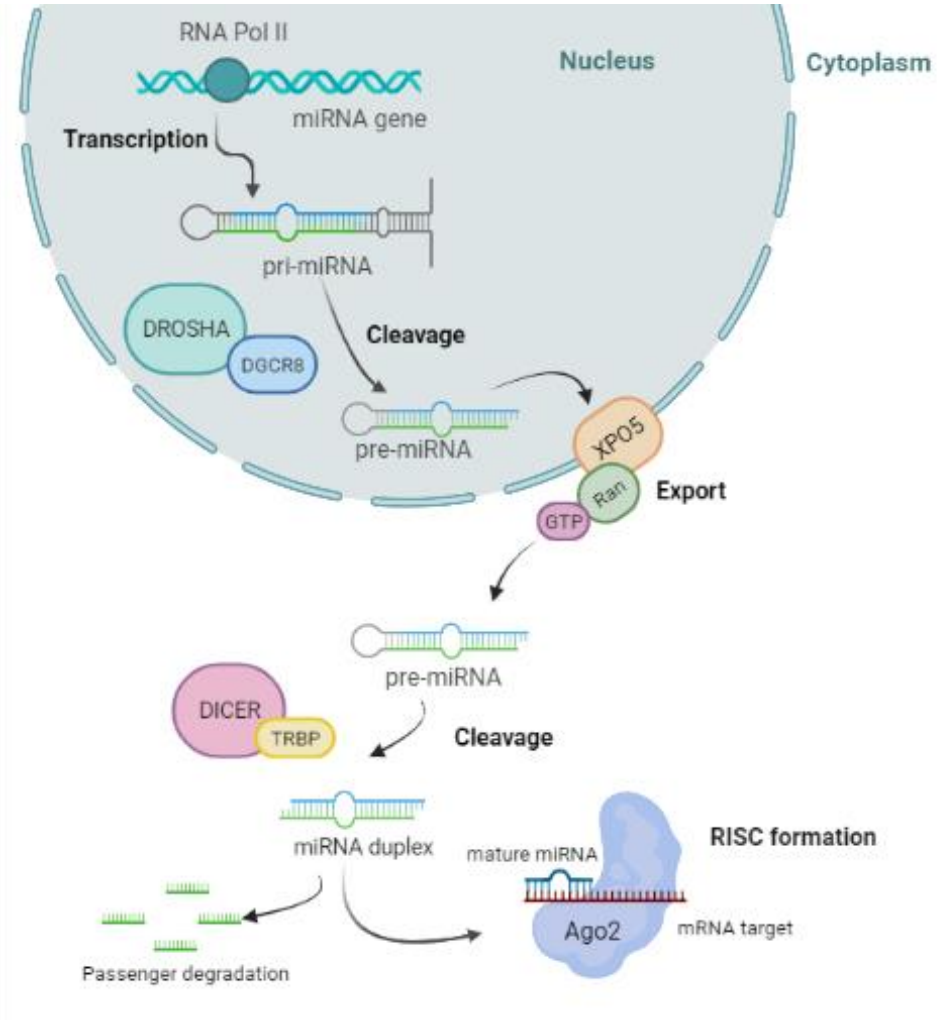

Figure I 19. miRNA biogenesis.
Transcription of miRNA genes is assured by RNA polymerase II (RNA Pol II) and produces a primary transcript (pri-miRNA). This pri-miRNA is then cleaved by the microprocessor complex (Drosha and its cofactor DGCR8) and exported in the cytoplasm trough the action of the exportin 5 (XPO5) and a Ran-GTPase. Once in the cytosol, the precursor miRNA (pre-miRNA) undergoes another round of cleavage by the enzyme Dicer and its cofactor TRBP which generates the miRNA duplex. One strand will be degraded and the other will be loaded onto Ago protein (Ago2) to produce RISC complex which allows target recognition. Figure created with Biorender.com.

4.2.1. Transcription

MiRNAs transcription is carried out by RNA polymerase II (RNA Pol II), however, some miRNAs can be transcribed by RNA Pol III. 30% of miRNA loci are processed from intronic regions of protein-coding genes but only few in exonic regions. Other miRNAs genes are located into intergenic regions or in antisense orientation and, thus, are regulated by their own promotor and can be transcribed independently of the protein-coding genes (Lee *et al.*, 2004). When miRNAs loci are located at short distance, they form a cluster and are transcribed together. Nevertheless, those miRNAs may have variable expression. The transcripts, usually longer than 1kb, are named primary miRNAs (pri-miRNAs). Those precursors are capped in

their 5' extremity with a 7-methyl guanylate motif (m7G) and possess a poly-adenylated tail in 3'. Pri-miRNAs generally consist of a stem-loop structure of 33-35bp, a terminal loop and single-stranded RNA (ssRNA) extensions at both extremities. The same mechanism governs both miRNAs and protein-coding genes transcription even if particular transcription factors are involved (Macfarlane & Murphy, 2010; Ha & Kim, 2014; Kabekkodu *et al.*, 2018).

4.2.2. Nuclear cleavage

Freshly transcribed, the pri-miRNA undergoes a maturation process. This process begins in the nucleus where the Microprocessor complex, formed by the RNAse III Drosha and its cofactor, DGCR8 (DiGeorge syndrome Critical Region gene 8), governs its cleavage. Upon binding of pri-miRNAs, DGCR8; also known as Pasha in *D.melanogaster*) trimerizes and form a protein-pri-miRNA complex that determines the cleavage site. Drosha manages the degradation of the hairpin precursor at both 3' and 5' arms, 22 bases away from the junction linked to the terminal loop and 11 bp from the bon between the ssRNA and double-stranded RNA (dsRNA). This mechanism releases another hairpin precursor of about ~60 nt called pre-miRNA (Denli *et al.*, 2004; Ha & Kim, 2014; Cammaerts *et al.*, 2015; Bartel, 2018).

4.2.3. Nuclear export

The following steps of pre-miRNAs maturation occur in the cytoplasm. Therefore, nuclear export of those precursors represents a critical step in miRNAs biogenesis. Once generated, pre-miRNAs are exported through the action of the nucleocytoplasmic factor Exportin-5 (XPO5) and its cofactor Ran (RAs-related Nuclear protein), essential for the export of RNA and proteins. XPO5 pinpoints dsRNA regions of ~17 nt with a short 3' extension and, in this way, only well processed pre-miRNAs are correctly exported. Finally, in the cytoplasmic compartment, Ran hydrolyzes GTP and the pre-miRNAs are liberated (Yi *et al.*, 2003; Bohnsack, Czaplinski & Görlich, 2004; Lund *et al.*, 2004).

4.2.4. Cytoplasmic processing

Once in the cytoplasm, the pre-miRNA pursues a second step of cleavage by the class III ribonuclease Dicer. The enzyme binds to the end of the precursor and leads to the cleavage of the terminal loop resulting in a short (~22nt) miRNA duplex with 2 nucleotides overhangs at each 3' extremities. Dicer comprises two catalytic RNAse III domains in C-terminal, responsible of the pre-miRNA cleavage, a N-terminal helicase domain that interact with the pre-miRNA terminal loop, increasing its processing, and the PAZ (PIWI-AGO-ZWILLE)

domain, which binds to the pre-miRNA 3' and 5' ends. Dicer interacts with two cofactors: PACT (Protein Activator of PKR) and TRBP (Tar RNA Binding Protein). Even if these double-stranded RNA binding cofactors enlarge Dicer activity, they do not seem essential for the pre-miRNAs maturation efficiency. Nevertheless, it has been shown that TRBP increases the stability of Dicer (Winter *et al.*, 2009; Lin & Gregory, 2015; Matsuyama & Suzuki, 2020).

4.2.5. RNA-induced silencing complex formation (RISC)

To degrade mRNA targets, the miRNA duplex produced by Dicer is afterwards loaded onto an Argonaute (AGO) protein forming the effector complex, RISC. This multiprotein complex is responsible for the RNA interference mediated by miRNAs. The RISC-Loading Complex (RLC), composed of Dicer and its cofactor TRBP (and/or PACT) allows the loading on AGO, usually Ago2. This ATP-dependent process requires the assistance of the chaperones proteins HSC70/HSP90. Thenceforth, the miRNA duplex comprises the guide strand, also called the mature miRNA, and its opposite sequence, the passenger strand. The thermodynamic stability of the 5' ends of both strands determines which strand will accumulate as mature miRNA. Thenceforth, the less stable strand in 5' is selected and the passenger is evicted and degraded by the AGO2. Nevertheless, other Ago proteins do not seem to present an endonuclease activity, another protein such as an RNA helicase mediates to slicing of the passenger strand. Another miRNA duplex characteristic may be chosen to identify the guide strand. Indeed, Ago proteins select the strand presenting a uridine (U) at the first position. Subsequently to the loading, Dicer is removed from the RISC and the miRNA-AGO complex interacts with the complementary mRNA targets and the mature RISC is formed (Khvorova *et al.*, 2003; Ha & Kim, 2014; Nakanishi, 2016).

4.2.6. Non-canonical pathways of miRNAs biogenesis

While the majority of miRNAs are generated by the canonical pathway, previously discussed, a sizeable amount of miRNAs is also produced by non-canonical pathways. Those non-conventional processes involve different combinations of the proteins involved in the canonical pathway such as Drosha, XPO5, Dicer and AGO2. There are two main pathways: Drosha/DGCR8-independent and Dicer-independent. For instance, (m^7G)-capped pre-miRNAs and mirtrons, pre-miRNAs originated from introns of mRNAs during splicing, are released in a Drosha/DGCR8-independent manner. The lacking of one helical turn, required for Drosha slicing, these pre-miRNAs are directly exported to the cytoplasm via exportin 1 and without any cleavage by Drosha and then pursue the canonical way. On the other hand, small hairpin

RNAs (shRNAs) biogenesis requires a Dicer-independent pathway. ShRNAs transcripts are cleaved by the Microprocessor complex but are loaded on AGO2 to continue their maturation (O'brien *et al.*, 2018; Salim *et al.*, 2022).

4.3. Mechanisms of action

4.3.1. Argonaute proteins

As discussed previously, miRNAs act as components of ribonucleoproteins (RNPs) complexes or RISCs, also called micro-ribonucleoproteins (miRNPs) or miRNA-induced silencing complexes (miRISCs), respectively. The most characterized components of miRNPs are Argonaute proteins. Among eukaryotes, Argonaute are highly conserved proteins playing major roles in many different RNA silencing pathways (**Fig. I 20**). This family is separated into two subfamilies: Ago and Piwi. The Piwi subfamily binds to piwiRNAs and is restricted to germ cells while Ago proteins are ubiquitous and bind to miRNAs and siRNAs. The number of Ago differs between species. For instance, in humans, four Ago proteins are listed: hsAgo1-4. These proteins are composed of four domains: N-terminal (N), PIWI-AGO-Zwille (PAZ), middle (MID) and PIWI domains. Two linkers are also present: L1 and L2 linkers. L1 allows the direct interaction between the N and PAZ domains while the L2 linker strengthens the N-L1-PAZ bond and connects it with the MID-PIWI part. Due to its basic characteristics, the MID domain binds the 5' phosphate end of the guide miRNA. The 2 nt 3' end is anchored at the PAZ domain. The PIMI domain contains the endonucleolytic capacity which is responsible for target mRNAs slicing. Interestingly, PIWI domain folds similar to RNAse H. In humans, only hsAgo2 presents this endonuclease activity that is able to cleave complementary mRNA targets via its catalytic triad: two aspartates D(597)-D(669) and one histidine H(807). Interestingly, the identical catalytic triad is also found in hsAgo3 even though it is catalytically inactive. Nevertheless, every Ago protein is able to initiate target mRNAs degradation and repression of their translation (Peters & Meister, 2007; Nakanishi, 2016; Wilson & Doudna, 2018; Iwakawa & Tomari, 2022).

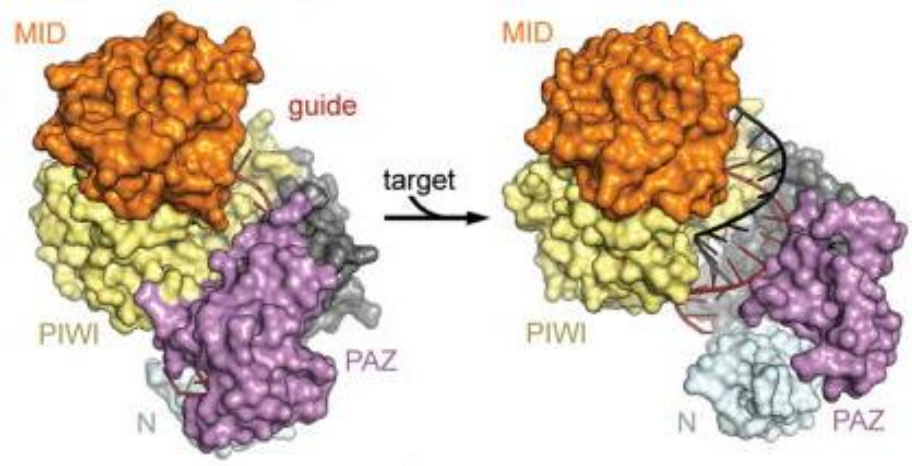

Figure I 20. Crystal structure of Ago protein in interaction with a guide miRNA.
The PAZ and the N-terminal domains interacts with the 3' extremity of the miRNA, whereas the 5' end is linked to the MID domain. The PIWI domain contains the catalytic activity of Ago protein. When the miRNA binds to its mRNA target, it induces a conformation switch. The PAZ domain releases the 3' extremity of the miRNA and Ago present a more open configuration. Figure adapted from Wilson & Doudna, 2013.

4.3.2. Ago cofactor, GW182, and P-Bodies

Because Ago proteins are not sufficient to promote silencing by their own, interactions of other proteins are required. Among the cofactors of Ago proteins, GW182 (glycine-tryptophan protein of 182 kDa) is required for RISC-mediated silencing. Its glycine and tryptophan repetitions enable the interaction between this cofactor and Ago. The C-terminal domain of the protein interacts directly with mRNAs and induces, together with the MID domain, mRNA decay. Interestingly, the affinity of GW182 for guide miRNA-loaded Ago is increased in comparison with unloaded Ago proteins. GW182 and Ago proteins localize in the Processing bodies (P-bodies). P-bodies are cytoplasmic foci where mRNA turnover (degradation and repression processes) occurs. Those sites contain a multitude of RNPs and enzymes involved in mRNA deadenylation, decapping and translational repression. Furthermore, the activity of the effector complex, RISC, and P-bodies are closely related. Verily, the inhibition of miRNA biogenesis inhibits P-bodies generation (Behm-Ansmant *et al.*, 2006; Macfarlane & Murphy, 2010; Nakanishi, 2016; Niaz & Hussain, 2018).

4.3.3. Target mRNAs recognition

The recognition of specific target mRNAs by miRNAs relies on the rules of base-pairing discovered by Watson & Crick. miRNAs share complementary with a protein-coding transcript. The pairing occurs between the 3'-UTR (Untranslated Region) of the mRNA and a specific region in the 5' of the guide miRNA. The latter is called seed region (**Fig. I 21**). Seed-matched site is composed of seven nucleotides which include nucleotides 2-8 (Bartel, 2009). This

particular sequence may be conserved between miRNAs and determines families of paralog miRNAs. One miRNA can target a large spectrum of mRNAs, but, a mRNA can also be regulated by many miRNAs. The degree of complementary of miRNA-mRNA duplex establishes the gene silencing mechanism. For instance, mRNA cleavage by Ago2 is broadly chosen when the pairing is almost perfect whereas the translation repression is favored by moderate base-pairing. Moreover, the multitude of miRNA-targets interactions show that miRNAs possess a huge regulatory power (Ambros, 2004; Macfarlane & Murphy, 2010).

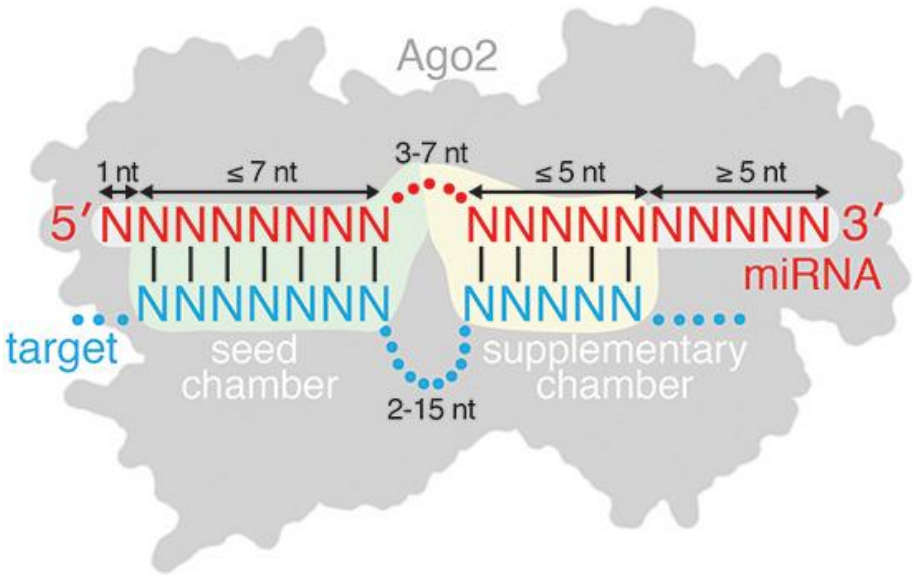

Figure I 21. Schematic representation of the interaction between a miRNA and its mRNA target through the seed sequence.
The seed sequence comprises the nucleotides 2-8 from the 5' extremity of the miRNA. This sequence represents the crucial step for target recognition. The supplementary region, at the 3' end, might increase the interaction between the seed region and the target. Figure adapted from Sheu-Gruttadauria et al., 2019.

4.3.4. mRNAs endonucleolytic cleavage

The miRNA-mediated target cleavage can be induced by Ago2 and its cofactor, GW182. This miRNAs-mediated silencing mechanism requires a fully complementary mRNA. This process is often happening in plants. In animals, however, the majority of targets are partially complementary therefore another miRNA-silencing process is often chosen: the target translation repression (Bartel, 2009; Huntzinger & Izaurralde, 2011).

4.3.5. Translation inhibition and mRNA decay

Considering that the vast majority of the miRNA-mRNA interactions are not perfectly complementary, the target undergoes a translational repression that can occur at every stage: post-initiation, initiation, elongation and termination (**Fig. I 22**). Ago is able to bind the 5' cap

of mRNAs and, therefore, prevents the binding of translation initiation factors such as eIF4F. It has also been shown that RISC can promote ribosome disassembly by interacting with another factor, eIF4G leaving the translation incomplete (Filipowicz *et al.*, 2008). Another miRNA-mediated silencing mechanism seems to prevail the others: the target degradation or mRNA decay (Huntzinger & Izaurralde, 2011). MiRNAs can also induce mRNA destabilization by a deadenylation process through the protein GW182. The latter recruits two deadenylase complexes, CCR4-NOT and PAN2-PAN3 complexes. MiRNA-mediated mRNA decay can also involve the poly(A)-binding proteins (PABPs). Indeed, it has been reported that miRNA induces the dissociation of PABP before deadenylation begins. Consequently, deadenylation and dissociation of PABP promote a translational repression and afterwards, mRNA decay. Once deadenylated, miRNAs induce target degradation. Indeed, RISC recruits decapping factors such as the DCP1:DCP2 complex. DCP2 possesses the catalytic activity while DCP1 activates the latter. By removing the tail and the cap, miRNAs enable the mRNA digestion by exonucleases at both extremities (Orang *et al.*, 2014; Iwakawa & Tomari, 2015).

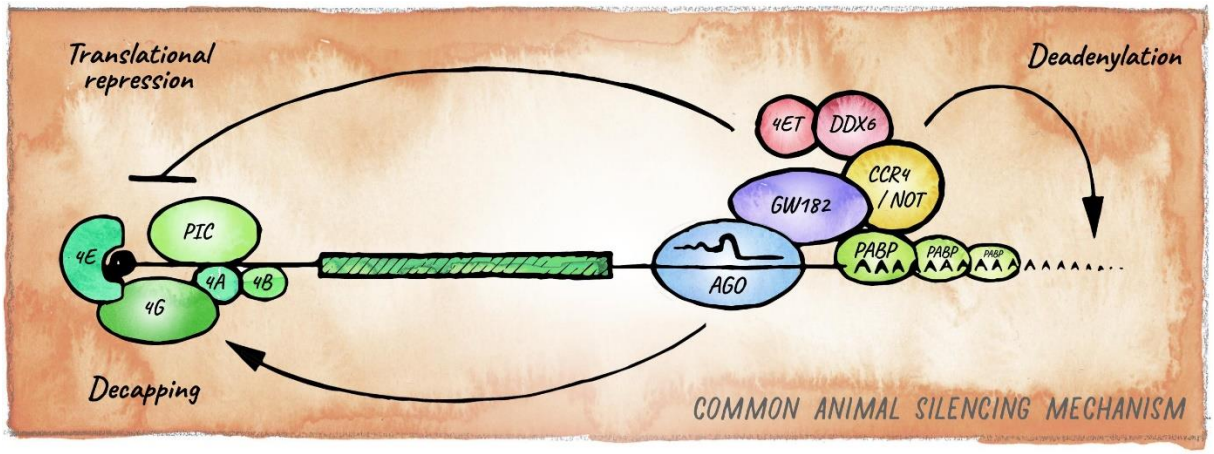

Figure I 22. Mechanisms of action of miRNA silencing in animals
miRNAs modulate gene expression through various pathways. Generally, miRNAs repress target genes through translational repression and promotion of mRNA decay. To degrade its mRNA targets, the miRNA is anchored within the RISC complex composed by Ago protein (usually, Ago2) and its cofactor GW182. This cofactor can interact with PABP, recruits CCR4-NOT which leads to targets deadenylation, decapping or cleavage. The translational repression is mostly linked to the binding of Ago2 to the 5' end of the mRNA which prevents the binding of translation initiation factors such as eIF4F and, therefore, represses target translation. Figure adapted from Dexheimer & Cochella,2020.

4.3.6. Translation induction

Interestingly, under specific conditions, miRNAs can also act as translation activators. For instance, miR-16 up-regulates the expression of Myt1 mRNA in oocytes from xenopus (Mortensen *et al.*, 2011). Vasudevan and colleagues demonstrated that, under serum starvation, the miRNA miR-369-3 recruits Ago2 which induces the activation of translation (Vasudevan,

Tong & Steitz, 2007). Nevertheless, switches between posttranscriptional upregulation and downregulation by miRNAs remains unclear (Vasudevan, 2012).

4.3.7. Regulation of miRNA activity and biogenesis

The fact that miRNAs regulate the expression of their mRNA targets is well established. However, miRNA expression is also regulated by several factors. Modifications of miRNAs occur and may affect their activity and biogenesis. For instance, single nucleotide polymorphisms (SNPs) in genes encoding miRNAs can modulate their processing. The generation of pri-miRNAs can also be affected by epigenetic modifications such as methylation. Moreover, RNA-binding proteins (RBPs) may also impede their processing. And, finally, miRNA editing. This mechanism refers to alternations in the sequence of miRNAs and is characterized by nucleotide modifications by, mainly, two families of deaminases: adenosine deaminases acting on RNA (ADARs) and cytidine deaminases from the activation induced cytidine deaminases/apolipoprotein B mRNA editing enzyme cytidine deaminases (AID/APOBEC). ADARs lead to the deamination of adenosine (A) to inosine (I) while AID/APOBEC is responsible for the editing cytidine (C)-to-U. miRNA editing plays an important role in miRNA regulation and function. Indeed, it has been shown that editing processes can alter miRNA maturation. Furthermore, interactions between miRNAs and mRNA or competing endogenous RNAs (ceRNAs) can be affected by these RNA modifications. MiRNA editing process is a specific mechanism producing various miRNAs under specific conditions. This may provide new biomarkers and create a great interest in the understanding of several pathologies such as cancer (Pasquinelli, 2012; L. Li *et al.*, 2018; Correia De Sousa *et al.*, 2019).

4.4. MiRNAs in cancer

MiRNAs mediate several biological processes such as proliferation, migration, differentiations, etc. As a consequence, they play important roles in multiple diseases such as cancer. They can act as tumor suppressors or oncogenes, respectively, if they help to decrease or increase tumor growth. Oncogenes miRNAs are also called oncogenic miRNAs (oncomiRs). However, depending on the cell type and the abundancy of its targets, the same miRNA can act as an oncomiR or a tumor suppressor (Svoronos *et al.*, 2016). The involvement of miRNAs in cancer was first described in the context of chronic lymphocytic leukaemia. Indeed, two miRNAs genes, miR-15a and miR-16-1 were downregulated in patients presenting this pathology. Interestingly, those non-coding RNAs were responsible for the inhibition of B-cell

lymphoma 2 (Bcl-2), an apoptosis inhibitor (Reddy, 2015). MiRNAs are also considered for their potential as therapeutic tools and biomarkers for several diseases, especially for cancer. Here are a few examples of miRNAs implications in the hallmarks of cancer.

The dysregulation of miRNA expression in cancer cells can partly be ascribed to the amplification, deletion or translocation of miRNA genes. For instance, in lung cancer, the cluster comprising two tumor suppressor miRNAs, miR-143 and miR-145, is frequently deleted (Das and Pillai, 2015). Alterations of transcription factors may also affect the miRNAs abundancy. For example, c-Myc, a transcription factor often increased in multiple malignancies, induces the expression of the oncogenic miR-17-92 cluster. Another example is the implication of p53, a tumor suppressor, on miR-34 expression. Indeed, miR-34 levels are upregulated upon p53 action and, therefore, reducing apoptosis (Peng & Croce, 2016). Finally, defects in some of the elements required for miRNAs biogenesis can induce abnormal miRNA expression and, consequently, promote tumor appearance. For instance, in Wilms cancers, SNPs in genes coding for DGCR8 and Drosha induce the repression of two mesenchymal-to-epithelial transition (MET) regulators, let-7a and miR-200 (Walz *et al.*, 2015). Likewise, Dicer is often dysregulated in the majority of tumors. Effectively, Dicer downregulation promotes several pathways implicated in cancer progression such as cell proliferation and metastasis generation (Iliou *et al.*, 2014). Finally, miRNA expression can be affected by sponges. Those RNA molecules, also called miRNA sponges, are competitive inhibitors of miRNA. Sponges can be long non-coding RNAs (lncRNAs), circular RNAs (circRNAs), pseudogenes or even mRNAs. For instance, the lncRNA SNHG7 induce cancer progression through its binding to cyclin D1 by sponging miR-503 (Qi *et al.*, 2018). Moreover, circNRIP1 inhibits the action of miR-149-5p by affecting the expression of AKT1 (Zhang *et al.*, 2019).

4.4.1. Implications of miRNAs in drug resistance

Since miRNAs are key regulators of cancer progression, their potential role in resistance to anti-cancer therapies have been studied. Actually, many miRNAs are dysregulated in drug-resistant cells and promote cancer development. The up-regulation of oncogenic miRNAs is often correlated with the appearance of drug resistance. For instance, miR-21 can induce doxorubicin resistance in breast cancer cells by the downregulation of PTEN (Si *et al.*, 2019). The overexpression of miR-155 in adriamycin-resistant cells induces MET (Yu *et al.*, 2015). In MDA-MB-231 cell line, overexpression of miR-34a enhances chemoresistance to docetaxel through Bcl-2 and cyclin D1 inhibition (Kastl *et al.*, 2012). On the other hand, in resistant cancers, some tumor suppressors miRNAs are downregulated and their overexpression can

restore the tumor response to multiple drugs. For instance, mir-519 and miR-503 repress the expression of Bcl-2, hence restoring chemosensitivity in glioblastoma cells and in non-small cell lung cancer cells, respectively (Qiu *et al.*, 2013; Li *et al.*, 2018).

4.4.2. MiRNAs as therapeutic tools

Since miRNAs are implicated in physiological and pathological processes, a huge interest has emerged between researchers to study their capacities as therapeutic agents. In 2020, miRNA-based therapeutics counted thousands of patents delivered in the US and in Europe and constitutes a notable business segment (Chakraborty *et al.*, 2021). In miRNA therapeutics, the first strategy is to increase the levels of an anti-tumor miRNA. For instance, a phase I trial demonstrated the efficiency and safety of MRX34 treatment in patients with solid tumors. MRX34 is miR-34a mimic delivered in a liposomal particle. Since in many patients, miR-34a is downregulated, the aim of this miRNA mimic therapy is to enhance the levels of this tumor suppressor involved in resistance and metastasis formation (Beg *et al.*, 2017). On the other hand, oncogenic miRNAs can be repressed by using miRNA antagonists such as locked-nucleic acids (LNA). For instance, the repression of miR-21 by the LNA anti-miR-21 inhibits the progression of colorectal cancer (Nedaeinia *et al.*, 2016). However, major obstacles in RNA therapeutics are described. First, for an efficient delivery of miRNA to cells miRNAs degradation needs to be avoided, or at least, reduced. Moreover, RNA requires the crossing of the lipid bilayer. For that purpose, miRNA can be encapsulated in lipid carriers such as extracellular vesicles or liposomes. Nevertheless, other hurdles have to be considered such as the off-target effects, the activation of immune nucleic acids sensors and the dose accuracy (Lieberman, 2018; Damase *et al.*, 2021).

4.4.3. MiRNAs as biomarkers

MiRNAs are produced by all cell types under physiological and pathological conditions. However, since they also can be secreted into biofluids, miRNAs are studied as novel biomarkers for several diseases, including cancer. miRNAs present many features of ideal biomarkers: efficient, specific, robust, non-invasive and sensitive (Faruq & Vecchione, 2015). Aberrant expression of miRNAs is described in multiple cancer types. Among the dysregulated miRNAs, some may provide information on cancer stages and discriminate the benign and the malignant lesions. For instance, the levels of miR-21 were up regulated in serum from B-cell lymphoma patients compared to healthy patients (Li *et al.*, 2015). In breast cancer, patients with

a metastatic stage present higher levels of miR-21 and miR-494. This specific miRNA pattern is associated with a poor prognosis (Marino *et al.*, 2014).

4.4.3.1. Circulating miRNAs

Considering the presence of RNase in circulation, the existence of extracellular miRNAs was unexpected. As mentioned previously, miRNAs can be released in the extracellular milieu of almost all biofluids. Despite ribonuclease activity, extracellular miRNAs appear highly stable indicating that they are packed to prevent degradation. Indeed, there are two types of circulating miRNAs, vesicle-associated and non-vesicle-associated (Cui *et al.*, 2019). Nevertheless, the majority of circulating miRNAs is associated with ribonucleoprotein complexes. Among those proteins, the endonucleolytic protein Ago2 was described to transport miRNAs. For example, Ago2 can carry miR-16 and its catalytic activity of Ago2 may, consequently, have an impact on recipient cells (Arroyo *et al.*, 2011). Moreover, miRNAs can also be attached to high-density lipoprotein (HDL). HDL are lipoproteins transporting lipids, such as cholesterol, to the liver. For instance, HDL-transported miR-223 represses the expression of ICAM-1 in endothelial cells (Tabet *et al.*, 2014).

On the other hand, extracellular vesicles, major actors of cell-cell communication, can also deliver miRNAs to recipient cells. As discussed previously, cells release three types of EVs: exosomes, microvesicles and apoptotic bodies. The most studied vesicles are the exosomes. Multitude of studies have described the loading of miRNAs in those small vesicles. For instance, exosomal miR-567 can restore the chemosensitivity of breast cancer cells to trastuzumab by targeting a protein related to autophagy (Han *et al.*, 2020). Likewise, in response to epirubicin treatment, endothelial cells could produce miR-503-loaded exosomes and, therefore, participate in the anti-tumoral process by targeting cyclin D2 in triple negative breast cancer cells (Bovy *et al.*, 2015). The packaging of miRNAs in MVs is often used by cells. For instance, miR-34a and miR-145 are released in MVs derived from colon cancer cells (Akao *et al.*, 2014). It has also been shown that circulating miR-92a, an oncomiR, carried by MVs can promote tumor growth by reducing the levels of the tumor suppressor, Dickkopt-3, in other cancer cells or cells from the microenvironment (Yamada *et al.*, 2013).Likewise, miRNAs can also be transported by apoptotic bodies. Although the packaging of miRNAs in exosomes and in MVs is a process more studied, their transport in Abs is a process quite unknown. However, some studies report the implications of ABs-transported miRNAs in several pathologies. For instance, macrophages can release miR-221 and miR-222 in ABs inducing fibrosis by the induction of cell proliferation in lung epithelial cells (Zhu *et al.*, 2017).

4.4.3.1.1. Export of miRNAs in exosomes

Transfer of miRNAs in exosomes represents a new mode of cell to cell communication. However, the mechanism mediating the specific sorting of miRNAs remains unclear. Nevertheless, several studies demonstrate that proteins regulate this process. Based on motif recognition, the protein heterogeneous nuclear ribonucleoprotein A2B1 (hnRNPA2B1) binds to specific miRNAs leading to their export. Interestingly, miRNAs destined to be sorted in exosomes, also called exo-miRNAs, share a common motif (GGAG) in the 3' part of the miRNA. Likewise, cellular miRNAs also share a specific motif (UGCA) For instance, miR-601 and miR-17 possess, respectively, the exosomal motif or the cellular motif. Moreover, the binding of hnRNPA2B1 controlling miRNAs sorting requires the addition of a small ubiquitin-related modifier (SUMO) modification (Villarroya-Beltri et al., 2013). However, hnRNPA2B1 could have an opposite effect on a specific miRNA, miR-503. Indeed, hnRNPA2B1 binding inhibits the packaging of miR-503 in exosomes (Pérez-Boza, Boeckx et al., 2020). In hepatocytes, the sorting of exosomal miRNAs requires the action of the synaptotagmin-binding cytoplasmic RNA-interacting protein (SYNCRIP), also known as hnRNP-Q. This sorting process also involve the binding of a protein to specific motifs (Santangelo et al., 2016). Annexin A2 may also contribute to miRNA export in EVs (Hagiwara et al., 2015). Y-box protein 1 (YBX1), a component of exosomes, has been described to promote miRNA sorting into exosomes. Through YBX1 action, a particular miRNA, miR-223-3p, is selectively sorted into exosomes. Nevertheless, this miRNAs packaging does not involve a motif recognition (Shurtleff et al., 2016).

4.5. MiR-503

During this work, we have focus our interest on a specific miRNA, hsa-miR-503-5p. For ease of reading, the term miR-503 will be used.

MiR-503 was first described in human retinoblastoma tissues (Zhao *et al.*, 2009). This intragenic miRNA is located on the chromosome Xq26.3 and is clustered with miR-424 forming the miR-424(322)/503 cluster (Griffiths-Jones *et al.*, 2008). MiR-503 and miR-424, 383 bases away from each other, are transcribed together. Nearby in the genome, five other miRNAs are found within 7 kb to the cluster: miR-542-5p, miR-542-3p, miR-450a, miR-450b-5p et miR-450b-3p. Both miRNAs belong to the miR-16 family. Members of this family are miR-15a, miR-15b, miR-195, miR-424, miR-497 and miR-503. Nevertheless, based on the seed sequence, miR-103, miR-107 and miR-646 can also be included. In consequence, all the

members share a common seed region (AGCAGC) and, therefore, elicit similar biological functions (Caporali & Emanueli, 2011).

4.5.1. MiR-503 in cancer

Interestingly, miR-503 has paradoxical roles in cancer. In fact, depending on the tumor context and target genes, this miRNA can inhibit or improve tumor development. MiR-503 has been identified as a tumor suppressor in many cancer types, especially, in breast cancer. For instance, miR-503 is able to reduce MDA-MB-231 proliferation by targeting cyclin D1 (CCND1), D2 (CCND2) and D3 (CCND3). Those three proteins promote the progression through the G1-S phase of the cell cycle (Bovy *et al.*, 2015; Long *et al.*, 2015). Interestingly, the miR-424/503 locus is often deleted in breast cancer patients with poor prognosis. Indeed, the loss of the cluster expression promotes breast cancer progression by elevated levels of Bcl-2 and insulin growth factor 1 receptor (Rodriguez-barrueco *et al.*, 2017). The tumor suppressor role of miR-503 is not restricted to breast cancer. For instance, miR-503 inhibits osteosarcoma cells proliferation (Lv *et al.*, 2018). Down-regulation of miR-503 is associated with poor prognosis for lung cancer patients (Liu *et al*., 2015). Nevertheless, in rare cases, miR-503 may exert oncogenic actions. For instance, in colon cancer, miR-503 is able to induce oxaliplatin chemoresistance by targeting PUMA, a pro-apoptotic protein (K. Xu *et al.*, 2017).

Aim of the study

Aim of the study

The communication between cancer cells and their microenvironment is an essential aspect of cancerology. Therefore, understanding how the environment could affect tumor cell behavior is critical for the development of new anti-cancer strategies. In this study, we will focus on the communication between the endothelium and breast cancer cells by extracellular vesicles (EVs). During the past decade, EVs have emerged as a new communication tool involving the exchange of bioactive molecules such as microRNAs, small non-coding RNAs that act mostly in the repression of gene expression.

Previously, our laboratory identified a microRNA, miR-503 which exhibited upregulated levels in endothelial exosomes released by endothelial cells (ECs) upon epirubicin treatment. Moreover, this miRNA affected tumor growth. In this study, they highlighted an exosome-dependent transfer of microRNAs from endothelial to tumor cells (Bovy *et al.*, 2015). This suggests that there might be a specific mechanism that sorts miR-503 into EVs. Understanding how microRNAs are exported in EVs is currently an important challenge that we wanted to tackle in this project.

The aim of this study is to determine the molecular mechanism of miR-503 export and its impact on tumor cell behavior. In the first part of the thesis, we determined which proteins were involved in the miRNA export. We analyzed the interactions between the proteins and miR-503 and how epirubicin modulates them. These analyses highlighted two proteins that were involved in the sorting of this anti-tumoral miRNA upon epirubicin treatment. In the second part, we wanted to determine the impact of the proteins and the microRNA on tumor cell behavior. We silenced the proteins in endothelial cells, cocultured them with triple-negative breast cancer cells (MDA-MB-231) and measured the effects on tumorigenicity using various functional assays. The third part of this work asked if the effects of miR-503 on MDA-MB-231 cells that respond to chemotherapy, were conserved in epirubicin or paclitaxel-resistant tumor cells. Epirubicin and paclitaxel are chemotherapeutic drugs currently used to treat patients suffering from breast cancer. Graciously provided by Dr. Gorski and Dr. Spears, we performed functional assays on epirubicin and paclitaxel-resistant MDA-MB-231 cells. In the last part of this thesis, we asked if our findings were relevant for patients. Therefore, we used bioinformatics to determine the correlation between the proteins involved in the export and miR-503. We also analyzed the impact of miR-503 deletion on the survival rate of breast cancer patients.

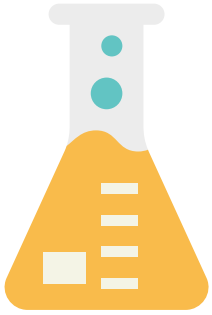

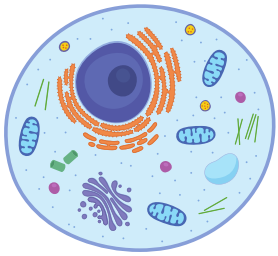
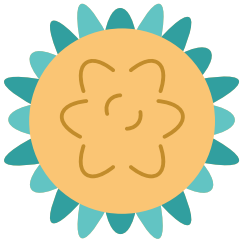

Materials & Methods

Materials and methods

Several materials and methods were also described in the article published in 2020 and presented in Results chapter 1. Therefore, these methods will not be included in the chapter "Materials and Methods" but are detailed in the methods of the article.

1. Cell lines

1.1. Cancer cells

All cancer cells were grown in an incubator at 37°C in a 5% CO_2 humid atmosphere. They were cultured in DMEM medium (Lonza) containing 4.5 g/L glucose, 110 mg/L sodium pyruvate, 584 mg/L L-glutamine, supplemented with 10% FBS (Lonza); and 1% of a mix of antibiotics (penicillin 10,000 units/ml, streptomycin 10,000 µg/ml) (Life technologies).

MDA-MB-231 (ATCC-HTB26; sex: F) (ATCC, Manassas, USA) are epithelial breast adenocarcinoma cells. These cells will be named "sensitive breast cancer cells" and were grown as described above. MDA-MB-231 Luc cells (expressing the gene coding for luciferase) were cultured in DMEM medium (Lonza) containing 4.5 g/L glucose, 110 mg/L sodium pyruvate, 584 mg/L L-glutamine, supplemented with 10% FBS (Lonza); and 1% of a mix of antibiotics (penicillin 10,000 units/ml, streptomycin 10,000 µg/ml) (Life technologies).

MDA-MB-231 resistant to epirubicin (MDA-MB-231 Epi-R) were kindly obtained by the courtesy of Dr. Shanon Gorski, BC Cancer Research Institute, Vancouver, Canada. Cells were cultured as described above for cancer cells, but implemented with 100 nM of epirubicin (Accord Healthcare, UK). Experiments were performed in drug-free medium.

MDA-MB-231 resistant to paclitaxel (MDA-MB-231 Pacli-R) were kindly obtained by the courtesy of Dr. Melanie Spears, MaRS Centre, Toronto, Canada. Cells were cultured as described above for cancer cells, but implemented with 25 nM of paclitaxel (Accord Healthcare). Experiments were performed in drug-free medium.

For exosome experiments, the media was depleted from the EVs naturally present in the serum, and then called "exosome-free". The serum was diluted 1:1 in culture medium and then centrifuged at 100,000g, 4°C for 18 h (Beckman Coulter, Optima XPN-80, SW32 rotor). The supernatant was then filtered through a 0.22µm filter (Millipore, Burlington, USA) and was added to the rest of the medium to reach 2% of exosome-free serum.

2. Epirubicin and paclitaxel treatments

The concentrations used in all experiments involving the treatment of the cells with epirubicin and paclitaxel were, respectively, 1µg/ml and 50 ng/ml in complete media (EGM-2 for HUVECs and DMEM 4.5g/L Glucose for cancer cells). The day after the treatment with chemotherapeutic agents, cells were gently washed twice with PBS and fresh medium was added.

3. EVs analysis

3.1. Electroporation

Pre-miRNAs (pre-miR-503 or pre-miR-67) were added to the freshly produced EVs in a ratio 1:6, i.e, one miRNA molecule for 6 µg of EVs. The mix was diluted in 500 µL of PBS in electroporation cuvettes (Eurogentec) and then electroporated for 5 seconds at 400V. The miRNA-loaded EVs were then stocked at -80°C.

3.2. EVs characterization

3.2.1. Transmission electron microscopy (TEM)

EVs were placed on a nickel grid coated with a thin layer of carbon for 1 h, washed three times with PBS, and then fixed with 2% paraformaldehyde (PFA) for 10 min. Then, the samples were incubated for 2 h with anti-CD63 and anti-CD81 antibodies. EVs were then washed five times and incubated with a 10 nm-gold labeled secondary antibody. Five more washes were applied and samples underwent another round of fixation with 2.5% glutaraldehyde for 10 min. Samples were contrasted using 2.5% uranyl acetate for 10 min, followed by four washes and an incubation of 10 min in lead citrate. The grids were finally washed four times in deionized water and analyzed with a JEM-1400 transmission electron microscope (JEOL) at 80 kV.

4. Transfection

4.1. Design of the synthetic miRNA.

The miRNA mimic miR-503-5p and cel-miR-67 (control) are double-stranded RNAs designed using the method of Betancur *et al.* (Betancur *et al.*, 2012). Briefly, the mature miRNA strand is modified by the addition of phosphorylation at the 5’ end and the carrier strand is the complementary RNA sequence, carrying a two base 3’ overhang with mutations near the 3’ end to thermodynamically destabilize the strand and induce faster degradation. Anti-miRs have

been designed to be fully complementary to the miR sequences (Lennox & Behlke, 2010). They are DNA/LNA mixmers with complete phosphorotioate backbones. LNAs were introduced to have a Tm between 70-75°C.

4.2. MiR-503 transfection

Cells were transfected as followed: for each milliliter of cells-containing-media, 700 µL represented media and cells while the remaining 300 µL were the transfection mix. The solution was prepared by the addition of 0.5 µL of Dharmafect-4 (Dharmacon, Lafayette, USA) to 149.5 µL of serum-free EBM-2 or DMEM for 10 minutes at RT. In parallel, a solution containing 149 µL of serum-free EBM-2 and 1µL of miRNA, at concentration of 10 µM, was mixed with the Dharmafect dilution and was incubated again at RT for another 20 minutes. Finally, the cells-containing solution was seeded in a flask/plate and the transfection solution was added. The final concentration of miR-503 was then 10 nM. After 16 hours, the supernatant was removed and fresh media (EGM-2 or DMEM) was added to the cells. After 24h of transfection, cells were washed three times with PBS and then stored at -80°C.

The same protocol was applied for the anti-miRNA transfection (anti-miR-503 and anti-cel-miR-67 also referred to as anti-miR-control).

4.3. Biotinylated miR-503 transfection

To determine the proteins attached to miR-503, endothelial cells were transfected, as described above, with a biotinylated form of miR-503 to achieve a concentration of 10 nM. After 16 hours, the supernatant was removed and fresh EGM-2 media was added to the cells. After 48h of transfection, cells were washed three times with PBS and then stored at -80°C. The design of biotinylated miRNA followed the protocol described by Ørom and Lund (Ørom & Lund, 2007) (**Figure. M 23**). In summary, miR-503 sequence was modified with an overhang of -UU and the addition of a C7 linker-biotin to the 3' –OH extremity and a phosphorylation in the 5' end. The carrier strand (miR-503-reverse) was the complementary RNA sequence, also phosphorylated in the 5' end and carrying a -UU 3' overhang but containing a mutation near to the 3'-end to destabilize the strand and induce its degradation.

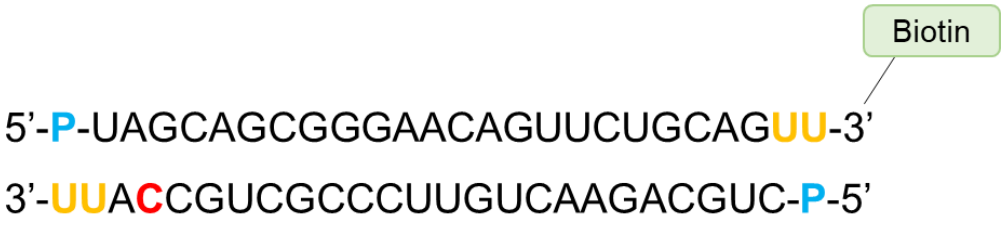

Figure M 23. Design of miR-503-biotin and miR-503-reverse.
In black is shown the natural miR-503 sequence and the modifications are indicated in colors: green represents the addition of biotin, blue is for the phosphorylation, orange for the 3' tailing and red represents the mismatch included to destabilize the carrier strand.

5. Plasmid construction

5.1. Amplification of DNA sequence

In a final volume of 25 µL, 5 ng of DNA were added to 0.75 µL of dNTP 10 mM (Promega, Madison, WI, USA), 0.75 µL of specific primers (10 µM) and 1 µl of Taq Kapa Hifi (Kapa Biosystems), diluted in the Kapa Hifi Buffer. The mix was then incubated in a T3 thermocycler (Westburg) and underwent several steps. First, DNA was denatured for five minutes at 95°C. The amplification step comprises 35 cycles of 20 seconds at 98°C, 15 seconds at 65°C and one minute at 72°C. Finally, a last step (5 minutes at 72°C) allowed the DNA elongation.

5.2. Cloning

To allow the cloning of the specific DNA sequence in the pCR8/GW/TOPO vector, the addition of a poly-A tail was required. For that purpose, 10 µL of the previous PCR were mixed to 1 µL of dNTP 10 nM, 0.5 µL of Go-Taq polymerase (Promega) and incubated in a T3 thermocycler for ten minutes at 72°C. Then, 2 µL of the poly-A tailed PCR product were added to 1 µL of vector, 1 µL of buffer and 2 µL of water (Invitrogen). The mix was incubated for five minutes at RT. Right after, the bacteria transformation could take place.

5.3. Bacterial transformation

To incorporate the plasmid of interest, 2 µL of plasmid were added to TOP10 chemically competent cells. The mix incubated for 30 minutes on ice. Then, cells underwent a heat shock at 42°C for, precisely, 30 seconds and, right after, were placed on ice. 250 µL of LB medium were added and the solution was then incubated for one hour at 37°C. Few microliters (~50 µL) were spread out on a Petri dish containing LB medium which included agar and the antibiotic for the clone selection.

5.4. DNA digestion

The cleavage of DNA fragments is performed by various restriction enzymes: NheI, XhoI and BstXI (Biolabs, Ipswich, MA, USA). The restriction was performed for one hours at 37°C, following manufacturer's protocol.

5.5. DNA fragments separation

The separation of DNA fragments was performed via electrophoresis on 1% agarose gels containing 0.01% of SYBR Safe DNA Gel Stain (Invitrogen) diluted in TE Buffer. 10% of loading buffer was added to the samples and the sizes of DNA were then analyzed.

5.6. Plasmid DNA extraction (miniprep)

An isolated colony was incubated, in 3 ml of LB medium that contained the adequate antibiotic, overnight at 37°C. The following day, the *Miniprep ZR Plasmid* (Zymo research, CA, USA) kit allowed us to purify plasmid DNA following manufacturer's protocol. In summary, 2 ml of bacterial culture were centrifuged at 14,000g for 30 seconds. The pellet was resuspended in 200 µL of P1 Buffer. Then, 200 µL of P2 and P3 buffers were added to the mix to, respectively, lyse the cells and neutralize the reaction. The solution incubated for two minutes at room temperature and was centrifuged for two minutes at 14,000g. The supernatant was transferred in a column which was centrifuged at 14,000g for 30 seconds. The eluate was discarded and 200 µL of Endo-wash buffer were added to the column and centrifuged again (14,000g, 30 seconds). Again, eluate was discarded and 400 µL of Plasmid-wash buffer were added to the column for one minute of centrifugation at 14,000g. Finally, DNA was eluted by the addition of 30 µL of water.

5.7. Plasmid DNA extraction (Endo-free maxiprep)

The endotoxin-free (Endo-free) DNA purification was performed using the *EndoFree Plasmid Maxi* kit (Qiagen), following manufacturer's instructions. In summary, bacteria were pelleted for 15 minutes at 6,000g, 4°C and resuspended in 10 ml of P1 buffer. 10 ml of P2 and P3 buffers were also added and the mix was loaded into a column. Then, the column was washed with 30 ml of QC buffer. DNA was eluted with 15 ml of QN Buffer and precipitated by the addition of isopropanol. The solution was then centrifuged for half an hour at 15,000g, 4°C. The pellet was washed with 70% Ethanol and centrifuged for ten more minutes. The supernatant was discarded and the DNA was resuspended in endotoxin-free water.

6. Fluorescent cell lines production

6.1. Viral vectors production

The production of viral vectors has been realized by the viral vectors platform. They incorporated the plasmids pLenti6-PALM-GFP, pLenti6-PALM-m-Cherry, pLenti6-V5-CD63-eGFP and pLenti6-V5-CD63-m-Cherry, previously produced, into lentivirus.

6.2. Fluorescent cells production

Within the L2 platform, 100,000 HUVECs and MDA-MB-231 were seeded in a 24-well plate and cultured overnight at 37°C. The following day, viruses and protamine sulfate (MP Biomedicals) were added to the cells and incubated overnight at 37°C. Twenty-four hours later, to select cells which had incorporated the vector, blasticidin (Invivogen) was supplemented to media. Cells were cultivated within the L2 until their media were virus-free.

HUVECs and MDA-MB-231 were, respectively, transduced with pLenti6-V5-CD63-eGFP or pLenti6-PALM-GFP and pLenti6-V5-CD63-m-Cherry or pLenti6-PALM-m-Cherry.

7. Transwell coculture assay

For HUVEC-GFP and MDA-MB-231-m-Cherry cocultures, 200,000 recipient cells were seed onto 6-wells plates previously coated with 0.2% gelatin and incubated overnight at 37°C. Then, donor cells were seeded onto the inner part of a 0.4 µm transwell (Corning). The transwell was then added to the well (**Figure. M 24**). After 6h of coculture, cells from the bottom chamber were visualized via a high-resolution confocal microscope LSM 880 (Zeiss).

For HUVECs and MDA-MB-231 cocultures, donor cells (HUVECs) were seeded, as described previously, and transfected with siRNA against the identified proteins (siANXA2, sihnRNPA2B1, siVIM and siTSP1) or with the unrelveant siRNA (UNREL) at a final concentration of 20 nM. The following day, MDA-MB-231 were seeded onto the inner part of a 0.4 µm transwell which was then added to the well. After 48h, cancer cells underwent a variety of functional assays.

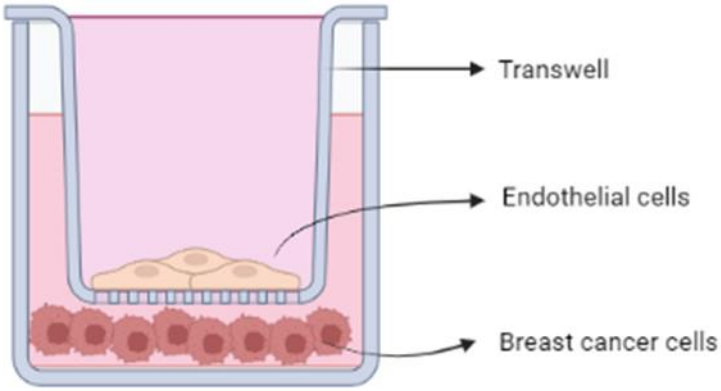

Figure M 24. Schematic representation of a transwell coculture system.
Donor cells, in this case endothelial cells, were seeded in the inner part of the transwell and cocultivated with recipient cells, in this case breast cancer cells. Figure created with Biorender.com.

8. Functional assays

8.1. Apoptosis assay

The amount of cells undergoing apoptosis was measured by flow cytometry using the kit *Roche Annexin-V-Fluos Staining Kit* (Roche). 10^5 cancer cells were transfected and seeded in T-25 flasks with 4 ml of complete DMEM. After 24h, cells were gently detached with trypsin. Cells were then stained, following the manufacturer's instructions (eBioscience), with Annexin-V-FITC and propidium iodide (PI) and analyzed on the FACS Calibur (BD Biosciences). Three controls were realized: the buffer alone, the Annexin-V-FITC only and the PI alone. The Annexin-V is the ligand of phosphatidylserine, which is expressed on the surface of dying cells. Viable cells with intact membranes exclude PI, whereas the surface of damaged cells are permeable to PI. The combination of the two dyes allows the discrimination of living cells (Annexin-V -, PI -) and cells undergoing early (Annexin-V +, PI -) or late (Annexin-V -, PI +) apoptosis.

8.2. Cell adhesion assay

When the cells were transfected with the pre-miRNAs or the anti-miRNAs, they were seeded in a 6-well plate for 24h. The next day, the wells of a 96-well plate were coated with 20 µg/ml of fibronectin (BD-Biosciences) for an hour at 37°C. Then, 30,000 transfected cells were seeded on fibronectin-coated 96-wells plate for an hour at 37°C, washed with PBS and fixed with ice cold absolute methanol for 10 minutes. Cells, including 3 control blank wells, were then stained with 0.1% crystal violet (Sigma-Aldrich), previously solubilized in acetic acid, for 15 minutes and washed three times with water to remove the excess of staining solution. The

absorbance was measured at 562 nm with VICTOR X3 Multilabel Reader (PerkinElmer). This functional assay allows the quantification of attached cells by colorimetry.

8.3. Invasion assay

The generation of spheroids followed the method previously described by Correa and colleagues (Correa de Sampaio *et al.*, 2012). A thousand of cancer cells were seeded, in 96-well suspension plates (Greiner), in 200 µL of a mix of 3:2 DMEM/1.2% Methylcellulose (Sigma-Aldrich) and incubated for 48h at 37°C. Once the spheroids were formed, they were collected and delicately seeded in a three dimensional collagen matrix. This matrix was composed of a solution of 1:1 collagen (Corning)/pepsin and 1.2% methylcellulose. Six spheroids were plated per well, in a 48-well plate, in 300 µL of the collagen matrix solution. After 30 minutes of collagen polymerization, 500 µL of DMEM 2% FBS were added per well. Twenty-four hours after their incorporation in the matrix, spheroids were visualized via a microscope Olympus CKX41 (Olympus Life Science) at 10x-magnification objective. To measure the invasion rate of cancer cells, the area of the spheroids and the area of invasion were taken by ImageJ software.

The same protocol was used for heterospheroids composed of 500 transfected HUVEC CD63-GFP and 500 MDA-MB-231 CD63-m-Cherry. In this case, spheroids acquisition was performed by epifluorescence Nikon Eclipse Ti microscope (Nikon instruments) at 10x-magnification objective.

8.4. Migration assays

8.4.1. Scratch wound migration assay

Cells were directly seeded in a 48-well plate, 80,000 cells/well in 300 µL of DMEM 4.5 g/L glucose for 24h and the head of a 200 µL tip was used to perform a wound. Migration of cells into the wound was measured 6 h later. The percentage of coverage was calculated using the following formula:

$$\%Coverage = \left[\frac{Widht\ t0 - Widht\ t6}{Widht\ t0}\right] * 100$$

8.4.2. Migration assay in Boyden chamber

The Boyden chamber consists of a membrane pierced with 8 µm micropores. Cells seeded on the upper part of the membrane might be attracted by molecules present in the other

compartment, and migrate through it by chemotaxis. 30,000 HUVECs were transfected and seeded in 300 µL of DMEM 1g/ml Glucose without serum on the upper wells of the Boyden chambers (24-well Transwell, Costar Corp). In parallel, 20,000 MDA-MB-231 cells were seeded in the lower chamber. Two days after, the inserts were added to the wells. To induce migration, the lower chamber was filled with 600 µL of DMEM supplemented with 10% FBS. Cells were allowed to migrate for 8 h at 37 °C. The membrane insert was removed and flipped so that the side towards the lower chamber faced the operator. Cells were fixed for 20 min in ice cold absolute methanol, stained with 4% Giemsa and the insert was mounted on microscope slides. Cells were imaged using an Olympus CKX41 microscope (Olympus Life Science) and counted using ImageJ (NIH).

8.5. Proliferation assays

8.5.1. Proliferation assay with BrdU

Transfected cells were directly seeded in a 96-well plate, 3,000 cells/well in 100 µL of DMEM 4.5 g/L glucose for 24h. The following day, medium was changed with DMEM supplemented with 10% FBS to induce proliferation. The thymidine analogue 5-bromo-2-deoxyuridine (BrdU) was added and incubated for 16 h. The proliferation rate was then analyzed by measuring the BrdU incorporation with the kit *Cell proliferation ELISA BrdU colorimetric* (Roche) according to manufacturer's protocol. Absorbance at 355 nm was measured with VICTOR X3 Multilabel Reader (PerkinElmer). Nevertheless, in some cases, sulfuric acid was added to the wells to neutralize the reaction. Therefore, absorbance was measured at 590 nm. This functional assay allows the detection of the BrdU incorporated in genomic DNA of dividing cells by using antibodies and colorimetry.

8.5.2. Proliferation assay with luciferin

For the luminescence proliferation assay, endothelial cells were transfected with siRNAs against the identified proteins (20 nM). In parallel, 50,000 MDA-MB-231 cells were seeded in 24-well plates. After 48h, endothelial cells were detached by trypsin and seeded again in a 0.4 µm transwell. The day after, the transwell was added to the well. After 24h of coculture, 150 µg/ml of luciferin were added per well, and the luminescence was quantified using the bioluminescent IVIS imaging system (Xenogen-Caliper).

8.6. Survival assay

2,000 cancer cells were transfected and seeded in a 96-well plate, in 100 µL of complete medium. The cells were grown in the incubator at 37°C, 5% CO_2, for 24h. The cells treated with chemotherapies were incubated after 16h in complete medium. Then, cells were gently washed twice with PBS and fresh DMEM was added. 1h before the experiment endpoint, 10 µL of WST1 reagent (Roche) were added to the wells, including three control wells. Absorbance was measured after 30 minutes at 450 nm using the VICTOR X3 Multilabel Reader (PerkinElmer). WST1 is a colorimetric assay based on the cleavage of a tetrazolium salt, MTS, by the mitochondrial dehydrogenase to form formazan in viable cells.

9. Quantitative analysis of genes and microRNA expression by qRT-qPCR

Three different approaches were used to measure the levels of several RNAs.

9.1. miRNAs

For the detection of microRNAs (Cel-miR-67, RNU44, RNU48, and miR-503), 3.33ng of RNA were retrotranscribed using the *TaqMan Reverse Transcription Kit* (Applied Biosystems) with the *TaqMan microRNA Assay* (Applied Biosystems). The detection of the levels of these genes was performed using 2.2µL of the cDNA product, 1.7 µL of *TaqMan microRNA Assay* (Applied Biosystems) and *TaqMan Universal Master Mix* (Applied Biosystem) (16.5 µL of enzyme diluted with 12.6 µL of RNAse-free water). 10 µL of mix were added per well. The average levels of RNU44 and RNU48 were used to normalize the miRNA of interest. In the case of EVs, (Cel-miR-67, let-7d, miR-16 and miR-503), 1.67µL of RNA samples were used per reaction and the normalization was performed against the average levels of let-7d and miR-16. Since this system of detection does not amplify DNA products, only the negative control lacking primers was prepared per experiment. In all cases, gene levels were assessed using the $2^{-(\Delta\Delta Ct)}$ method. This method was used for the Chapter 1 experiments.

For both chapters two and three, the synthesis of cDNA (from 20 to 200 ng of RNA) first required the addition of a poly-A tail by an *E. coli PolyA polymerase* (New England Biolabs, MA, USA) for an hour at 42°C. Then, tailed RNA were retrotranscribed into cDNA by the addition of 0.45 µL of MMLV-retrotranscriptase (New England Biolabs). The cDNAs produced were used for quantitative PCR reaction, using *Takyon SYBR Green* (Eurogentec). The thermal cycles were performed on the PCR cycler Applied Biosystems 7900 HT (Applied Biosystems). The relative levels of mRNAs were quantified using the $2^{-(\Delta\Delta Ct)}$ method and were normalized against the average of two housekeeping genes: Small Nucleolar RNA, C/D Box 44 (SNORD44 aka RNU44) and Small Nucleolar RNA, C/D Box 48 (SNORD48 aka RNU48).

9.2. Coding genes

The synthesis of cDNA was performed using the *iScript DNA synthesis kit* (Biorad), following manufacturer's protocol, starting from 500 to 1,000 ng of total RNA. The cDNAs produced were used for quantitative PCR reaction, using *Takyon SYBR Green* (Eurogentec). The thermal cycles were performed on the PCR cycler Applied Biosystems 7900 HT (Applied Biosystems). For each experiment, two controls were done: the first without cDNA and the other without the reverse transcriptase (RT-). The relative levels of mRNAs were quantified

using the $2^{-(\Delta\Delta Ct)}$ method and were normalized against the average of two housekeeping genes: β2-microglobulin (B2M) and peptidylprolyl isomerase (PPIA).

10. Orthotopic MDA-MB-231 adenocarcinoma xenografts

Subconfluent MDA-MB-231 cells were trypsinized, washed and resuspended in PBS. The MDA-MB-231 cell suspensions (100,000 cells in 100 µL of PBS) were injected in the fourth mammary gland of each NOD-SCID mouse. For microRNAs-loaded EVs treatment, 3 µg of EVs containing miR-503 or the control Cel-miR-67 were injected peritumorally from day 21 which consists of the time when tumor size reached 50 mm^3) every three days. Approximately, thirty-six days after tumor cells injection, mice were euthanized, and their tumors harvested.

Tumor growth of MDA-MB-231 cells was assessed by measuring the length and width of each tumor every day. Tumor volume was calculated using the following formula:

$$V = l\ x\ w\ ^2x\ 0.5$$

Where V: volume; w: width and l: length.

11. Statistical analysis

All experiments were performed a minimum of 3 times otherwise stated. The values plotted represent the mean of the biological replicates ± the standard error of the mean (SEM) or the standard deviation (SD), the technique used is specified for each case in the figure's legend. The statistical significance of the results was assessed using an unpaired t-test. All p-values and n are reported in the figure legends. Results are considered significant when $p < 0.05$.

12. Buffers, antibodies and sequences

12.1. Buffers

12.1.1. Protein extraction and Western Blotting

Buffer	Composition
Exosome lysis buffer	1% triton, 0.1% SDS, PBS
Electrophoresis buffer	25 mM Tris-HCl; 192 mM glycine; SDS 0,1%
Transfer buffer	24 mM Tris HCl; 192 mM glycine; 20% méthanol
4x loading buffer	5% Glycerol, 30mM Tris-HCl pH=6.8, 5% SDS, 0.002% Bromophenol Blue and 5% β-mercaptoethanol
4x non-reducing loading buffer	5% Glycerol, 30mM Tris/HCl pH=6.8, 5% SDS, 0.002% Bromophenol Blue
RIPA buffer	50mM Tris pH 7.5, 150mM NaCl, 10 mM $CaCl_2$, 0.5% NP40, 0.25% Sodium deoxycholate and 0.1% SDS
Trypsin-EDTA	0.5% trypsin (Difco, MI, USA); 0.2% EDTA; PBS; pH=7.6

12.1.1. Subcellular fractionation

Buffer	Composition
Buffer A	50 µL Hepes 1M pH=7.9, 50 µL KCl 1M, 7,5 µL MgCl2 1M, 1.7 ml Sucrose 1M, 500 µL Glycérol, 5 µL DTT 1M, one pill of proteinase and phosphatase inhibitors (Roche), 5 µL Triton X100, 2.6 ml water
Buffer B	150 µL EDTA 100 mM pH=8, 20 µL EGTA 50 mM pH=8, 5 µL DTT 1M, one pill of proteinase and phosphatase inhibitors, 4.8 ml water

12.1.2. Immunofluorescence

Buffer	Composition
Fixation Buffer	4% PFA
Blocking Buffer	5% BSA, 0.5% saponin, PBS
Antibody diluent Buffer	0.5% BSA, PBS

12.1.3. miR-503 pull-down

Buffer	Composition
Pull-Down Lysis Buffer 1	20mM Tris-HCl pH=7.5, 0.5% SDS, 1mM EDTA, 200U/ml RNAse Inhibitor (Roche), 1x Halt Protease and phosphatase inhibitor cocktail (Thermofisher) and 1pill/10ml of cOmplete Protease Inhibitor (Roche)
Pull-Down Washing Buffer 1	20mM Tris-HCl pH=7.5, 500 mM LiCl, 0.1% SDS, 1 mM EDTA
Pull-Down Washing Buffer 2	20mM Tris-HCl pH=7.5, 500 mM LiCl, 1 mM EDTA
Pull-Down Washing Buffer 3	20mM Tris-HCl pH=7.5, 200 mM LiCl, 1 mM EDTA

12.1.4. Immunoprecipitation

Buffer	Composition
IP Washing Buffer	50mM HEPES, 150mM NaCl and 1% Triton

12.2. Antibodies

Protein	Host	Blocking	Conc	Brand	Reference
β-tubulin	Rabbit	8% Milk	1:4000	Abcam	Ab6046
ANXA2	Rabbit	8% Milk	1:1000	Cell signaling	#8235
FN1	Mouse	8% Milk	1:1000	BD Biosciences	610077
HNRNPA2B1	Mouse	5% BSA	1:1000	Abcam	Ab6102
TSP1	Mouse	8% Milk	1:1000	Thermofisher	MA5-13398
VIM	Mouse	8% Milk	1:1000	Dako	MO725229
VINCULIN	Rabbit	8% Milk	1:1000	Abcam	Ab129002
HISTONE H3	Rabbit	8% Milk	1:1000	Cell signaling	9715S
GAPDH	Mouse	8% Milk	1:1000	Abcam	Ab8245
CD9	Mouse	8% Milk	1:1000	Santa Cruz	Sc20048
CD63	Mouse	8% Milk	1:1000	Invitrogen	10628D
CD81	Mouse	8% Milk	1:1000	Invitrogen	103630D
Cytochrome c	Rabbit	8% Milk	1:500	Oncogene research	PC333
Syntenin	Rabbit	8% Milk	1:1000	Abcam	ab133267
Anti-mouse FC-HRP	Horse	-	1:2000	Cell signaling	7076
Anti-rabbit FC-HRP	Goat	-	1:2000	Cell signaling	7074
Alexa488-conjugated anti-mouse IgG	Goat	-	1:300	Thermofisher	A32723
Alexa555-conjugated anti-rabbit IgG	Goat	-	1:300	Thermofisher	A32732

12.3. Sequences

12.3.1. Small interfering RNAs

Gene	siRNA	Carrier
Scramble (SCR) or UNREL	CUUCCUCUCUUUCUCUCCCUUGATT	UCACAAGGGAGAGAAAGAGAGGAAGGA
ANXA2	GAAAACCAGCUUGCGAAUAACAGTC	GACUGUUAUUCGCAAGCUGGUUUUCUA
FN1	GUGGUCCUGUCGAAGUAUUTT	AAUACUUCGACAGGACCACTT
HNRNPA2B1	GGAACAUCACCUUAGAGAUUACUTT	AAAGUAAUCUCUAAGGUGAUGUUCCUC
TSP1	GGAGUUCAGUACAGAAAUATT	UAUUUCUGUACUGAACUCCTT
VIM	GAAUGGUACAAAUCCAAGUTT	ACUUGGAUUUGUACCAUUCTT

12.3.2. List of miRNA mimics.

Bio-labeled miRs are the same duplexes but with a biotin the 3' end of the sense strand.

Gene	Sense strand	Antisense strand
miR-503-5p	5' P-UAGCAGCGGGAACAGUUCUGCAG-bio	5' GCAGAACUGUUCCCGCUGCGAAG 3'
cel-miR-67-3p	5' P-UCACAACCUCCUAGAAAGAGUAGA 3'	5' UACUCUUUCUAGAAGGUGGUGCUU 3'

12.3.3. List of anti-miRs

Anti-miRs are made with complete phosphorothioate backbone with a mix of DNA and LNA bases, represented in the brackets.

miRNA	Sequence
Anti-miR-503	5'(CT)GCAG(A)ACTGTTCCC(G)CTG(CTA)3'
Anti-miR-67	5'(TC)GATCTA(C)TCTTTCTAGG(A)GGTTG(T)GATG(CT) 3'

12.3.4. Primers for coding genes qRT-PCR

Primer sequences are annotated from 5’ to 3’.

Gene	Forward	Reverse
B2M	GAGTATGCCTGCCGTGTG	AATCCAAATGCGGCATCT
PPIA	CCAACACAAATGGTTCCCAGT	CCATGGCCTCCACAATATTCA
ABCB1	TGCATTTGGAGGACAAAAGA	AGCAGGAAAGCAGCACCTAT
MDH2	GACCTGTTCAACACCAATGC	TGAAAACTTCTGCTGTGATGG
POR	CGGCTGAAGAGCTACGAGA	AGTCCGAGATGTCCAATTCC
TOP2A	GGATCCACCAAAGATGTCAA	CCAGTTTCATCCAACTTGTCC
GADD45A	GAGCTCCTGCTCTTGGAGAC	CCCGGCAAAAACAAATAAGT
SIRT6	GCAGTCTTCCAGTGTGGTGT	CTCTCAAAGGTGGTGTCGAA
GAPDH	TGCCCCCATGTTTGTGATG	GGTGGTGCAGGAGGCATT
ANXA2	GAGCGGGATGCTTTGAACATT	TAGGCGAAGGCAATATCCTGT
FN1	CGGTGGCTGTCAGTCAAAG	AAACCTCGGCTTCCTCCATAA
HNRNPA2B1	ATTGATGGGAGAGTAGTTGAGCC	AATTCCGCCAACAAACAGCTT
TSP1	AGACTCCGCATCGCAAAGG	TCACCACGTTGTTGTCAAGGG
VIM	GACGCCATCAACACCGAGTT	CTTTGTCGTTGGTTAGCTGGT
CCND1	CAATGACCCCGCACGATTTC	CATGGAGGGCGGATTGGAA
CCND2	CTCGAGGGATGCCAGTTGGGCC	GCGGCCGCCAAAAGCGTGAATCATTGCC
CCND3	TACCCGCCATCCATGATCG	AGGCAGTCCACTTCAGTGC
BCL2	GGTGGGGTCATGTGTGTGG	CGGTTCAGGTACTCAGTCATCC
MYB	GAAAGCGTCACTTGGGGAAAA	TGTTCGATTCGGGAGATAATTGG
AKT3	TGGCATGCTGGGTAACTGGA	CAGGCCACACATCTCGCTTC
DGCR2	CGAGGATGAGAGCGACGAAG	CCTAGGAAACTGCTGAAGCGA
FGF2	GGGAGAAGAGCGACCCTCAC	AGCCAGGTAACGGTTAGCACA
FGF7	TGGTAATCCAGCTCCTGGCG	CCATGTTGCCATTCGGAGAGC
L1CAM	ATCCTCCTGCTCCTCGTCCT	CGTTGTCACTGTACTCGCCG
PTGFR	GGCTCCGTCTTCTGCTCCTC	TCCGTCTGGCAGGTTGTGTT
SDCBP2	CAGCTGGAGAAGGTCGTGG	CCTGAATGGCTTGGTCCACT

12.3.5. Primers for miRNAs qRT-PCR

miRNA	Sequence
miR-503-5p	CGTAGCAGCGGGAACAGT
miR-16	TAGCAGCACGTAAATATTGGCG
RNU44	GCAAATGCTGACTGAACATGAA
RNU48	CTCTGAGTGTGTCGCTGATGC
Universal primer	GCATAGACCTGAATGGCGGTA

Results

Chapter I

hnRNPA2B1 inhibits the exosomal export of miR-503 in endothelial cells

Results

The results are divided into four chapters.

Data from the first chapter, entitled “hnRNPA2B1 inhibits the exosomal export of miR-503 in endothelial cells” were published in 2020 and both, Jennifer Pérez-Boza and I, are co-first authors (Pérez-Boza, Boeckx *et al*., 2020). Jennifer Pérez-Boza identified the proteins in interaction with miR-503.

The second chapter will discuss the effects of the exosomal export of miR-503 on breast cancer cells behavior.

Then, we will discuss the role of miR-503 in breast cancer tumorigenicity and its implication in resistance to chemotherapy.

Finally, in the last chapter, we will study the clinical implications of miR-503 for breast cancer patients.

1. hnRNPA2B1 in the exosomal export of miR-503 in endothelial cells

hnRNPA2B1 inhibits the exosomal export of miR-503 in endothelial cells

Pérez-Boza, Jennifer*[1-2]; Boeckx, Amandine*[1]; Lion, Michele[1]; Dequiedt, Franck.[3], Struman, Ingrid[1]

[1]Molecular Angiogenesis Laboratory, GIGA Research, ULiege, B34, Avenue de l'Hôpital, 1, B-4000 Liège, Belgium.

[2] Current address: Exosome Research Group and Medical Oncology, VUmc Cancer Center Amsterdam, 1118 De Boelelaan, 1182 DB Amsterdam, The Netherlands

[3] Laboratoire de Signalisation et Interactions des Protéines, GIGA-Research, ULiege, B34, Avenue de l'Hôpital, 1, B-4000 Liège, Belgium

Correspondence should be addressed to I.S. (i.struman@uliege.be)

*These authors contributed equally to the work

Manuscript published in **Cellular and Molecular Life Sciences (2020)** 77:4413–4428 https://doi.org/10.1007/s00018-019-03425-6.

1.1. Abstract

The chemotherapeutic drug Epirubicin increases the exosomal export of miR-503 in endothelial cells. To understand the mechanisms behind this process, we transfected endothelial cells with miR-503 carrying a biotin tag. Then, we pulled-down the proteins interacting with miR-503 and studied their role in microRNA exosomal export. A total of four different binding partners were identified by mass spectrometry and validated by Western Blotting and negative controls, among them ANXA2 and hnRNPA2B1. By using knock-down systems combined with pull-down analysis, we determined that Epirubicin mediates the export of miR-503 by disrupting the interaction between hnRNPA2B1 and miR-503. Then, both ANXA2 and miR-503 are sorted into exosomes while hnRNPA2B1 is relocated into the nucleus. The combination of these processes culminates in the increased export of miR-503. These results suggest, for the first time, that RBPs can negatively regulate the exosomal sorting of microRNAs.

1.2. Introduction

Exosomes are small bilipidic vesicles ranging in size between 30 and 150nm (van Niel et al., 2018) produced in the endosomal compartment of virtually all cells. These vesicles mediate extracellular communication through the exchange of information via receptor signaling and/or by absorption, via either endocytic processes or pinocytosis/phagocytosis (McKelvey et al., 2015). The content of exosomes is dictated by the parent cell type, as well as by the status and the environment of the cells at the time of production (Dreyer and Baur, 2016).

Even though exosomes may carry different cargo (coding and non-coding RNA (Pérez-Boza et al., 2018), DNA (Kalluri and LeBleu, 2017), lipids (Record et al., 2014) and proteins (Beach et al., 2014)), multiple studies have shown that the loading of specific RNAs (in disease) can promote phenotypic changes in the recipient cells (Li et al., 2015).

MicroRNAs are small non-coding RNAs involved in the negative regulation of gene expression. Although changes in the exosomal RNA profiles often reflect changes in the parental cells, cellular stimulus can also modify the encapsulation of specific microRNAs. An example of this mechanism is the anti-tumoral microRNA miR-503. Our group previously reported that breast cancer patients receiving the neoadjuvant Epirubicin had increased circulating levels of miR-503. We then demonstrated that this chemotherapeutic drug could promote, in endothelial cells, the production of exosomes with anti-tumoral properties loaded with miR-503 (Bovy et al., 2015). In conclusion, we highlighted an exosome-dependent transfer of microRNAs from endothelial to tumor cells that contributes to the anti-tumoral effect of Epirubicin. Our data suggested the presence of an underlying mechanism leading to the selective export of miR-503 in endothelial cells. To date, several studies have focused on motif-based RBP recognition to explain exosomal microRNA export, but the mechanisms behind this process still remain mostly unknown. In this study, combining microRNA pull-down techniques along with proteomic assays and knock down studies, we discovered that Epirubicin promotes the exosomal export of miR-503 by destabilizing the interaction between this microRNA and hnRNPA2B1. Process that culminates in the increased exosomal encapsulation of miR-503.

1.3. Methods

Cells and culture conditions

HUVECs were isolated as previously described by Jaffe et al (1973). HUVECs were amplified in flasks coated with gelatin (0.2%) in Endothelial Cell Growth Media-2 (EGM2) (Lonza, Germany)) lacking heparin and supplemented with 5% donor bovine serum (DBS) at 37°C and 5% CO_2. HMVECs (Human microvascular endothelial cells) (Lonza, Germany) were cultured in EGM2 lacking heparin and supplemented with 5% fetal bovine serum (FBS) at 37°C and 5% CO_2. All exosomes experiments were performed in exosome-depleted media prepared using serum that had been centrifuged at 110,000 g for 16 h at 4°C to remove exosomes (Beckman Coulter Optima L-90K, SW32 Rotor). Cells were stored in liquid nitrogen for further use and used for experimental procedures from passage 6 (P6) to P10. The concentration of

epirubicin used in all experiments was 1 µg/ml in complete EGM2. The levels used for this test were decided after calculating the circulating concentration of this drug in patients (Bovy et al., 2015).

Exosome purification and characterization

HUVECs and HMVECs were cultured in heparin-free EGM2 supplemented with full 5 % DBS (v/v) or exosome depleted DBS (exosomes were depleted from the serum by overnight centrifugation at 110,000 g and 4 ºC). Cells were incubated at 37 °C and 5 % CO_2 up to P10 at a seeding density of $1.8.10^6$ cells per 175 cm^2 flask. Three days later, the supernatant was recovered, and exosomes were purified by sequential ultracentrifugation. The media was first centrifuged at 2000 g for 20 minutes at 4°C to remove unattached cells, followed by a second round of centrifugation at 12,000 g (45 minutes at 4°C) to remove cell debris and large vesicles. The supernatant was then collected and passed through a 0.2 µm filter and ultracentrifuged at 110,000 g for 2 h at 4°C to pellet the exosomes (Beckman Coulter Opitima L-90K, SW32 rotor). The pellet was washed with PBS to remove any possible coprecipitated protein complexes, and with a final round of centrifugation at 110,000 g for 2 h at 4°C, the pellet was recovered and stored in PBS at -80°C. Exosomes were characterized by Dynamic Light Scattering (DLS) for vesicle size and by Western blotting for protein composition. In brief, the protein characterization of cells and exosomes was performed following the MISEV 2018 guidelines using the following antibodies: CD63 (#106228D, Invitrogen), CD9 (#sc20048, Santa Cruz), CD81 (#10630D, Invitrogen), syntenin (#ab133267, Abcam), or cytochrome c (#556433, BD Pharmingen) for immune detection.

Electron microscopy of whole-mounted immuno-labelled exosomes

Isolated exosomes were placed on Formvar-carbon coated nickel grids for 1 h, washed 3 times with PBS and fixed with 2% paraformaldehyde for 10 min. After 3 washes, grids were then incubated for 2 h with the following antibodies: anti-CD63 or anti-CD105. Exosomes were then washed 5 times and incubated with a 10 nm-gold labeled secondary antibody. They were washed 5 more times and post-fixed with 2.5% glutaraldehyde for 10 min. Samples were contrasted using 2.5% uranyl acetate for 10 min followed by 4 washes and an incubation of 10 min in lead citrate. Grids were finally washed 4 times in deionized water and examined with a JEOL JEM-1400 transmission electron microscope at 80 kV.

Design of the synthetic microRNA

The microRNA mimics miR-503-biotin cel-miR-67-biotin are double stranded RNAs designed following the publications by Orom and Lund [12] and Betancur et al.[13]. In summary, the mature microRNA strand was modified by the addition of a biotin to the 3' –OH and a phosphorylation at the 5' end. The carrier strand (miR-503-reverse or cel-miR-67 reverse) was the complementary RNA sequence, which was also phosphorylated at the 5' end and carried a two bases 3' overhang with mutations near the 3' end to thermodynamically destabilize the strand and induce faster degradation. **Supplementary Figure S1** shows the sequence and modifications induced in the microRNA duplexes. Oligonucleotides were purchased from Eurogentec.

Preparation of protein lysates and Western blotting

HUVECs were washed with PBS 1x and RIPA buffer was added (50mM Tris pH 7.5, 150mM NaCl, 10 mM $CaCl_2$, 0.5% NP40, 0.25% Sodium deoxycholate and 0.1% SDS) at 75 µl/10^6 cells. The plates/flasks were then scratched and the cellular lysate was centrifuged at 10.000g and 4°C for 15 minutes. The cleared supernatant was then recovered and the pellet (cellular debris) discarded. The quantification of cellular lysates was performed using the BCA Protein Assay Kit (Pierce) following the manufacturer's instructions. For exosomes, the lysis of the samples was performed using exosome lysis buffer (10% Triton, 1% SDS) and the quantification of exosomal protein was performed with BCA Protein Assay Kit (Pierce) incubating the samples at 60°C for 60 minutes. Prior gel loading, samples were denatured by boiling at 95°C for 7 minutes in 1x loading buffer (40% Glycerol, 240mM Tris/HCl pH=6.8, 8%SDS, 0.025% Bromophenol Blue) without 5% β-mercaptoethanol for the detection of tetraspanins (CD9, CD63 and CD81) and with the reducing agent for all the other proteins. Equal amounts of protein lysates (10µg) were electrophoresed on a 12 % SDS-polyacrylamide gels and transferred to a polyvinylidene fluoride membrane using a wet transfer system. The blots were then blocked with either 5% BSA (in the case of hnRNPA2B1) or commercial powdered milk at 8% for 1h. Blots were then incubated overnight at 4°C with the primary antibody (ANXA2 (#8235, Cell Signaling), FN1 (#610077, BD Phamingen), HNRNPA2B1(#Ab6102, Abcam), TSP1(# MA5-13398, Thermo Fisher), VIM (#MO72529, DAKO), VINC (#Ab129002, Abcam), SYN (#Ab133267, Abcam)). After 3 washes of 10 minutes with TBS/0.1% Tween-20 (TBST), the membranes were incubated for 1h at room temperature with an HRP-conjugated secondary antibody (anti-rabbit (#7074S, Cell Signaling), anti-mouse (#7076S, Cell Signaling) and washed twice with TBST and once with TBS. The

blots were then incubated with enhanced chemiluminiscence (ECL) substrate (Pierce Biotechnology) and exposed to films. All films were scanned and the intensity of the bands was quantified using ImageJ.

MiR-503 and cel-miR-67 pull-down

To detect the proteins associated with miR-503, HUVECs or HMVECs were transfected with 10nM miR-503-biotin or cel-miR-67-biotin duplexes at the time of seeding. For this purpose, 7.5µl of DharmaFECT 4 (Dharmacon) were mixed with 2242.5µl of serum free EBM2 (Lonza) and incubated at room temperature for 10 minutes. After this, a second solution containing 2235 µl of EBM2 and 15 µl of 10 µM miR-503-biotin/reverse was prepared. Both solutions were mixed and incubated at room temperature for 20 more minutes. In parallel, $1.8.10^6$ cells were seeded in 10.5 ml of full EGM2 (supplemented with 5% DBS) in a 145 cm^2 round dish previously coated with gelatine 0.2 %. The transfectant-miRNA solution was then added to the cells to achieve a final microRNA concentration of 10nM in 15 ml. The next day, the media was replaced with 20ml of fully supplemented EGM2 and two days later we proceeded to pull down the microRNA and its putative partners. Forty plates were used for the identification of the miR-503-biotin partners by mass spectrometry (see supplementary methods for detailed protocol), and 10 plates were used for the validation of the results.

The protocol used in the pull down followed the methodology described by Rambout X (Rambout et al., 2016) with some modifications. Two cross-linking steps were performed. First, after washing twice with ice-cold PBS, 5ml of a 1 mM 3,3-dithiobis(sulfosuccinimidylpropionate) (DTSSP) solution was added to the plates and incubated for 2h at 4°C to induce the crosslinking between proteins. The supernatant was removed and the cells were incubated with 20 mM Tris HCl pH 7.6 for 30 minutes to stop the crosslinking reaction. Then, the plates were washed twice with ice-cold PBS. In a second crosslinking step, the formation of covalent bonds between proteins and RNA was induced via UV irradiation. For that purpose, the cells were set on an ice tray and UV-irradiated (0.4 J/cm^2 of 365-nm UV light with a Stratalinker 2400). Then, 2 ml of Pull-Down Lysis Buffer 1 (20 mM Tris-HCl pH 7.5, 0.5% SDS, 1 mM EDTA, 200 U/ml RNAse Inhibitor (Roche-Sigma Aldrich), 1x Halt Protease and phosphatase inhibitor cocktail (Thermo Scientific) and 1 pill/ 10 ml of cOmplete Protease Inhibitor (Roche-Sigma Aldrich)) was added per plate and the cells scratched. The lysate was recovered and passed through a needle (22G) 2 to 3 times to reduce viscosity. At this point, an aliquot of the lysate (1%) was recovered and stored at -20°C as input. Then, 25µl (per plate) of magnetic streptavidin-coated beads (New England BioLabs) was added to the lysate

and the mix was incubated in soft agitation for 2h at 4°C. The beads were then separated using a magnet for 30 minutes and washed with Pull-Down Washing Buffer 1 (20 mM Tris-HCl pH 7.5, 500 mM LiCl, 0.1% SDS, 1 mM EDTA). The beads were then washed again with Washing buffer 2 (20 mM Tris-HCl pH 7.5, 500 mM LiCl, 1 mM EDTA), separated for 20 minutes and washed one last time with Washing buffer 3 (20mM Tris-HCl pH 7.5, 200 mM LiCl, 1 mM EDTA) followed by magnetic separation for 15 minutes. After all the washes, the beads were resuspended again in denaturing 4x loading buffer and boiled for 10 minutes at 97°C. Next, the different pulled-down components were separated by electrophoresis on a 12% SDS-polyacrylamide gel until the loading buffer left the gel. The protocol used for the identification of the putative partners of miR-503 by mass spectrometry can be found in the Supplementary Methods.

Immunoprecipitation assays and qPCR

To detect the affinity of the identified proteins with miR-503, HUVECs or HMVECs were transfected with a synthetic miR-503 (10 nM) (identical to the native mature miR-503) following the same protocol used for miR-503-biotin transfection. Twenty-four hours after removing the media and 48h after transfection, cells were washed twice with ice cold PBS and incubated with 1 mM dithiobis (succinimidyl propionate) DSP (ThermoFisher) in soft agitation for 2 h at 4°C. Then, the reaction was stopped by removing the supernatant, adding 20 mM Tris HCl and incubating at room temperature for additional 30 minutes. After washing twice with ice-cold PBS, the plates were set on an ice tray and irradiated with UV light to induce RNA-protein crosslinking (0.4 J/cm2 of 365-nm UV light with a Stratalinker 2400). Then, 25 µl of RIPA buffer was added to the plates and these were scratched using a scraper. The lysate was then recovered into an Eppendorf tube and incubated on ice for 15 minutes. Then, the samples were centrifuged, and the pellet (cellular debris) discarded. A preclearing of the samples (to reduce nonspecific binding of peptides to the beads), was performed by adding 50 µl of Protein A agarose beads (per plate) (Sigma-Aldrich, 11719408001) and incubating the sample for 2 h at 4 °C with rotation. After that, the samples were centrifuged at 2.800 rpm and 4°C for 3 minutes to pellet the beads. The supernatant was recovered and 5µl of antibody was added per plate used. The samples were left to incubate and rotate overnight at 4°C. The following day, 50 µl of Protein A agarose beads (per plate) was added, and the samples were incubated again for 2 h more at 4°C in rotation. Then, the beads were recovered by centrifugation (3 minutes at 2800 g and 4 °C) and washed three times with IP Lysis Buffer (50 nM Hepes pH 7.5; 150 nM NaCl; 1% Triton X-100) (lacking protease inhibitors) for 1 h. After the final wash, the beads

were resuspended in 100 µl of PBS and RNA extraction was performed using miRNEasy kit (Qiagen) following the manufacturer instructions. The antibodies used for immunoprecipitation were ANXA2 (#610069, BD Pharmingen), FN1 (#610077, BD Phamingen), HNRNPA2B1(#Ab6102, Abcam), TSP1(# MA5-13398, Thermo Fisher) and VIM (#MO72529, DAKO)). To identify unspecific interactions, HUVECs were transfected with 10 nM of cel-miR-67 and the same protocol was followed.

Small-interfering RNA assays

Small interfering RNAs (siRNAs) were used to knock down the levels of expression of anxa2, fn1, hnrnpA2B1, TSP1, and vim. A scramble siRNA (a siRNA without targets in the human genome) was used as a control in all experiments at the same concentration used for the knock down of the other proteins. Oligonucleotides were purchased from Eurogentec and sequences are shown in the supplementary material. The transfection protocol was as follows per ml of final volume to transfect: 700 µl of a solution of EGM2 and cells was combined with 300 µl of a solution containing the transfectant and siRNA in EBM2. To prepare this mixture, 0.5 µl of DharmaFECT 4 (Dharmacon) was mixed with 149.5 µl of serum-free EBM2 (for each milliliter) and incubated for 10 minutes at room temperature. Posteriorly, a solution containing 149 µl of serum-free EBM2 and 1 µl of siRNA at a concentration of 20 µM was mixed with the DharmaFECT dilution and incubated again at room temperature for another 20 minutes. Finally, the cells (700 µl) were seeded in a plate or flask previously coated with gelatine, and the siRNA-DharmaFECT solution was added. The following day, the supernatant was removed, and full media (EGM2) was added to the cells. To validate the efficiency of protein knockdown, 100,000 HUVECs were seeded in a 6-well plate and transfected with the siRNAs. The plates/flasks were then scratched, and the cells were either lysed with RIPA buffer for further protein analysis or mixed with TRIzol for RNA extraction. The time points used for the validation were 24, 48 and 72 h for RNA and 48, 72 and 96 h for proteins. The rationale behind the 24 h delay (for protein level assessment) was to allow the normal levels of the protein in the cell to naturally decrease and thus more reliably observe the effect of the gene knockdown at the protein level. For the production of exosomes after protein knockdown and treatment with epirubicin, $1.8.10^6$ cells (for the nontreated conditions (NT)) and $5.5.10^6$ cells (for cells treated with epirubicin) were seeded in each T175 flask and transfected to a final volume of 18 ml following the protocol mentioned above. Then, the next day, the supernatant was fully recovered and replaced with 20 ml of full EGM2 supplemented (or not) with 1 µg/ml epirubicin. The next day, the entire supernatant was discarded, and 20 ml of exosome-depleted (exofree)

EGM2 was added. Four T175 flasks were used per condition. The cells were incubated in these conditions for 72 h, after which the exosomes were purified. The levels of miR-503 in the cells after the knockdown of the genes were assessed 24 after the addition of the exosome-depleted media.

Quantitative analysis of gene and microRNA expression by RT-qPCR

The purification of RNA from cellular sources was performed using the miRNeasy kit (Qiagen) following the manufacturer's instructions. The RNA was resuspended in RNAse-free water and quantified by Nanodrop (ThermoFisher). The same kit was used to extract RNA from exosomes although a modification step was added: five volumes of TRIzol were added to the exosomes and the volumes of chloroform and ethanol were adjusted accordingly. RNA was suspended in RNAse-free water and quantified with the Quant-it Ribogreen RNA assay kit (R11490, ThermoFisher) on black 96-well plates. The emitted fluorescence was assessed using a spectrophotometer (2030 Multilabel Reader VICTORTM X3 from Perkin Elmer) at 592 nm (emission range of fluorescein).

Two different approaches were used to measure the levels of different genes depending on their type. The variation in coding genes (gapdh, anxa2, hnRNPA2B1, TSP1, vim) were assessed by qRT-PCR. For that purpose, the synthesis of cDNA was performed starting from 500ng of RNA using the iScript Kit (BioRad) following the manufacturer's instructions. The levels of mRNA in the samples were then assessed by qPCR using a SYBER system (Takyon – Eurogentec) and detected with a thermocycler (Applied Biosystems 7900HT – Applied Biosystems). gapdh was used as housekeeping gene to normalized variations in the levels of input RNA. For each experiment performed, two negative controls were used: a sample lacking retrotranscriptase enzyme (RT-) and one lacking primers. Only experiments with undetected gene levels for these two controls were considered. The sequences used for the design of the probes are in the Supplementary Methods.

For the detection of cellular non-coding RNAs (RNU44, RNU48, miR-503, let-7d, miR-16 miR-210, and cel-miR-67), 3.33 ng of RNA were retrotranscribed using the TaqMan Reverse Transcription Kit (Applied Biosystem) with the TaqMan microRNA Assay (Applied Biosystems). The detection of the levels of these genes was performed using 2.2 µl of the cDNA product, 1.7 µl of TaqMan microRNA Assay Reagent (Applied Biosystem) and a dilution of TaqMan Universal Master Mix (Applied Biosystem) (16.5 µl of enzyme diluted with 12.6 µl of RNAse free water). The mix was prepared prior to plating and 10 µl of solution was added

per well. The average levels of RNU44 and RNU48 were used to normalize RNA input in the cells. In the case of exosomal RNA detection, 1.67 µl of RNA extract were used per reaction and the normalization was performed against the average levels of let-7d and miR-16. Since this system of detection does not amplify DNA products, only the negative control lacking primers was prepared per experiment. In all cases, the level of the genes was assessed using the $^{\Delta\Delta Ct}$ method (Livak and Schmittgen, 2001).

Immunofluorescence assays

HUVECs were seeded in coverslips at a density of $2.5.10^4$ cells/well and treated (or not) with epirubicin, from 24 to 72 hours. Cells were then washed three times with PBS, fixed for ten minutes with 4% paraformaldehyde (PFA) and then permeabilized with 70% ethanol overnight. After permeabilization, the cells were washed again three times with PBS and blocked with 5% BSA for 30 min at room temperature. Then, the cells were incubated with anti-ANXA2 (1:100; #8235, Cell Signaling), anti-hnRNPA2B1 (1:100; #Ab6102, Abcam), anti-VIM (1:100; #MO72529, DAKO) and anti-TSP1 (1:100; # MA5-13398, Thermo Fisher) for 1h at room temperature. After incubation, cells were washed three times with PBS, and incubated an additional 1h with Alexa488-conjugated goat anti-mouse IgG (1:300; Thermo Fisher Scientific) and DAPI (1:500; Thermo Fisher Scientific). Then, cells were washed three times with PBS and once with distilled water. Finally, the coverslips were mounted on slides using Prolong (Thermo Fisher Scientific) and visualized under a confocal microscope (Leica SP5, Leica Microsystems, Wetzlar, Germany). The fluorescence intensity of hnRNPA2B1 staining in HUVEC cells was assessed using the plugin "Intensity Ratio Nuclei-Cytoplasm" on ImageJ-FIJI.

Subcellular fractionation

Endothelial cells were treated (or not) with epirubicin (1µg/ml; Sigma-Aldrich, Saint-Louis, Missouri, USA) for 24h. At 24, 48 and 72h after starting treatment, cells were trypsinized and pelleted by centrifugation at 1000g for 5 minutes at 4°C. Later, the cells were washed twice with cold PBS and permeabilized with 0.5 % PBS-Tween for 10 minutes. Then, the cells were resuspended in Buffer A (1M Hepes pH 7.9; 1M KCl; 1M $MgCl_2$; 1 M Sucrose; 10 % Glycerol; 1M, Dithiothreitol 0.01 ‰; Triton X-100 protease and phosphatase inhibitors (Sigma-Aldrich, Saint-Louis, Missouri, USA); diethylpyrocarbonate-(DEPC) water) and incubated on ice for 5 minutes. The lysates were then centrifuged at 1300 g for 4 minutes at 4°C. The supernatant (S1) was recovered and centrifuged at 20,000g for 15 minutes at 4°C. The cytosolic fraction (second

supernatant, S2) was recovered and stored at -20°C. The pellet (P1) was washed with Buffer A twice, and resuspended in Buffer B (EDTA 100 mM pH 8; EGTA 50 mM pH 8; Dithiothréitol 1M; protease and phosphatase inhibitors (Sigma-Aldrich, Saint-Louis, Missouri, USA); DEPC-water). The solution was then incubated on ice for 30 minutes followed by centrifugation at 1700g for 4 minutes (4°C°). The nuclear fraction present in the supernatant (S3), was recovered and stored at -20°C. The different fractions were characterized by Western Blotting using the nuclear marker Histone H3 (#ab1791, Abcam) and the cytoplasmic marker GAPDH (#ab8245; Abcam). The levels of hnRNPA2B1 were detected by Western blotting in equimolar quantities of protein (10µg) from the cytoplasmic and nuclear fractions and quantified using ImageJ.

Statistical analysis

All experiments were performed a minimum of 3 times unless otherwise stated. The plotted values represent the mean of the biological replicates ± the standard error of the mean (SEM) or the standard deviation (SD); the technique used is specified for each case in the figure legend. The statistical significance of the results was assessed using an unpaired t-test.

1.4. Results

1.4.1. Characterization of exosomes and identification of miR-503 binding partners

Extracellular vesicles (EVs) were purified using ultracentrifugation and characterized by Western blotting detecting the following exosomal (CD63, CD9, CD81, syntenin) and cellular markers (mitochondrial cytochrome C) (**Fig. R 25a**). Dynamic light scattering revealed vesicles with an average size of 100 nm (**Fig. R 25b**), suggesting an enrichment of exosomes in our preparation. Electronic microscopy analysis confirms the size as well as the presence the tetraspanin CD63 and the endothelial marker CD105 (**Fig. R 25c**).

As previously shown (Bovy et al., 2015), Epirubicin increases the export of miR-503 into exosomes in human umbilical vein endothelial cells (HUVECs) (**Fig. R 25d**). To identify the binding partners of miR-503 we transfected HUVECs with a synthetic miR-503-biotin. We then determined if the biotinylation of miR-503 interfered with the mechanism of export triggered by Epirubicin by assessing the levels of miR-503 in exosomes after treatment (**Suppl. Fig. S1**). We found little to no effect linked to the presence of a biotin tag in the selective export of miR-503 in response to Epirubicin, ranging around the 2-fold increase in native conditions (**Fig. R 25d**) and after miR-503 biotin transfection (**Suppl. Fig. S2a**).

To identify the miR-503 binding partners, we transfected HUVECs with the biotin-microRNA construct and followed a double crosslinking strategy (**Fig. R 25e**): first, by inducing the formation of RNA-protein bonds and, second, by stabilizing protein-protein interactions. Following this methodology, we pulled down the microRNA and identified its binding protein partners by mass spectrometry. The efficiency of the transfection of miR-503-Biotin was assessed by qPCR on cellular lysates (**Suppl. Fig. S2b**).

A total of 9 different proteins were identified by mass spectrometry: Propionyl-CoA carboxylase alpha subunit (PCCA), Pyruvate Carboxilase (PC), Heparan sulfate proteoglycan 2 (Perlecan), Fibronectin 1 (FN1), Thrombospondin-1 (TSP1), β-Actin (ACTB), Vimentin (VIM), Annexin A2 (ANXA2) and heterogeneous nuclear ribonucleoprotein A2/B1 (hnRNPA2B1). A brief description of their main roles in the cell is summarized in **Supplementary Table S 5**. Both PCCA and PC are binders of endogenous biotin, hence their identification (Tong, 2013); they were not considered for further analysis. Perlecan, TSP1 and FN1 are both part of the extracellular matrix (Hellewell et al., 2015; Neill et al., 2013; Viana et al., 2013), while ACTB and VIM are main components of the cytoskeleton and regulate motility, cellular stability and cellular division (Dave and Bayless, 2014; Dominguez and Holmes, 2011). ANXA2, via its involvement in cellular transduction, can modulate cellular growth and various signaling processes. In addition, it was also recently discovered that ANXA2 can bind to mRNAs (Aukrust et al., 2007; Luo and Hajjar, 2013; Vedeler et al., 2012) and mediate the exosomal export of microRNAs. The most well-known function of hnRNPA2B1 is shuttling mRNA from the nucleus to the cytoplasm and regulating post-transcriptional gene expression (He and Smith, 2009). Interestingly, hnRNPA2B1 can also bind microRNAs with a specific sequence and promote their export into exosomes (Villarroya-Beltri et al., 2013).

The microRNA-protein association between miR-503 and its putative partners was then validated by Western blotting with the proteins of interest in the biotinylated-miR-503 pull down fraction. Figure 1f shows that, ACTB and Perlecan were not found in association with miR-503-botin while FN1, TSP1, hnRNPA2B1 and, to a lesser extent, VIM and ANXA2, were enriched in the pull-down fraction.

To mitigate bias associated with the unspecific detection of proteins, we transfected HUVECs with a c. elegans microRNA carrying a biotin tag (cel-miR-67-biotin). The efficiency of the transfection is shown in **Suppl. Figure S2c** and the effect of Epi on the exosomal export of cel-miR-67 in **Suppl. Figure S2d**. Then, we pulled down the microRNA and detected by

Western Blot the proteins previously validated. Our results (**Fig. R 25f**) pointed to FN1 as a non-specific contaminant of our pull down and was excluded from further analysis.

The putative complex formed by miR-503 in combination with ANXA2, hnRNPA2B1, TSP1 and VIM will be referred to in the following sections as the MicroRNA Exporting Complex or MEC.

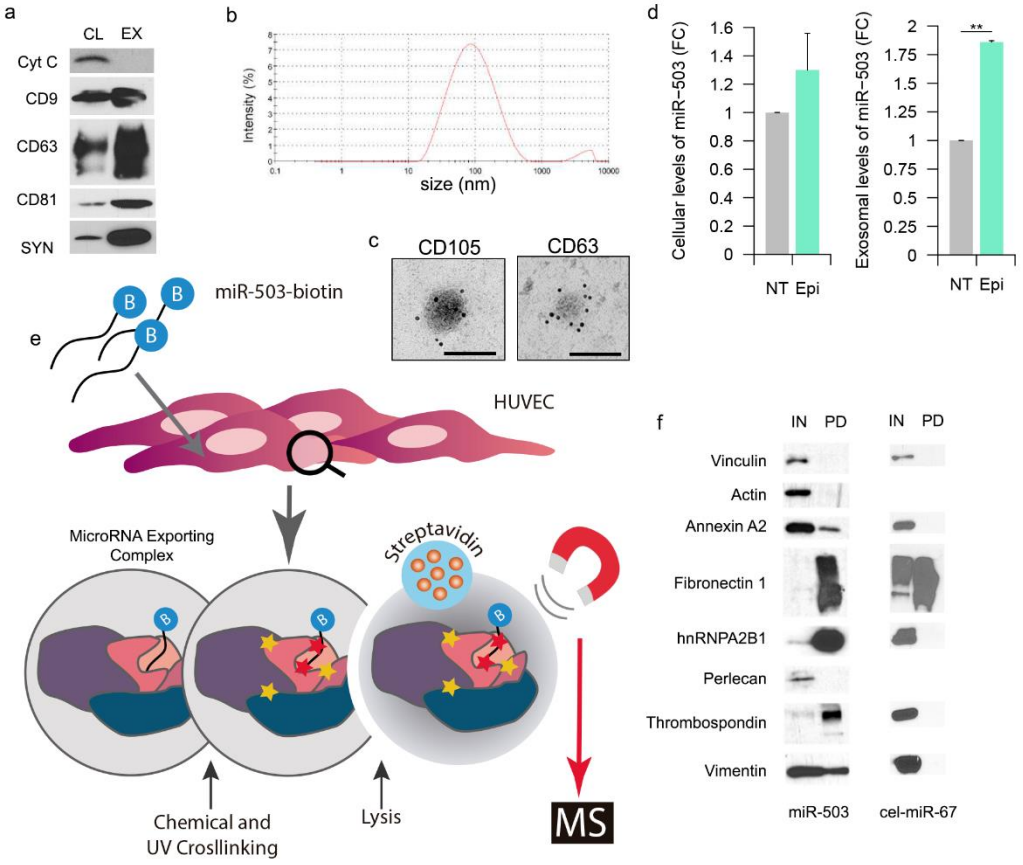

Figure R 25. Exosome characterization and identification of miR-503 binding proteins.
a *exosome characterization of HUVEC lysates and exosomes (10 µg) against the EV markers: CD9, CD63, CD81, syntenin (SYN), and the cellular marker cytochrome C (Cyt C).* ***b*** *Dynamic light scattering analysis of exosomal preparations.* ***c*** *Electron microscopy images of HUVEC exosomes labeled with anti-CD63 and anti-CD105, scale bars = 100 nm.* ***d*** *Cells were treated with epirubicin for 24h. Cell lysates were prepared 24h after treatment and exosomes were collected 72h after removing the chemotherapeutic drug. Cellular and exosomal levels of miR-503 were evaluated by qPCR. Data show mean ± SEM (n = 3). **p < 0.01 vs. respective control.* ***e*** *Schematic representation of the protocol used to identify the MEC proteins. HUVECs (30×10^6 cells) were transfected with miR-503-biotin (10 nM). The following day, the cells were crosslinked with DTSSP and UV. HUVECs lysates were incubated with streptavidin beads. Both input (IN)(cellular lysate) and pull-down fractions (PD) were separated by SDS-PAGE. Isolated proteins were identified by mass spectrometry and f validated by western blotting against pull-down (PD) and input (IN) (1% of cell lysate) fractions using vinculin as loading control. Cel-miR-67 was used as a negative control for the pull-down.*

1.4.2. Epirubicin does not regulate the expression of the MEC components

To study whether Epirubicin regulates the expression of some of the components of the MEC in HUVECs, we assessed the mRNA and protein abundance in cells after treatment. As shown in **figure R 26a**, Epirubicin reduces the expression of TSP1 and hnRNPA2B1. Interestingly, the regulation is only significant 24h after treating the cells with Epirubicin. At protein level (**Fig. R 26b**), we observe that Epirubicin has little effect on the protein abundance of the MEC components: while changes in the abundance of ANXA2 and TSP1 follow a similar trend to the changes observed at RNA level, the effect is too modest to be significant. These results suggest that Epirubicin does not affect the export of miR-503 by regulating the abundance of the MEC components.

1.4.3. The exosomal export of ANXA2 is regulated by Epirubicin

To determine if miR-503 is co-exported with all or some of the components of the MEC, we treated HUVECs with Epirubicin and then collected the exosomes produced during the following 72h. With the exception of VIM, all MEC proteins were detected in exosomes (**Fig. R 26d**). Interestingly, only ANXA2 showed a strong enrichment (average 8-fold) in exosomes after the treatment with Epirubicin. Taken together, these results suggest that the MEC is, at least, partially destabilized upon Epirubicin treatment.

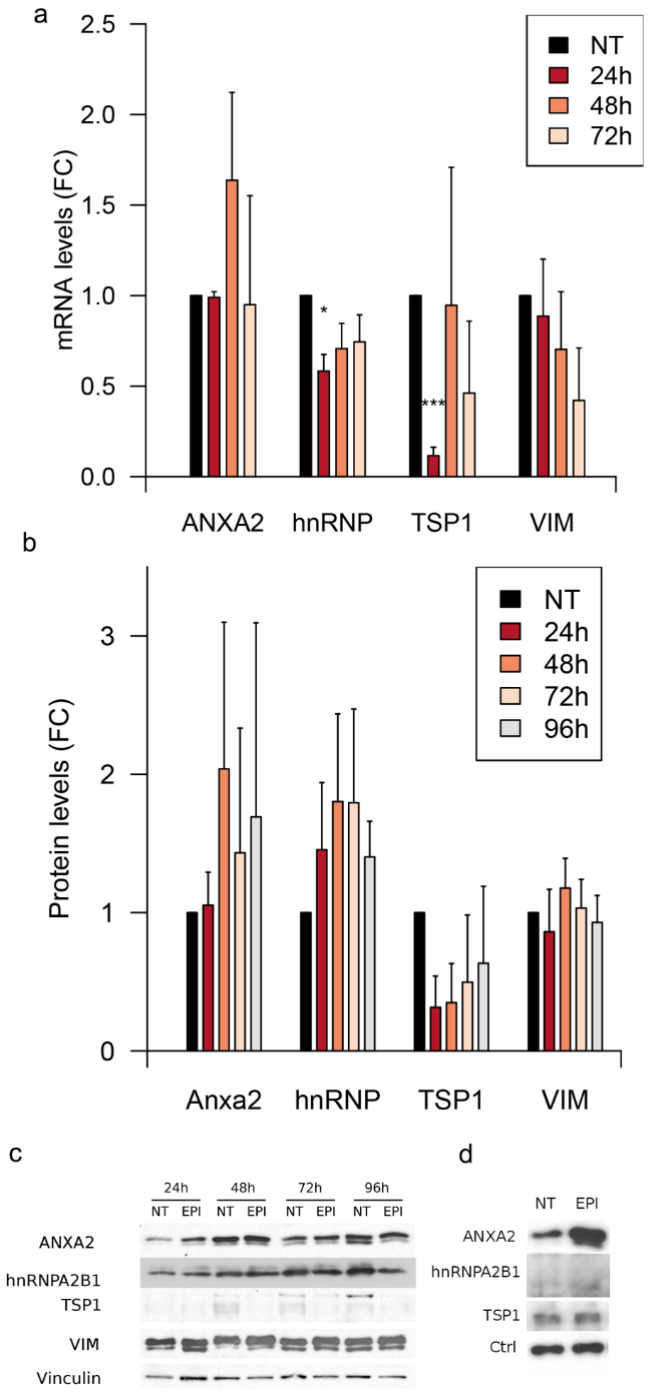

Figure R 26. Epirubicin regulates the mRNA levels of TSP1 and hnRNPA2B1.
HUVECs were treated with epirubicin for 24h and the levels of (a) RNA and (b) proteins were assessed, respectively, by qPCR at 24, 48 and 72h after treatment and western blotting at 24, 48, 72 and 96 h after treatment. Data represent fold change against non-treated cells. Plots show mean and SEM from three independent experiments (, p<0.05; ***, p<0.001). (c) Representative western blot. (d) HUVECs were treated with epirubicin for 24h and exosomes were produced for additional 72h. Exosomes were purified by ultracentrifugation and the levels of proteins were determined by western blotting (10 µg). Representative example of n = 3.*

1.4.4. ANXA2 and miR-503 present the most stable interaction among the MEC components

To study the composition of the MEC, we decided to pull down miR-503 prior any crosslinking and after only inducing the formation of protein-RNA bonds with UV crosslinking. Theoretically, the strongest interaction between the components of the MEC and the microRNA should be maintained in non-crosslinked conditions while the weakest interactions would only be detected when both UV and chemical crosslinkings were performed. Our results (**Fig. R 27a**) suggest that in the absence of crosslinking, ANXA2 is the most abundant MEC protein present in the pull down. To a much lesser extent, VIM can also be detected in non-crosslinked conditions. Interestingly, both TSP1 and hnRNPA2B1 can only be detected when both crosslinkings are performed.

1.4.5. Epirubicin disrupts the interaction between miR-503 and hnRNPA2B1 and VIM

We then assessed if the interaction between miR-503 and the MEC components was affected by Epirubicin treatment. For that purpose, the components of the MEC were immuno-precipitated and the levels of miR-503 determined by qPCR. A shown in **Fig. R 27b**, in untreated conditions, miR-503 was co-precipitated with all MEC components, although the levels bound to ANXA2 were minimal. Interestingly, hnRNPA2B1 showed very high affinity for miR-503 (10, 36 and 79-fold change when compared to the cellular lysate).

To study if the interaction between the components of the MEC and miR-503 was affected by the chemotherapeutic drug, we treated endothelial cells with Epirubicin and measured the levels of miR-503 in the immunoprecipates before and after treatment (**Fig. R 27c**). In the cases of VIM, and hnRNPA2B1 a significant reduction of miR-503 in the immunoprecipitates was observed after treatment ($p = 0.025$, $p = 0.002$ and $p = 0.00003$, respectively). Strikingly, the opposite effect was observed for ANXA2 (~2.3-fold increase, $p=0.019$). In addition, when using the transfection of cel-miR-67 as a negative control (**Suppl. figures S3a and S3b**), we observed that Epirubicin does not have any effect on the interaction between these proteins and the exogenous RNA. In combination, these results suggest that Epirubicin modulates the interaction between miR-503 and some components of the MEC (ANXA2, VIM and hnRNPA2B1).

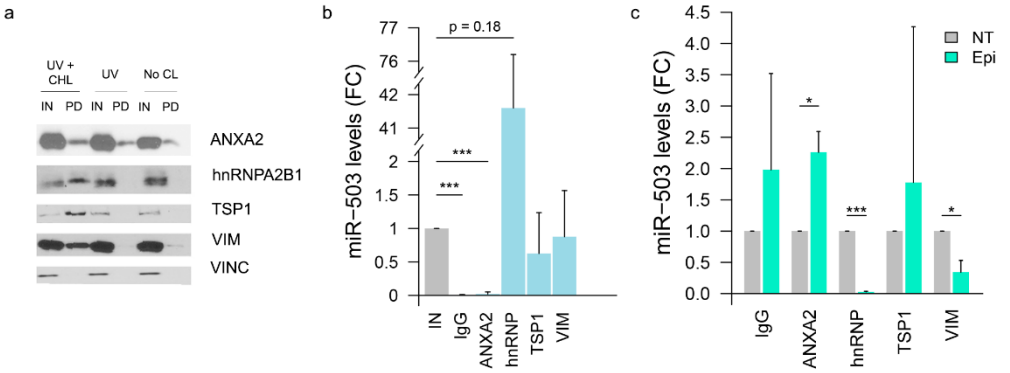

Figure R 27. Epirubicin disrupts the interaction between miR-503 and VIM and hnRNPA2B1.
*(**a**) HUVEC (30.10^6 cells) were transfected with miR-503-biotin (10 nM). The following day, cells were crosslinked with DTSSP and UV (UV + CHL), only UV (UV) or not subjected to any crosslinking (No CL). HUVECs lysates were incubated with streptavidin beads. Both input (IN) (cellular lysate) and pull-down fractions (PD) were separated by SDS-PAGE and revealed by western-blotting using indicated proteins. Input (IN) = 1% of cell lysate. Vinculin was used as loading control. (**b**,**c**) HUVECs were transfected with miR-503 (10 nM). 48h later, immunoprecipitation assays were performed using the indicated antibodies or an IgG control and the levels of miR-503 were evaluated by qPCR. Plots show (**b**) fold change of miR-503 in the immunoprecipitated (IP) vs input fractions (IN) in non-treated cells and (**c**) fold change of immunoprecipitated miR-503 in epirubicin-treated (EPI) vs non-treated cells (NT). Plots represent mean and SEM from three independent experiments (*p<0.05; **p<0.01;***p<0.001). IN = 1% of the cellular lysate before immunoprecipitation.*

1.4.6. Epirubicin treatment promotes the relocation of hnRNPA2B1 into the nucleus

Aiming to assess whether the changes in affinity between MEC components and miR-503 were associated to fluctuations in protein distribution, we decided to study the effect of Epirubicin on protein localization. Confocal analysis revealed that, in untreated conditions, hnRNPA2B1 is mainly located in the nucleus and in some cytoplasmic granules (**Fig. R 28a** and **28b**). Interestingly, Epirubicin treatment promotes the relocation of hnRNPA2B1 into the nucleus 24 and 48 h after treatment. This migration was not observed for any of the other MEC components (**Suppl. Figure S4a**). The relocation of hnRNPA2B1 was confirmed by Western blotting analysis of subcellular fractions (validation of the technique in **Supplementary figure S4b**) showing an increase in the ratio between cytoplasmic and nuclear abundance at 24 and 48 h that is partially reverted at 72h (**Fig. R 28a** and **R 28d**).

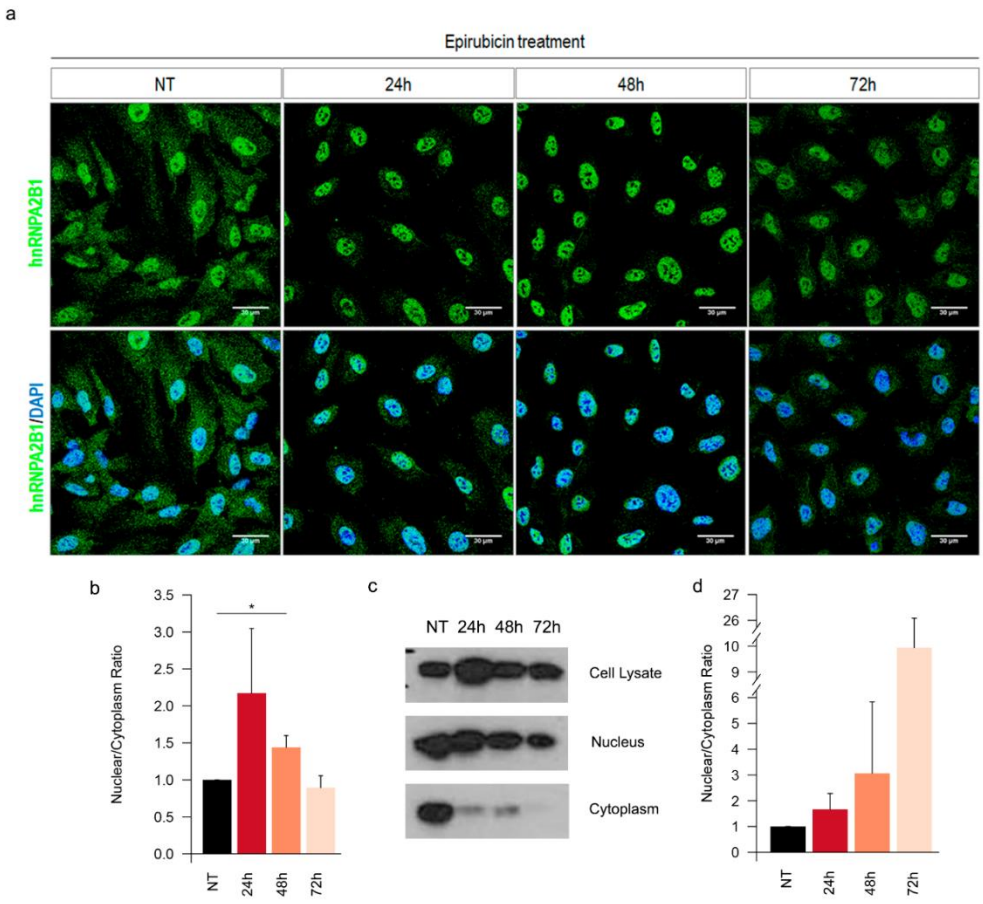

Figure R 28. hnRNPA2B1 relocalizes into the nucleus after epirubicin treatment.
*(**a**) Confocal images of hnRNPA2B1 (green) and DAPI (blue) of HUVECs treated with epirubicin for 24h. Pictures taken at the indicated times after starting the treatment. (**b**) Quantification of the intensity in the cytoplasm and nucleus were performed using ImageJ on epifluorescence images. (**c**) Nuclear and cytoplasmic fractions from HUVECs treated with epirubicin and analyzed by western blotting for hnRNPA2B1 localization. (**d**) Abundance ratio of hnRNPA2B1 between nucleus and cytoplasm in subcellular fractions. All plots show results from three independent experiments (*p<0.05). Validation of subcellular fractionation method in in Supplementary Figure S4.*

1.4.7. ANXA2 and hnRNPA2B1 are key mediators of the exosomal export of miR-503

To study the role of the MEC components in the export of miR-503, we used a dual approach. First, we studied if the abundance of the components of the MEC could determine the fate of miR-503 or miR-210, a microRNA-control present in the cell at similar concentrations than miR-503. For that purpose, we knocked down the putative partners of the microRNA (validation of siRNA knock-down in **Supplementary figure S5**) and assessed the exosomal export of the microRNAs. Our results (**Fig. R 29a**) suggest that the knock down of TSP1 reduces significantly the export of miR-503, although the level by which is reduced is minimal (fold change 0.8). Interestingly, both the knock down of ANXA2 and hnRNPA2B1 increased the export of miR-503. While lower levels of ANXA2 induce a 1.5-fold increase,

slightly below the increase observed upon Epirubicin treatment in non-transfected conditions, the knock down of hnRNPA2B1 reproduced the effect of the chemotherapeutic drug to the same levels (ranging in 2-3 fold change increase). No significant differences were observed for the knock down of vim in untreated conditions and none of the MEC protein knock-downs affected significantly the export of miR-210 (**Fig. R 29d**).

Second, we studied whether the knockdown of the MEC proteins could affect the incorporation of miR-503 into exosomes triggered by the treatment with Epirubicin. For that purpose, cells transfected with siRNA against the components of the MEC (or siScramble) were treated with Epirubicin and the levels of exosomal miR-503 were assessed. Our results show that, the knock down of any of the components of the MEC reduced the exosomal encapsulation of miR-503 upon Epirubicin treatment (**Fig. R 29b**). Interestingly, the knock down of both ANXA2 and hnRNPA2B1 had the most dramatic effect on the exosomal encapsulation of miR-503. While no effect was observed in untreated conditions, Epirubicin seemed to reduce the exosomal export of miR-210 in most conditions, although when compared to siScr, none of the knockdowns had any effect (**Fig. R 29e**).

Finally, we determined whether the changes observed in the exosomal microRNA profiles were a reflection of changes in the cellular levels of miR-503, or the consequence of a specific export mechanism (**Fig. R 29c**). The knock down of any of the components of the MEC failed to increase the cellular production of miR-503. Only when hnRNPA2B1 was knocked down did we observe a modest but significant reduction in the cellular levels of miR-503. In the case of miR-210 (**Fig. R 29f**), any treatment of the cells with either siRNA or Epirubicin induced the production of reduced levels of this microRNA.

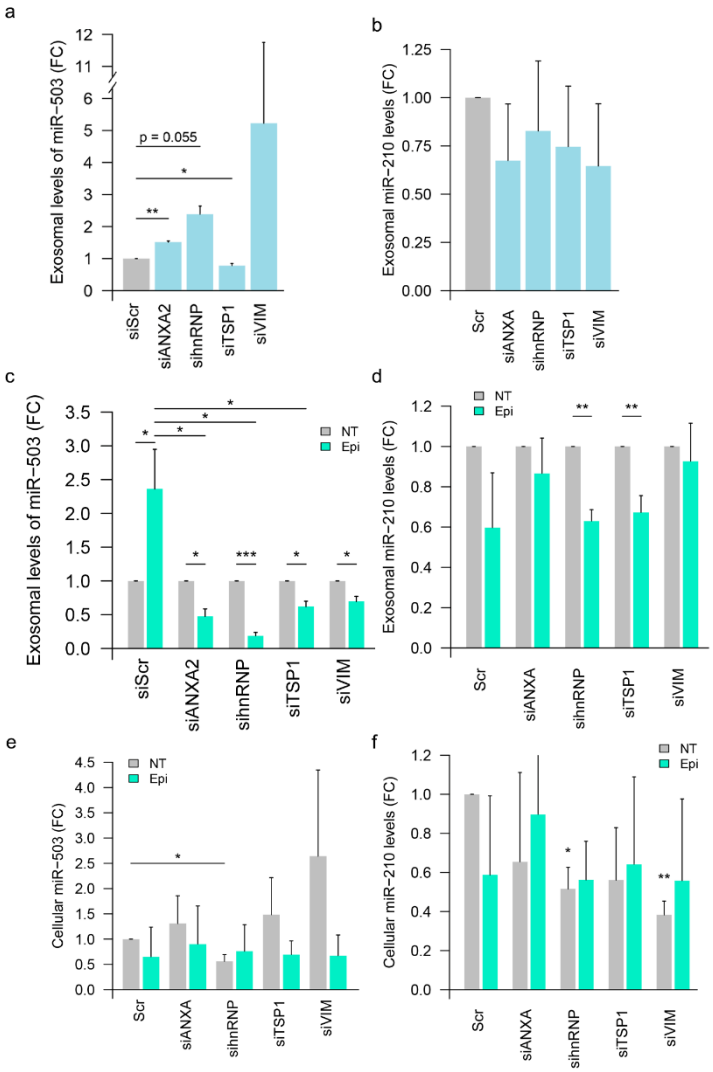

Figure R 29. ANXA2, hnRNPA2B1, TSP1 and VIM are necessary for the effect of epirubicin on the exosomal export of miR-503.

*HUVECs were transfected with siRNA for the indicated protein or control siRNA (siScr) (20 nM). Then, cells were treated with epirubicin for 24 h (or not) and exosomes were produced for the following 72 h. The levels of miR-503 (**a**, **c**, **e**) and miR-210 (**b**, **d**, **f**) in purified cells and exosomes were then assessed via qPCR. Data show fold change of miR-503 (**a**) and miR-210 (**b**) in exosomes from siRNA-transfected cells vs Scramble RNA-transfected (siScr) cells in non-treated conditions. Fold change of miR-503 and mR-210 respectively in exosomes (**c**, **d**) and cells (**e**, **f**) after siRNA transfection and epirubicin treatment normalized to untreated conditions. Plots show mean and SEM of three independent experiments (*p < 0.05; **p < 0.01, ***p < 0.001).*

1.4.8. Exosomal export of miR-503 is conserved in microvascular cells

To validate our findings, we confirmed our results with microvascular cells (HMVECs), endothelial cells presenting a closer phenotype to cells located in the tumor microenvironment. First, we assessed whether Epirubicin also induced the exosomal export of miR-503. For that purpose, we isolated HMVEC exosomes from Epirubicin-treated or untreated cells. Our findings suggest (**Fig. R 30a**) that the treatment with the chemotherapeutic drug also induces

miR-503 sorting into exosomes. Then, we determined if miR-503 also interacted with the same MEC partners in HMVEC. Our results showed (**Fig. R 30b**) that, after pulling down miR-503-biotin, we could detect two of the previously identified MEC components (ANXA2 and hnRNPA2B1) while TSP1 and VIM were not detected.

To study if Epirubicin also affects the interaction between miR-503 and some components of the MEC in HMVECs, we treated these cells with Epirubicin and then immuno-precipitated the proteins of interest. Our results show that, both in untreated conditions (**Fig. R 30c**) and after treatment (**Fig. R 30d**), the interaction between miR-503 and the MEC components follow the same trends observed for HUVECs: before treatment, the levels of ANXA2 binding miR-503 are low while the opposite is observed for hnRNPA2B1 (**Fig. R 30c**). After treatment, these interactions are reversed and increased miR-503 is found in the immunoprecipitated of ANXA2 while less microRNA is associated to hnRNPA2B1.

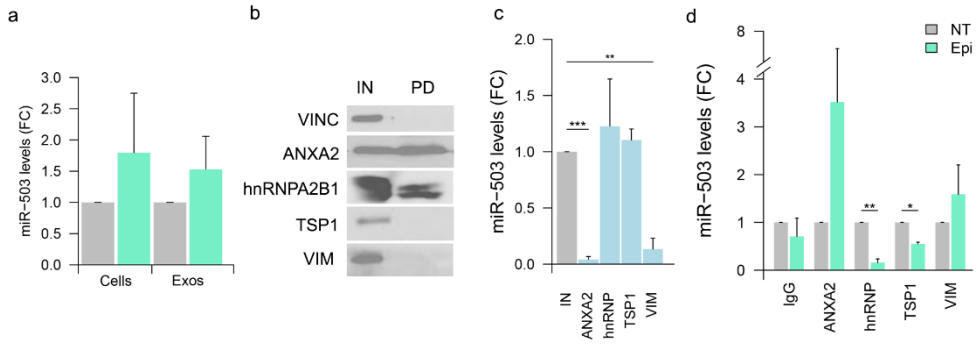

Figure R 30. ANXA2 and hnRNPA2B1 are necessary for the effect of epirubicin on the exosomal export of miR 503 in microvascular endothelial cells.

HMVECs were treated with epirubicin for 24h. Cell lysates were prepared 24 h after treatment and exosomes were collected 72h after removing the chemotherapeutic drug. Cellular and exosomal levels of miR-503 were evaluated by qPCR. Plot represents mean and SEM (n = 3). ***(b)*** *HMVECs were transfected with miR-503-biotin (10 nM). The following day, the cells were crosslinked with DTSSP and UV. HMECs lysates were incubated with streptavidin beads. Both input (IN) (cellular lysate) and pull-down fractions (PD) were separated by SDS-PAGE. Previously identified components of the MEC complex were validated by western blotting against pull-down (PD) and input (IN) (1% of cell lysate) fraction using vinculin as loading control.* ***(c)*** *HMVECs were transfected with 10 nM of miR-503. 48h later, immunoprecipitation assays were performed using the indicated antibodies and the levels of miR-503 were evaluated by qPCR. Plot shows fold change of miR-503 in the immunoprecipitated (IP) vs input fractions (IN) in non-treated cells and* ***(d)*** *fold change of immunoprecipitated miR-503 in epirubicin-treated (EPI) vs non-treated cells (NT). Plots represent mean and SEM from three independent experiments (*p<0.05; **p<0.01; ***p<0.001). IN = 1% of the cellular lysate before immunoprecipitation.*

1.5. Discussion

In previous work we showed that the treatment with the chemotherapeutic agent Epirubicin induces the over-export of the anti-tumoral miRNA-503 in endothelial cells. These results suggested the presence of a specific mechanism behind the sorting of this microRNA. Unfortunately, little is known about the machinery regulating the exosomal export of microRNAs. Only a few studies have reported the role of RNA-binding proteins in promoting the export of some subclasses of microRNAs (hnRNPA2B1 (Villarroya-Beltri et al., 2013), Syncrip (Santangelo et al., 2016), MVP (Teng et al., 2017), MEX3C (Lu et al., 2017) and Y-Box (Shurtleff et al., 2016)). Surprisingly, in this study we show that the exosomal sorting of miR-503 is negatively regulated by its binding to hnRNPA2B1. This is the first evidence showing that RBPs can bind and prevent the export of miRNAs into exosomes.

The proteomic analysis of the binding partners of miR-503 revealed 9 potential proteins possibly involved in exosomal miR-503 export. Leaving aside the two proteins identified as natural biotin binders, one protein identified as a non-specific contaminant and those not validated by Western blotting, the identified partners of miR-503 were TSP1, VIM, ANXA2 and hnRNPA2B1.

While no relationship has been established between TSP1 and the binding or export of RNAs, thrombospondin-1 has often been studied in the extracellular compartment. This protein is underrepresented in exosomes derived from nasopharyngeal carcinoma cells (Chan et al., 2015) and in EVs derived from cells undergoing epithelial to mesenchymal transition (EMT) (Tauro et al., 2013). Despite this, most of the publications studying circulating TSP1 have focused on its role in angiogenesis (Dudek and Mahaseth, 2005; Gonzalez et al., 2004) and as a marker of EMT (Kudo-Saito et al., 2009). Our results propose an ambiguous role for TSP1 in the MEC: the knock down of this protein suggests that TSP1 has a modest but significant effect in the exosomal export of miR-503 independently of the treatment with Epirubicin. However, no significant differences were observed when the interaction between TSP1 and miR-503 was studied. These results suggest that TSP1 may be involved in the interaction between secondary partners of the MEC and the microRNA export machinery but not directly binding the microRNA and regulating its export.

Our study suggests that VIM could be involved in the export of miR-503: in cells with reduced VIM abundance, Epirubicin fails to promote the exosomal export of miR-503. Given that in untreated conditions the knock down of this protein does not have any significant effect,

it is possible that VIM regulates the localization of the MEC before the release of miR-503 for exosomal encapsulation. This hypothesis is supported by two factors: first, this protein was mostly pulled down after inducing the formation of protein-protein bonds. Second, by the physiological role of VIM in the cell: vimentin regulates the reorganization of the cellular cytoskeleton and the rearrangement of extracellular adhesion molecules (Liu et al., 2015). Several publications have also found that VIM can be encapsulated into exosomes and that the levels at which it can be found often correlate with aggressiveness in the parent cells (Jeppesen et al., 2014). Unfortunately, in the cellular model used in this study, we could not detect this protein in the extracellular fraction. In addition, VIM was recently found to bind RNAs: VIM can stabilize collagen mRNA by binding to a stem loop region found at the 5'UTR (Challa and Stefanovic, 2011). After this study, it has been repeatedly showed that VIM can stabilize several other mRNAs following the same mechanism: alkaline phosphatase mRNA (Schmidt et al., 2015), mu-opioid receptor (Song et al., 2013) and eIF2α (Chatterjee et al., 2013). Even though our experiments failed to prove direct binding between VIM and miR-503, we show that Epirubicin can disrupt the interaction between these partners and propose a role for VIM during microRNA exosomal export.

ANXA2 is one of the top 20 most common proteins found in exosomes (Mathivanan et al., 2012) and mediates EV uptake via the immobilization of the vesicles to the surface of the recipient cells (Koumangoye et al., 2011). At the cellular level, ANXA2 has been associated with exo- and endocytosis, as well as with the traffic of membranous bodies, lipid raft formation, and signal transduction (reviewed in Wang and Lin, 2014). Moreover, ANXA2 can induce EMT by increasing the migration and invasion capacities of cancer cells (Wang et al., 2015, p. 3), reducing apoptosis and mediating multi-drug resistance (Zhang et al., 2014). At the extracellular level, ANXA2 can induce pro-angiogenic processes and metastatic phenotypic switch by promoting cellular motility (Ling et al., 2004; Maji et al., 2016; Sharma et al., 2006). Regarding RNA, some studies have found that ANXA2 can bind some mRNAs such as c-myc (Filipenko et al., 2004) and "Infectious Bronchitis Virus pseudoknot" RNA (Kwak et al., 2011). Additionally, another recently published study shows that some proteins of the same calcium-biding signaling family regulate the export of exosomal microRNAs. Although promising, these results showed that ANXA2 only participates in the encapsulation of 6 specific microRNAs without shared motifs (Hagiwara et al., 2015) (none of them miR-503). According to our results, ANXA2 has an affinity for miR-503 stable enough that it is pulled down without any sort of crosslinking. These results, in combination with previous evidence showing that ANXA2 can bind RNA suggest that ANXA2 is the main protein in the MEC directly interacting with miR-

503. Although the treatment with Epirubicin only increases modestly but not significantly the levels of cellular ANXA2, its exosomal export is increased by 8-fold. Even though the relative quantity of ANXA2 binding to miR-503 under untreated conditions is very low, likely due to the high abundance of this protein in the cell, the treatment with Epirubicin strongly increases the pull down of miR-503-bound ANXA2 (2.5-fold). This switch could indicate that either Epirubicin induces the binding of ANXA2 to the microRNA promoting its exosomal export or that epitopes unavailable for IP are revealed upon treatment. Since in untreated conditions, ANXA2 already shows a strong interaction with miR-503, our results support the latter hypothesis. At the same time, given that reduced levels of ANXA2 promote the export of miR-503 in untreated conditions but impair the export induced by Epirubicin, our results point to a crucial role for ANXA2 in the microRNA export mechanism triggered by chemotherapy.

The second component of the MEC, key in the export of miR-503 into exosomes is hnRNPA2B1. The known roles of hnRNPA2B1 include DNA replication and repair, RNA nuclear export, pre-mRNA splicing, mRNA stability (He and Smith, 2009), pri-miRNA processing and mediation of splicing events (Alarcón et al., 2015), among others. In addition, hnRNPA2B1 can also bind to lncRNAs and regulate the expression of some genes at post-transcriptional level (Lan et al., 2016). Several studies have also focused on the role of this protein in disease. In hepatocellular carcinoma, hnRNPA2B1 can act as an oncogene via the control of alternative splicing processes (Shilo et al., 2014) and induction of EMT (Zhou et al., 2014). Moreover, hnRNAP2B1 has been found to be a circulating biomarker of lung cancer (Dowling et al., 2015) and a dual mediator of the development of breast cancer. First, hnRNPA2B1 is associated with the loss of breast cancer susceptibility gene 1 (brca1) (Santarosa et al., 2010) and, second, by being a regulator of the STAT3-ERK1/2 signaling pathway (Hu et al., 2017). hnRNPA2B1 has also been linked to the efficiency of chemotherapy in vitro: Inhibition of hnRNPA2B1 expression improved chemosensitivity to gemcitabine, 5-fluorouracil (5-FU), and oxaliplatin in pancreatic cancer cell lines (Gu and Liu, 2013).

Regarding exosomal RNA loading, hnRNPA2B1 was the first RBP known to regulate the export of microRNAs. In their study, Villarroya et al discovered that this protein binds to microRNAs with a specific motif and promotes their exosomal export upon sumoylation (Villarroya-Beltri et al., 2013). Interestingly, miR-503 does not have the “exo-motif” described in this study, likely suggesting that the involvement of hnRNPA2B1 in the export of this microRNA does not follow the same mechanism. Moreover, unlike in their study, we did not observe any differences in the sumoylation of hnRNPA2B1 between cells and exosomes, likely

due to differences in the cellular model used. Another recent study showed that hnRNPA2B1 can bind the host gene of miR-503 (Wang et al., 2018). These results suggest that the binding region of this RBP falls outside the coordinates of the mature miR-503, thus supporting the hypothesis that hnRNPA2B1 does not directly bind to miR-503. Our data showed that hnRNPA2B1 can only be identified along with miR-503 when both protein-protein and protein-UV crosslinking is induced. These results propose the hypothesis that hnRNPA2B1 does not bind directly to miR-503 but to other components of the MEC. Our findings also point to hnRNPA2B1 having high affinity for miR-503 (avg 40-fold) and that, upon Epirubicin treatment, this affinity is strongly reduced. At the same time, we have shown that Epirubicin induces the relocation of cytoplasmic hnRNPA2B1 towards the nucleus. Interestingly, reduced levels of hnRNPA2B1 also promote the export of exosomal miR-503 to the same levels observed by the treatment with Epirubicin alone (~2.5-fold).

The combination of these results suggests that Epirubicin induces the increased exosomal export of miR-503 by disrupting the interaction between hnRNPA2B1 and miR-503/ANXA2. Then, hnRNPA2B1 is relocated into the nucleus and a fraction of the initial MEC, composed by ANXA2 binding to miR-503, is sorted into exosomes. Our findings suggest that ANXA2 mediates the interaction between miR-503 and hnRNPA2B1. These results are supported by the evidence showing that when the levels of ANXA2 are reduced (by siRNA), Epirubicin cannot promote the over export of miR-503 because hnRNPA2B1 is no longer associated to this microRNA. The validation of our results in HMVECs prove the conservation of a miR-503/ANXA2/hnRNPA2B1 axis across different subtypes of endothelial cells thus supporting the role of both RBPs in mediating the export of microRNAs. Given that hnRNPA2B1 mediates repair processes at sites of DNA double strand break (DBS) hotspots (Tchurikov et al., 2013), we hypothesize that the relocation of hnRNPA2B1 towards the nucleus upon Epirubicin treatment could respond to a recycling mechanism initiated by the DNA destabilization triggered by the chemotherapeutic drug. Whether this relocation is the cause of the MEC destabilization or its consequence, remains unknown. Although several independent studies (Santangelo et al., 2016; Villarroya-Beltri et al., 2013) have found a series of RBPs that can bind and promote the export of microRNAs, this study is the first one to propose a mechanism by which proteins can promote cellular retention and inhibit the exosomal export of a specific microRNA.

Acknowledgements

We thank the technology platforms support staff at the GIGA Research Center. We thank Marie-Alice Meuweis for her support in designing and interpreting the mass spectrometry data. This study was supported by the University of Liège (ULg), the Fonds National de la Recherche Scientifique (FNRS), Télévie and the Fonds Léon Frédéricq. The authors declare that they have no competing interests.

AUTHOR CONTRIBUTIONS

JPB designed, supervised, conducted and performed experiments and statistical analyses, interpreted the data, and wrote the manuscript. AB performed the experiments with HMVECs, immunofluorescence, fractionation experiments and exosome characterization. performed experiments and provided technical backup. FD participated in data analysis and provided scientific suggestions. IS conceived and designed the study, coordinated the experiments, and wrote the manuscript. All authors read and approved the final manuscript.

Competing interests

The authors declare no competing interests.

1.6. References

Alarcón CR, Goodarzi H, Lee H, Liu X, Tavazoie S, Tavazoie SF. 2015. HNRNPA2B1 Is a Mediator of m(6)A-Dependent Nuclear RNA Processing Events. Cell 162:1299–1308. doi:10.1016/j.cell.2015.08.011

Aukrust I, Hollås H, Strand E, Evensen L, Travé G, Flatmark T, Vedeler A. 2007. The mRNA-binding Site of Annexin A2 Resides in Helices C–D of its Domain IV. J Mol Biol 368:1367–1378. doi:10.1016/j.jmb.2007.02.094

Beach A, Zhang H-G, Ratajczak MZ, Kakar SS. 2014. Exosomes: an overview of biogenesis, composition and role in ovarian cancer. J Ovarian Res 7:14. doi:10.1186/1757-2215-7-14

Bovy N, Blomme B, Frères P, Dederen S, Nivelles O, Lion M, Carnet O, Martial JA, Noël A, Thiry M, Jérusalem G, Josse C, Bours V, Tabruyn SP, Struman I. 2015. Endothelial exosomes contribute to the antitumor response during breast cancer neoadjuvant chemotherapy via microRNA transfer. Oncotarget 6:10253–10266. doi:10.18632/oncotarget.3520

Challa AA, Stefanovic B. 2011. A novel role of vimentin filaments: binding and stabilization of collagen mRNAs. Mol Cell Biol 31:3773–3789. doi:10.1128/MCB.05263-11

Chan Y-K, Zhang H, Liu P, Tsao S-W, Lung ML, Mak N-K, Ngok-Shun Wong R, Ying-Kit Yue P. 2015. Proteomic analysis of exosomes from nasopharyngeal carcinoma cell identifies intercellular transfer of angiogenic proteins. Int J Cancer 137:1830–1841. doi:10.1002/ijc.29562

Chatterjee S, Panda AC, Berwal SK, Sreejith RK, Ritvika C, Seshadri V, Pal JK. 2013. Vimentin is a component of a complex that binds to the 5'-UTR of human heme-regulated eIF2α kinase mRNA and regulates its translation. FEBS Lett 587:474–480. doi:10.1016/j.febslet.2013.01.013

Dave JM, Bayless KJ. 2014. Vimentin as an integral regulator of cell adhesion and endothelial sprouting. Microcirc (New York, NY 1994) 21:333–344. doi:10.1111/micc.12111

Dominguez R, Holmes KC. 2011. Actin structure and function. Annu Rev Biophys 40:169–186. doi:10.1146/annurev-biophys-042910-155359

Dowling P, Pollard D, Larkin A, Henry M, Meleady P, Gately K, O'Byrne K, Barr MP, Lynch V, Ballot J, Crown J, Moriarty M, O'Brien E, Morgan R, Clynes M. 2015. Abnormal levels of heterogeneous nuclear ribonucleoprotein A2B1 (hnRNPA2B1) in tumour tissue and blood samples from patients diagnosed with lung cancer. Mol Biosyst 11:743–752. doi:10.1039/c4mb00384e

Dreyer F, Baur A. 2016. Biogenesis and Functions of Exosomes and Extracellular Vesicles. Methods Mol Biol 1448:201–216. doi:10.1007/978-1-4939-3753-0_15

Dudek AZ, Mahaseth H. 2005. Circulating angiogenic cytokines in patients with advanced non-small cell lung cancer: correlation with treatment response and survival. Cancer Invest 23:193–200.

Filipenko NR, MacLeod TJ, Yoon C-S, Waisman DM. 2004. Annexin A2 is a novel RNA-binding protein. J Biol Chem 279:8723–8731. doi:10.1074/jbc.M311951200

Gonzalez FJ, Rueda A, Sevilla I, Alonso L, Villarreal V, Torres E, Alba E. 2004. Shift in the balance between circulating thrombospondin-1 and vascular endothelial growth factor in cancer patients: Relationship to platelet a-granule content and primary activation. Int J Biol Markers 19:221–228. doi:10.5301/JBM.2008.1959

Gu W-J, Liu H-L. 2013. Induction of pancreatic cancer cell apoptosis, invasion, migration, and enhancement of chemotherapy sensitivity of gemcitabine, 5-FU, and oxaliplatin by hnRNP A2/B1 siRNA. Anticancer Drugs 24:1. doi:10.1097/CAD.0b013e3283608bc5

Hagiwara K, Katsuda T, Gailhouste L, Kosaka N, Ochiya T. 2015. Commitment of Annexin A2 in recruitment of microRNAs into extracellular vesicles. FEBS Lett 589:4071–4078. doi:10.1016/j.febslet.2015.11.036

Hamidi H, Ivaska J. 2017. Vascular Morphogenesis: An Integrin and Fibronectin Highway. Curr Biol 27:R158–R161. doi:10.1016/j.cub.2016.12.036

He Y, Smith R. 2009. Nuclear functions of heterogeneous nuclear ribonucleoproteins A/B. Cell Mol Life Sci 66:1239–1256. doi:10.1007/s00018-008-8532-1

Hellewell AL, Gong X, Schärich K, Christofidou ED, Adams JC. 2015. Modulation of the extracellular matrix patterning of thrombospondins by actin dynamics and thrombospondin oligomer state. Biosci Rep 35. doi:10.1042/BSR20140168

Hu Y, Sun Z, Deng J, Hu B, Yan W, Wei H, Jiang J. 2017. Splicing factor hnRNPA2B1 contributes to tumorigenic potential of breast cancer cells through STAT3 and ERK1/2 signaling pathway. Tumour Biol J Int Soc Oncodevelopmental Biol Med 39:1010428317694318. doi:10.1177/1010428317694318

Jaffe EA, Nachman RL, Becker CG, Minick CR. 1973. Culture of human endothelial cells derived from umbilical veins. Identification by morphologic and immunologic criteria. J Clin Invest 52:2745–2756. doi:10.1172/JCI107470

Jeppesen DK, Nawrocki A, Jensen SG, Thorsen K, Whitehead B, Howard KA, Dyrskjøt L, Ørntoft TF, Larsen MR, Ostenfeld MS. 2014. Quantitative proteomics of fractionated membrane and lumen exosome proteins from isogenic metastatic and nonmetastatic bladder cancer cells reveal differential expression of EMT factors. Proteomics 14:699–712. doi:10.1002/pmic.201300452

Kalluri R, LeBleu VS. 2017. Discovery of Double-Stranded Genomic DNA in Circulating Exosomes. Cold Spring Harb Symp Quant Biol LXXXI:030932. doi:10.1101/sqb.2016.81.030932

Koumangoye RB, Sakwe AM, Goodwin JS, Patel T, Ochieng J. 2011. Detachment of Breast Tumor Cells Induces Rapid Secretion of Exosomes Which Subsequently Mediate Cellular Adhesion and Spreading. PLoS One 6:e24234. doi:10.1371/journal.pone.0024234

Kudo-Saito C, Shirako H, Takeuchi T, Kawakami Y. 2009. Cancer metastasis is accelerated through immunosuppression during Snail-induced EMT of cancer cells. Cancer Cell 15:195–206. doi:10.1016/j.ccr.2009.01.023

Kwak H, Park MW, Jeong S. 2011. Annexin A2 Binds RNA and Reduces the Frameshifting Efficiency of Infectious Bronchitis Virus. PLoS One 6:e24067. doi:10.1371/journal.pone.0024067

Lahav J, Lawler J, Gimbrone MA. 1984. Thrombospondin interactions with fibronectin and fibrinogen. Eur J Biochem 145:151–156. doi:10.1111/j.1432-1033.1984.tb08534.x

Lan X, Yan J, Ren J, Zhong B, Li J, Li Y, Liu L, Yi J, Sun Q, Yang X, Sun J, Meng L, Zhu W, Holmdahl R, Li D, Lu S. 2016. A novel long noncoding RNA Lnc-HC binds hnRNPA2B1 to regulate expressions of Cyp7a1 and Abca1 in hepatocytic cholesterol metabolism: Hepatology, Vol. XX, No. X, 2015 Lan et al. Hepatology 64:58–72. doi:10.1002/hep.28391

Li Q, Shao Y, Zhang X, Zheng T, Miao M, Qin L, Wang B, Ye G, Xiao B, Guo J. 2015. Plasma long noncoding RNA protected by exosomes as a potential stable biomarker for gastric cancer. Tumour Biol J Int Soc Oncodevelopmental Biol Med 36:2007–2012. doi:10.1007/s13277-014-2807-y

Ling Q, Jacovina AT, Deora A, Febbraio M, Simantov R, Silverstein RL, Hempstead B, Mark WH, Hajjar KA. 2004. Annexin II regulates fibrin homeostasis and neoangiogenesis in vivo. J Clin Invest 113:38–48. doi:10.1172/JCI19684

Liu C-Y, Lin H-H, Tang M-J, Wang Y-K. 2015. Vimentin contributes to epithelial-mesenchymal transition cancer cell mechanics by mediating cytoskeletal organization and focal adhesion maturation. Oncotarget 6:15966–15983.

Livak KJ, Schmittgen TD. 2001. Analysis of relative gene expression data using real-time quantitative PCR and the 2(-Delta Delta C(T)) Method. Methods 25:402–408.

Lötvall J, Hill AF, Hochberg F, Buzás EI, Di Vizio D, Gardiner C, Gho YS, Kurochkin I V, Mathivanan S, Quesenberry P, Sahoo S, Tahara H, Wauben MH, Witwer KW, Théry C. 2014. Minimal experimental requirements for definition of extracellular vesicles and their functions: a position statement from the International Society for Extracellular Vesicles. J Extracell vesicles 3:26913. doi:http://dx.doi.org/10.3402/jev.v3.26913

Lu P, Li H, Li N, Singh RN, Bishop CE, Chen X, Lu B. 2017. MEX3C interacts with adaptor-related protein complex 2 and involves in miR-451a exosomal sorting. PLoS One 12:1–25. doi:10.1371/journal.pone.0185992

Luo M, Hajjar KA. 2013. Annexin A2 system in human biology: cell surface and beyond. Semin Thromb Hemost 39:338–346. doi:10.1055/s-0033-1334143

Maji S, Chaudhary P, Akopova I, Nguyen PM, Hare RJ, Gryczynski I, Vishwanatha JK. 2016. Exosomal Annexin A2 Promotes Angiogenesis and Breast Cancer Metastasis. Mol cancer Res MCR. doi:10.1158/1541-7786.MCR-16-0163

Mathivanan S, Fahner CJ, Reid GE, Simpson RJ. 2012. ExoCarta 2012: database of exosomal proteins, RNA and lipids. Nucleic Acids Res 40:D1241–D1244. doi:10.1093/nar/gkr828

McKelvey KJ, Powell KL, Ashton AW, Morris JM, McCracken SA. 2015. Exosomes: Mechanisms of Uptake. J Circ Biomarkers 4. doi:10.5772/61186

Neill T, Jones HR, Crane-Smith Z, Owens RT, Schaefer L, Iozzo R V. 2013. Decorin evokes rapid secretion of thrombospondin-1 in basal breast carcinoma cells via inhibition of RhoA/ROCK1. FEBS J 280:2353–2368. doi:10.1111/febs.12148

Ørom UA, Lund AH. 2007. Isolation of microRNA targets using biotinylated synthetic microRNAs. Methods 43:162–165. doi:10.1016/j.ymeth.2007.04.007

Pérez-Boza J, Lion M, Struman I. 2018. Exploring the RNA landscape of endothelial exosomes. RNA 24:423–435. doi:10.1261/rna.064352.117

Purushothaman A, Bandari SK, Liu J, Mobley JA, Brown EE, Sanderson RD. 2016. Fibronectin on the Surface of Myeloma Cell-derived Exosomes Mediates Exosome-Cell Interactions. J Biol Chem 291:1652–1663. doi:10.1074/jbc.M115.686295

Rambout X, Detiffe C, Bruyr J, Mariavelle E, Cherkaoui M, Brohée S, Demoitié P, Lebrun M, Soin R, Lesage B, Guedri K, Beullens M, Bollen M, Farazi TA, Kettmann R, Struman I, Hill DE, Vidal M, Kruys V, Simonis N, Twizere J-C, Dequiedt F. 2016. The transcription factor ERG recruits CCR4-NOT to control mRNA decay and mitotic progression. Nat Struct Mol Biol 23:663–672. doi:10.1038/NSMB.3243

Record M, Carayon K, Poirot M, Silvente-Poirot S. 2014. Exosomes as new vesicular lipid transporters involved in cell-cell communication and various pathophysiologies. Biochim Biophys Acta 1841:108–120. doi:10.1016/j.bbalip.2013.10.004

Santangelo L, Giurato G, Cicchini C, Montaldo C, Mancone C, Tarallo R, Battistelli C, Alonzi T, Weisz A, Tripodi M. 2016. The RNA-Binding Protein SYNCRIP Is a Component of the Hepatocyte Exosomal Machinery Controlling MicroRNA Sorting. Cell Rep 17:799–808. doi:10.1016/j.celrep.2016.09.031

Santarosa M, Del Col L, Viel A, Bivi N, D'Ambrosio C, Scaloni A, Tell G, Maestro R. 2010. BRCA1 modulates the expression of hnRNPA2B1 and KHSRP. Cell Cycle 9:4666–4673. doi:10.4161/cc.9.23.14022

Schmidt Y, Biniossek M, Stark GB, Finkenzeller G, Simunovic F. 2015. Osteoblastic alkaline phosphatase mRNA is stabilized by binding to vimentin intermediary filaments. Biol Chem 396:253–260. doi:10.1515/hsz-2014-0274

Sharma MR, Rothman V, Tuszynski GP, Sharma MC. 2006. Antibody-directed targeting of angiostatin's receptor annexin II inhibits Lewis Lung Carcinoma tumor growth via blocking of plasminogen activation: possible biochemical mechanism of angiostatin's action. Exp Mol Pathol 81:136–145. doi:10.1016/j.yexmp.2006.03.002

Shilo A, Ben Hur V, Denichenko P, Stein I, Pikarsky E, Rauch J, Kolch W, Zender L, Karni R. 2014. Splicing factor hnRNP A2 activates the Ras-MAPK-ERK pathway by controlling A-Raf splicing in hepatocellular carcinoma development. RNA 20:505–515. doi:10.1261/rna.042259.113

Shurtleff M, Karfilis K V., Temoche-Diaz M, Ri S, Schekman R. 2016. Y-box protein 1 is required to sort microRNAs into exosomes in cells and in a cell-free reaction. Elife 5:e19276. doi:10.1101/040238

Song KY, Choi HS, Law P-Y, Wei L-N, Loh HH. 2013. Vimentin interacts with the 5'-untranslated region of mouse mu opioid receptor (MOR) and is required for post-transcriptional regulation. RNA Biol 10:256–266. doi:10.4161/rna.23022

Tauro BJ, Mathias RA, Greening DW, Gopal SK, Ji H, Kapp EA, Coleman BM, Hill AF, Kusebauch U, Hallows JL, Shteynberg D, Moritz RL, Zhu H-J, Simpson RJ. 2013. Oncogenic H-ras reprograms Madin-Darby canine kidney (MDCK) cell-derived exosomal proteins following epithelial-mesenchymal transition. Mol Cell proteomics MCP 12:2148–2159. doi:10.1074/mcp.M112.027086

Tchurikov NA, Kretova O V., Fedoseeva DM, Sosin D V., Grachev SA, Serebraykova M V., Romanenko SA, Vorobieva N V., Kravatsky Y V. 2013. DNA Double-Strand Breaks Coupled with PARP1 and HNRNPA2B1 Binding Sites Flank Coordinately Expressed Domains in Human Chromosomes. PLoS Genet 9:e1003429. doi:10.1371/journal.pgen.1003429

Teng Y, Ren Y, Hu X, Mu J, Samykutty A, Zhuang X, Deng Z, Kumar A, Zhang L, Merchant ML, Yan J, Miller DM, Zhang HG. 2017. MVP-mediated exosomal sorting of miR-193a promotes colon cancer progression. Nat Commun 8:1–16. doi:10.1038/ncomms14448

Tong L. 2013. Structure and function of biotin-dependent carboxylases. Cell Mol life Sci C 70:863–891. doi:10.1007/s00018-012-1096-0

van Niel G, D'Angelo G, Raposo G. 2018. Shedding light on the cell biology of extracellular vesicles. Nat Rev Mol Cell Biol. doi:10.1038/nrm.2017.125

Vedeler A, Hollås H, Grindheim AK, Raddum AM. 2012. Multiple roles of annexin A2 in post-transcriptional regulation of gene expression. Curr Protein Pept Sci 13:401–412.

Viana L de S, Affonso RJ, Silva SRM, Denadai MVA, Matos D, Salinas de Souza C, Waisberg J. 2013. Relationship between the expression of the extracellular matrix genes SPARC, SPP1, FN1, ITGA5 and ITGAV and clinicopathological parameters of tumor progression and colorectal cancer dissemination. Oncology 84:81–91. doi:10.1159/000343436

Villarroya-Beltri C, Gutiérrez-Vázquez C, Sánchez-Cabo F, Pérez-Hernández D, Vázquez J, Martin-Cofreces N, Martinez-Herrera DJ, Pascual-Montano A, Mittelbrunn M, Sánchez-Madrid F. 2013. Sumoylated hnRNPA2B1 controls the sorting of miRNAs into exosomes through binding to specific motifs. Nat Commun 4:2980. doi:10.1038/ncomms3980

Wang C-Y, Lin C-F. 2014. Annexin A2: Its Molecular Regulation and Cellular Expression in Cancer Development. Dis Markers 2014. doi:10.1155/2014/308976

Wang H, Liang L, Dong Q, Huan L, He J, Li B, Yang C, Jin H, Wei L, Yu C, Zhao F, Li J, Yao M, Qin W, Qin L, He X. 2018. Long noncoding RNA miR503HG, a prognostic indicator, inhibits tumor metastasis by regulating the HNRNPA2B1/NF-κB pathway in hepatocellular carcinoma. Theranostics 8:2814–2829. doi:10.7150/thno.23012

Wang T, Yuan J, Zhang J, Tian R, Ji W, Zhou Y, Yang Y, Song W, Zhang F, Niu R. 2015. Anxa2 binds to STAT3 and promotes epithelial to mesenchymal transition in breast cancer cells. Oncotarget 6:30975–30992. doi:10.18632/oncotarget.5199

Zhang F, Zhang H, Wang Z, Yu M, Tian R, Ji W, Yang Y, Niu R. 2014. P-glycoprotein associates with Anxa2 and promotes invasion in multidrug resistant breast cancer cells. Biochem Pharmacol 87:292–302. doi:10.1016/j.bcp.2013.11.003

Zhou Z-J, Dai Z, Zhou S-L, Hu Z-Q, Chen Q, Zhao Y-M, Shi Y-H, Gao Q, Wu W-Z, Qiu S-J, Zhou J, Fan J. 2014. HNRNPAB induces epithelial-mesenchymal transition and promotes metastasis of hepatocellular carcinoma by transcriptionally activating SNAIL. Cancer Res 74:2750–2762. doi:10.1158/0008-5472.CAN-13-2509

1.7. Supplementary Methods

Protein identification by Mass Spectrometry

HUVECs were transfected with miR-503 biotin as described in miR-503 pulldown section. Forty plates were used for the experiments of identification of the miR-503-biotin partners by Mass Spectrometry and 10 for the validation of the results by Western Blotting.

Following, the gel was fixed for 3h with a solution of 50% ethanol and 3% phosphoric acid. Then it was washed three times in milliQ water for 20 minutes each time. Next, the gel was incubated for 1h in a solution of 34% methanol, 3% phosphoric acid and 17% ammonium sulphate. Passed that time, Coomassie Blue G250 was added to the previous incubation (to a concentration of 360mg/L) and it was left in incubation for 3 days at room temperature. Following that period, the gel was washed with MilliQ water to de-stain unspecific color binding.

Proteins bands were excised from the gel. Each spot was placed in a well of a multi-well plate for automatic digestion using Janus liquid handling station (Perkin Elmer). Each spot was washed for 5 minutes with 50 µl of 50 mM ammonium bicarbonate solution, the liquid was then removed and 50 µl of 50/50 50 mM ammonium bicarbonate solution/acetonitrile were used to wash each spot during 5 minutes then the liquid was removed. These 2x washes were repeated once more. Then reduction of disulfide bonds was done by adding 50 µl of DTT (dithiothreitol) 10 mM per well, the plate was maintained at 56°C under agitation for 45 minutes. The DTT solution was removed after cooling of the multi-well plate at 20°C and 40 µl of iodoacetamide 55 mM was added to each well, mix for 1 minute by agitation and then allow to react during 1 hour at 20°C. The liquid was then removed.

The spots were washed again using the procedure described above. Then the spots were dehydrated by adding 60 µl of acetonitrile per well, mix for 5 minutes. Then the liquid was removed and the spots were dried 1 hour at 40°C then 1 hour at 20°C. The multi-well was then cooled to 4°C. For digestion, 3 µl of 10 ng/µl trypsin in 25 mM ammonium bicarbonate solution were added to each well, mix for 1 minute and incubate for 1 hour at 4°C and then for 4 hours at 37°C. The peptides were extracted using 15 µl of a solution 1% trifluoroacetic acid under agitation for 30 minutes at 40°C, then 2 hours at 20°C with a mixing of 5 minutes every 2 hours.

The peptide extracts were pooled if several spots came from the same 1D gel band. Then the volume of the pool was reduced under vacuum using a speed-vacuum (Thermo Scientific) to 25 µl (except for sample 16_3575 for which we reduced the volume to 50 µl). From these

pools, 9 µl (for file A3184-C-160930-AXT) or 10 µl (for file A3420*-C-161018-AXT) were injected onto the LC-MS/MS system. The UPLC system is a NanoAcquity (Waters) equipped with an Acquity UPLC M-Class HSS T3 Column, 1.8µm, 75µm*250mm (Waters) as analytical column and a Acquity UPLC M-Class Symmetry C18 Trap Column, 100A, 5µm, 180µm*20mm, 2G V/M (Waters) as Trap column. This UPLC system is hyphenated to a nano-ESI ion trap mass spectrometer Amazon Speed ETD (Bruker) operated in positive ion mode. The main parameters used for the analyses are given below:

A) Gradients

a. Trapping

Time (min)		Flow (µl/min)		%A1	%B1
0	20	98.0	2.0		
3	20	98.0	2.0		

This step allows to load the sample on the TRAP column during 3 minutes, then the valve change position and what has been trapped on the trap column is eluted on the analytical column (mode analytical) and sent to the mass spectrometer.

b. Analytical

Time (min)		Flow (µl/min)		%A1	%B1
0	0.3	98.0	2.0		
3	0.3	93.0	7.0		
25	0.3	70.0	30.0		
30	0.3	60.0	40.0		
34	0.3	10.0	90.0		
38	0.3	10.0	90.0		
42	0.3	98.0	2.0		
57	0.3	98.0	2.0		

The gradient « Analytical » allows the peptides elution from the Trap and analytical columns. The eluate is sent to the mass spectrometer.

B) MS Method

The principal parameters for the run were the following: nanoflow: ESI; capillary: 4500V; endplate offset: 500V; nebulizer: 15psi; dry gas: 5.0L/min; dry temperature: 220°C; target mass: 900m/z; compound stability: 100%; trap drive level: 100%; autoMS: 2; number of precursor ions: 8; MS mode: enhanced; MS/MS mode: Xtreme; ICC target: 200000; Max time: 200.00ms; scan range 200 to 1500m/z and excluse after 2 Spectra/Release after 2min.

The raw data were searched against SwissProt database (release 2014_05, 545388 sequences) limited to Human taxonomy (20339 sequences) using Mascot 2.2.06 (Matrix Science) for sequence alignment and ProteinScape software (Bruker) for generating output files for database search. Significant identifications were considered when at least 2 unique peptides (with Mascot score of at least 15) were identified per protein hits with at least one peptide showing an identity Mascot Score. False discovery rate associated with significant score was <0.1%.

Results

Chapter II

Impact of endothelial hnRNPA2B1 silencing on breast cancer cells behavior

2. Impact of endothelial hnRNPA2B1 silencing on breast cancer cells behavior

Previous work in the lab has shown that a tumor mimicking environment reduced the sorting of the anti-tumoral miRNA, miR-503. Moreover, the chemotherapeutic agent epirubicin increased the export of this particular miRNA in exosomes released by endothelial cells. miR-503-loaded exosomes could then affect tumor behavior (Bovy *et al.*, 2015). In the first part of this work, we found that miR-503 is present in the cell in a complex composed of several proteins also called miR-EXO proteins. One of them, hnRNPA2B1, binds miR-503 in the cytoplasm. Epirubicin disrupt this binding leading to the release and export of miR-503 into EVs. Indeed, hnRNPA2B1 inhibits the exosomal export of miR-503 in endothelial EVs (Pérez-Boza, Boeckx, *et al*., 2020). In the present work, we wanted to assess if the miR-EXO proteins silencing would affect breast cancer cell behavior. To study the impact of miR-EXO proteins on cancer cell behavior, we decided to use a transwell-coculture system where endothelial cells, transfected with siRNA against the identified proteins, were cocultured with MDA-MB-231 cells for 48 hours (**Fig. R 31**).

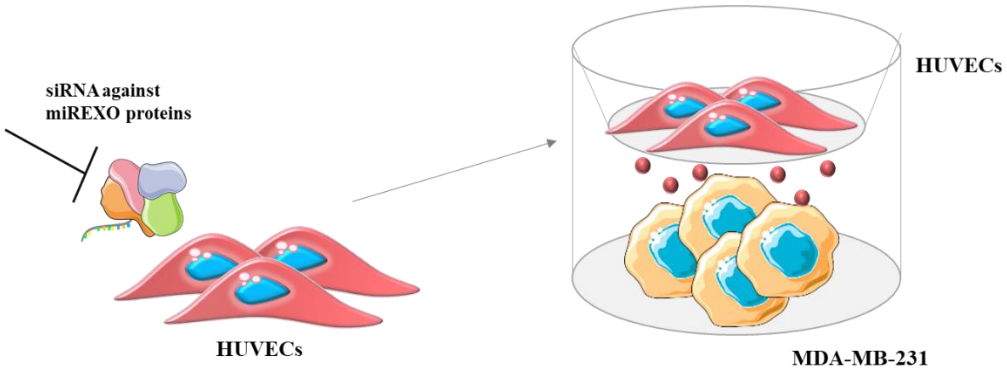

Figure R 31. Schematic representation of the endothelial-cancer cells coculture.
Endothelial cells (HUVECs) were transfected with siRNA against miR-EXO proteins and then cocultivated with MDA-MB-231 cells for 48 hours in a transwell coculture system. This system allows the passage of molecules and particles smaller than 0.4 µm, such as exosomes.

We first validated the efficiency of the siRNA transfection. **Supplementary figure S5** showed that all of the miR-EXO proteins are efficiently knock downed 48h after transfection, we thus decided to select this time point for further studies.

2.1. Impact of endothelial miR-EXO protein silencing on the proliferation and the migration of breast cancer cells

We further studied the effect of the silencing of ANXA2, hnRNPA2B1, TSP1 and VIM in MDA-MB-231 cells, to determine how endothelial EVs could modify breast cancer cell behavior. To determine their effects, we reduced the levels of miR-EXO proteins in HUVECs by transfection with siRNAs against these proteins and cocultivated them with breast cancer cells for 48h. MDA-MB-231 were then used to perform several functional assays.

We first analyzed the capacity of transfected endothelial cells to regulate the MDA-MB-231 proliferation. For that purpose, we used MDA-MB-231 expressing the luciferase coding gene. Proliferation is assessed by measuring the luminescence of MDA-MB-231 LUC after the coculture with HUVECs. These assays showed that hnRNPA2B1, TSP1 and VIM silencing reduced the proliferation of MDA-MB-231 cells while ANXA2 did not seem to influence it (**Fig. R 32**).

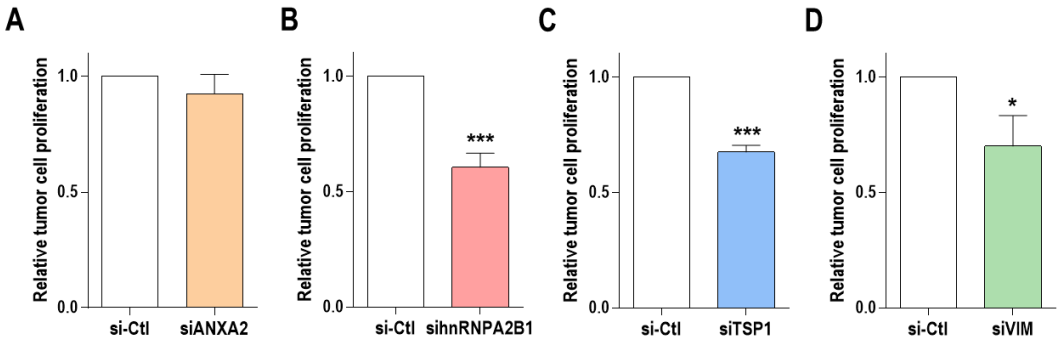

Figure R 32. Endothelial knock-down of hnRNPA2B1, TSP1 and VIM reduces breast cancer cells proliferation. *HUVECs were transfected with 20 nM of siRNAs against ANXA2, hnRNPA2B1, TSP1, VIM and the siRNA control (si-Ctl). The proliferation was assessed by the measure of the luminescence of MDA-MB-231 cells after 48 hours of coculture (**A-D**). Data are expressed as mean ± SD from at least three independent experiments and compared to the control (si-Ctl) (n=3; *, p<0.05, ***, p< 0.001).*

The potential of the proteins to modulate breast cancer cell migration was assessed in Boyden chamber assays. Migration results of hnRNPA2B1 knock-out in HUVECs showed a tendency to reduce the migratory capacity of the tumor cells (**Fig. R 33**). Whereas, the silencing of the other miR-EXO proteins did not influence MDA-MB-231 migration.

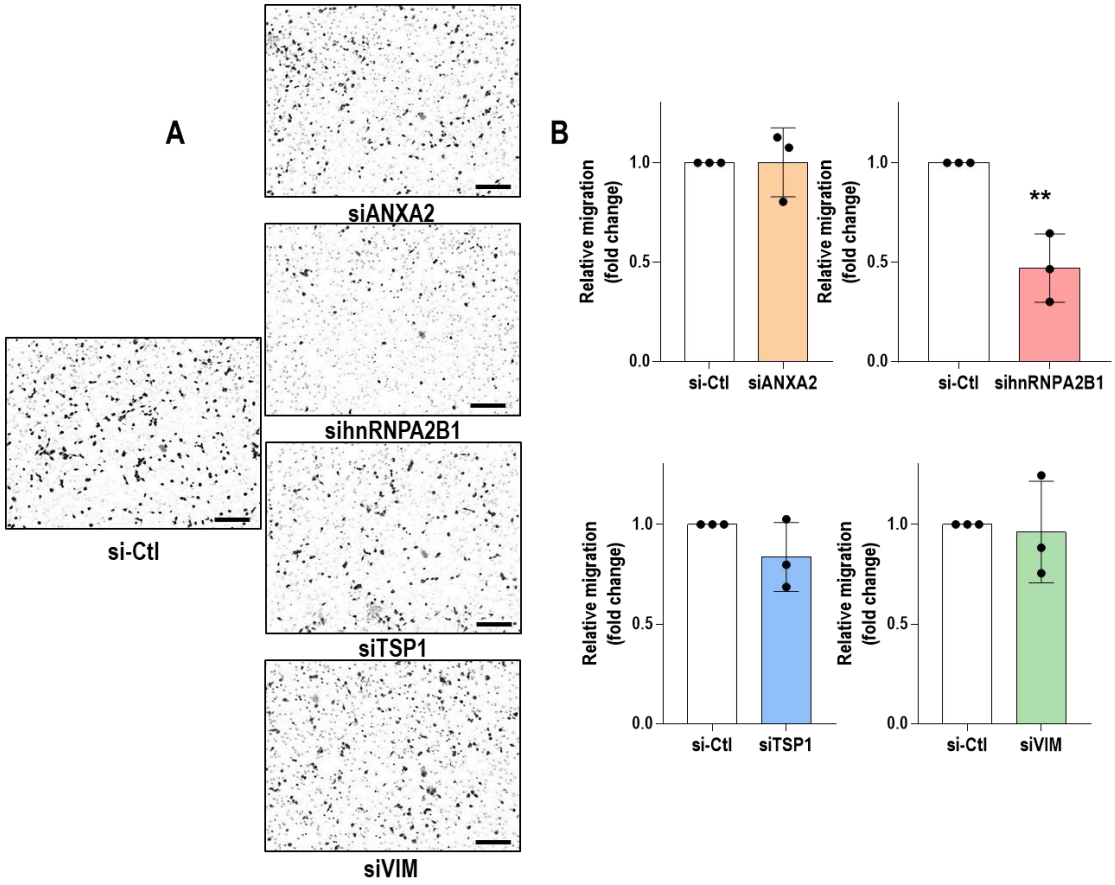

Figure R 33. Endothelial knock-down of hnRNPA2B1 impacts negatively breast cancer cells migration.
*HUVECs were transfected with 20 nM of siRNAs against ANXA2, hnRNPA2B1, TSP1, VIM and the siRNA control (si-Ctl). (**A**) After 48 h of transfection, endothelial cells were seeded in a 24-well plate and, in parallel, MDA-MB-231 were seeded onto the inner part of the Boyden chamber and cocultivated with HUVECs and allowed to migrate for 16h. The cells were then fixed, the porous membrane removed and stained with Giemsa. Scale bar = 200µm. (**B**)The migratory capacities of MDA-MB-231 cells were counted and reported on plots. Data are expressed as mean ± SD from three independent experiments compared to the control (si-Ctl) (n=3; **, p<0.01).*

2.2. Impact of endothelial miR-EXO protein silencing on the invasion of breast cancer cells

To determine how modified endothelial EVs can affect breast cancer behavior, we further studied the effects of the silencing of miR-EXO proteins on MDA-MB-231 invasive capacities. To study tumor cell invasion in presence of endothelial cells, we setup an experiment allowing the visualization of exosomes released by the two cell types.

For that purpose, we designed and generated lentiviral vectors expressing an exosome marker: CD63. We created two new cell lines: HUVECs CD63-GFP and MDA-MB-231 CD63 mCherry which expressed the tetraspanin CD63 coupled with two different fluorophores, respectively, GFP and mCherry. We then performed coculture experiments in transwell and analyzed the fluorescence using a high resolution confocal microscope. When HUVEC CD63-

GFP are cocultured with non-fluorescent breast cancer cells, green spots are seen in cancer cells indicating that endothelial EVs were incorporated within cancer cells (**Fig. R 34a**). Then we performed the reverse experiment to assess the transfer of exosomes between fluorescent breast cancer cells (MDA-MB-231 CD63-m-Cherry) and non-fluorescent endothelial cells. Interestingly, **figure R 34b** confirmed that the transfer of EVs could either be effective from endothelial cells to cancer cells, but also in the opposite way.

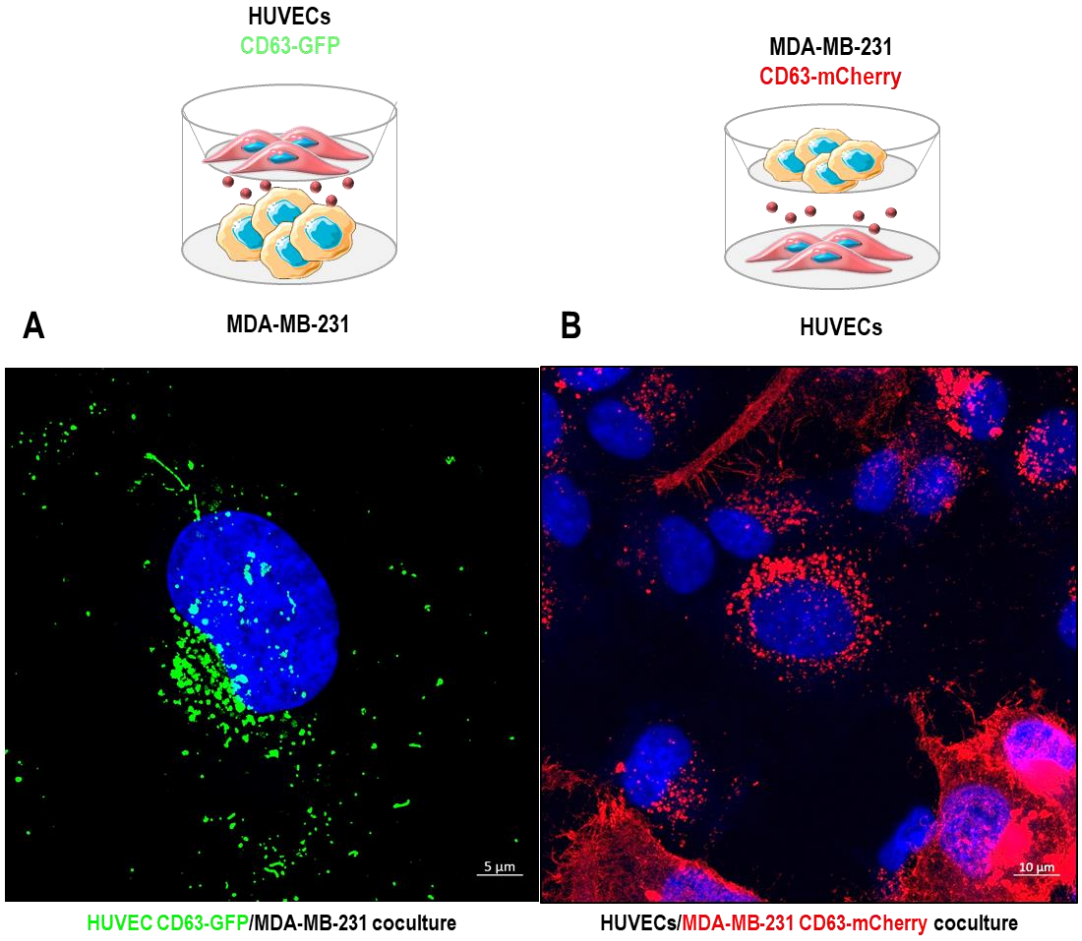

Figure R 34. Transfer of EVs between endothelial and triple-negative breast cancer cells.
(A) HUVEC CD63-GFP were cocultivated with MDA-MB-231 for 6h. Cancer cells were then visualized using the high-resolution microscope LSM 880 (Zeiss). Scale bar = 5 µm. (B) MDA-MB-231 CD63-m-Cherry were cocultivated with HUVECs for 6h. Endothelial cells were then visualized using the high-resolution microscope LSM 880 (Zeiss). Scale bar = 10µm.

To assess the impact of miR-EXO proteins on breast tumor cell invasiveness, we performed 3D culture model of spheroids assays with the same fluorescent cells. In this case, we generated heterospheroids, i.e, spheroids composed of HUVECs CD63-GFP and MDA-MB-231 CD63-mCherry. Interestingly, as showed in the spheroid assays, the silencing of only one protein, hnRNPA2B1, reduced drastically breast cancer cell invasion, whereas ANXA2, TSP1 and VIM knockdown did not affect the invasive capacities of tumor cells (**Fig. R 35**). All functional assays suggest that hnRNPA2B1 could be an interesting target for breast cancer treatment.

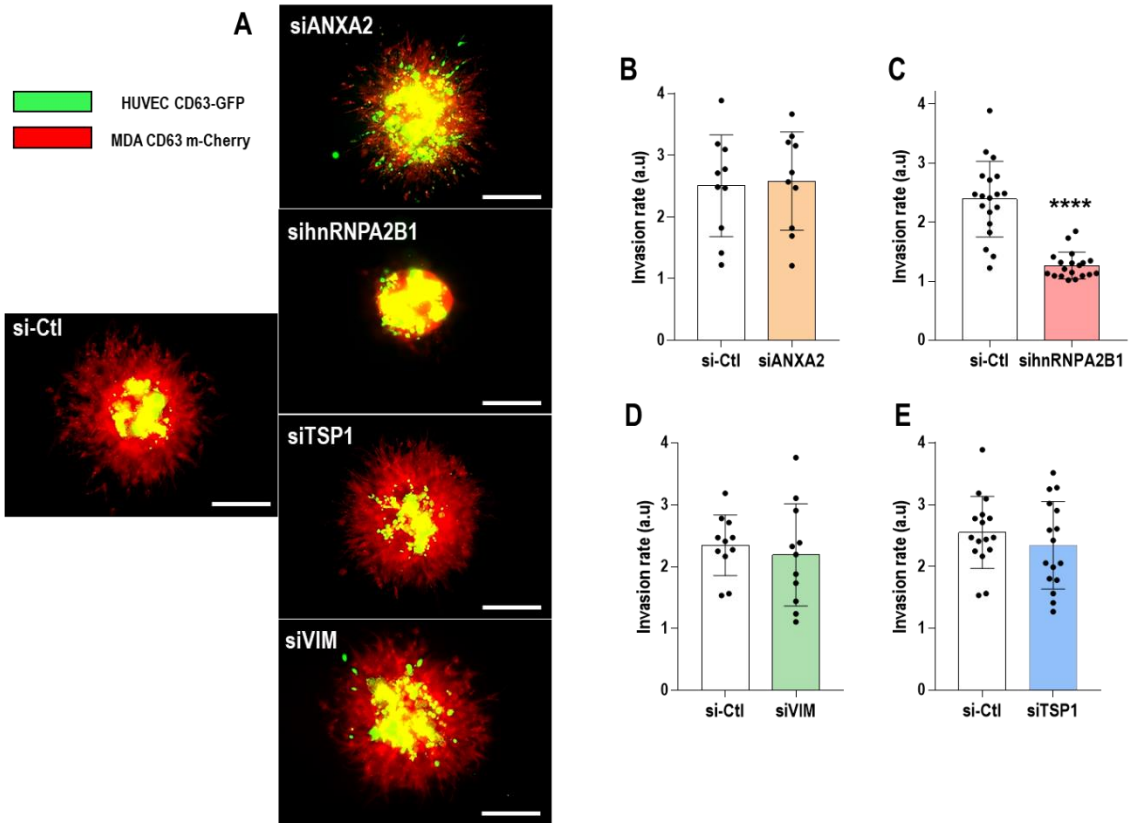

Figure R 35. Endothelial silencing of hnRNPA2B1 reduces breast cancer cell invasiveness.
*HUVEC CD63-GFP were transfected with 20 nM of siRNAs against ANXA2, hnRNPA2B1, TSP1, VIM and the control (si-Ctl). After transfection, endothelial cells were cocultivated with MDA-MB-231 CD63-m-Cherry cells in a 96-well suspension plate for 48h, then, both cell lines were seeded in a collagen 3D matrix and allowed to invade. (**A**) Heterospheroids acquisition was taken after a 24h-incubation in the 3D matrix by epifluorescence analysis on a Nikon Eclipse Ti microscope (Nikon instruments) with a 10x-magnification objective, scale bar =200 µm. Relative invasion of MDA-MB-231 CD63-m-Cherry cells, in coculture with HUVEC transfected with siANXA2 (**B**), sihnRNPA2B1 (**C**), siTSP1 (**D**) and siVIM (**E**), was calculated with the following formula: (Area of sprout-central area)/central area. Dots represents the number of spheroids. Data are expressed as mean ± SD from at least three independent experiments compared to the control (si-Ctl) (n=3; ****, p<0.0001).*

2.3. Impact of endothelial miR-EXO protein silencing on the expression of miR-503 and its targets in breast cancer cells

Based on our functional results, we decided to quantified the levels of miR-503 and its targets in MDA-MB-231 cells, to determine if the effects could be linked to the miRNA. For that purpose, we used a computational approach involving the Targetscan algorithm (http://www.targetscan.org/) to obtain a list of genes predicted to be targets of miR-503. miR-503 possesses thousands of targets, but we decided to select five of them: cyclin D2 (CCND2) and D3 (CCND3), MYB and Bcl-2. The functions of these target genes are detailed in **Supplementary Table S6**. For that purpose, we cocultivated, for 24h, cancer cells with HUVEC cells, previously transfected with siRNA against the miR-EXO proteins. **Fig. R 36a** shows that when hnRNPA2B1 is silenced, miR-503 was significantly upregulated in MDA-MB-231 compared to the control condition while none of the other proteins seem to influence the miRNA expression. Those data suggest that the increased secretion of miR-503 upon hnRNPA2B1 knockdown lead to an increase level of this microRNA in the cancer cell. To determine if the elevated level of miR-503 in the cancer cells results in the repression of its targets we analyzed the level of CCND2, CCND3, MYB and BCL2. While some miR-503 targets were downregulated in the hnRNPA2B1 silencing: CCND2 and CCDN3, BCL2 and MYB level is unaffected. ANXA2, TSP1 and VIM did not impact the expression of miR-503 (**Fig. R 36**).

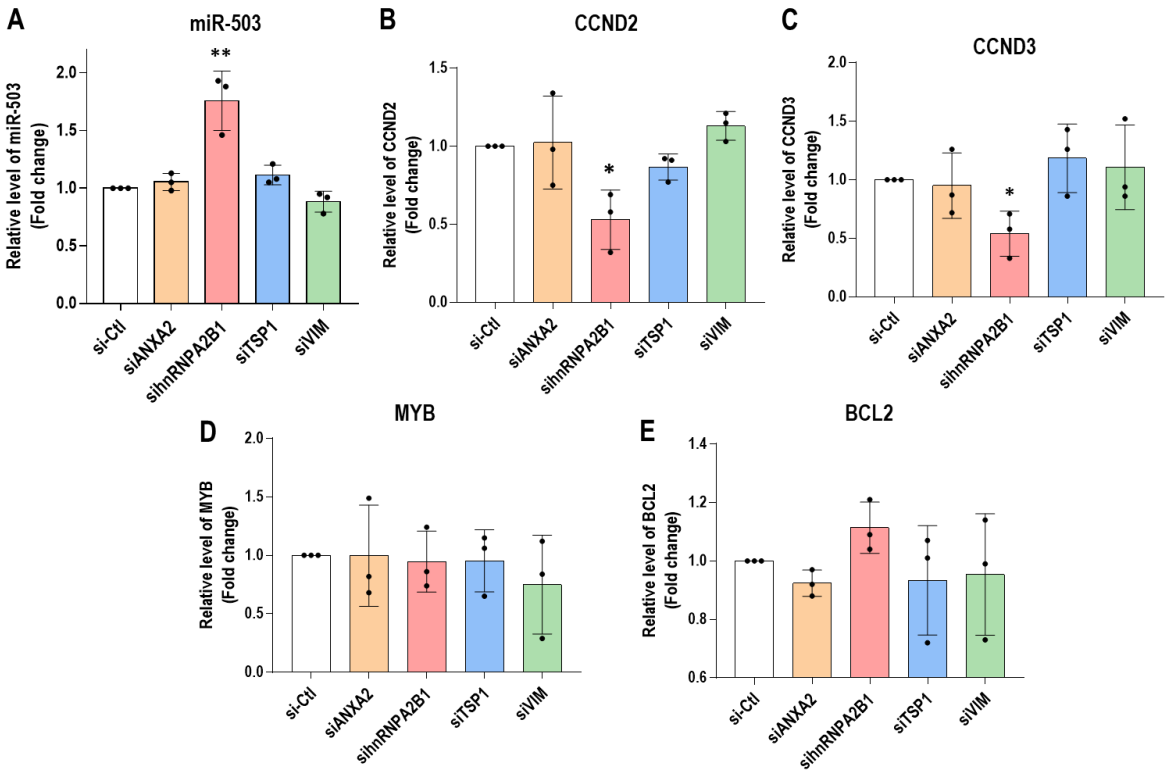

Figure R 36. Endothelial silencing of hnRNPA2B1 increases the levels of miR-503 and a downregulation of its targets in breast cancer cells.
*HUVEC were transfected with 20 nM of siRNAs against ANXA2, hnRNPA2B1, TSP1, VIM and the control (si-Ctl). After transfection, endothelial cells were cocultivated with MDA-MB-231 in a 6-well plate for 48h. RNAs were extracted from MDA-MB-231 cells. The levels of expression of miR-503 (**A**), CCND2 (**B**), CCND3 (**C**), MYB (**D**) and BCL2 (**E**) are represented as fold change of their level in the control condition. The values are normalized to the mean Ct of RNU44 and RNU48 (**A**) or to the mean Ct of B2M and PPIA (**B-E**). Data are expressed as mean ± SD from three independent experiments compared to the control (si-Ctl) (n=3; *, p<0.05, **, p<0.01).*

We also aimed to verify that the endothelial knockdown of the miR-EXO proteins did not affect the expression of these proteins in breast cancer cells. Data showed that sihnRNPA2B1 transfection in HUVECs did not affect the cancerous mRNA levels of hnRNPA2B1 (**Suppl. Fig S6**). The same results were obtained for all of the other miR-EXO proteins.

2.4. Impact of epirubicin treatment on breast cancer cell behavior

As mentioned previously, hnRNPA2B1 knockdown mimics the treatment with epirubicin which induces the sorting of miR-503 within endothelial exosomes (Pérez-Boza, Boeckx, *et al.*, 2020). For this reason, we decided to treat endothelial cells with epirubicin for 24h. Cells were then washed twice with PBS and cocultivated with MDA-MB-231 cells for 24h. Then, we analyzed the proliferation rate of luminescent cancer cells and we observed that after epirubicin treatment, the relative proliferation of MDA-MB-231 LUC was reduced compared to non-treated condition (**Fig. R 37**).

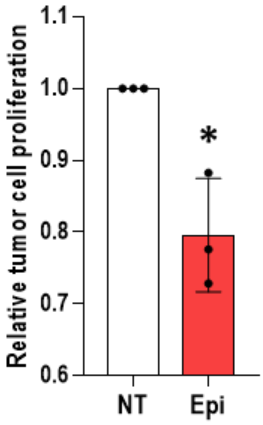

Figure R 37. Epirubicin treatment of endothelial cells reduces the proliferative properties of breast cancer cells. *HUVECs were incubated 24h with 1µg/ml epirubicin, or non-treated (NT) and cocultivated with MDA-MB-231 LUC cells. The proliferation was assessed by the measure of the luminescence of MDA-MB-231 cells after 24 hours of coculture. Data are expressed as mean ± SD from at least three independent experiments and compared to the control (NT) (n=3; *, p<0.05).*

We further quantified the levels of miR-503 and its targets after epirubicin treatment. We showed that, compared to the non-treated condition, epirubicin treatment could induce the up-regulation of the miRNA in breast cancer cells. Curiously, none of its targets seem to be affected by the coculture with treated HUVECs (**Fig. R 38**).

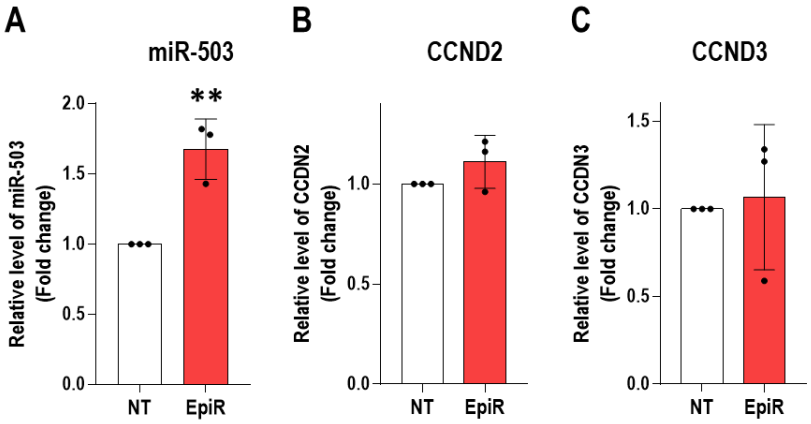

Figure R 38. miR-503 levels are up-regulated in cancer cells cocultured with epirubicin-treated endothelial cells. *HUVECs were incubated 24h with 1µg/ml epirubicin, or non-treated (NT) and cocultivated with MDA-MB-231 cells. RNAs were extracted from MDA-MB-231 cells. The levels of expression of miR-503 (**A**), CCND2 (**B**) and CCND3 (**C**) are represented as fold change of their level in the control condition. The values are normalized to the mean Ct of RNU44 and RNU48 (**A**) or to the mean Ct of B2M and PPIA (**B-E**). Data are expressed as mean ± SD from three independent experiments compared to the control (NT) (n=3; **, p<0.01).*

2.5. Endothelial EVs influence tumor cell behavior

Then we wanted to determine if the effects of hnRNPA2B1 knockdown observed in the coculture experiments was due to the EVs released by endothelial cells.

First, we proceeded to the characterization of these vesicles. For that purpose, we purified EVs from HUVEC supernatants using differential ultracentrifugation method. The size of the vesicles was assessed by Dynamic Light Scattering (DLS), and their size and morphology by transmission electron microscopy (TEM).

As shown in **figure R 39**, the vesicles display a diameter around 85 nm. Transmission electron microscopy confirmed that the vesicles ranged between 60 and 100 nm, and that some vesicles were enriched in exosomal markers such as CD63 and CD81.

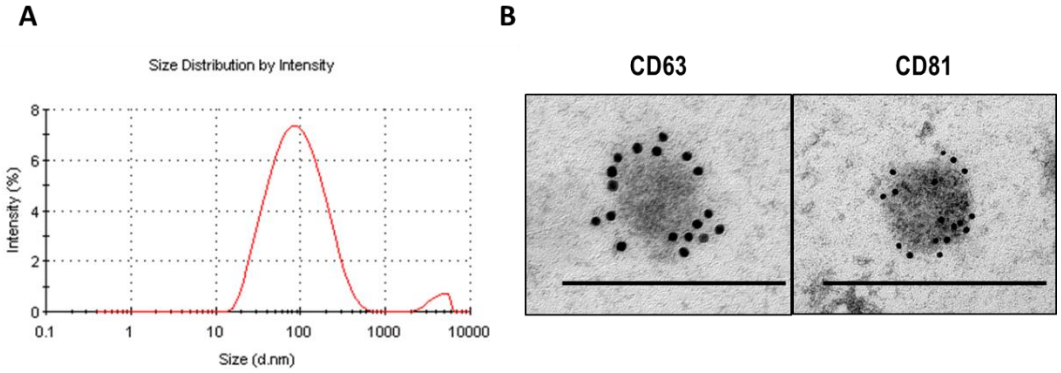

Figure R 39. Size and morphology of endothelial extracellular vesicles.
*EVs were isolated from HUVECs supernatant and purified by differential ultracentrifugation. (**A**) The size of the vesicles was assessed by DLS where the peak represents the diameter average of the particles. (**B**) Purified EVs were visualized by TEM and immunogold staining (black dots) for CD63 and CD81 were applied to the particles. Scale bar = 200 nm. In collaboration with Pr. M. Thiry.*

We also compared the relative protein abundance of CD9, CD63, CD81, syntenin-1 and Cytochrome C (Cyt C) either in the vesicles and in endothelial cells by Western Blotting (**Fig. R 40**). As expected, the tetraspanins CD9, CD63 and CD81 were present in both fractions although, these exosomal markers were enriched in the EVs fraction such as syntenin-1. Nevertheless, as a cellular marker, we evaluated the expression of Cyt C, a mitochondrial protein which is present in cells and in apoptotic bodies but not in exosomes. Our results showed that endothelial vesicles were indeed devoid of Cyt C.

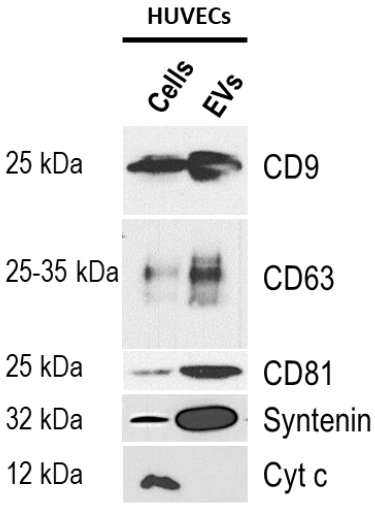

Figure R 40. Protein composition of endothelial extracellular vesicles.
10 µg of proteins extracted from total HUVEC lysates or EVs produced from HUVECs were separated by SDS-PAGE and subjected to Western blotting using the specific antibodies: the exosome markers CD9, CD63 and CD81 and the cellular marker, cytochrome C.

Considering that the EVs characterization was as expected, we decided to incubate these vesicles on breast cancer cells and evaluate their impact on their growth. For that purpose, we cultured HUVECs and transfected them with 20 nM siRNA against the miR-EXO proteins (ANXA2, hnRNPA2B1, TSP1 and VIM) for 48h and, then, we produced EVs for 72h in *exofree* media. Particles were purified using differential ultracentrifugation and incubated with MDA-MB-231 for 6h (**Fig. R 41**). We then wanted to determine if these EVs could impact tumor cell proliferation. Therefore, right after the coculture, we proceeded to a proliferation assay. This experiment required the incorporation of BrDU within genomic DNA of cancer cells. Results of the incorporation showed that, compared to the non-treated condition but also the transfection control (si-Ctl), only exosomes produced by hnRNPA2B1-silenced HUVECs reduce the proliferation of MDA-MB-231.

Moreover, we also demonstrated that exosomes produced by hnRNPA2B1-silenced HUVECs enhanced the levels of miR-503 and down-regulated one of its targets, CCND2. Whereas, the mRNA levels of CCDN3 weren't affected.

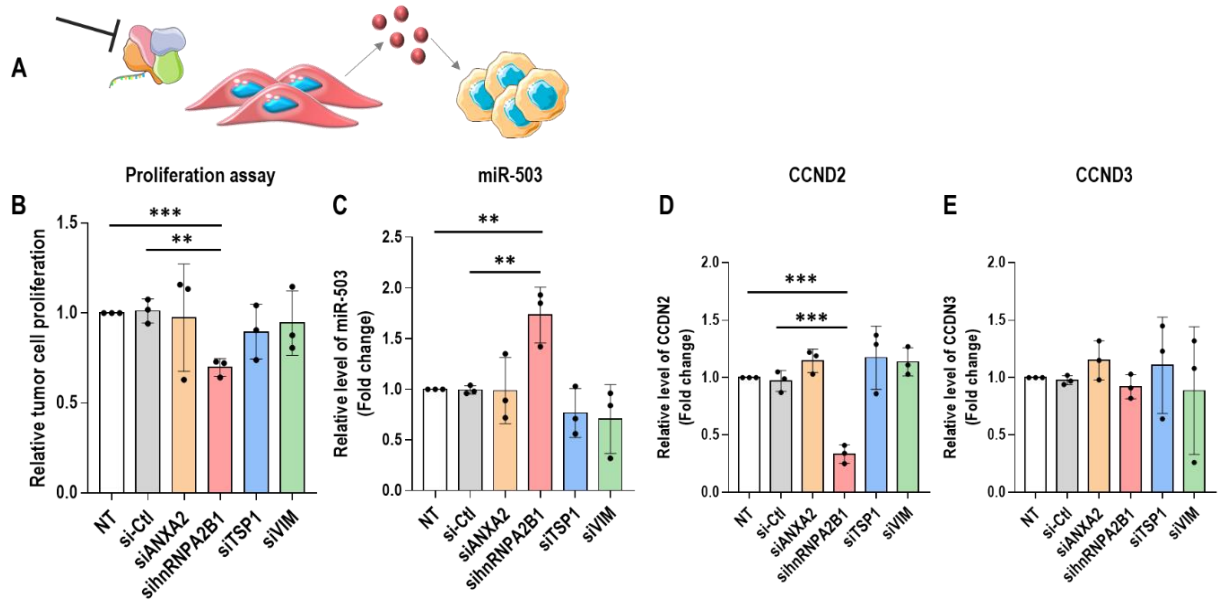

Figure R 41. hnRNPA2B1 knockdown in endothelial cells induce the production of EVs with anti-proliferative capacities.

*(**A**) HUVECs were transfected, for 48h, with 20 nM siRNA against ANXA2, hnRNPA2B1, TSP1 and VIM and compared to the non-treated condition (NT), i.e without EVs treatment, or the control condition (si-Ctl). Then, HUVECs were cultured in exofree media for 72h and EVs were isolated from HUVECs supernatant and purified by differential ultracentrifugation. These particles (5 µg) were added to MDA-MB-231 cells which underwent for 6 h (**B**) a proliferation assay by the measurement of BrDU incorporation after 16 h. Moreover, RNAs were extracted from MDA-MB-231 cells. The levels of miR-503 (**C**), CCND2 (**D**) and CCND3 (**E**) are represented as fold change of their level in the control condition (in this case, NT). The values are normalized to the mean Ct of RNU44 and RNU48 (**B**) or to the mean Ct of B2M and PPIA (**D** and **E**). Data are expressed as mean ± SD from three independent experiments compared to the NT or si-Ctl conditions (n=3; **, p<0.01; ***, p< 0.001).*

Results

Chapter III

miR-503 curtails sensitive and resistant breast cancer cell tumorigenicity

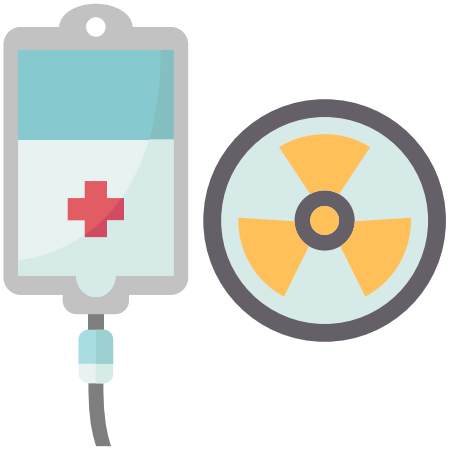

3. miR-503 curtails sensitive and resistant breast cancer cell tumorigenicity

During tumor evolution, cancer cells might acquire drug resistance. Therefore, we decided to investigate the potential impact of miR-503 in the resistance to chemotherapy. To assess that, we obtained epirubicin- or paclitaxel-resistant triple breast cancer cells, respectively referred as Epi-R or Pacli-R. MDA-MB-231 Epi-R and Pacli-R cells were generously provided by Dr. Shanon Gorski and Dr. Melanie Spears. Polyclonal epirubicin-resistant cells were produced by growing in increasing concentrations of epirubicin (up to 100 nM) for almost one year (Chittaranjan *et al.*, 2014). Polyclonal paclitaxel-resistant MDA-MB-231 cells were cultured in increasing concentration of paclitaxel (up to 25 nM) until the resistance to taxanes was acquired (Kenicer *et al.*, 2014). For all cell types, we proceeded to functional assays and target analysis. To confirm that cells were truly resistant to chemotherapy, we analyzed the survival rate of those cells and compared to the native cells upon treatment with the respective chemotherapeutic agent. Survival curves showed a difference in sensibility to epirubicin or paclitaxel between native or resistant MDA-MB-231 (**Fig. R 42**).

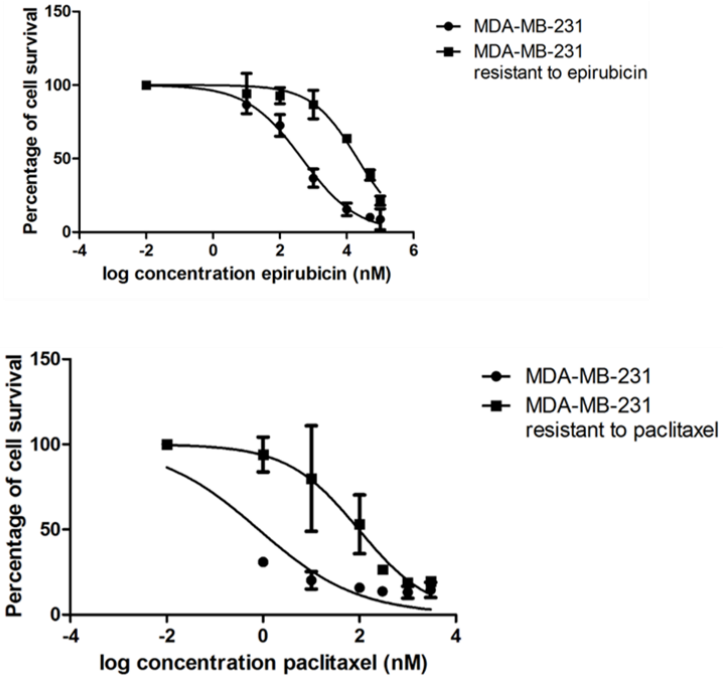

Figure R 42. Difference in the sensibility to epirubicin or paclitaxel between native and resistant MDA-MB-231. *Cells were incubated with various concentration of respective drugs for 48h (epirubicin for MDA-MB-231 Epi-R or paclitaxel for MDA-MB-231 Pacli-R). WST1 was added to the cells and their viability was assessed by measuring the absorbance. The IC50 corresponding to epirubicin treatment shifts from 252.2 ng/mL (560 nM) for native cells to 11,415 ng/mL (21,000 nM) in Epi-R. The IC50 relative to paclitaxel shifts from 0.71 ng/mL (0.8 nM) for native cells to 82.6 ng/mL (97 nM) in Pacli-R cells. Data are expressed as mean ± SD from three independent experiments. These data have been generated by Stella Dederen.*

Moreover, we decided to measure the mRNA levels of well-known resistance genes: ABCB1, GADD45A, MDH2, POR, SIRT6 and TOP2A. The functions of these genes in multi-drug resistance are described in **Supplementary Table S7**. Interestingly, in both resistant cell lines, the majority of resistance genes were upregulated compared to native MDA-MB-231. However, the levels of TOP2A were, in contrast, downregulated (**Fig. R 43-44**).

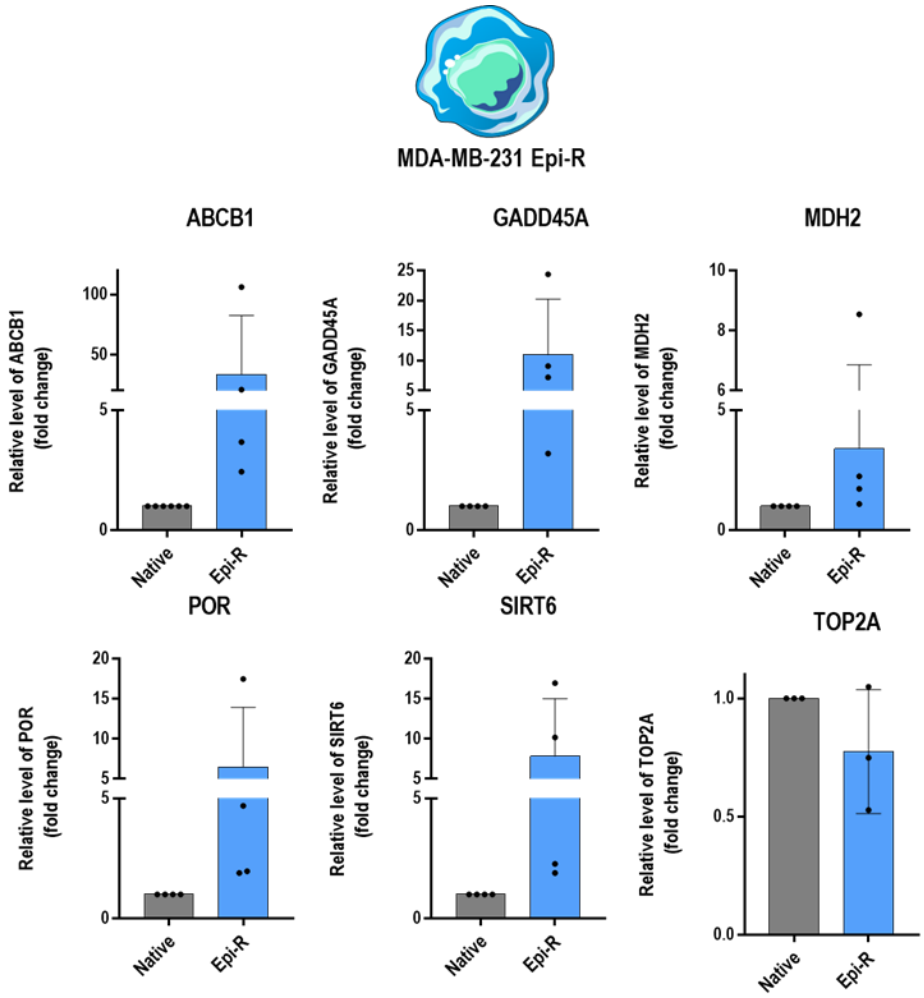

Figure R 43. Genes involved in the resistance to chemotherapy are modulated in epirubicin-resistant cells.
RNAs were extracted from either native (grey) or Epi-R (blue) MDA-MB-231 cells. The expression level of resistance genes (ABCB1, GADD45A, MDH2, POR, SIRT6 and TOP2A) are represented as fold change of their level in native cells. The values are normalized to the mean Ct of B2M and PPIA. Data are expressed as mean ± SD from at least three independent experiments.

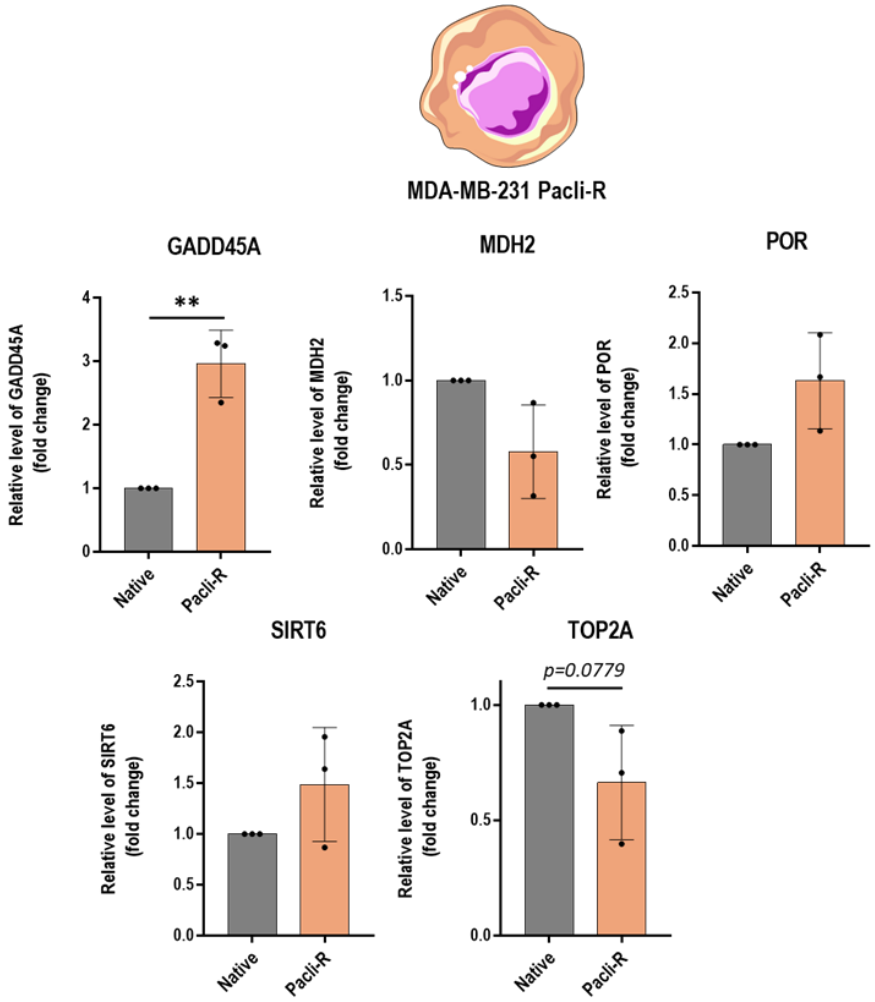

Figure R 44. Genes involved in the resistance to chemotherapy are modulated in paclitaxel-resistant cells.
*RNAs were extracted from either native (grey) or Pacli-R (orange) MDA-MB-231 cells. The expression level of resistance genes (GADD45A, MDH2, POR, SIRT6 and TOP2A) are represented as fold change of their level in native cells. The values are normalized to the mean Ct of B2M and PPIA. Data are expressed as mean ± SD from three independent experiments (**, p<0.01).*

We further decided to quantified the levels of miR-503 to determine if the acquisition of resistance to chemotherapy would affect its expression. Interestingly, as shown in figure **R 45**, the levels of miR-503 were indeed affected and drastically reduced in epirubicin- or paclitaxel-resistant breast cancer cells. These results suggest that miR-503 could play a role in resistance to chemotherapy.

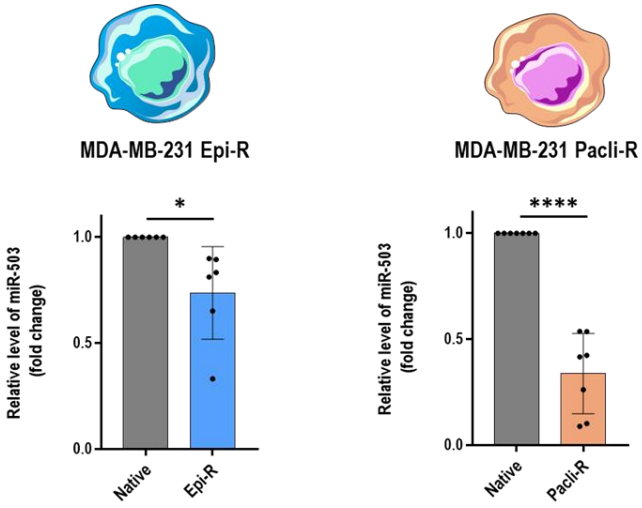

Figure R 45. miR-503 expression is reduced in breast cancer cells resistant to chemotherapy.
RNAs were extracted from sensitive (Native) or epirubicin- (Epi-R) or paclitaxel- resistant (Pacli-R) breast cancer cells. The expression levels of miR-503 are represented as fold change of their level in the control condition (Native). The values are normalized to the mean Ct of RNU44 and RNU48. Data are expressed as mean ± SD from at least three independent experiments compared to the control (, p< 0.05; ****, p<0.0001).*

3.1. Functional effects of miR-503 on sensitive and resistant triple-negative breast cancer cells

We further studied the effects of miR-503 on breast cancer cells which were sensitive or resistant to epirubicin or paclitaxel, to determine the potential role of this specific miRNA in tumor progression and in resistance to chemotherapy. To evaluate the impact of miR-503 on cancer cells, we transiently transfected the MDA-MB-231 cells with a microRNA mimic designed to generate the mature miR-503-5p (miR-503) and a respective control cel-miR-67 (miR-Ctl). In parallel, to knockdown the endogenous miR-503, cells were also transfected with an anti-miRNA targeting miR-503 (anti-miR-503) and its respective control anti-cel- miR-67 (anti-Ctl). These transfected cells were used to perform functional assays. Indeed, we analyzed the potential implication of the miRNA on tumor proliferation, adhesion, migration, invasion and apoptosis. Results of BrDU incorporation showed that miR-503 overexpression reduces drastically the proliferation of both native or resistant breast cancer cells (**Fig. R 46**). In contrast, the downregulation of miR-503 showed a tendency to increase the proliferation of tumor cells but was not significant.

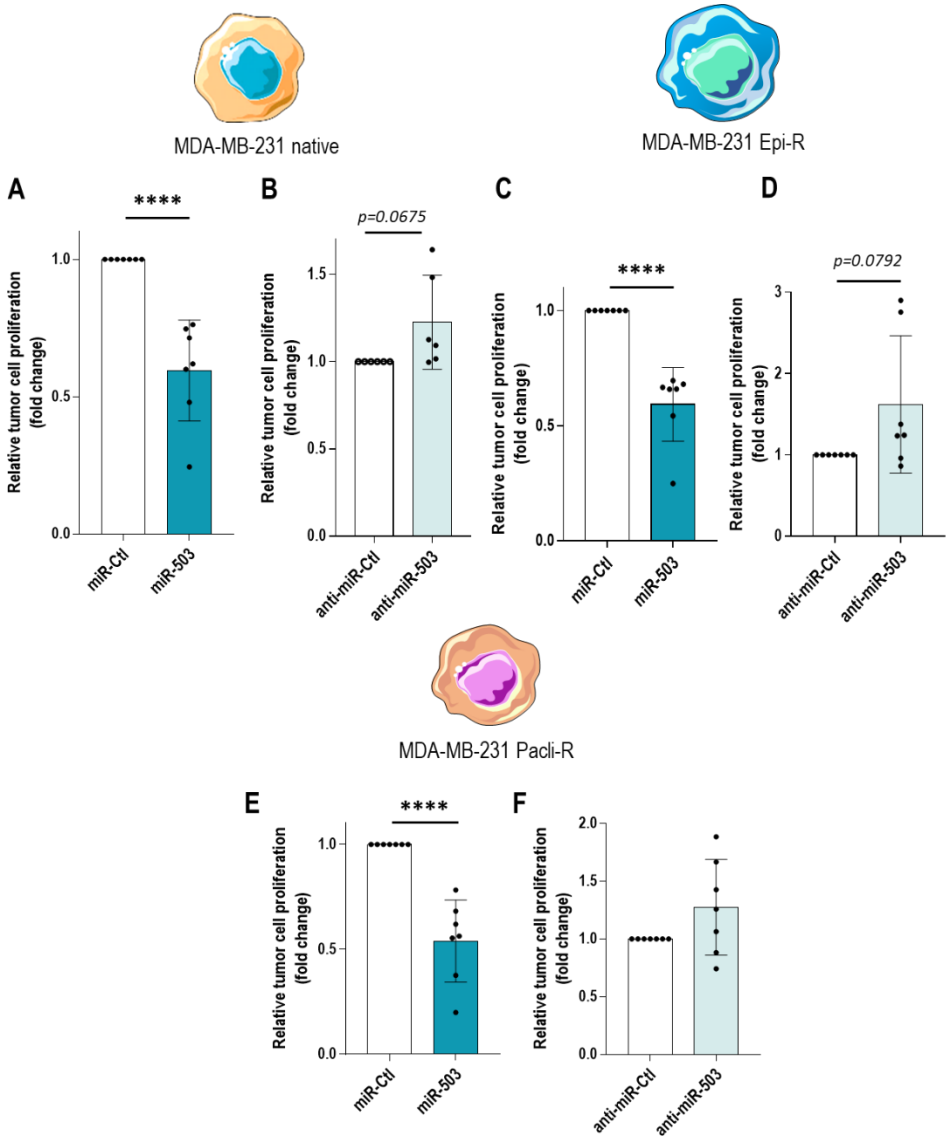

Figure R 46. miR-503 reduces the proliferation of sensitive and epirubicin or paclitaxel resistant breast cancer cells.

*Native (**A**-**B**), Epi-R (**C**-**D**) and Pacli-R (**E**-**F**) resistant MDA-MB-231 cells were transfected with 10 nM of miR-503 or anti-miR-503, and their respective controls: miR-Ctl and anti-miR-Ctl. miR-503 and anti-miR-503 are, respectively, represented in dark and light blue. 24 h after transfection; the proliferation was assessed by the measure of the incorporation of BrDU during 16h. Data are expressed as mean ± SD from at least three experiments and compared to the control (miR-Ctl or anti-miR-Ctl) (****, p< 0.0001).*

Adhesion assays, on a fibronectin matrix, revealed that miR-503 led to a strong reduction of cancer cell adhesion (**Fig. R 47**) while the inhibition of miR-503 increased the adhesion. The impact of miR-503 seems to be more efficient on Pacli-R and Epi-R cells than natives.

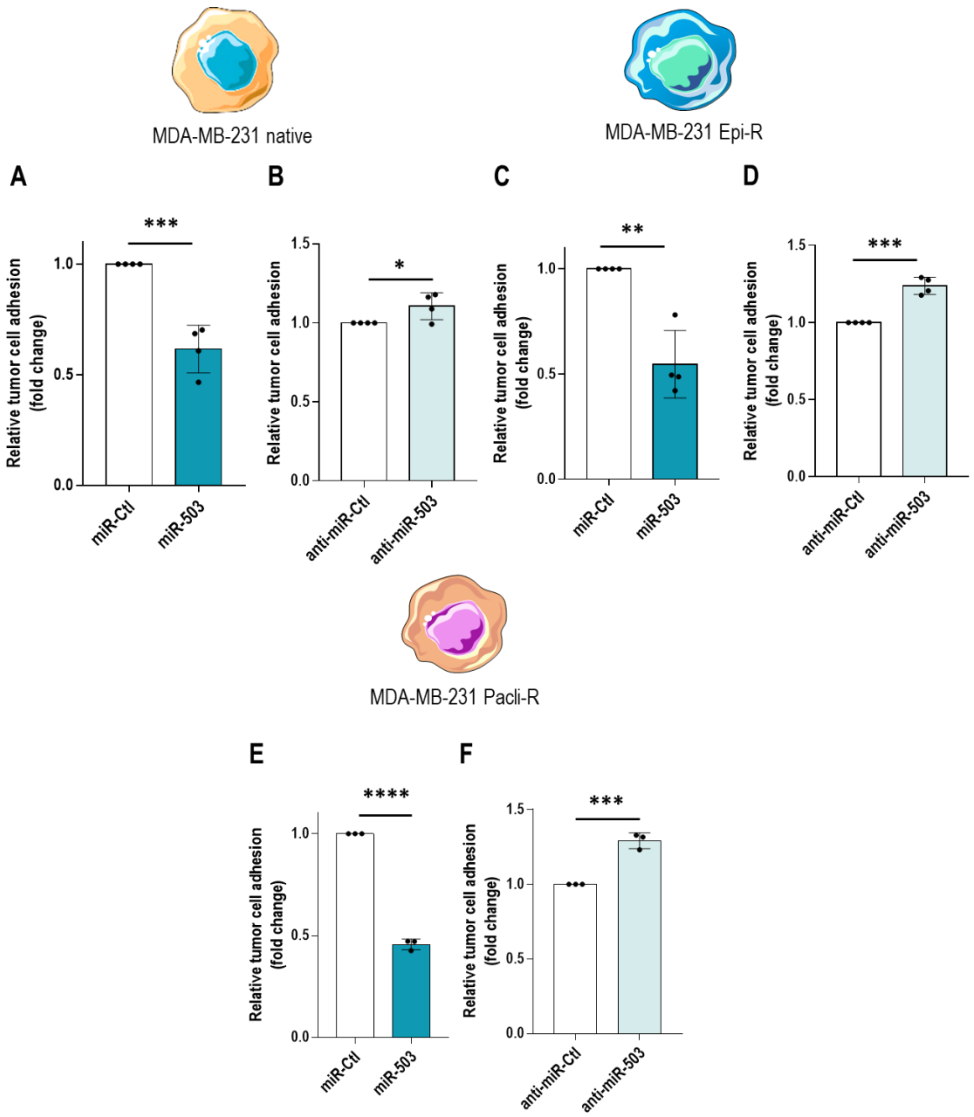

Figure R 47. miR-503 reduces sensitive and epirubicin or paclitaxel resistant breast cancer cell adhesion.
*Native (**A-B**), Epi-R (**C-D**) and Pacli-R (**E-F**) resistant MDA-MB-231 cells were transfected with 10 nM of miR-503 or anti-miR-503, and their respective controls: miR-Ctl and anti-miR-Ctl. miR-503 and anti-miR-503 are, respectively, represented in dark and light blue. Adhesion of tumor cells was assessed using a fibronectin matrix. 24 h after transfection, cells were seeded on fibronectin (20 ng/ml) for 1 hour. Cells were then stained and measured by absorbance. Data are expressed as mean ± SD from at least three experiments and compared to the control (miR-Ctl or anti-miR-Ctl) (*, p<0.05, ***, p< 0.001, ****, p< 0.0001).*

Moreover, we performed scratch-wound assays to evaluate the potential effects of miR-503 on tumor cells which respond (native) or not (resistant) to epirubicin or paclitaxel. Results from scratch-wound assays showed that miR-503 overexpression reduced significantly the migratory properties of both cells (**Fig. R 48**). Nevertheless, miR-503 seems to have a greater impact on sensitive cells but still reduces considerably Epi-R and Pacli-R migration. The opposite effects were observed for the inhibition of miR-503 with the anti-miRNA.

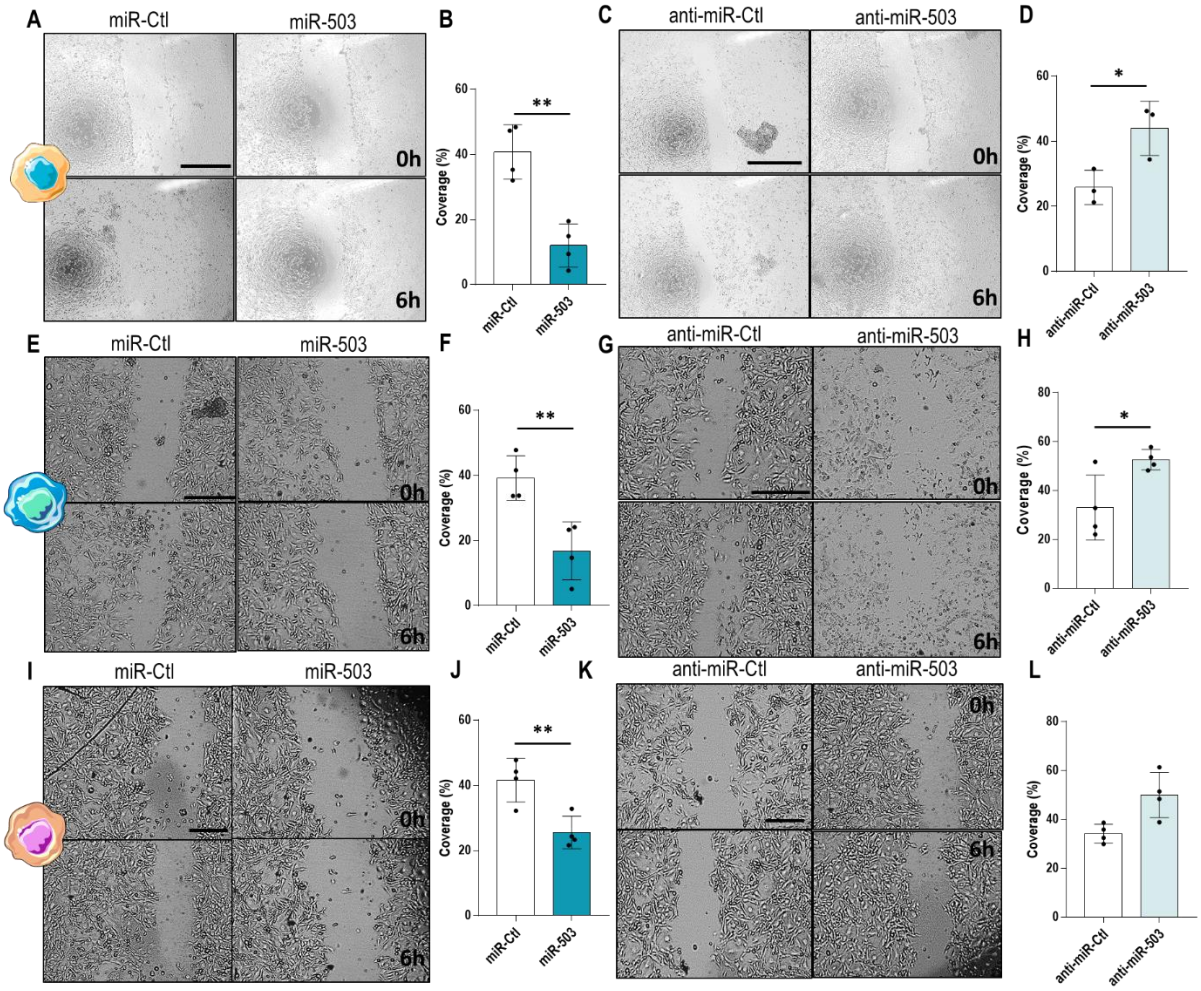

Figure R 48. miR-503 reduces sensitive, Epi-R and Pacli-R breast cancer cell migration.
*Native (**A-D**), Epi-R (**E-H**) and Pacli-R (**I-L**) MDA-MB-231 were transfected with 10 nM of miR-503 or anti-miR-503, and their respective controls: miR-Ctl and anti-miR-Ctl. miR-503 and anti-miR-503 are, respectively, represented in dark and light blue. Scratch-wound assays were performed after 24 h of transfection. (**A**, **C**, **E**, **G**, **I**, **K**) Representative brightfield images of scratch-wound assays were acquired at the indicated time points. Scale bar: 250 µm. (**B**, **D**, **F**, **H**, **J**, **L**) Quantification of cell migration was assessed after 6 h. Data are expressed as mean ± SD from at least three experiments and compared to the control (miR-Ctl or anti-miR-Ctl) (*, p<0.05, **, p< 0.01).*

Triple-negative breast cancer is a very aggressive disease that might spread within other organs. Therefore, we decided to investigate the role of miR-503 on the invasiveness of sensitive and resistant breast cancer cells and we observed that the miR-503 mimic decreased the invasive capacities of both native and Epi-R tumor cells. The opposite effects were obtained with the anti-miR-503 (**Fig. R 49**). Furthermore, we aimed to study the implication of miR-503 on paclitaxel-resistant breast cancer cell invasion using spheroids assays. However, these cells were not able to grow as spheroids in the methylcellulose matrix.

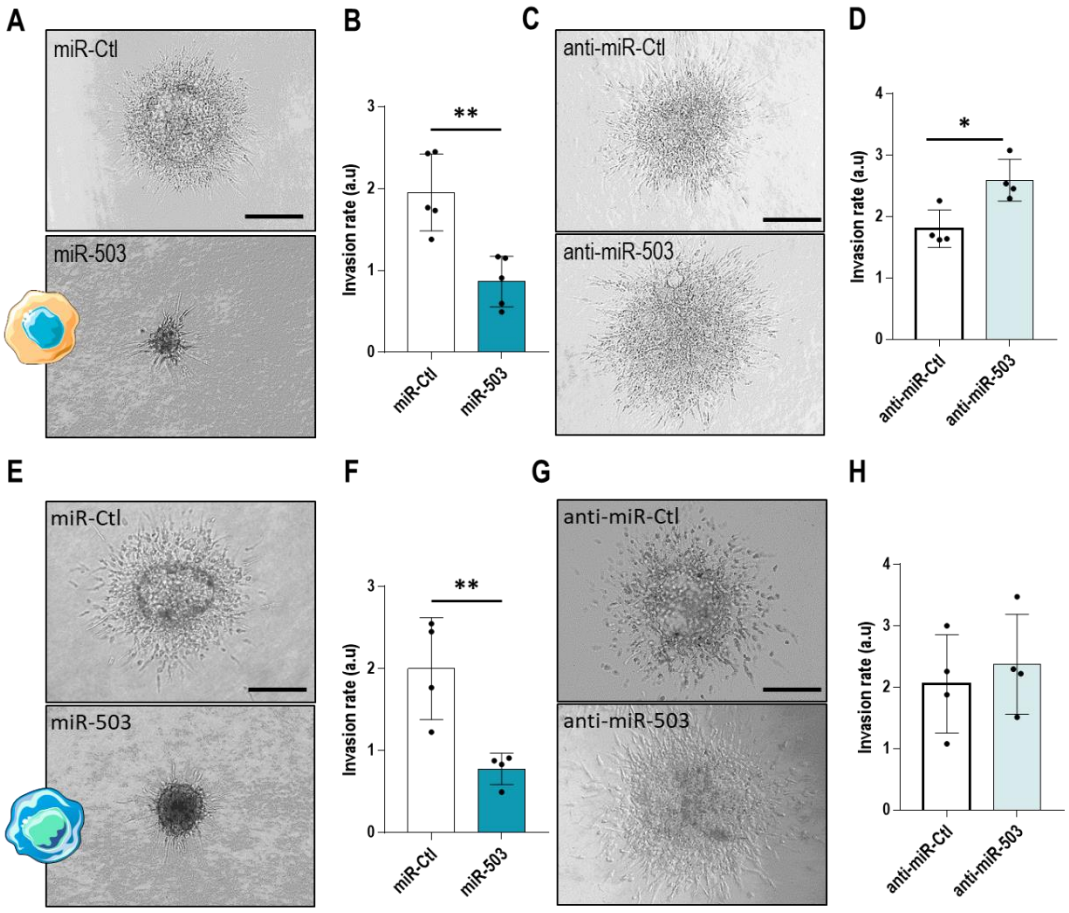

Figure R 49. miR-503 curtails sensitive and Epi-R breast cancer cell invasiveness.
*Native (**A-D**) and Epi-R (**E-H**) MDA-MB-231 were transfected with 10 nM of miR-503 or anti-miR-503, and their respective controls: miR-Ctl and anti-miR-Ctl. miR-503 and anti-miR-503 are, respectively, represented in dark and light blue. Spheroids assay. 24 h after transfection, MDA-MB-231 cells were seeded in methylcellulose and, 48 h later, within a collagen matrix to form spheroids. Pictures were taken after 24h of incubation, scale bar = 250 µm. (**B**, **D**, **F**, **H**) Invasion rate was calculated by the following formula: (Area of sprout-central area/central area). Data are expressed as mean ± SD from at least three experiments and compared to the control (miR-Ctl or anti-miR-Ctl) (*, p<0.05, **, p< 0.01).*

We further studied the miRNA implications on tumor cell death. For that purpose, native and resistant MDA-MB-231 cells were transfected with miR-503 mimic and anti-miR-503, and compared to their respective controls, for 24h. The level of apoptosis and necrosis was performed by staining Annexin-V and propidium iodide (PI) measured by flow cytometry. As described in **figure R 50**, for all cell types, miR-503 did not affect their death. Indeed, the percentage of dying cells was unchanged between conditions.

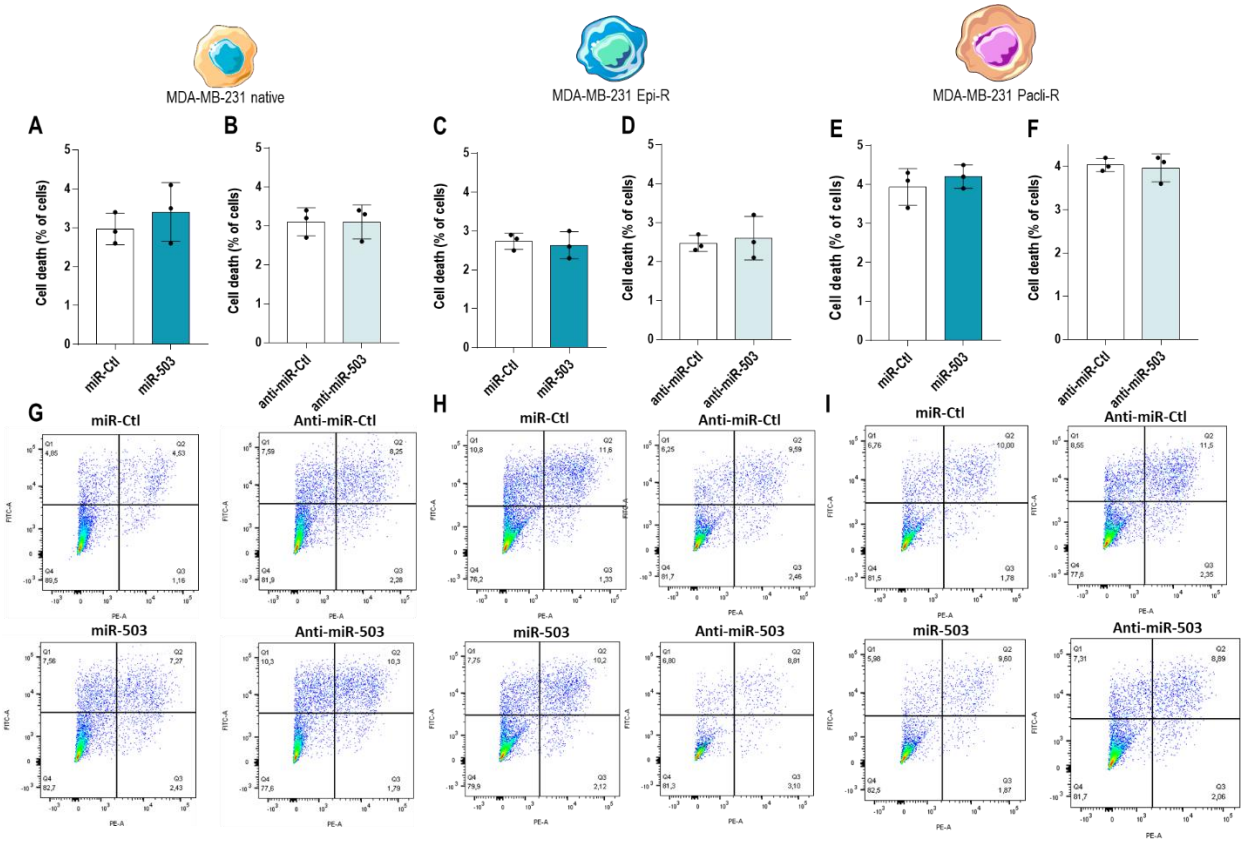

Figure R 50. Cell death is not affected by miR-503.
*After 24h of transfection with 10 nM of miR-503 (**A**, **C**, **E**) or anti-miR-503 (**B**, **D**, **F**), and their respective controls (miR-Ctl or anti-miR-Ctl), native (**A**, **B**), Epi-R (**C**, **D**) and Pacli-R (**E**, **F**) MDA-MB-231 were harvested and stained with Annexin-V and PI to characterize cell status. Scatter plots of flow cytometry analysis of native (**G**), Epi-R (**H**) and Pacli-R (**I**). Data are expressed as mean ± SD from at least three experiments and compared to the control (miR-Ctl or anti-miR-Ctl) (n = 3).*

Finally, we decided to determine how resistant cell could survive with the overexpression of miR-503. To do so, we proceeded to survival assays with WST1. Results showed that after 24h of transfection, miR-503 reduced significantly the survival rate of both epirubicin or paclitaxel-resistant tumor cell (**Fig. R 51**). Moreover, the down-regulation of miR-503 led to a small increase of cell survival.

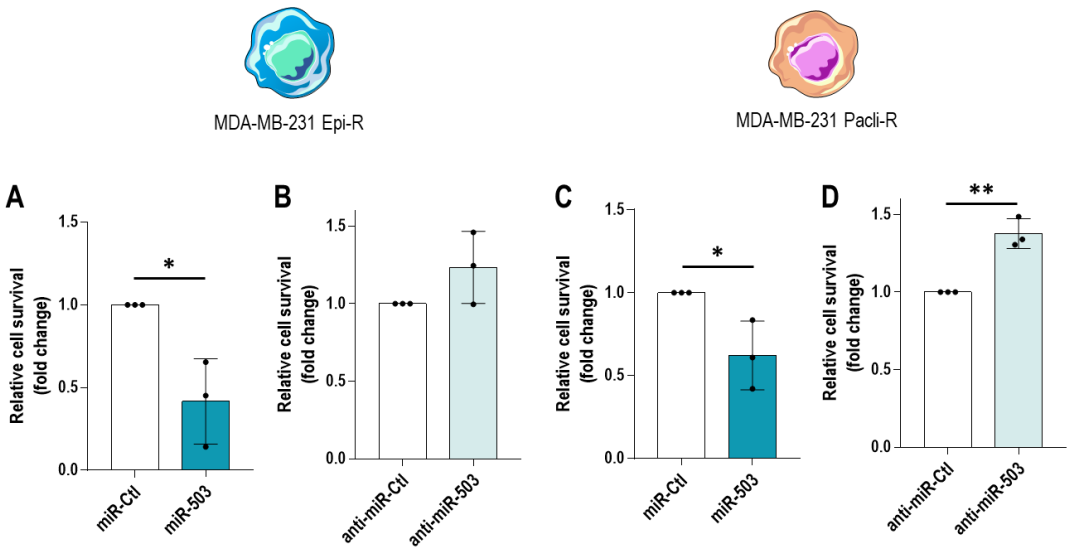

Figure R 51. miR-503 reduces epirubicin-resistant and paclitaxel-resistant breast cancer cell survival.
*MDA-MB-231 Epi-R (**A**, **B**) or Pacli-R (**C**, **D**) were transfected with 10 nM of miR-503 (**A**, **C**) or anti-miR-503 (**B**, **D**) and their respective controls (miR-Ctl and anti-miR-Ctl) for 24h. miR-503 and anti-miR--503 are, respectively, represented in dark and light blue. Analysis of the survival capacity of cells was assessed by a colorimetric assay. WST1 was added to the cells and the absorbance was measured after 1h. Data are expressed as mean ± SD from three experiments and compared to the control (miR-Ctl or anti-miR-Ctl) (*, p<0.05; **, p<0.01).*

These results indicate that genetic miR-503 overexpression reduces significantly breast cancer cell proliferation, migration and invasiveness. Interestingly, epirubicin and paclitaxel-resistant cells respond also to the miRNA treatment and the same phenotype is observed.

3.2. miR-503 reduces the expression of CCND1 and CCND3

To explore the molecular mechanism responsible for the inhibition of tumorigenicity by miR-503, we selected putative target genes involved in proliferation, migration, adhesion and invasion. We used a computational approach involving the Targetscan algorithm (http://www.targetscan.org/) to obtain a list of genes predicted to be targets of miR-503. We observed the presence of proteins that influence cell cycle, proliferation, migration and adhesion pathways. Using qRT-PCR, we tested a subset of miR-503 target genes that displayed pro-tumoral properties (**Suppl. Table S6**.). From this subset of genes, we identified three targets of miR-503, CCND1, CCND2 and CCND3. As shown in **figure R 52**, CCND1 and CCND3 were downregulated at the RNA levels upon overexpression of the miRNA while CCND2 level was not affected. Interestingly, the diminution of both cyclins was observed in native and in Epi-R and Pacli-R cells.

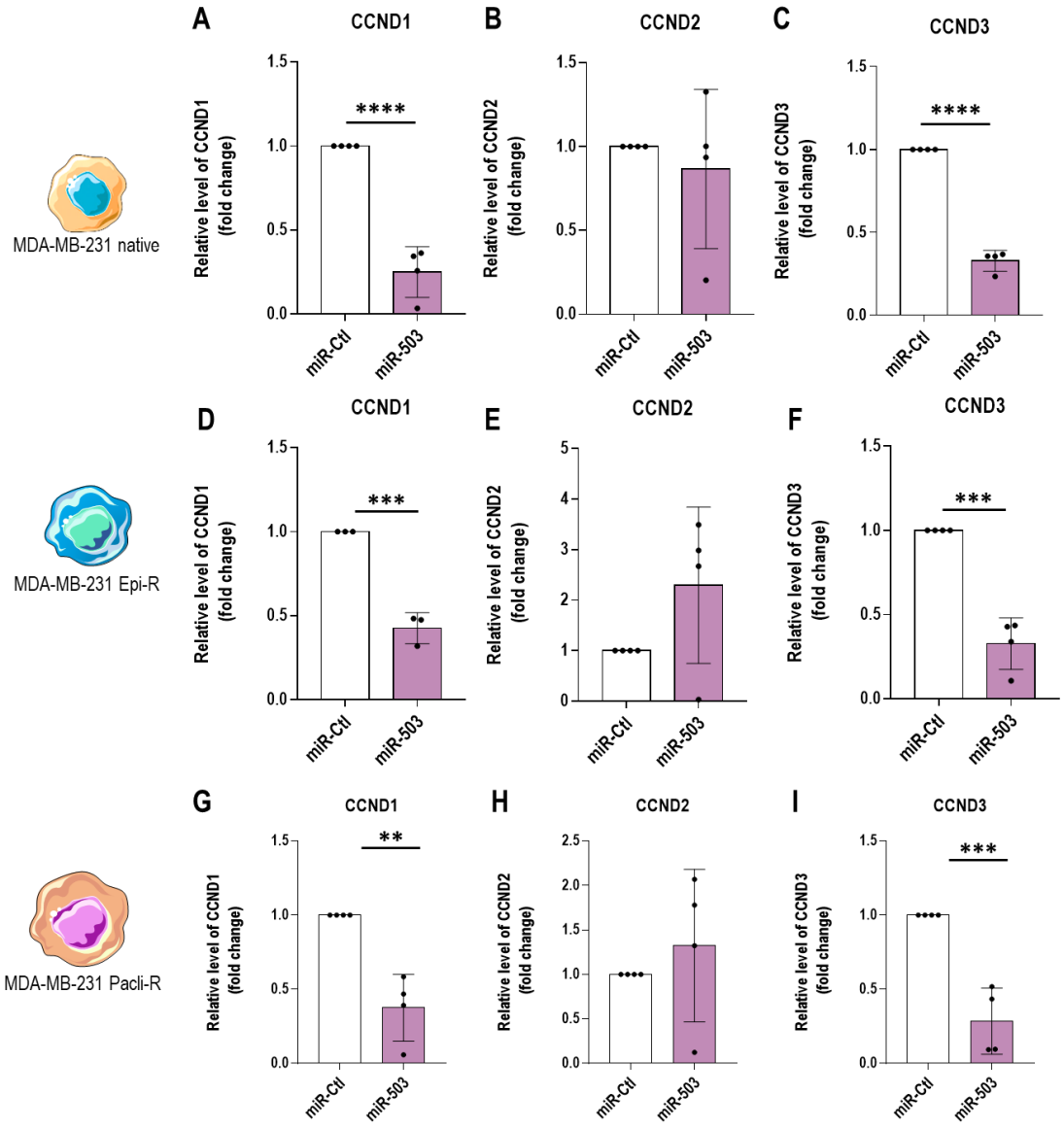

Figure R 52. miR-503 targets CCND1 and CCND3.
*After 24h of transfection with 10 nM of miR-503 and its control (miR-Ctl), RNAs were extracted from MDA-MB-231 cells (Native, Epi-R and Pacli-R). The levels of expression of CCND1 (**A**, **D**, **G**), CCND2 (**B**, **E**, **H**) and CCND3 (**C**, **F**, **I**) are represented as fold change of their level in the control condition. The values are normalized to the mean Ct of B2M and PPIA. Data are expressed as mean ± SD from three independent experiments compared to the control (**, p<0.01; ***, p<0.001).*

Moreover, the inhibition of miR-503 downregulated the levels of CCND1 and CCDN3 whereas CCND2 expression is not affected. The same results were obtained for both sensitive and resistant cell lines (**Fig. R 53**).

These results demonstrate that miR-503 curtails tumor cell proliferation through the inhibition of two of its targets: CCND1 and CCND3.

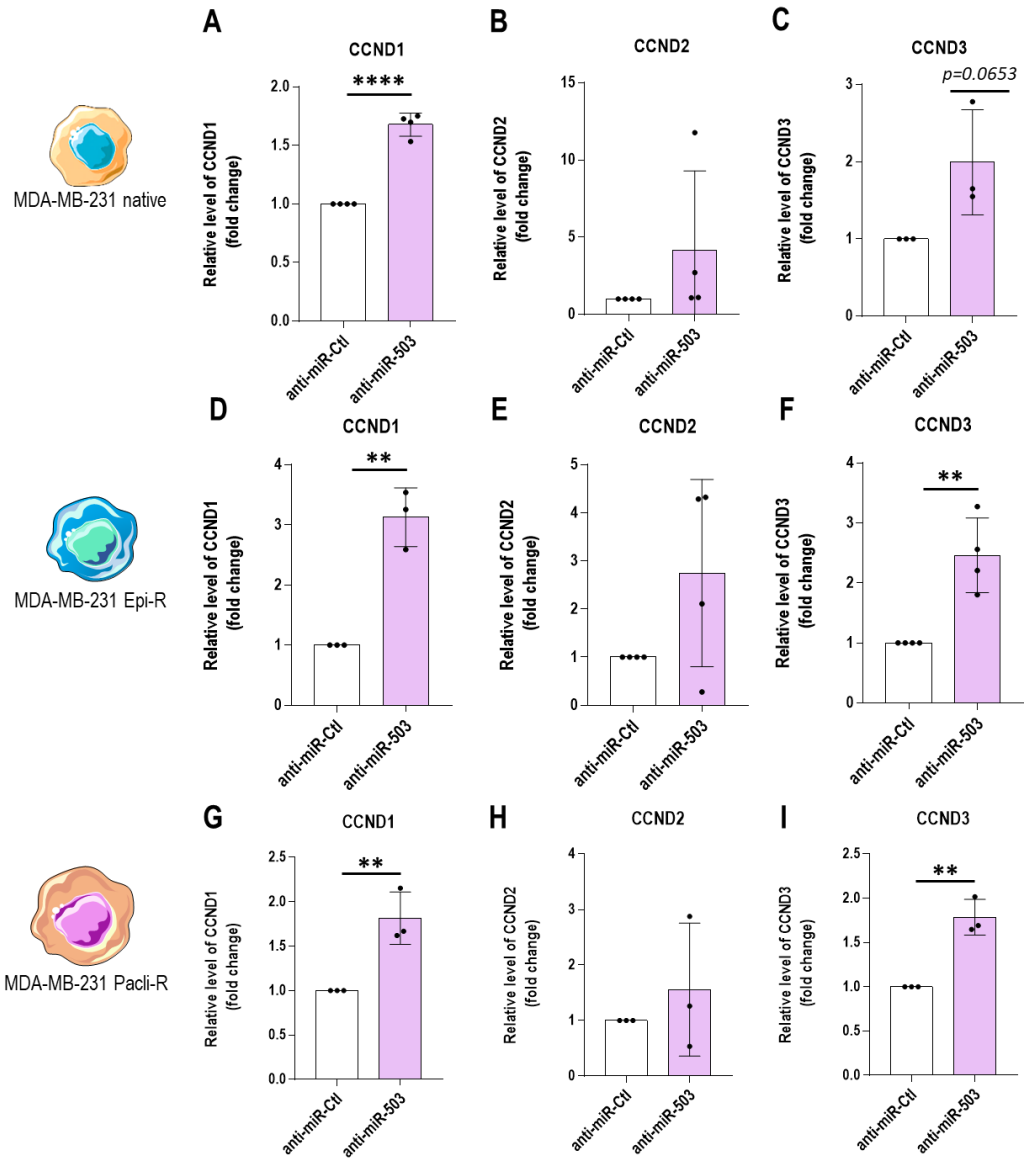

Figure R 53. miR-503 targets CCND1 and CCND3.
*After 24h of transfection with 10 nM of anti-miR-503, and its controlss (anti-miR-Ctl), RNAs were extracted from MDA-MB-231 cells (Native, Epi-R and Pacli-R). The levels of expression of CCND1 (**A**, **D**, **G**), CCND2 (**B**, **E**, **H**) and CCND3 (**C**, **F**, **I**) are represented as fold change of their level in the control condition. The values are normalized to the mean Ct of B2M and PPIA. Data are expressed as mean ± SD from three independent experiments compared to the control (**, p<0.01).*

3.3. Functional effects of miR-503-loaded EVs on sensitive and resistant triple-negative breast cancer cells

The communication between cells within the tumor microenvironment is crucial for tumor growth and is involved in the acquisition of drug resistance. For that purpose, we decided to determine the effects of endothelial extracellular vesicles on sensitive and resistant breast cancer cells. These EVs were electroporated with the miR-503 and incubated for 6h on natives, Epi-R or Pacli-R MDA-MB-231 cells (**Fig. R 54**). To confirm that miR-503 electroporation was efficient, we measured by qRT-PCR the levels of miR-503 and the miR control (Cel-miR-67) in all cell lines. The validation showed that miR-503 was overexpressed in cancer cells previously incubated with miR-503 enriched EVs. Interestingly, the incorporation of endothelial miR-503-loaded EVs into resistant cells was more efficient compared to native cells (**Fig. R 54c, f, i**).

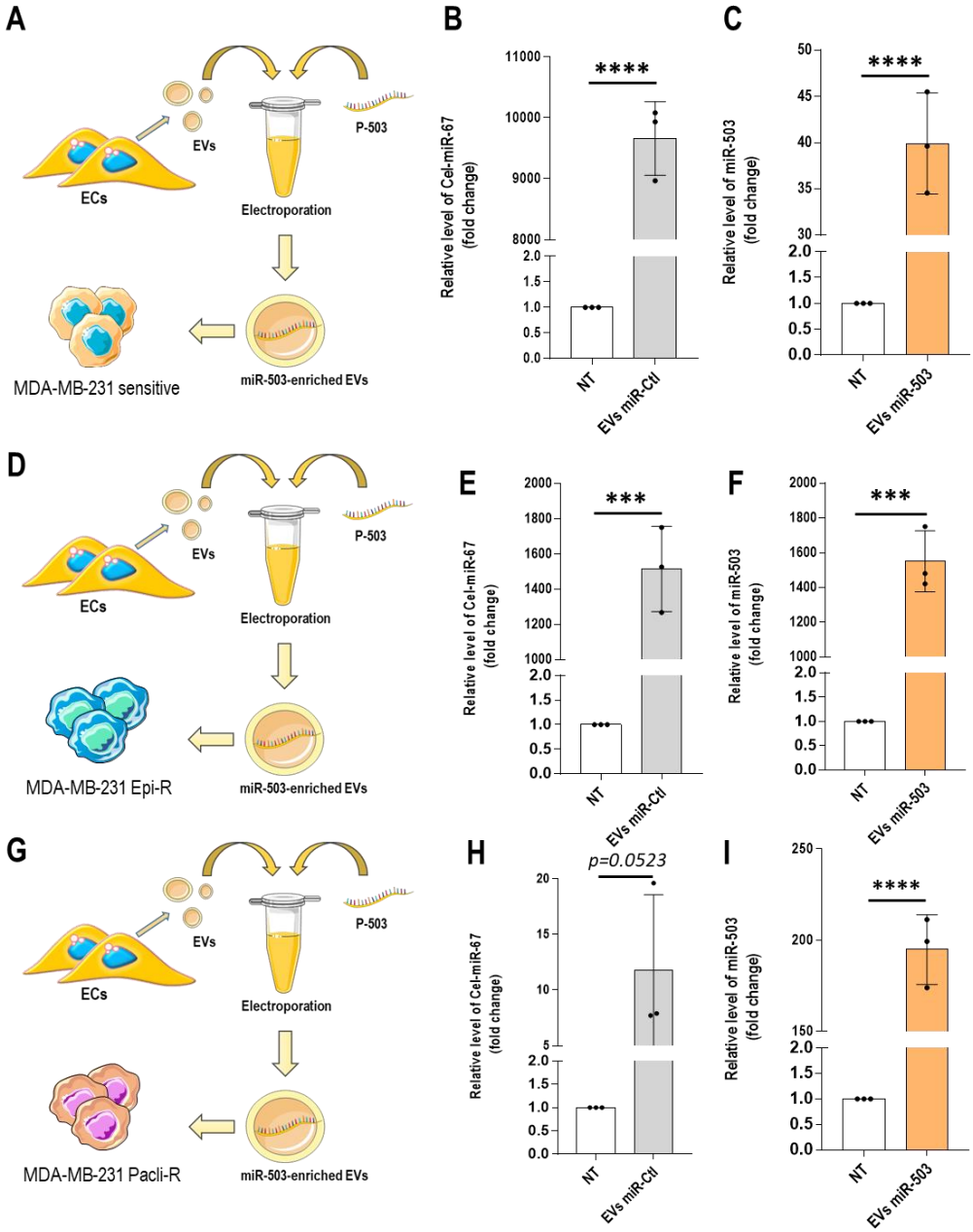

Figure R 54. miR-503-enriched EVs are efficiently incorporated in sensitive and resistant cells.
*Schematic representation of miR-503 electroporation and incubation for 6h on MDA-MB-231 native (**A**), Epi-R (**D**) and Pacli-R (**G**) cells. Cells were treated with 5 µg of EVs. RNAs were extracted from MDA-MB-231 cells. Cel-miR-67 and miR-503 electroporated EVs are, respectively, represented in grey and orange. The levels of expression of Cel-miR-67 (**B**, **E**, **H**) and miR-503 (**C**, **F**, **I**) are represented as fold change of their level in the control condition (non-treated). The values are normalized to the mean Ct of RNU44 and RNU48. Data are expressed as mean ± SD from three independent experiments compared to the control (***, p<0.001; ****, p<0.0001).*

Then, we decided to analyze the functional impact of these endothelial EVs on tumor cell proliferation and migration. Results of BrDU incorporation showed that, compared to non-treated or miR-Ctl conditions, miR-503-loaded EVs reduces significantly breast cancer cell proliferation (**Fig. R 55**).

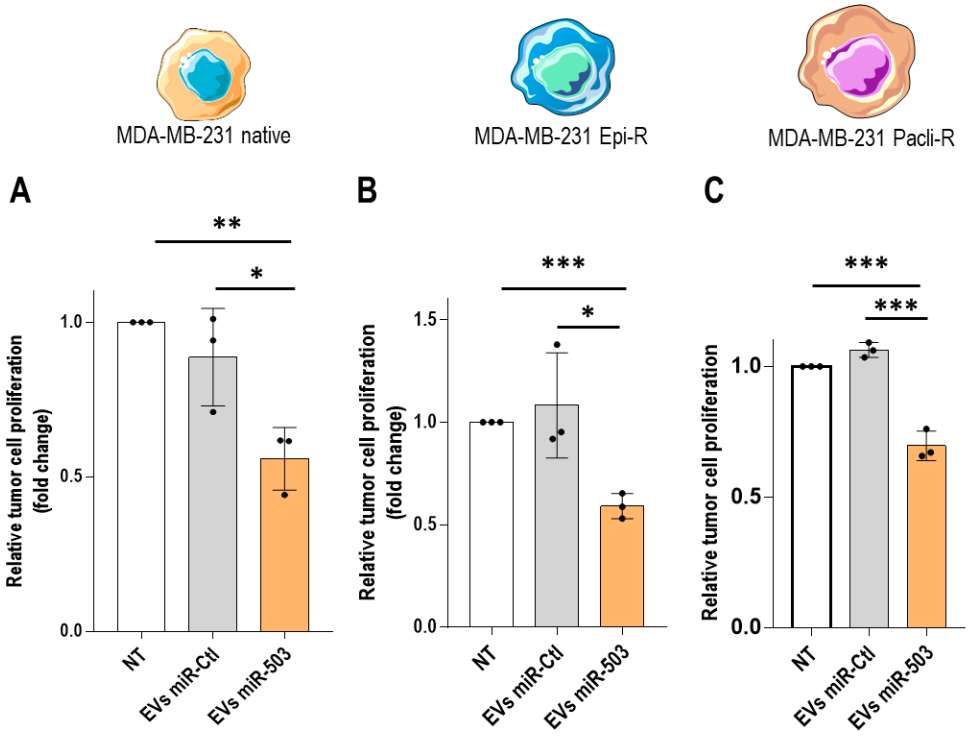

Figure R 55. miR-503-enriched EVs curtails sensitive and resistant triple-negative breast cancer cell proliferation.
*After 6 h of EVs incubation, the proliferation of native (**A**), Epi-R (**B**) and Pacli-R (**C**) was assessed by the measure of the incorporation of BrDU during 16h. Cells were treated with 5 µg of EVs. Scale bar: 250 µm. Data are expressed as mean ± SD from three independent experiments compared to the control (*, p<0.05; **, p<0.01; ***, p<0.001).*

The migratory capacities, assessed by scratch-wound assays, showed that the incorporation of miR-503 within both sensitive and resistant tumor cells decreases significantly their proliferation (**Fig. R 56**). These results establish the role of miR-503 as an inhibitor of breast cancer cell progression.

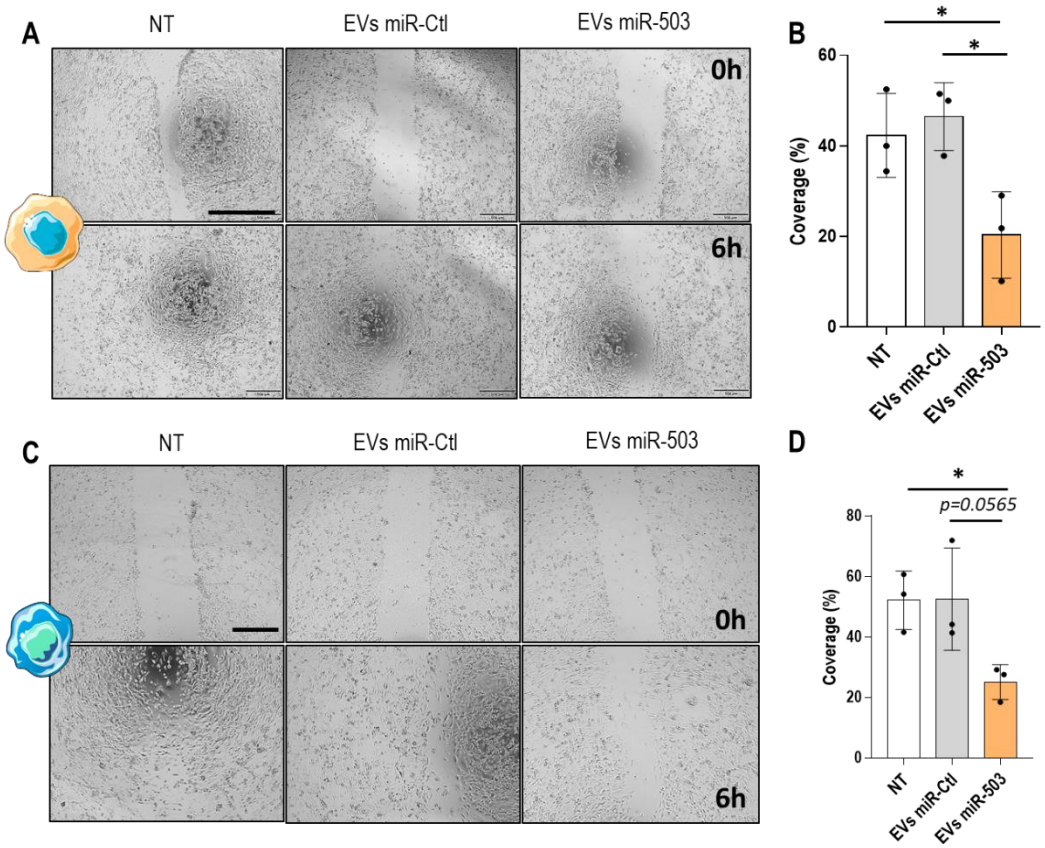

Figure R 56. miR-503-enriched EVs curtails sensitive and resistant triple-negative breast cancer cell migration. *Scratch-wound assays were performed after 24 h of incubation with electroporated EVs. (**A**, **C**) Representative brightfield images of scratch-wound assays were acquired at the indicated time points. Scale bar: 250 µm. (**B**, **D**) Quantification of cell migration after 6 h. Data are expressed as mean ± SD from three independent experiments compared to the control (*, p<0.05).*

3.4. miR-503-loaded EVs impair breast cancer growth in vivo

We next investigated whether miR-503 could impair TNBC cells for growth in *vivo*. We implanted sensitive MDA-MB-231 cells orthotopically in the mammary gland of 6-weeks old NOD-SCID mice (**Fig. R 57**). At day 18, tumors were visible and we started the injection of electroporated EVs every three days until the tumor reach a certain volume. The efficiency of EV incorporation within tumors was assessed by qRT-PCR. As shown in **Fig. R 57c**, miR-503 levels were up-regulated in the corresponding tumors. Therefore, EVs were effectively incorporated. Interestingly, miR-503-loaded EVs impaired drastically breast cancer growth in vivo.

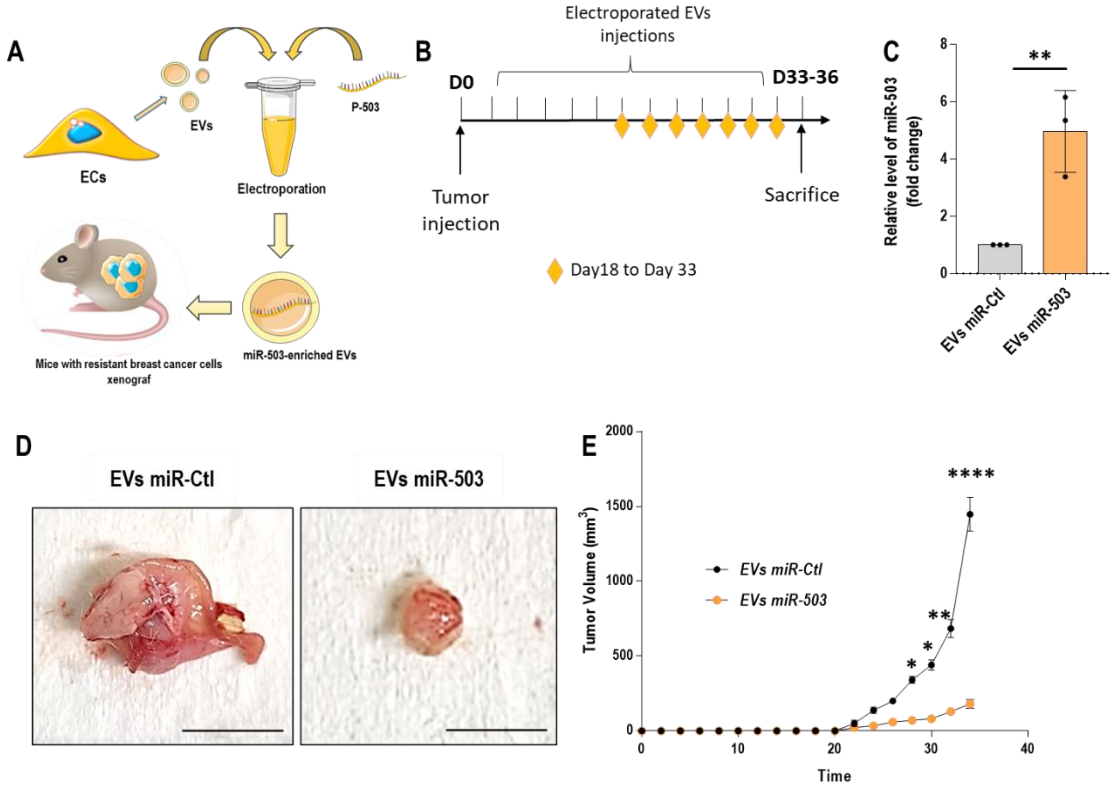

Figure R 57. miR-503-enriched EVs curtails sensitive breast tumor growth.
*(**A**) Schematic representation of miR-503 electroporation and injection in 6-week-old mice NOD-SCID mice orthotopically implanted with 5 × 10^4 MDA-MB-231. (**B**) Schematic illustration of the injection protocol. At day 0, cells were injected. Tumors appeared after 18 days and the EVs injection started the same day until the day of sacrifice (Day 33). (**C**) RNAs were extracted from tumors treated with miR-503 or miR-Ctl-loaded EVs. The levels of expression of miR-503 is represented as fold change of its level in the control condition. The values are normalized to the mean Ct of RNU44 and RNU48. Data are expressed as mean ± SD from three independent experiments compared to the control (**, p<0.01). (**D**) Representative photographs of breast adenocarcinoma removed after 33 days from orthotopically implants of 5 × 10^4 MDA-MB-231 native cells in 6-week-old mice treated with the indicated vesicles. Scale bar: 0.5 cm.(**E**) Growth curves of orthotopically implanted 5 × 10^4 MDA-MB-231 native cells treated with the indicated EVs at day 0 in 6-week-old mice. Data are expressed as mean ± SEM from two independent experiments compared to the control (n = 10; **, p<0.01, ****, p<0.0001).*

Results

Chapter IV

miR-503 and hnRNPA2B1:
implications for breast cancer patients

4. miR-503 and hnRNPA2B1: implications for breast cancer patients

In this final chapter, we decided to study the potential implications of miR-503 and hnRNPA2B1 for breast cancer patients. First, we decided to perform bioinformatics to determine if miR-503 expression was linked to breast cancer progression. Moreover, we evaluated the potential correlation between miR-503 and the miR-EXO protein levels within breast cancer tissue samples using Molecular Taxonomy of Breast Cancer International Consortium (METABRIC) and/or The Cancer Genome Atlas (TCGA) databases.

Interestingly, as shown in **figure R 58**, the deletion of miR-503 locus negatively altered breast cancer patient survival. Nevertheless, this decrease was greater using METABRIC, a database focusing on breast cancer, than TGCA analysis.

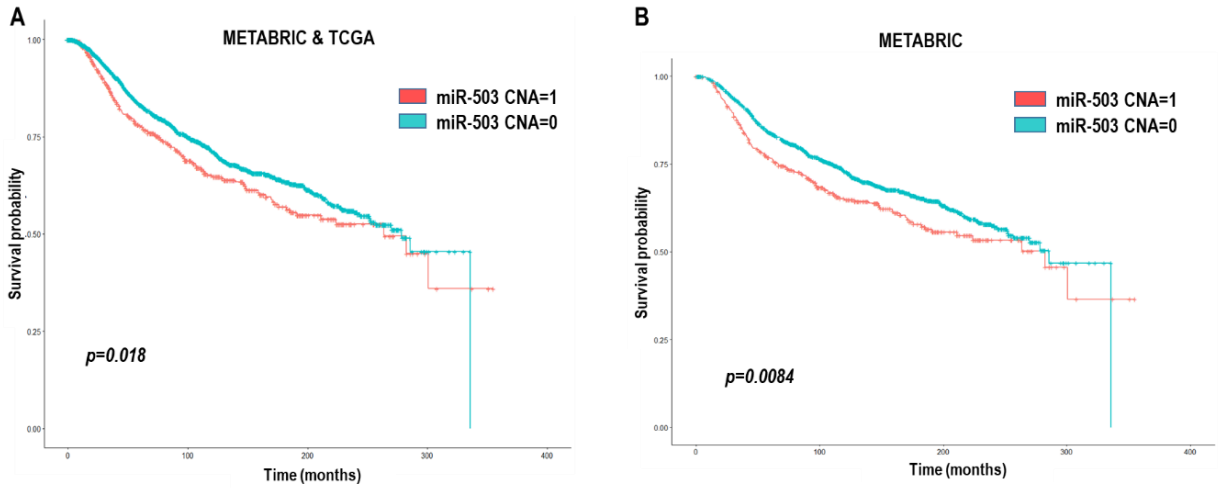

Figure R 58. miR-503 deletion reduces breast cancer patient survival.
*Kaplan-Meier survival curve showed data extracted from TCGA or METABRIC databases. Kaplan-Meier curve from (**A**) TCGA and METABRIC databases. Blue curves represent patients without any mutation in miR-503 locus (n = 2296), while red curves represent patients carrying a mutation in the locus (n = 315). (**B**) Kaplan-Meier survival curve from METABRIC database. Patients without copy number alterations (CNA) (n = 1574) and patients carrying one CNA (n = 159).*

Then we performed correlation studies to determine if miR-503 levels were related to the miR-EXO in patients. To do so, we sorted TCGA data into two categories, high or low levels of 503, and compared them to the expression of hnRNPA2B1. Box plots (**Fig. R 59**) showed that hnRNPA2B1 and miR-503 levels were positively associated. Indeed, high levels of miR-503 were correlated with high levels of hnRNPA2B1. Interestingly, for ANXA2, the levels were inversely correlated with miR-503 expression.

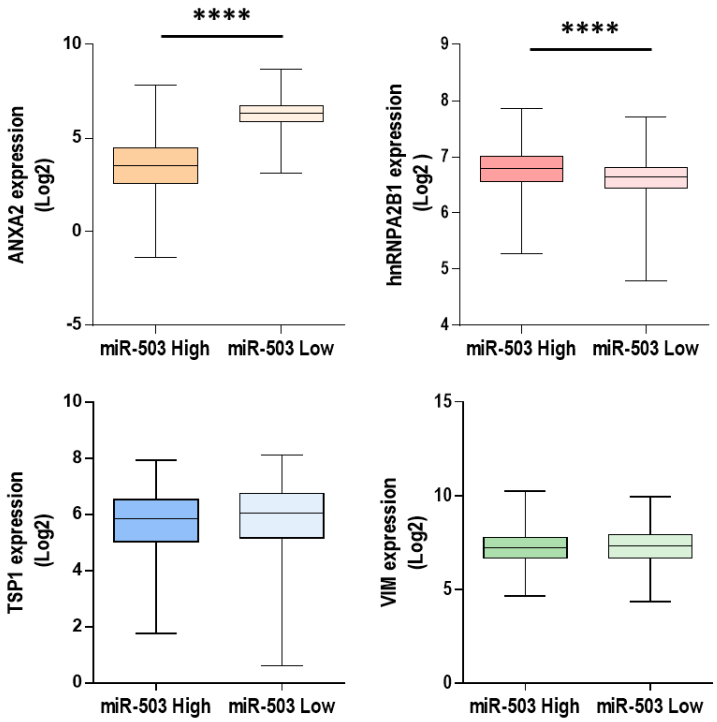

Figure R 59. hnRNPA2B1 levels are positively correlated with miR-503 expression.
*Box plots represent data from breast cancer patients (n = 1084) from the TCGA database. In this analysis, we sorted the 20% samples where miR-503 was less or more expressed (****; p<0.0001).*

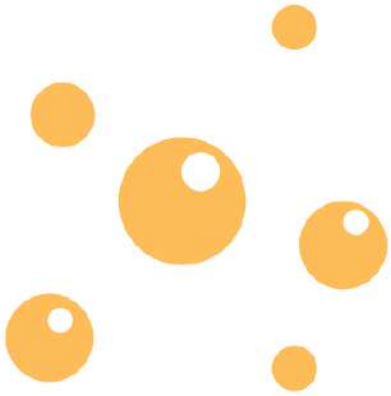
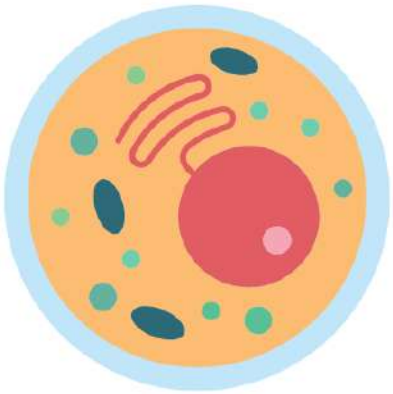


Discussion, Conclusion & Perspectives

Discussion, conclusion and perspectives

The work presented in this dissertation provides new insights into the mechanism of miR-503 export into EVs and its implications in breast cancer.

First, we aimed to unravel the exosomal export of the anti-tumoral miRNA, miR-503, released by the endothelium. For that purpose, we decided to study the molecular mechanism responsible for miR-503 export in endothelial EVs. As previously described in our laboratory, exosome composition can be modulated under specific conditions. For instance, the chemotherapeutic agent epirubicin increase mir-503 levels in exosomes released from HUVEC without affecting its levels within the cell.

miR-503 levels were upregulated in exosomes released from HUVECs upon treatment with the chemotherapeutic agen epirubicin. Interestingly, the levels of this particular miRNA were not changed within the cell (Bovy *et al.*, 2015). These data prompt us to hypothesize that chemotherapeutic agents, including epirubicin, specifically enhance the export of mir-503 in endothelial exosomes by an unknown mechanism. So far, only few papers propose partial mechanisms responsible for miRNA sorting within EVs.

For instance, it has been shown that, through a motif-dependent process, hnRNPA2B1 links specific miRNAs inducing their export in exosomes (Villarroya-Beltri *et al.*, 2013a). hnRNP-Q (aka SYNCRIP) and hnRNPU could also induce miRNA sorting, sharing an exo-motif, in EVs (Santangelo *et al.*, 2016; Zietzer *et al.*, 2020). However, other motif-independent mechanisms exist. For instance, Y-Box binding protein 1 (YBX1), MEX3C, and ANXA2 were also described to induce specific miRNA export (Hagiwara *et al.*, 2015; Shurtleff *et al.*, 2016; Lu *et al.*, 2017).

Interestingly, our unbiased approach, pull-down of biotinylated miRNA followed by mass spectrometry analysis revealed nine potential miR-503 partners: Annexin A2 (ANXA2), heterogeneous Nuclear Ribonucleoprotein A2/B1 (hnRNPA2B1), fibronectin 1 (FN1), thrombospondin-1 (TSP1), vimentin (VIM), Perlecan, β-actin, Propionyl-CoA carboxylase (PCCA), and pyruvate carboxylase (PC). As native biotin binders, the two latter were considered as positive control of the experiments. The validation of the proteomic analysis by pull-down assay followed by western blotting highlighted that both Perlecan and β-actin were not specific and were, therefore, eliminated.

To confirm that these putative partners were specific to miR-503, we decided to transfect HUVECs with a biotinylated form of the miRNA control (cel-miR-67 or miR-Ctl) and only ANXA2, hnRNPA2B1, TSP1, and VIM were found in the miR-503 pulldown condition while FN1 was present in both samples. Because of its role and abundance in the extracellular matrix of endothelial cells (Spada *et al.*, 2021), FN1 was found in both conditions and thus considered as a contaminant.

Interestingly, the pull-down assays revealed the presence of the RNA-Binding protein (RBP) hnRNPA2B1. As mentioned previously, a sumoylated form of this protein can regulate the export of specific miRNAs in exosomes in a motif sequence-dependent manner. These ncRNAs shared a sequence motif, also called EXO-motif: GGAG. The others, maintained within the cells, presented a cellular motif: UGCA (Villarroya-Beltri *et al.*, 2013). Interestingly, miR-503 possesses this cellular motif, thus, hnRNPA2B1 might maintain the miRNA within the cells. TSP1 is a major component of the ECM. This protein is a well-known angiogenesis inhibitor (Bornstein, 2009) and promotes EMT (Ribatti *et al.*, 2020). VIM is a cytoskeleton protein and composes intermediate filaments. This protein maintains cell integrity and is involved in adhesion, migration, and EMT (Wu *et al.*, 2018).

Our previous results suggest that miR-503 interacts with some "sorting proteins". Our goal is to understand why epirubicin treatment enhances the release of miR-503. Therefore, we postulate that epirubicin could affect the mRNA and protein levels of the miR-EXO proteins. We evaluated these levels inside the cells upon epirubicin treatment to verify our hypothesis. Surprisingly, epirubicin did not seem to regulate the cellular expression of miR-EXO proteins. Nevertheless, the treatment affected the exosomal amount of one miR-EXO protein, ANXA2, which exhibited up-regulated levels. These results are not surprising. Indeed, this protein is a member of the annexin family expressed on the surface of endothelial and other types of cells. ANXA2 is involved in many cellular processes such as vesicle transport, endo- and exocytosis (Ma et al., 2021). Furthermore, ANXA2 is one of the top twenty most common proteins found in extracellular vesicles (Mathivanan et al., 2012). Interestingly, this protein has been described to recruit miRNAs into EVs in a sequence-independent manner. However, ANXA2 did not modulate the loading of miR-503 (Hagiwara et al., 2015).

We then aimed to study the bindings between the miRNA and the proteins. The several crosslinking conditions (No CL, UV, UV+CHL) showed that ANXA2 was found in each condition. Since the strongest links are maintained with or without UV crosslinking, ANXA2 presented the strongest interaction with miR-503. Whereas hnRNPA2B1, VIM and TSP1 were

not found in the UV lysate, the crosslinking allowing the interaction between protein and RNA, we demonstrated that they were in the periphery of the miR-EXO complex.

Immunoprecipitation assays followed by miR-503 quantification by qRT-PCR showed that epirubicin disrupted the interaction between the miRNA, hnRNPA2B1, and VIM. Whereas, the interaction between miR-503 and ANXA2 was strengthened. These results are in line with the export of ANXA2 within exosomes after epirubicin treatment and suggest that ANXA2 acts as an enhancer of miR-503 export while hnRNPA2B1 inhibits it.

To better understand the effects of epirubicin on the localization of the miR-EXO proteins, especially hnRNPA2B1, we proceeded to immunofluorescence and subcellular fractionation assays. Interestingly, hnRNPA2B1 was the only protein affected by the treatment and was relocalized within the nucleus where it could play its major functions. Indeed, hnRNPA2B1 is a RBP involved in alternative splicing, transcription, translation, telomere maintenance and RNA transport (Moran-Jones *et al.*, 2005; Liu and Shi, 2021). This protein has also been reported to promote tumor growth (Yu Yang *et al.*, 2020). Through its N6-methyladenosine (m^6A) reader function, hnRNPA2B1 can also mediate the processing of pri-miRNAs (Alarcón *et al.*, 2015). Interestingly, this RBP has been described to bind double-strand breaks and modulate the mRNA splicing after DNA damages caused by chemotherapy (Tchurikov *et al.*, 2013; Cloutier *et al.*, 2018). Indeed, it is well established that chemotherapeutic agents can induce DSB (Woods and Turchi, 2013). Therefore, epirubicin treatment may induce a relocalization of hnRNPA2B1, and thus disrupts the interaction between the protein and miR-503, to play its major roles within the nucleus.

Finally, we demonstrated that the two miR-EXO proteins, ANXA2 and hnRNPA2B1, were required for miR-503 sorting into EVs. Due to its overexpression in EVs and its higher affinity for the miRNA upon treatment, ANXA2 seemed to induce miR-503 sorting. Indeed, the protein has been described to facilitate the endosomal trafficking of RNAs (Wang *et al.*, 2016). On the other hand, hnRNPA2B1 inhibited miR-503 export within EVs. However, this protein could also maintain miRNAs carrying a cellular motif (UGCA) such as miR-503.

Figure D 60 summarizes the molecular mechanism of miR-503 export in EVs upon epirubicin treatment. First, the drug enhances the interaction between miR-503 and ANXA2 but disrupts the binding with hnRNPA2B1. These changes induce a switch in the localization of hnRNPA2B1 that returns to the nucleus. Finally, together with ANXA2, miR-503 is exported

within endothelial EVs. Our findings were the first to describe the roles of a RBP in the sorting of miRNAs and were published in 2020 in CMLS (Pérez-Boza *et al.*, 2020).

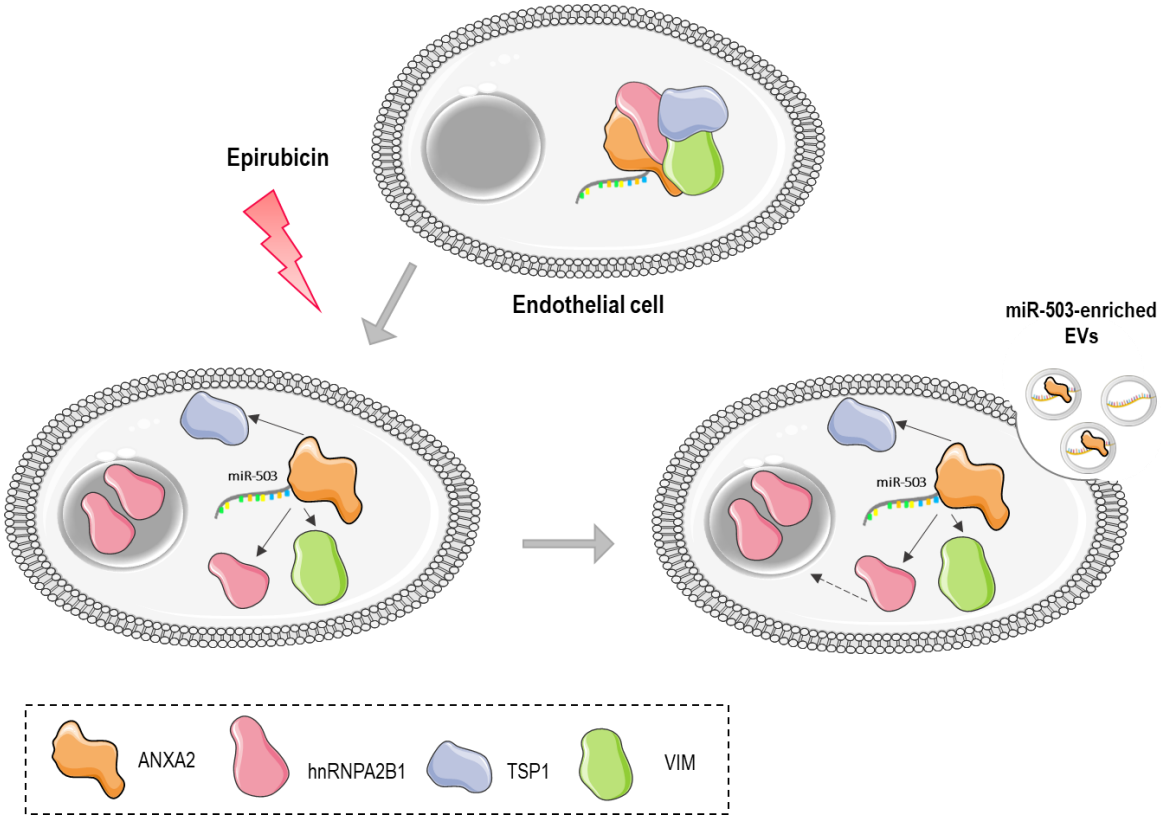

Figure D 60. Schematic representation of miR-503 export in EVs upon epirubicin treatment.
When endothelial cells are treated with epirubicin, the miR-EXO complex, composed of miR-503 and the miR-EXO proteins, disrupts. ANXA2 (in orange) remains strongly attached to the miRNA while hnRNPA2B1 (in pink), TSP1 (in blue) and VIM (in green) are detached. Then, hnRNPA2B1 returns within the nucleus to play its key role in RNA processing. All of these processes allow the sorting of miR-503, accompanied by ANXA2, into EVs.

When endothelial cells are treated with epirubicin, the miR-EXO complex, composed of miR-503 and the miR-EXO proteins, disrupts. ANXA2 (in orange) remains strongly attached to the miRNA while hnRNPA2B1 (in pink), TSP1 (in blue) and VIM (in green) are detached. Then, hnRNPA2B1 returns to the nucleus to play its key role in RNA processing. All of these processes allow the sorting of miR-503, accompanied by ANXA2, into EVs.

In the second part of the project, we were interested in the putative role of mir-503 enriched-endothelial EVs on triple-negative breast cancer cell behavior. Indeed, we previously observed that epirubicin treatment increased the levels of miR-503 within endothelial EVs. Since EVs play a crucial role in cell communication and tumor microenvironment, we postulated that miR-503 enriched endothelial EVs could affect the tumor cells behavior.

Since epirubicin treatment can affect both endothelial and tumor cells, to simplify our model for the next step of the investigation, we decided to investigate the effect of the miR-EXO protein knockdown in endothelial cells on breast cancer cells. Of note, hnRNA2B1 inhibits the sorting of miR-503 in EVs, whereas ANXA2 enhances it.

To do so, we cocultured silenced HUVECs with MDA-MB-231 and performed several assays.

MDA-MB-231	siANXA2	sihnRNPA2B1	siTSP1	siVIM
Proliferation	=	↓	↓	↓
Migration	=	↓	=	=
Invasion	=	↓	=	=

Table D 1. Summary table of the functional effects of miR-EXO endothelial silencing on MDA-MB-231.

As shown in **table D 1**, the silencing of hnRNPA2B1 had drastic effects on triple-negative breast cancer cell tumorigenicity. Indeed, hnRNPA2B1 endothelial inhibition impacted negatively proliferative, migratory and invasive capacities of triple-negative cells. Of course, we discarded the possibility of a transfer of sihnRNPA2B1 from endothelial to cancer cells-since hnRNPA2B1 is known to promote the progression of many cancer types such as breast, colon, and liver (Hu *et al.*, 2017; Yu Yang *et al.*, 2020; J. Tang *et al.*, 2021) and, interestingly, tumor cells cultured in presence of hnRNPA2B1-silenced HUVECs showed increased levels of miR-503. These results could be explained by our previous study which has demonstrated that hnRNPA2B1 silencing upregulated the exosomal levels of miR-503 (Pérez-Boza, Boeckx, *et al.*, 2020). To confirm that miR-503 was responsible for reducing breast cancer cell tumorigenicity, we decided to select putative targets of miR-503 that could explain the phenotype observed. Using the Targetscan algorithm, we selected four miR-503 targets that could potentially explain our phenotype: CCND2, CCND3, BCL2 and MYB. Cyclins D2 and D3 play critical roles in the cell cycle progression, and thus in proliferation, by their association with cyclin-dependent kinases during the G1 phase. Moreover, these proteins are classified as oncogenes by promoting tumor development (Büschiges *et al.*, 1999; Moreno-Bueno *et al.*, 2003). Bcl-2 is an anti-apoptotic protein that increases cell survival but has no effect on proliferation (Hardwick & Soane, 2013). The oncogene MYB codes for a transcription factor promoting cell proliferation (Sala, 2005). Interestingly the levels of two of them were impaired by hnRNPA2B1 silencing: CCND2 and CCND3, two pro-proliferative proteins. However, these targets do not help us understand the changes in the migratory of invasive properties.

Since epirubicin treatment could also induce the sorting of miR-503 within EVs, we decided to treat endothelial cells with the drug and assess breast cancer cell proliferation. Likewise, epirubicin reduced drastically their proliferative capacities. By quantifying miR-503 levels, we confirmed that the miRNA was overexpressed within cancer cells cocultured with epirubicin-treated HUVECs. Therefore, we speculated that hnRNPA2B1 silencing mimics the effects of epirubicin on endothelial cells which leads to the sorting of miR-503 in EVs. Nevertheless, the proliferation impairment was not due to the downregulation of pro-proliferative targets such as CCND2 and CCDN3.

Comforted by our interesting results, we wished to investigate deeply the transfer of EVs between HUVECs and MDA-MB-231. Therefore, we generated fluorescent cell lines, HUVECs CD63-GFP and MDA-MB-231 CD63-mCherry. CD63 is a tetraspanin family member, similar to CD9 and CD81. However, although CD9 and CD81 are enriched in both exosomes and microvesicles, CD63 enrichment seems to be only detected on the exosome surface (Van Niel *et al*., 2018). Moreover, this tetraspanin has been reported in the surface of late endosomes, ILVs, and lysosomes (Pols & Klumperman, 2009). Fluorescent cells allowed us to observe the transfer of EVs between HUVECs and MDA-MB-231, in both directions.

We wanted to determine if endothelial EVs, alone, could affect the tumor phenotype. First, we characterized the particles generated by silenced HUVECs. The size and morphology, analyzed by DLS and TEM, are in agreement with the size of small EVs (up to 150 nm). The expression of EV markers such as CD9, CD63, and CD81 was analyzed by Western blotting, and we observed an enrichment in all three tetraspanins in the EV samples. The same characterization was realized for EVs produced by normal HUVECs, and we observed the same tetraspanin pattern and enrichment in syntenin-1, an exosomal marker. Syntenin is a protein implicated in exosome biogenesis through its interaction with ALIX (Roucourt *et al.*, 2015). Moreover, Cytochrome c, associated with mitochondria and apoptotic bodies, was absent from EVs fractions. This EV composition corresponds to small vesicles, potentially exosomes, but we cannot exclude the presence of other types of vesicles. Nevertheless, the guidelines to characterize exosomes were redefined in 2018 and comprises multiple methods of isolation and characterization (Théry *et al.*, 2018). Small EVs, produced by miR-EXO-silenced-HUVECs, were incorporated within cancer cells and curtailed, on their own, the proliferation of MDA-MB-231 cells. The up-and down-regulation of miR-503 and its target confirmed that EVs released from hnRNPA2B1-silenced endothelial cells could affect cancer cell behavior through

the transfer of miR-503. Furthermore, the incorporation of miR-503 led to the inhibition of CCND2 which reduced breast cancer cell proliferation.

In summary, hnRNPA2B1 silencing mimics epirubicin treatment in HUVECs, causing the export of miR-503, an anti-tumoral miRNA. miR-503-enriched EVs are incorporated within breast tumor cells where the miRNA acts as an inhibitor of, mostly, proliferation through the downregulation of Cyclin D, but also migration and invasion (**Fig. D 61**). These results offer new possibilities for the development of anti-cancer drugs.

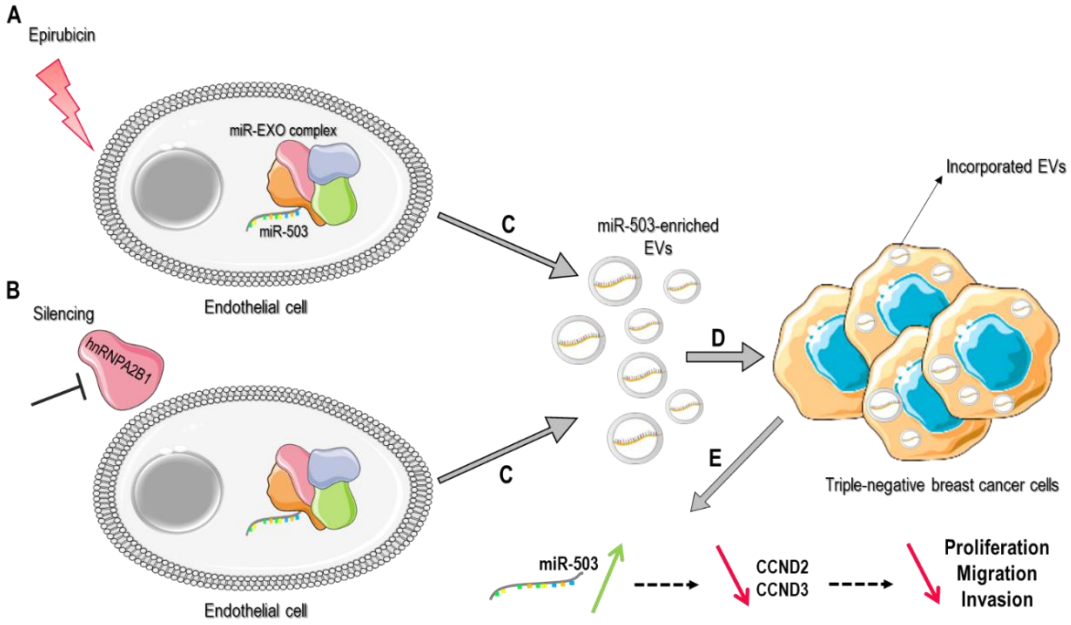

Figure D 61. Endothelial hnRNPA2B1 silencing mimics epirubicin treatment and leads to the sorting of miR-503 into EVs, which are incorporated within cancer cells.
*Both epirubicin treatment (**A**) and hnRNPA2B1 silencing (**B**) of endothelial cells induce the export of miR-503 (**C**) into EVs. These particles are then incorporated by breast tumor cells and release miR-503 within the cytosol, where it can play its anti-tumoral roles by inhibiting CCND2 and CCDN3. These proteins, involved in cell cycle progression, reduce cancer cell proliferation. Nevertheless, other targets inhibit the migratory and invasive capacities of these cells.*

Both epirubicin treatment (**A**) and hnRNPA2B1 silencing (**B**) of endothelial cells induce the export of miR-503 (**C**) into EVs. These particles are then incorporated by breast tumor cells and release miR-503 within the cytosol where it can play its anti-tumoral roles through the inhibition of CCND2 and CCDN3. These proteins, involved in cell cycle progression, reduce cancer cell proliferation. Nevertheless, other targets inhibit migratory and invasive capacities of these cells.

Besides inhibiting cancer cells, epirubicin seems to impact other TME cells such as endothelial cells. Indeed, the chemotherapeutic agent, epirubicin, increases the EV levels of

miR-503. We also demonstrated that this mechanism leads to the incorporation of miR-503-loaded EVs within breast cancer cells and, thus, curtails their capacity to grow. Many papers describe the impact of TME EVs on cancer cell progression. Cells can produce EVs that will rather promote or reduce tumor growth. For instance, tumor-derived exosomes (TDEs) can induce angiogenesis by transferring bioactive molecules, such as miRNAs, to endothelial cells (Ahmadi & Rezaie, 2020). On the other hand, the incorporation of endothelial exosomes into tumor cells suppresses angiogenesis via the down-regulation of VEGF-A (Lee *et al.*, 2013). As described previously, EVs, and their miRNA cargo, play major roles in the acquisition, but also in the inhibition, of multidrug resistance (MDR) (Bach *et al.*, 2017). Considering that chemoresistance is a major problem in breast cancer treatments, we decided to study the impact of miR-503 on drug-resistant breast cancer cells. First, we wanted to know if the effects of the miRNA observed in sensitive cells (Bovy *et al.*, 2015) were conserved in resistant cells or if miR-503 was only effective in cells responding to chemotherapy. Epirubicin and paclitaxel are the two main chemotherapeutic agents used for breast cancer treatments. Thus, thanks to Dr. Gorski and Dr. Spears, we obtained epirubicin or paclitaxel-resistant MDA-MB-231 cells. The IC50 after exposure to the chemotherapeutic agent showed that Epi-R and Pacli-R were indeed less sensitive than native breast cancer cells. Moreover, we quantified the levels of genes involved in MDR: ABCB1, GADD45A, MDH2, POR, SIRT6, and TOP2A.

MDA-MB-231	Epi-R	Pacli-R
ABCB1	↑	/
GADD45A	↑	↑
MDH2	↑	↓
POR	↑	↑
SIRT6	↑	↑
TOP2A	↓	↓

Table D 2. Summary table of the expression levels of genes involved in multi-drug resistance.

As shown in **table D 2**, the levels of ABCB1, GADD45A, POR, and SIRT6 were upregulated in resistant cells. ABCB1 gene codes for the protein P-gp, an efflux pump that allows the release of drugs without cells. Overexpression of this protein has been associated with the acquisition of chemoresistance. Furthermore, therapeutic agents that target P-glycoprotein have been developed (Choi & Yu, 2014). Growth arrest and DNA damage-inducible 45 (Gadd45) is a stress response protein that interacts with BRCA1 and promote

cancer pathogenesis (Pietrasik *et al.*, 2020). Interestingly, its levels have been found increased in doxorubicin-resistant cells (Sherman-Baust *et al.*, 2011). The malate dehydrogenase 2 (MDH2) is an enzyme that catalyzes the reversible oxidation of malate in oxaloacetate through a NAD/NADH dependent system (Minárik *et al.*, 2002). MDH2 has been described to confer resistance to taxanes and anthracyclines in, respectively, prostate and uterine sarcoma cancer cells (Liu *et al.*, 2013; Lo *et al.*, 2015). Nevertheless, this protein is not responsible for the acquisition of resistance in our MDA-MB-231 Pacli-R cells. The enzyme cytochrome P450 oxidoreductase (POR) is present at the endoplasmic reticulum surface and allows the transfer of electrons from NADPH to P450 (Lu *et al.*, 1969). Increased levels of POR have been associated with the acquisition of doxorubicin resistance (Villeneuve *et al.*, 2006). Sirtuin 6 (SIRT6) is a member of the deacetylase family which is involved in multiple pathways such as DNA repair and telomere maintenance. SIRT6 confers chemoresistance to several cancer cells. For instance, SIRT6 increases drug resistance of lymphoma cells (Juan Yang, Li, *et al.*, 2020). Interestingly, its levels have been found increased in epirubicin or paclitaxel-resistant cancer cells (Khongkow *et al.*, 2013). On the other hand, SIRT6 is also described as a tumor suppressor protein (Fiorentino *et al.*, 2021). Finally, TOP2A levels have been found reduced in both epirubicin and paclitaxel-resistant cells. Indeed, Top2α protein, encoded by TOP2A, is one of the main epirubicin targets (Munro *et al.*, 2010). Moreover, its levels are reduced in paclitaxel-resistant cells (Villeneuve *et al.*, 2006). The characterization of resistant MDA-MB-231 confirmed that our breast tumor cells were indeed resistant to epirubicin or paclitaxel.

Interestingly, the basal levels of miR-503 were reduced in both Epi-R and Pacli-R compared to sensitive cells. Among the tumor suppressor roles of this miRNA, several studies have demonstrated that miR-503 curtailed the resistance to chemotherapy (Qiu *et al.*, 2013b). Moreover, the loss of the miR-424/503 cluster favors breast cancer chemoresistance (Rodriguez-Barrueco *et al.*, 2017). However, miR-503 has also been found to confer MDR to colorectal cancer cells (K. Xu *et al.*, 2017). Thus, we were wondering if its overexpression could resensitize resistant breast cancer cells.

MDA-MB-231	Proliferation	Adhesion	Migration	Invasion	Apoptosis
Sensitive	↓	↓	↓	↓	=
Epi-R	↓	↓	↓	↓	=
Pacli-R	↓	↓	↓	/	=

Table D 3. Summary table of the functional effects of miR-503 on sensitive and resistant MDA-MB-231 cells.

The functional assays (**Table D 3**) revealed that miR-503 could, as previously described, impair sensitive breast cancer cell tumorigenicity (Long *et al.*, 2015; Baran-Gale *et al.*, 2016) but also curtails the progression of both epirubicin and paclitaxel-resistant MDA-MB-231 cells. Interestingly, the impact of miR-503 is equivalent between native and Epi-R and Pacli-R cells. Notably, the relative proliferation and migration of resistant and sensitive cell lines were equivalent.This miRNA is often considered as a tumor suppressor and has been shown to reduce breast cancer cell proliferation, migration and invasion (Peng *et al.*, 2014; Long *et al.*, 2015). Our results showed that miR-503 had no impact on both sensitive and resistant cell death. Indeed, in the second chapter, we found that miR-503 did not target BCL2 in our MDA-MB-231 cells. However, the miRNA has been previously described to reduce cancer chemoresistance through the targeting of BCL2 and, therefore, promoted cancer cell apoptosis (Qiu *et al.*, 2013). Another interesting fact is that Pacli-R cells could not grow as spheroids in a collagen matrix. Reynolds and colleagues have demonstrated that paclitaxel treatment modulated spheroid shape. However, these results were obtained with another breast cancer cell type, the MCF7 cells (Reynolds *et al.*, 2017). The phenotype observed in sensitive and resistant tumor cells after miR-503 overexpression can be associated with the cell cycle arrest through the inhibition of CCND1 and CCND3, and, therefore, proliferation. Nevertheless, our previous results have shown that CCND2 was indeed a target of miR-503. Also, the downregulation of cyclins could not explain the impact of miR-503 on tumor migration, survival, invasion, and adhesion.

Since miR-503 is exported in EVs released by HUVECs upon epirubicin and paclitaxel treatments, we wanted to assess their impact on sensitive and resistant cell behavior. The functional assays (**table D 4**) showed that miR-503-enriched EVs reduce the proliferation and migration of sensitive and resistant tumor cells. Considering that EVs might, on their own, either promote or inhibit tumor growth (Bruno *et al.*, 2014), we decided to add another control, the non-treated condition, and we observed that MDA-MB-231 treated with control EVs proliferate and migrate with the same ratio than non-treated cells. Therefore, cel-miR-67-loaded EVs are considered as a good control for miR-503 experiment.

MDA-MB-231	Proliferation	Migration
Sensitive	↓	↓
Epi-R	↓	↓
Pacli-R	↓	/

Table D 4. Summary table of the functional effects of miR-503-loaded EVs on sensitive and resistant MDA-MB-231 cells.

These results suggest that the overexpression of miR-503 curtails sensitive and epirubicin or paclitaxel-resistant breast cancer cell tumorigenicity *in vitro*. We then decided to study the involvement on breast cancer growth *in vivo*. Many studies have previously shown that miR-503 could impair tumor growth. For instance, the loss of miR-424/503 cluster promotes breast cancer progression (Rodriguez-barrueco *et al.*, 2017). In this case, mice experiments revealed that the treatment with miR-503-loaded EVs reduced drastically breast tumor volumes. Taken together, in vitro and in vivo data confirmed that miR-503 acts as a tumor suppressor in breast cancer (**Fig. D 62**). We believe that our study nominates miR-503 as a potential therapeutic agent for breast cancer therapy. Furthermore, its incorporation within EVs improves its therapeutic potential.

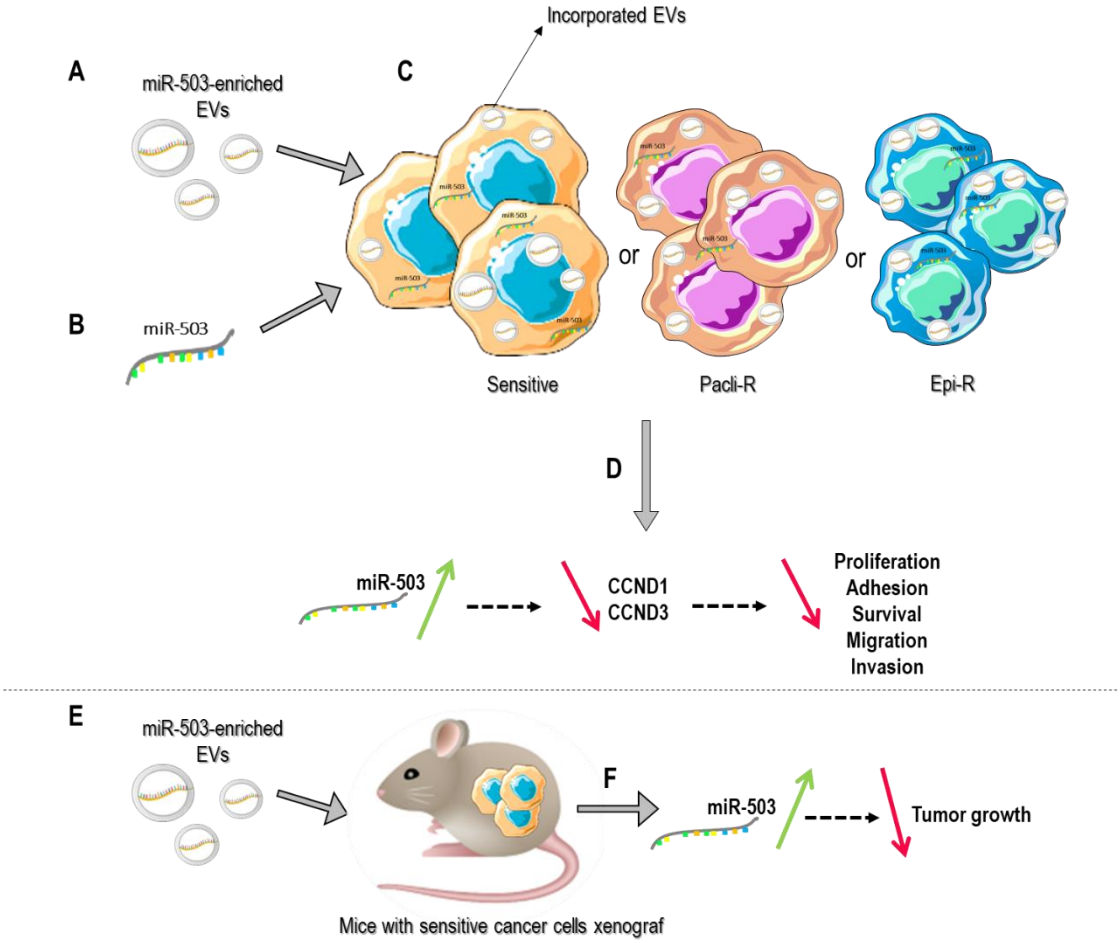

Figure D 62. miR-503 curtails breast cancer progression in vitro and in vivo.
*(**A**) miR-503-loaded EV treatment and (**B**)miR-503 overexpression. The levels of miR-503 are up-regulated within sensitive and resistant cancer cells due to the overexpression and the EV transfer (**C**) and lead to a reduction of tumorigenicity of both cell lines through the targeting of CCND1 and CCND3 (**D**). Moreover, mice injected with miR-503-enriched EVs (**E**) showed a drastic decrease in tumor growth (**F**).*

In the last chapter, we combined the previous results and aimed to determine the implications of miR-503 and the miR-EXO proteins in breast cancer patients. Bioinformatics revealed that the survival rate was reduced when patients carried a deletion in the locus of miR-503. Interestingly, another study revealed that the miR-424/503 locus is deleted in ~14% of breast cancers and was associated with poor survival (Rodriguez-Barrueco *et al.*, 2017).

Regarding the perspectives of this work, it would be very interesting to study the molecular mechanism of miR-503 export more deeply. Indeed, the relocalization of hnRNPA2B1 into the nucleus after epirubicin treatment aroused our interest. To better understand this process, we could realize immunofluorescence assays to visualize the potential interaction between hnRNPA2B1 and DSB markers such as γH2XA and 53BP1. Indeed, chemotherapeutic agents, which provoke DSB, can induce cell death. However, DSB also occur

in normal cells and this phenomenon is thwarted by proteins involved in DNA repair. For instance, DSB induce histone H2AX phosphorylation around the break, which recruits other proteins involved in the repair. 53BP1 (p53 binding protein 1) is a protein involved in the repair of DSB (Popp *et al.*, 2017). Considering the functions of those two proteins in DSB repair, their visualization by immunofluorescence microscopy may be useful to detect DSB caused by epirubicin which might be associated with hnRNPA2B1.

The proliferative capacities of sensitive and resistant cancer cells could be explained by the decrease of targets involved in the cell cycle. Nevertheless, the migratory, adhesion and the invasive phenotypes observed in sensitive and resistant cells require the measurement of other targets. Therefore, selecting new putative miR-503 targets and quantifying their levels after miR-503 overexpression could be interesting. Targetscan algorithm allowed us to find putative target mRNAs: AKT3, DGCR2, FGF2, FGF7, L1CAM, and SDCBP2. AKT3, a member of the AKT kinases family, is part of the PI3K (phosphatidylinosito3-kinase)/AKT signaling and is involved in cell survival and proliferation (Madhunapantula & Robertson, 2009). DiGeorge syndrome critical region gene 2 (DGCR2) and L1 Cell Adhesion Molecule (L1CAM) are involved in cell adhesion (Van der Maten *et al.*, 2019). Fibroblast growth factors 2 and 7 (FGF2 and FGF7) are implicated in cell migration, invasion and proliferation (Korc & Friesel, 2009). Syndecan binding protein 2 (SDSBP2) has been linked to cancer progression through the activation of pro-proliferative pathways (Qian *et al.*, 2013). Thus, it could be interesting to quantify the levels of the putative targets involved in these pathways to explain our invasive, adhesion, and migratory phenotypes.

MiR-503 curtails both sensitive and chemoresistant breast cancer cells. However, our results did not demonstrate that miR-503 could restore the sensitivity of resistant cells. To further study this mechanism, it could be very interesting to overexpress miR-503 and, at the same time, treat the cells with epirubicin or paclitaxel and measure their survival, and the other cancerous phenotypes. It could bring novel treatments possibilities for patients who do not respond to chemotherapy. During the last decade, EVs have emerged for their biomarker and therapeutic interest. Many studies have demonstrated that EVs carry bioactive molecules such as miRNAs. These ncRNAs are widely studied, conserve high plasmatic stability, and thus, are considered as a good source of biomarkers. In miRNA therapeutics, a strategy is to increase the levels of an anti-tumor miRNA. For instance, a phase I trial demonstrated the efficiency and safety of miR-34a overexpression in patients with solid tumors. Since in many patients, miR-34a is downregulated, the aim of this miRNA mimic therapy is to enhance the levels of this

tumor suppressor involved in resistance and metastasis formation (Beg *et al.*, 2017). EVs and its cargo, miR-503, through its anti-cancerous properties, could offer new opportunities for breast cancer treatment. Therefore, it would be interesting to study deeper the impact of enriched EVs on cells that are not responding to chemotherapy.

Considering that miR-503 inhibits angiogenesis, it could be interesting to perform immunohistochemistry on tumors and quantify the number of vessels using CD31 staining (Hirakawa *et al.*, 2016; Wen *et al.*, 2018). Since miR-503 targets CCND1 and CCDN3, it could be interesting to quantify their protein levels within the tumors.

MiR-503 affects the epirubicin and paclitaxel-resistant breast tumor cells in vitro. However, to reinforce our study, we want to determine if these electroporated EVs could also impact the resistant tumor growth in vivo.

Plasma for patients that underwent neoadjuvant chemotherapy presented up-regulated levels of miR-503 (Bovy *et al.*, 2015). Nevetheless, to strengthen our study, it would be very interesting to measure the levels of this particular miRNA into plasmatic EVs and determine if the up-regulation observed is due to the circulating of the exosomal form of miR-503. Furthermore, it could be very interesting to analyze this potential up-regulation and if it has a link between patient subgroups based on receptor expression classification.

Collectively, this study delivers new evidences that miR-503 sorting into EVs requires the inhibition of hnRNPA2B1 which traps the miRNA within the cell. This inhibition mimics the effects of epirubicin treatment. Using several approaches, we attest that miR-503 overexpression curtails TNBC growth in vitro and in vivo, by counteracting tumor proliferation, migration, survival, adhesion and invasion. Interestingly, the miRNA influences both sensitive and resistant breast cancer cell behavior. Finally, miR-503 locus deletion is associated with poor survival. Therefore, we believe that our study nominates miR-503 and miR-503-loaded EVs as potential therapeutic tools for breast cancer therapy.

Supplementary data

Supplementary data

1. Supplementary figures

miR-503

5'-P- UAGCAGCGGGAACAGUUCUGCAG-3'
3'-GAA**G**CGUCGCCCUUGUCAAGACG-P-5'

miR-503-biotin

5'-P- UAGCAGCGGGAACAGUUCUGCAG-biotin 3'
3'-GAA**G**CGUCGCCCUUGUCAAGACG-P-5'

cel-miR-67

5'-P-UCACAACCUCCUAGAAAGAGUAGA-3'
3'-UU**C**GUG**G**UGGA**A**GAUCUUUCUCAU-P-5'

cel-miR-67-biotin

5'-P-UCACAACCUCCUAGAAAGAGUAGA-biotin 3'
3'-UU**C**GUG**G**UGGA**A**GAUCUUUCUCAU-P-5'

Suppl. Figure S 1. miR-503, miR-503-biotin, cel-miR-67 and cel-miR-67-biotin sequences.
In black is shown the natural miR-503 or cel-67 sequences and the modifications are indicated in colors: orange represents the addition of biotin, violet is for the phosphorylation, blue is for the 3' tailing and bold black represents the mismatch included to destabilize the carrier strand.

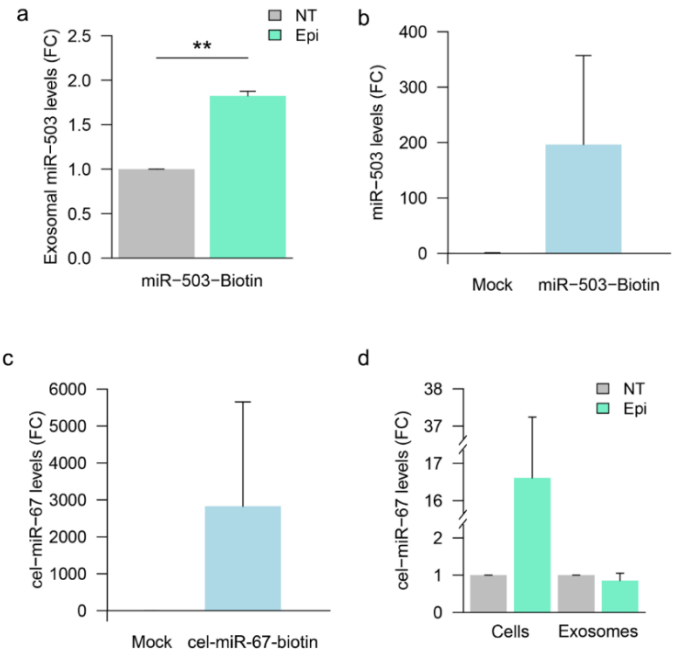

Suppl. Figure S 2. Validation of miR-503-biotin export upon epirubicin treatment and validation of its transfection.
*(**a**, **d**) Exosomes were purified from HUVECs non-treated (NT) or treated with epirubicin (Epi) for 24h and cultivated in exofree medium for 72 more hours. RNAs were extracted from these exosomes and the levels of miR-503 or cel-miR-67 were assessed by qRT-PCR. (**b**) Validation of miR-503-biotin transfection or (**c**) cel-miR-67-biotin. Data are expressed as mean and SEM from three independent experiments (**p<0.01).*

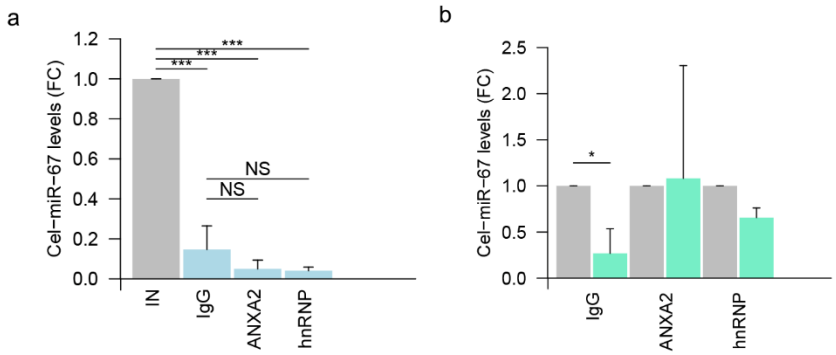

Suppl. Figure S 3. miR-EXO proteins are not linked to cel-miR-67.
*(**a**) HUVECs were transfected with cel-miR-67 (10 nM). Cell lysates were then immunoprecipitated with the selected antibodies and compared to the input (IN) (cellular lysate) in non-treated condition or compared to (**b**) epirubicin-treated cells. Data are expressed as mean and SEM from three independent experiments (*p<0.05; ***p<0.001).*

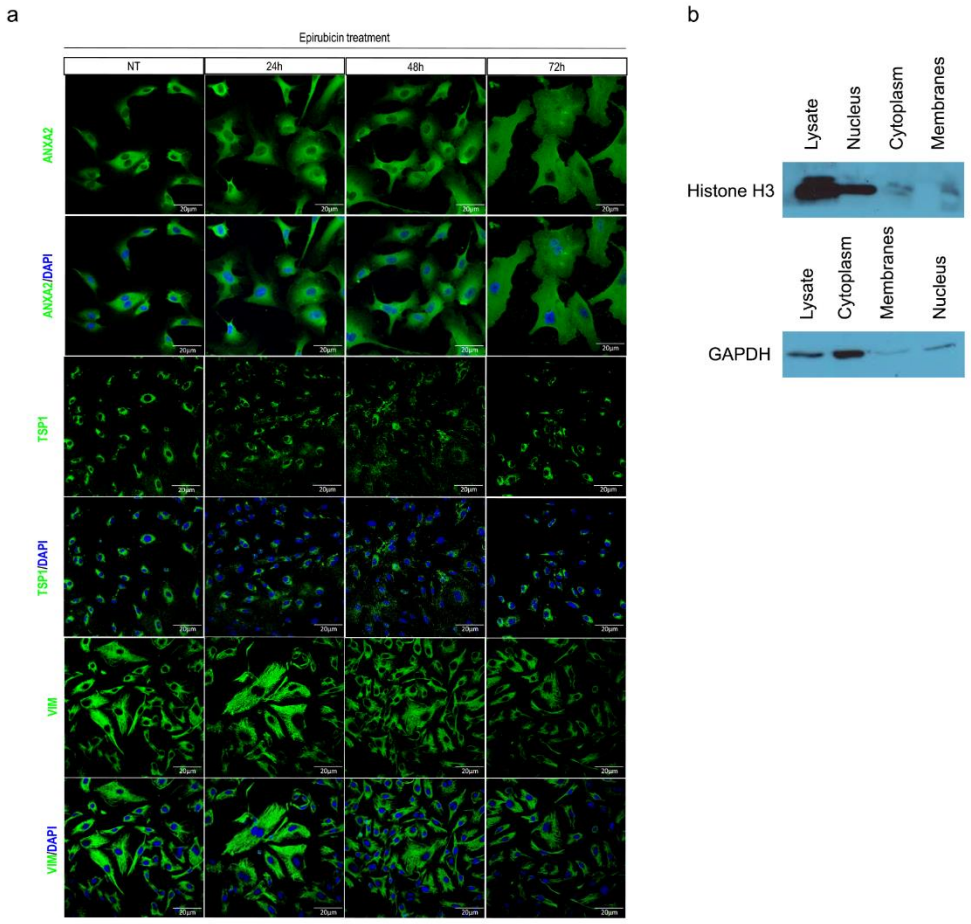

Suppl. Figure S 4. Localization of ANXA2, TSP1 and VIM is not altered by epirubicin.
(a) HUVECs were treated with epirubicin for 24h (1 µg/mL) and stained with antibodies against the respective proteins. Immunofluorescence assays were visualized using a confocal microscope. Scale bar = 200 µm. (b) Validation of Histone H3 and GAPDH subcellular localization by western blotting.

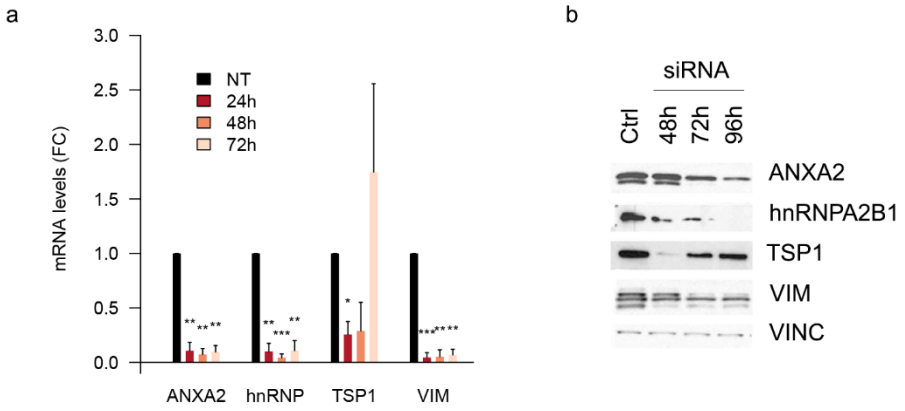

Suppl. Figure S 5. MiR-EXO protein knockdown validation.
(a) *HUVECs were transfected 20 nM of siRNAs for 24 to 72h and the mRNA levels were assessed by qRT-PCR.* ***(b)*** *Validation of protein knockdown (48 to 96h) by western blotting. Data are expressed as mean and SEM from three independent experiments (*p<0.05; **p<0.01, ***p<0.001).*

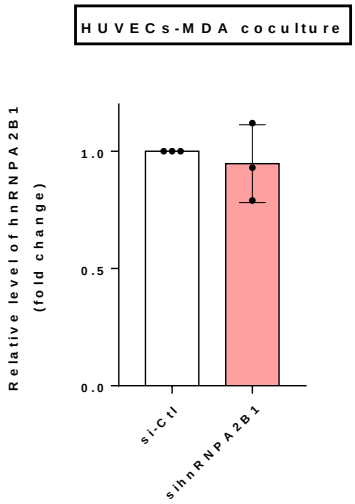

Suppl. Figure S 6. Endothelial silencing of hnRNPA2B1 does not reduce hnRNPA2B1 levels in MDA-MB-231 cells.
HUVECs were transfected with 20 nM of siRNAs against hnRNPA2B1 and the control (si-Ctl). After transfection, endothelial cells were cocultivated with MDA-MB-231 cells for 24h. RNAs were extracted from tumor cells and the expression level of hnRNPA2B1 was is represented as fold change of their level in the control condition. The values are normalized to the mean Ct of B2M and PPIA. Data are expressed as mean ± SD from three independent experiments compared to the control (si-Ctl).

2. Supplementary tables

Protein	Symbol	Description
Propionyl-CoA carboxylase alpha subunit	PCCA	The protein encoded by this gene is the alpha subunit of the heterodimeric mitochondrial enzyme Propionyl-CoA carboxylase. PCCA encodes the biotin-binding region of this enzyme.
Pyruvate Carboxylase	PC	This gene encodes pyruvate carboxylase, which requires biotin and ATP to catalyse the carboxylation of pyruvate to oxaloacetate. The active enzyme is a homotetramer arranged in a tetrahedron which is located exclusively in the mitochondrial matrix. Pyruvate carboxylase is involved in gluconeogenesis, lipogenesis, insulin secretion and synthesis of the neurotransmitter glutamate.
Heparan sulfate proteoglycan 2	HSPG2 (Perlecan)	This gene encodes the perlecan protein, which consists of a core protein to which three long chains of glycosaminoglycans (heparan sulfate or chondroitin sulfate) are attached. The perlecan protein is a large multidomain proteoglycan that binds to and cross-links many extracellular matrix components and cell-surface molecules. It has been shown that this protein interacts with laminin, prolargin, collagen type IV, FGFBP1, FBLN2, FGF7 and transthyretin, etc., and it plays essential roles in multiple biological activities. Perlecan is a key component of the vascular extracellular matrix, where it helps to maintain the endothelial barrier function. It is a potent inhibitor of smooth muscle cell proliferation and is thus thought to help maintain vascular homeostasis. It can also promote growth factor (e.g., FGF2) activity and thus stimulate endothelial growth and re-generation. It is a major component of basement membranes, where it is involved in the stabilization of other molecules as well as being involved with glomerular permeability to macromolecules and cell adhesion.
Fibronectin 1	FN1	This gene encodes fibronectin, a glycoprotein present in a soluble dimeric form in plasma, and in a dimeric or multimeric form at the cell surface and in extracellular matrix. The encoded preproprotein is proteolytically processed to generate the mature protein. Fibronectin is involved in cell adhesion and migration processes including embryogenesis, wound healing, blood coagulation, host defense, and metastasis. The gene has three regions subject to alternative splicing, with the potential to produce 20 different transcript variants, at least one of which encodes an isoform that undergoes proteolytic processing.

Thrombospondin 1	TSP1	The protein encoded by this gene is a subunit of a disulfide-linked homotrimeric protein. This protein is an adhesive glycoprotein that mediates cell-to-cell and cell-to-matrix interactions. This protein can bind to fibrinogen, fibronectin, laminin, type V collagen and integrins alpha-V/beta-1. This protein has been shown to play roles in platelet aggregation, angiogenesis, and tumorigenesis.
β-Actin	ACTB	This gene encodes one of six different actin proteins. Actins are highly conserved proteins that are involved in cell motility, structure, integrity, and intercellular signaling. The encoded protein is a major constituent of the contractile apparatus and one of the two nonmuscle cytoskeletal actins that are ubiquitously expressed.
Vimentin	VIM	This gene encodes a type III intermediate filament protein. Intermediate filaments, along with microtubules and actin microfilaments, make up the cytoskeleton. The encoded protein is responsible for maintaining cell shape and integrity of the cytoplasm, and stabilizing cytoskeletal interactions. This protein is involved in neuritogenesis and cholesterol transport and functions as an organizer of a number of other critical proteins involved in cell attachment, migration, and signaling.
Annexin A2	ANXA2	This gene encodes a member of the annexin family. Members of this calcium-dependent phospholipid-binding protein family play a role in the regulation of cellular growth and in signal transduction pathways. This protein functions as an autocrine factor which heightens osteoclast formation and bone resorption.
heterogeneous nuclear ribonucleoprotein A2/B1	hnRNPA2B1	This gene belongs to the A/B subfamily of ubiquitously expressed heterogeneous nuclear ribonucleoproteins (hnRNPs). The hnRNPs are RNA binding proteins and they complex with heterogeneous nuclear RNA (hnRNA). These proteins are associated with pre-mRNAs in the nucleus and appear to influence pre-mRNA processing and other aspects of mRNA metabolism and transport. While all of the hnRNPs are present in the nucleus, some seem to shuttle between the nucleus and the cytoplasm. The hnRNP proteins have distinct nucleic acid binding properties. The protein encoded by this gene has two repeats of quasi-RRM domains that bind to RNAs.

Table S 5. List and functions of miR-503 partners in HUVECs.
Mass spectroscopy (MS) allowed us to identify several proteins that were attached to the miRNA. Both PCCA and PC binds naturally biotin making them positive controls for the miR-503 pull-down. Perlecan, TSP1 and FN1 are components of the ECM. β-actin and vimentin are cytoskeleton proteins. Interestingly, ANXA2 and hnRNPA2B1 are RNA-binding proteins (RBPs) involved, respectively, in cell transduction or in RNA processing. Table adapted from ***Pérez-Boza, Boeckx, et al., 2020****.*

Gene	Symbol	Functions
Cyclin D1, D2 and D3	CCND1, CCND2, CCND3	D-type cyclins are proteins that mediate the G1/S phase transition and have been described to participate to cancer proliferation (Pestell, 2013). Moreover, miR-503 has been reported to target CCND1, CCND2 and CCND3 (Bovy *et al.*, 2015; Long *et al.*, 2015).
B-Cell lymphoma 2	BCL2	Bcl-2 is an anti-apoptotic protein and, thus, a pro-tumoral protein. BCL2 has been described to be targeted by miR-503 (Qiu *et al.*, 2013b).
MYB	MYB	MYB is a transcription factor involved in differentiation pathways. Alterations in MYB have been found in ~30% of tumors from patients carrying BRCA1 mutations (Ramsay & Gonda, 2008).

Table S 6. List and functions of miR-503 targets.

Gene	Symbol	Functions
ATP-Binding Cassette Subfamily B Member 1	ABCB1	ABCB1, also known as P-glycoprotein (P-gp) or MDR1, is an efflux pump that allows the release of drugs without cells. Overexpression of this protein has been associated with the acquisition of chemoresistance (Choi & Yu, 2014).
Growth arrest and DNA-damage-inducible protein 45a	GADD45A	GADD45A, a stress response protein, promotes cancer progression (Pietrasik et al., 2020) and its levels have been associated with doxorubicin-resistance (Sherman-Baust et al., 2011)
Malate dehydrogenase 2	MDH2	MDH2 catalyzes the oxidation of malate in oxaloacetate (Minárik et al., 2002) and can confer resistance to taxanes and anthracyclines in cancer cells (Liu et al., 2013; Lo et al., 2015).
Cytochrome P450 Oxidoreductase	POR	POR allows the electrons transfer from NADPH to P450 (Lu et al., 1969). Increased levels of POR have been associated with the acquisition of doxorubicin resistance (Villeneuve et al., 2006)
Sirtuin 6	SIRT6	SIRT6 is a histone deacetylase involved in telomere maintenance. Increased levels of SIRT6 have been demonstrated in epirubicin and paclitaxel-resistant breast cancer cells.
Topoisomerase II	TOP2A	Top2α protein is targeted by epirubicin (Munro et al., 2010). Moreover, its levels have been shown reduced in paclitaxel-resistant cells (Villeneuve et al., 2006).

Table S 7. List and functions of resistance genes.

References

References

Abe, O. *et al.* (2005) 'Effects of radiotherapy and of differences in the extent of surgery for early breast cancer on local recurrence and 15-year survival: An overview of the randomised trials', *The Lancet*, 366(9503), pp. 2087–2106. doi: 10.1016/S0140-6736(05)67887-7.

Abu Samaan, T. M. *et al.* (2019) 'Paclitaxel's Mechanistic and Clinical Effects on Breast Cancer', *Biomolecules*. doi: 10.3390/biom9120789.

Ades, F. *et al.* (2014) 'Luminal B breast cancer: Molecular characterization, clinical management, and future perspectives', *Journal of Clinical Oncology*, 32(25), pp. 2794–2803. doi: 10.1200/JCO.2013.54.1870.

Ahmadi, M. and Rezaie, J. (2020) 'Tumor cells derived-exosomes as angiogenenic agents: Possible therapeutic implications', *Journal of Translational Medicine*. BioMed Central, 18(1), pp. 1–17. doi: 10.1186/s12967-020-02426-5.

Akao, Y. *et al.* (2014) 'Extracellular disposal of tumor-suppressor miRs-145 and -34a via microvesicles and 5-FU resistance of human colon cancer cells', *International Journal of Molecular Sciences*, 15(1), pp. 1392–1401. doi: 10.3390/ijms15011392.

Akers, J. C. *et al.* (2013) 'Biogenesis of extracellular vesicles (EV): Exosomes, microvesicles, retrovirus-like vesicles, and apoptotic bodies', *Journal of Neuro-Oncology*, pp. 1–11. doi: 10.1007/s11060-013-1084-8.

Akram, M. *et al.* (2017) 'Awareness and current knowledge of breast cancer', *Biological Research*, p. 33. doi: 10.1186/s40659-017-0140-9.

Al-Mahayri, Z. N., AlAhmad, M. M. and Ali, B. R. (2021) 'Current opinion on the pharmacogenomics of paclitaxel-induced toxicity', *Expert Opinion on Drug Metabolism and Toxicology*. Taylor & Francis, 17(7), pp. 785–801. doi: 10.1080/17425255.2021.1943358.

Alarcón, C. R. *et al.* (2015) 'HNRNPA2B1 Is a Mediator of m6A-Dependent Nuclear RNA Processing Events', *Cell*, 162(6), pp. 1299–1308. doi: 10.1016/j.cell.2015.08.011.

Alitalo, A. and Detmar, M. (2012) 'Interaction of tumor cells and lymphatic vessels in cancer progression', *Oncogene*, pp. 4499–4508. doi: 10.1038/onc.2011.602.

Alitalo, K. (2011) 'The lymphatic vasculature in disease', *Nature Medicine*. Nature Publishing Group, 17(11), pp. 1371–1380. doi: 10.1038/nm.2545.

Alluri, P. and Newman, L. A. (2014) 'Basal-like and triple-negative breast cancers. Searching for positives among many negatives', *Surgical Oncology Clinics of North America*, pp. 567–577. doi: 10.1016/j.soc.2014.03.003.

Ambros, V. (2004) 'miRNAs found by genomics and reverse genetics', *Nature*, 431, p. 350. Available at: www.nature.com/nature.

Ambudkar, S. V., Kim, I. W. and Sauna, Z. E. (2006) 'The power of the pump: Mechanisms of action of P-glycoprotein (ABCB1)', *European Journal of Pharmaceutical Sciences*, 27(5), pp. 392–400. doi: 10.1016/j.ejps.2005.10.010.

Anstey, E. H. *et al.* (2017) 'Breastfeeding and Breast Cancer Risk Reduction: Implications for Black Mothers', *American Journal of Preventive Medicine*. Elsevier Inc., 53(3), pp. S40–S46. doi: 10.1016/j.amepre.2017.04.024.

Arroyo, J. D. *et al.* (2011) 'Argonaute2 complexes carry a population of circulating

microRNAs independent of vesicles in human plasma', *Proceedings of the National Academy of Sciences of the United States of America*, 108(12), pp. 5003–5008. doi: 10.1073/pnas.1019055108.

Attwell, D. *et al.* (2016) 'What is a pericyte?', *Journal of Cerebral Blood Flow and Metabolism*, 36(2), pp. 451–455. doi: 10.1177/0271678X15610340.

Aumailley, M. (2013) 'The laminin family', *Cell Adhesion and Migration*, 7(1), pp. 48–55. doi: 10.4161/cam.22826.

Bach, D. H. *et al.* (2017) 'The role of exosomes and miRNAs in drug-resistance of cancer cells', *International Journal of Cancer*, pp. 220–230. doi: 10.1002/ijc.30669.

Badaoui, M. *et al.* (2018) 'Collagen type 1 promotes survival of human breast cancer cells by overexpressing Kv10.1 potassium and Orai1 calcium channels through DDR1-dependent pathway', *Oncotarget*, 9(37), pp. 24653–24671. doi: 10.18632/oncotarget.19065.

Baghban, R. *et al.* (2020) 'Tumor microenvironment complexity and therapeutic implications at a glance', *Cell Communication and Signaling*. Cell Communication and Signaling, 18(1), pp. 1–19. doi: 10.1186/s12964-020-0530-4.

Baietti, M. F. *et al.* (2012) 'Syndecan-syntenin-ALIX regulates the biogenesis of exosomes', *Nature Cell Biology*. Nature Publishing Group, 14(7), pp. 677–685. doi: 10.1038/ncb2502.

Baran-Gale, J., Purvis, J. E. and Sethupathy, P. (2016) 'An integrative transcriptomics approach identifies miR-503 as a candidate master regulator of the estrogen response in MCF-7 breast cancer cells', *Rna*, 22(10), pp. 1592–1603. doi: 10.1261/rna.056895.116.

Barlow, K. D. *et al.* (2013) 'Pericytes on the tumor vasculature: Jekyll or hyde?', *Cancer Microenvironment*, pp. 1–17. doi: 10.1007/s12307-012-0102-2.

Bartel, D. P. (2009) 'MicroRNAs: Target Recognition and Regulatory Functions', *Cell*, 136(2), pp. 215–233. doi: 10.1016/j.cell.2009.01.002.

Bartel, D. P. (2018) 'Metazoan MicroRNAs', *Cell*. Elsevier Inc., 173(1), pp. 20–51. doi: 10.1016/j.cell.2018.03.006.

Batagov, A. O. and Kurochkin, I. V (2013) *Exosomes secreted by human cells transport largely mRNA fragments that are enriched in the 3'-untranslated regions*. doi: 10.1186/1745-6150-8-12.

Battistelli, M. and Falcieri, E. (2020) 'Apoptotic bodies: Particular extracellular vesicles involved in intercellular communication', *Biology*, 9(1). doi: 10.3390/biology9010021.

Beg, M. S. *et al.* (2017) 'Phase I study of MRX34, a liposomal miR-34a mimic, administered twice weekly in patients with advanced solid tumors', *Investigational New Drugs*, 35(2), pp. 180–188. doi: 10.1007/s10637-016-0407-y.

Behm-Ansmant, I. *et al.* (2006) 'mRNA degradation by miRNAs and GW182 requires both CCR4:NOT deadenylase and DCP1:DCP2 decapping complexes', *Genes and Development*, 20(14), pp. 1885–1898. doi: 10.1101/gad.1424106.

Bella, J. and Hulmes, D. J. S. (2017) 'Fibrillar collagens', *Subcellular Biochemistry*, 82, pp. 457–490. doi: 10.1007/978-3-319-49674-0_14.

Bentrem, D. J. *et al.* (2001) 'Molecular mechanism of action at estrogen receptor α of a

new clinically relevant antiestrogen (GW7604) related to tamoxifen', *Endocrinology*, 142(2), pp. 838–846. doi: 10.1210/endo.142.2.7932.

Beretta, G. L. and Zunino, F. (2007) 'Molecularmechanisms of anthracycline activity', *Topics in Current Chemistry*, 283, pp. 1–19. doi: 10.1007/128_2007_3.

Betancur, J. G., Yoda, M. and Tomari, Y. (2012) 'miRNA-like duplexes as RNAi triggers with improved specificity', *Frontiers in Genetics*, 3(JUL), pp. 2008–2013. doi: 10.3389/fgene.2012.00127.

Binenbaum, Y. *et al.* (2018) 'Transfer of miRNA in macrophage-derived exosomes induces drug resistance in pancreatic adenocarcinoma', *Cancer Research*, 78(18), pp. 5287–5299. doi: 10.1158/0008-5472.CAN-18-0124.

Bobrie, A. *et al.* (2011) 'Exosome Secretion: Molecular Mechanisms and Roles in Immune Responses', *Traffic*, 12(12), pp. 1659–1668. doi: 10.1111/j.1600-0854.2011.01225.x.

Bohnsack, M. T., Czaplinski, K. and Görlich, D. (2004) 'Exportin 5 is a RanGTP-dependent dsRNA-binding protein that mediates nuclear export of pre-miRNAs', *Rna*, 10(2), pp. 185–191. doi: 10.1261/rna.5167604.

Boland, C. R. (2017) 'Non-coding RNA: It's Not Junk', *Dig Dis Sci.*, 62(5), pp. 1107–1109. doi: 10.1007/s10620-017-4506-1.Non-coding.

Bonnans, C., Chou, J. and Werb, Z. (2014) 'Remodelling the extracellular matrix in development and disease', *Nature reviews. Molecular cell biology*, 15(12), pp. 786–801. doi: 10.1038/nrm3904.Remodelling.

Bornstein, P. (2009) 'Thrombospondins function as regulators of angiogenesis', *Journal of Cell Communication and Signaling*, pp. 189–200. doi: 10.1007/s12079-009-0060-8.

Bovy, N. *et al.* (2015) 'Endothelial exosomes contribute to the antitumor response during breast cancer neoadjuvant chemotherapy via microRNA transfer', *Oncotarget*, 6(12), pp. 10253–10266. doi: 10.18632/oncotarget.3520.

Bruno, R. D. and Njar, V. C. O. (2007) 'Targeting cytochrome P450 enzymes: A new approach in anti-cancer drug development', *Bioorganic and Medicinal Chemistry*, pp. 5047–5060. doi: 10.1016/j.bmc.2007.05.046.

Bruno, S. *et al.* (2014) 'Effects of mesenchymal stromal cell-derived extracellular vesicles on tumor growth', *Frontiers in Immunology*. doi: 10.3389/fimmu.2014.00382.

Buchbinder, E. I. and Desai, A. (2016) 'CTLA-4 and PD-1 pathways similarities, differences, and implications of their inhibition', *American Journal of Clinical Oncology: Cancer Clinical Trials*, 39(1), pp. 98–106. doi: 10.1097/COC.0000000000000239.

Bukowski, K., Kciuk, M. and Kontek, R. (2020) 'Mechanisms of multidrug resistance in cancer chemotherapy', *International Journal of Molecular Sciences*. doi: 10.3390/ijms21093233.

Büschiges, R. *et al.* (1999) 'Amplification and expression of cyclin D genes (CCND 1, CCND2 and CCND3) in human malignant gliomas', *Brain Pathology*, 9(3), pp. 435–442. doi: 10.1111/j.1750-3639.1999.tb00532.x.

Buzdar, A. U. *et al.* (2013) 'Fluorouracil, epirubicin, and cyclophosphamide (FEC-75) followed by paclitaxel plus trastuzumab versus paclitaxel plus trastuzumab followed by FEC-75 plus trastuzumab as neoadjuvant treatment for patients with HER2-positive breast cancer

(Z1041): A random', *The Lancet Oncology*, 14(13), pp. 1317–1325. doi: 10.1016/S1470-2045(13)70502-3.

Cai, J. *et al.* (2013) 'Extracellular vesicle-mediated transfer of donor genomic DNA to recipient cells is a novel mechanism for genetic influence between cells', *Journal of Molecular Cell Biology*, 5(4), pp. 227–238. doi: 10.1093/jmcb/mjt011.

Cammaerts, S. *et al.* (2015) 'Genetic variants in microRNA genes: Impact on microRNA expression, function, and disease', *Frontiers in Genetics*, 6(MAY), pp. 1–12. doi: 10.3389/fgene.2015.00186.

Caporali, A. and Emanueli, C. (2011) 'MicroRNA-503 and the Extended MicroRNA-16 Family in Angiogenesis', *Trends in Cardiovascular Medicine*. Elsevier Inc., 21(6), pp. 162–166. doi: 10.1016/j.tcm.2012.05.003.

Carlson, R. W. *et al.* (2011) 'NCCN guideline invasive breast cancer, J Nat Compr Cancer Network, 2011', 9(2), pp. 136–222.

Carmeliet, P. and Jain, R. K. (2011) 'Molecular mechanisms and clinical applications of angiogenesis', *Nature*, pp. 298–307. doi: 10.1038/nature10144.

Caruso, S. and Poon, I. K. H. (2018) 'Apoptotic cell-derived extracellular vesicles: More than just debris', *Frontiers in Immunology*. doi: 10.3389/fimmu.2018.01486.

Carvalho, C. *et al.* (2009) 'Doxorubicin: The Good, the Bad and the Ugly Effect', *Current Medicinal Chemistry*, 16(25), pp. 3267–3285. doi: 10.2174/092986709788803312.

Casey, M. and Bewtra, C. (2004) 'Peritoneal carcinoma in women with genetic susceptibility: Implications for Jewish populations', *Familial Cancer*, 3(3–4), pp. 265–281. doi: 10.1007/s10689-004-9554-y.

Chakraborty, C. *et al.* (2021) 'Therapeutic advances of miRNAs: A preclinical and clinical update', *Journal of Advanced Research*. Cairo University, 28, pp. 127–138. doi: 10.1016/j.jare.2020.08.012.

Chen, I. X. *et al.* (2019) 'Blocking CXCR4 alleviates desmoplasia, increases T-lymphocyte infiltration, and improves immunotherapy in metastatic breast cancer', *Proceedings of the National Academy of Sciences of the United States of America*, 116(10), pp. 4558–4566. doi: 10.1073/pnas.1815515116.

Chen, S. *et al.* (2021) 'Retinoblastoma cell-derived exosomes promote angiogenesis of human vesicle endothelial cells through microRNA-92a-3p', *Cell Death and Disease*, 12(7). doi: 10.1038/s41419-021-03986-0.

Cheng, H. C., Abdel-Ghany, M. and Pauli, B. U. (2003) 'A Novel Consensus Motif in Fibronectin Mediates Dipeptidyl Peptidase IV Adhesion and Metastasis', *Journal of Biological Chemistry*. Â© 2003 ASBMB. Currently published by Elsevier Inc; originally published by American Society for Biochemistry and Molecular Biology., 278(27), pp. 24600–24607. doi: 10.1074/jbc.M303424200.

Chittaranjan, S. *et al.* (2014) 'Autophagy inhibition augments the anticancer effects of epirubicin treatment in anthracycline-sensitive and -resistant triple-negative breast cancer', *Clinical Cancer Research*, 20(12), pp. 3159–3173. doi: 10.1158/1078-0432.CCR-13-2060.

Choi, Y. and Yu, A.-M. (2014) 'ABC Transporters in Multidrug Resistance and Pharmacokinetics, and Strategies for Drug Development', *Current Pharmaceutical Design*, 20(5), pp. 793–807. doi: 10.2174/13816128200514021416521 2.

Chraa, D. *et al.* (2019) 'T lymphocyte subsets in cancer immunity: Friends or foes', *Journal of Leukocyte Biology*, pp. 243–255. doi: 10.1002/JLB.MR0318-097R.

Cloutier, A. *et al.* (2018) 'HnRNP A1/A2 and Sam68 collaborate with SRSF10 to control the alternative splicing response to oxaliplatin-mediated DNA damage', *Scientific Reports*. Springer US, 8(1), pp. 1–14. doi: 10.1038/s41598-018-20360-x.

Coleman, M. P. *et al.* (2008) 'Cancer survival in five continents: a worldwide population-based study (CONCORD)', *The Lancet Oncology*, 9(8), pp. 730–756. doi: 10.1016/S1470-2045(08)70179-7.

Colombo, M., Raposo, G. and Théry, C. (2014) 'Biogenesis, secretion, and intercellular interactions of exosomes and other extracellular vesicles', *Annual review of cell and developmental biology*, 30, pp. 255–289. doi: 10.1146/annurev-cellbio-101512-122326.

Conigliaro, A. *et al.* (2015) 'CD90+ liver cancer cells modulate endothelial cell phenotype through the release of exosomes containing H19 lncRNA', *Molecular Cancer*, 14(1). doi: 10.1186/s12943-015-0426-x.

Conte, P. F. *et al.* (2000) 'Role of epirubicin in advanced breast cancer.', *Clinical breast cancer*. Elsevier Ltd., 1 Suppl 1(September), pp. S46–S51. doi: 10.3816/cbc.2000.s.009.

Cooke, V. G. *et al.* (2012) 'Pericyte depletion results in hypoxia-associated epithelial-to-mesenchymal transition and metastasis mediated by met signaling pathway', *Cancer Cell*. Elsevier Inc., 21(1), pp. 66–81. doi: 10.1016/j.ccr.2011.11.024.

Corcoran, C. *et al.* (2012) 'Docetaxel-Resistance in Prostate Cancer: Evaluating Associated Phenotypic Changes and Potential for Resistance Transfer via Exosomes', *PLoS ONE*, 7(12). doi: 10.1371/journal.pone.0050999.

Correa de Sampaio, P. *et al.* (2012) 'A heterogeneous in vitro three dimensional model of tumour-stroma interactions regulating sprouting angiogenesis', *PLoS ONE*, 7(2). doi: 10.1371/journal.pone.0030753.

Correia De Sousa, M. *et al.* (2019) 'Molecular Sciences Deciphering miRNAs' Action through miRNA Editing'. doi: 10.3390/ijms20246249.

Coussens, L. M. and Werb, Z. (2002) 'Inflammation and cancer', *Nature*, 420(December), pp. 19–26. Available at: www.nature.com/nature.

Crescitelli, R. *et al.* (2013) 'Distinct RNA profiles in subpopulations of extracellular vesicles: Apoptotic bodies, microvesicles and exosomes', *Journal of Extracellular Vesicles*, 2(1). doi: 10.3402/jev.v2i0.20677.

Cui, M. *et al.* (2019) 'Circulating MicroRNAs in Cancer: Potential and Challenge', *Frontiers in Genetics*, 10. doi: 10.3389/fgene.2019.00626.

D'Souza-Schorey Crislyn, C. and Clancy, J. W. (2012) 'Tumor-derived microvesicles: Shedding light on novel microenvironment modulators and prospective cancer biomarkers', *Genes and Development*, 26(12), pp. 1287–1299. doi: 10.1101/gad.192351.112.

Dai, X. *et al.* (2015) 'Breast cancer intrinsic subtype classification, clinical use and future trends', *American Journal of Cancer Research*, pp. 2929–2943. Available at: www.ajcr.us/.

Damase, T. R. *et al.* (2021) 'The Limitless Future of RNA Therapeutics', *Frontiers in Bioengineering and Biotechnology*. doi: 10.3389/fbioe.2021.628137.

Dan, H. *et al.* (2020) 'RACK1 promotes cancer progression by increasing the M2/M1 macrophage ratio via the NF-κB pathway in oral squamous cell carcinoma', *Molecular Oncology*, 14(4), pp. 795–807. doi: 10.1002/1878-0261.12644.

Das, A. V. and Pillai, R. M. (2015) 'Implications of miR cluster 143/145 as universal anti-oncomiRs and their dysregulation during tumorigenesis', *Cancer Cell International*. BioMed Central, 15(1), pp. 1–12. doi: 10.1186/s12935-015-0247-4.

Debusk, K. *et al.* (2021) 'Efficacy of tucatinib for HER2-positive metastatic breast cancer after HER2-targeted therapy: A network meta-analysis', *Future Oncology*, 17(33), pp. 4635–4647. doi: 10.2217/fon-2021-0742.

Delenclos, M. *et al.* (2017) 'Investigation of endocytic pathways for the internalization of exosome-associated oligomeric alpha-synuclein', *Frontiers in Neuroscience*, 11(MAR), p. 172. doi: 10.3389/fnins.2017.00172.

Denli, A. M. *et al.* (2004) 'Processing of primary microRNAs by the Microprocessor complex', *Nature*, 432(7014), pp. 231–235. doi: 10.1038/nature03049.

Dexheimer, P. J. and Cochella, L. (2020) 'MicroRNAs: From Mechanism to Organism', *Frontiers in Cell and Developmental Biology*. doi: 10.3389/fcell.2020.00409.

Dierssen-Sotos, T. *et al.* (2018) 'Reproductive risk factors in breast cancer and genetic hormonal pathways: A gene-environment interaction in the MCC-Spain project', *BMC Cancer*. BMC Cancer, 18(1), pp. 1–9. doi: 10.1186/s12885-018-4182-3.

Donoso-Quezada, J., Ayala-Mar, S. and González-Valdez, J. (2021) 'The role of lipids in exosome biology and intercellular communication: Function, analytics and applications', *Traffic*, 22(7), pp. 204–220. doi: 10.1111/tra.12803.

Dou, D. *et al.* (2020) 'Cancer-Associated Fibroblasts-Derived Exosomes Suppress Immune Cell Function in Breast Cancer via the miR-92/PD-L1 Pathway', *Frontiers in Immunology*, 11. doi: 10.3389/fimmu.2020.02026.

Ebrahimkhani, S. *et al.* (2018) 'Deep sequencing of circulating exosomal microRNA allows non-invasive glioblastoma diagnosis', *npj Precision Oncology*, 2(1). doi: 10.1038/s41698-018-0071-0.

Elias, A. D. (2010) 'Triple-negative breast cancer: A short review', *American Journal of Clinical Oncology: Cancer Clinical Trials*, 33(6), pp. 637–645. doi: 10.1097/COC.0b013e3181b8afcf.

Eliyatkin, N. *et al.* (2015) 'Molecular Classification of Breast Carcinoma: From Traditional, Old-Fashioned Way to A New Age, and A New Way', *Journal of Breast Health*, 11(2), pp. 59–66. doi: 10.5152/tjbh.2015.1669.

Elston, C. W. and Ellis, I. O. (1991) 'pathological prognostic factors in breast cancer. I. The value of histological grade in breast cancer: experience from a large study with long-term follow-up', *Histopathology*, 19(5), pp. 403–410. doi: 10.1111/j.1365-2559.1991.tb00229.x.

Emens, L. A. (2018) 'Breast cancer immunotherapy: Facts and hopes', *Clinical Cancer Research*, pp. 511–520. doi: 10.1158/1078-0432.CCR-16-3001.

Erbas, B. *et al.* (2006) 'The natural history of ductal carcinoma in situ of the breast: A review', *Breast Cancer Research and Treatment*, pp. 135–144. doi: 10.1007/s10549-005-9101-z.

Esfahani, K. *et al.* (2020) 'A review of cancer immunotherapy: From the past, to the present, to the future', *Current Oncology*, 27(S2), pp. 87–97. doi: 10.3747/co.27.5223.

Fallahpour, S. *et al.* (2017) 'Breast cancer survival by molecular subtype: a population-based analysis of cancer registry data', *CMAJ open*, 5(3), pp. E734–E739. doi: 10.9778/cmajo.20170030.

Faruq, O. and Vecchione, A. (2015) 'microRNA: Diagnostic perspective', *Frontiers in Medicine*, 2(AUG), pp. 1–10. doi: 10.3389/fmed.2015.00051.

Feng, D. *et al.* (2010) 'Cellular internalization of exosomes occurs through phagocytosis', *Traffic*, 11(5), pp. 675–687. doi: 10.1111/j.1600-0854.2010.01041.x.

Filipowicz, W., Bhattacharyya, S. N. and Sonenberg, N. (2008) 'Mechanisms of post-transcriptional regulation by microRNAs: Are the answers in sight?', *Nature Reviews Genetics*, 9(2), pp. 102–114. doi: 10.1038/nrg2290.

Fiorentino, F. *et al.* (2021) 'The two-faced role of sirt6 in cancer', *Cancers*, pp. 1–26. doi: 10.3390/cancers13051156.

Fitzner, D. *et al.* (2011) 'Selective transfer of exosomes from oligodendrocytes to microglia by macropinocytosis', *Journal of Cell Science*, 124(3), pp. 447–458. doi: 10.1242/jcs.074088.

Fitzpatrick, J. M. and De Wit, R. (2014) 'Taxane mechanisms of action: Potential implications for treatment sequencing in metastatic castration-resistant prostate cancer', *European Urology*. European Association of Urology, 65(6), pp. 1198–1204. doi: 10.1016/j.eururo.2013.07.022.

Frantz, C., Stewart, K. M. and Weaver, V. M. (2010) 'The extracellular matrix at a glance', *Journal of Cell Science*, pp. 4195–4200. doi: 10.1242/jcs.023820.

Fridlender, Z. G. and Albelda, S. M. (2012) 'Tumor-associated neutrophils: Friend or foe?', *Carcinogenesis*, pp. 949–955. doi: 10.1093/carcin/bgs123.

Fridman, W. H. *et al.* (2012) 'The immune contexture in human tumours: Impact on clinical outcome', *Nature Reviews Cancer*, pp. 298–306. doi: 10.1038/nrc3245.

Ganapathi, R. N. and Ganapathi, M. K. (2013) 'Mechanisms regulating resistance to inhibitors of topoisomerase II', *Frontiers in Pharmacology*, 4 AUG. doi: 10.3389/fphar.2013.00089.

Gennari, A. *et al.* (2004) 'Activity of first-line epirubicin and paclitaxel in metastatic breast cancer is independent of type of adjuvant therapy', *British Journal of Cancer*, 90(5), pp. 962–967. doi: 10.1038/sj.bjc.6601634.

Girardi, E. *et al.* (2020) 'A widespread role for SLC transmembrane transporters in resistance to cytotoxic drugs', *Nature Chemical Biology*, 16(4), pp. 469–478. doi: 10.1038/s41589-020-0483-3.

Godet, I. and Gilkes, D. M. (2017) 'BRCA1 and BRCA2 mutations and treatment strategies for breast cancer', *Integrative Cancer Science and Therapeutics*, 4(1). doi: 10.15761/icst.1000228.

Graeser, M. K. *et al.* (2009) 'Contralateral breast cancer risk in BRCA1 and BRCA2 mutation carriers', *Journal of Clinical Oncology*, 27(35), pp. 5887–5892. doi: 10.1200/JCO.2008.19.9430.

Grein, A. (1987) ‘Antitumor Anthracyclines Produced by Streptomyces peucetius’, *Advances in Applied Microbiology*, 32(C), pp. 203–214. doi: 10.1016/S0065-2164(08)70081-9.

Griffiths-Jones, S. *et al.* (2006) ‘miRBase: microRNA sequences, targets and gene nomenclature.’, *Nucleic acids research*, 34(Database issue). doi: 10.1093/nar/gkj112.

Griffiths-Jones, S. *et al.* (2008) ‘miRBase: Tools for microRNA genomics’, *Nucleic Acids Research*, 36(SUPPL. 1), pp. 154–158. doi: 10.1093/nar/gkm952.

Gucalp, A. *et al.* (2019) ‘Male breast cancer: a disease distinct from female breast cancer’, *Breast Cancer Research and Treatment*, pp. 37–48. doi: 10.1007/s10549-018-4921-9.

Ha, M. and Kim, V. N. (2014) ‘Regulation of microRNA biogenesis’, *Nature Reviews Molecular Cell Biology*. Nature Publishing Group, 15(8), pp. 509–524. doi: 10.1038/nrm3838.

Hagiwara, K. *et al.* (2015) ‘Commitment of Annexin A2 in recruitment of microRNAs into extracellular vesicles’, *FEBS Letters*. Federation of European Biochemical Societies, 589(24), pp. 4071–4078. doi: 10.1016/j.febslet.2015.11.036.

Han, M. *et al.* (2020) ‘Exosome-transmitted miR-567 reverses trastuzumab resistance by inhibiting ATG5 in breast cancer’, *Cell Death and Disease*, 11(1). doi: 10.1038/s41419-020-2250-5.

Haraszti, R. A. *et al.* (2016) ‘High-resolution proteomic and lipidomic analysis of exosomes and microvesicles from different cell sources’, *Journal of Extracellular Vesicles*, 5(1), pp. 1–14. doi: 10.3402/jev.v5.32570.

Haussmann, J. *et al.* (2020) ‘Recent advances in radiotherapy of breast cancer’, *Radiation Oncology*. doi: 10.1186/s13014-020-01501-x.

Hayashi, Y. *et al.* (2016) ‘p53 functional deficiency in human colon cancer cells promotes fibroblast-mediated angiogenesis and tumor growth’, *Carcinogenesis*, 37(10), pp. 972–984. doi: 10.1093/carcin/bgw085.

Hennenfent, K. L. and Govindan, R. (2006) ‘Novel formulations of taxanes: A review. Old wine in a new bottle?’, *Annals of Oncology*. Elsevier Masson SAS, 17(5), pp. 735–749. doi: 10.1093/annonc/mdj100.

Hientz, K. *et al.* (2017) ‘The role of p53 in cancer drug resistance and targeted chemotherapy’, *Oncotarget*, 8(5), pp. 8921–8946. doi: 10.18632/oncotarget.13475.

Higgins, M. J. and Baselga, J. (2011) ‘Targeted therapies for breast cancer’, *Journal of Clinical Investigation*, 121(10), pp. 3797–3803. doi: 10.1172/JCI57152.

Hirakawa, T. *et al.* (2016) ‘MiR-503, a microRNA epigenetically repressed in endometriosis, induces apoptosis and cell-cycle arrest and inhibits cell proliferation, angiogenesis, and contractility of human ovarian endometriotic stromal cells’, *Human Reproduction*, 31(11), pp. 2587–2597. doi: 10.1093/humrep/dew217.

Holton, R. A. *et al.* (1994) ‘First total synthesis of taxol. 2. Completion of the C and D rings’, *Journal of the American Chemical Society*, 116(4), pp. 1599–1600. doi: 10.1021/ja00083a067.

Hoshino, A. *et al.* (2015) ‘Tumour exosome integrins determine organotropic metastasis’, *Nature*. Nature Publishing Group, 527(7578), pp. 329–335. doi: 10.1038/nature15756.

Hsu, M. T., Wang, Y. K. and Tseng, Y. J. (2022) 'Exosomal Proteins and Lipids as Potential Biomarkers for Lung Cancer Diagnosis, Prognosis, and Treatment', *Cancers*. doi: 10.3390/cancers14030732.

Hu, Y. *et al.* (2017) 'Splicing factor hnRNPA2B1 contributes to tumorigenic potential of breast cancer cells through STAT3 and ERK1/2 signaling pathway', *Tumor Biology*, 39(3), pp. 1–11. doi: 10.1177/1010428317694318.

Hu, Y. B. *et al.* (2015) 'The endosomal-lysosomal system: From acidification and cargo sorting to neurodegeneration', *Translational Neurodegeneration*. doi: 10.1186/s40035-015-0041-1.

Hughes, K. S. *et al.* (2013) 'Lumpectomy plus tamoxifen with or without irradiation in women age 70 years or older with early breast cancer: Long-term follow-up of CALGB 9343', *Journal of Clinical Oncology*, 31(19), pp. 2382–2387. doi: 10.1200/JCO.2012.45.2615.

Huntzinger, E. and Izaurralde, E. (2011) 'Gene silencing by microRNAs: Contributions of translational repression and mRNA decay', *Nature Reviews Genetics*. Nature Publishing Group, 12(2), pp. 99–110. doi: 10.1038/nrg2936.

Huotari, J. and Helenius, A. (2011) 'Endosome maturation', *EMBO Journal*. Nature Publishing Group, 30(17), pp. 3481–3500. doi: 10.1038/emboj.2011.286.

Hurwitz, H. *et al.* (2004) 'Bevacizumab plus Irinotecan, Fluorouracil, and Leucovorin for Metastatic Colorectal Cancer', *New England Journal of Medicine*, 350(23), pp. 2335–2342. doi: 10.1056/nejmoa032691.

Iliou, M. S. *et al.* (2014) 'Impaired DICER1 function promotes stemness and metastasis in colon cancer', *Oncogene*, 33(30), pp. 4003–4015. doi: 10.1038/onc.2013.398.

Imura, J. *et al.* (2012) 'Laminin-5 is a biomarker of invasiveness in cervical adenocarcinoma.', *Diagnostic pathology*, 7, p. 105. doi: 10.1186/1746-1596-7-105.

Iwakawa, H. oki and Tomari, Y. (2015) 'The Functions of MicroRNAs: mRNA Decay and Translational Repression', *Trends in Cell Biology*, pp. 651–665. doi: 10.1016/j.tcb.2015.07.011.

Iwakawa, H. oki and Tomari, Y. (2022) 'Life of RISC: Formation, action, and degradation of RNA-induced silencing complex', *Molecular Cell*. Elsevier Inc., 82(1), pp. 30–43. doi: 10.1016/j.molcel.2021.11.026.

Jabłońska-Trypuć, A., Matejczyk, M. and Rosochacki, S. (2016) 'Matrix metalloproteinases (MMPs), the main extracellular matrix (ECM) enzymes in collagen degradation, as a target for anticancer drugs', *Journal of Enzyme Inhibition and Medicinal Chemistry*, 31, pp. 177–183. doi: 10.3109/14756366.2016.1161620.

Jayadev, R. and Sherwood, D. R. (2017) 'Basement membranes', *Current Biology*. Elsevier, 27(6), pp. R207–R211. doi: 10.1016/j.cub.2017.02.006.

Johnstone, R. M. *et al.* (1987) 'Vesicle formation during reticulocyte maturation. Association of plasma membrane activities with released vesicles (exosomes).', *Journal of Biological Chemistry*, 262(19), pp. 9412–9420. doi: 10.1016/s0021-9258(18)48095-7.

Joyce, J. A. (2005) 'Therapeutic targeting of the tumor microenvironment', *Cancer Cell*, 7(6), pp. 513–520. doi: 10.1016/j.ccr.2005.05.024.

Kabekkodu, S. P. *et al.* (2018) 'Clustered miRNAs and their role in biological functions

and diseases', *Biological Reviews*, 93(4), pp. 1955–1986. doi: 10.1111/brv.12428.

Kahlert, C. *et al.* (2014) 'Identification of doublestranded genomic dna spanning all chromosomes with mutated KRAS and P53 DNA in the serum exosomes of patients with pancreatic cancer', *Journal of Biological Chemistry*. Â© 2014 ASBMB. Currently published by Elsevier Inc; originally published by American Society for Biochemistry and Molecular Biology., 289(7), pp. 3869–3875. doi: 10.1074/jbc.C113.532267.

Kalluri, R. and LeBleu, V. S. (2020) 'The biology, function, and biomedical applications of exosomes', *Science*. doi: 10.1126/science.aau6977.

Kamerkar, S. *et al.* (2017) 'Exosomes facilitate therapeutic targeting of oncogenic KRAS in pancreatic cancer', *Nature*. Nature Publishing Group, 546(7659), pp. 498–503. doi: 10.1038/nature22341.

Kamińska, M. *et al.* (2015) 'Breast cancer risk factors', *Przeglad Menopauzalny*, pp. 196–202. doi: 10.5114/pm.2015.54346.

Karkkainen, M. J. *et al.* (2004) 'Vascular endothelial growth factor C is required for sprouting of the first lymphatic vessels from embryonic veins', *Nature Immunology*, 5(1), pp. 74–80. doi: 10.1038/ni1013.

Kastl, L., Brown, I. and Schofield, A. C. (2012) 'MiRNA-34a is associated with docetaxel resistance in human breast cancer cells', *Breast Cancer Research and Treatment*, 131(2), pp. 445–454. doi: 10.1007/s10549-011-1424-3.

Katz, T. A. (2016) 'Potential mechanisms underlying the protective effect of pregnancy against breast cancer: A focus on the IGF pathway', *Frontiers in Oncology*, p. 228. doi: 10.3389/fonc.2016.00228.

Kavallaris, M. (2010) 'Microtubules and resistance to tubulin-binding agents', *Nature Reviews Cancer*, 10(3), pp. 194–204. doi: 10.1038/nrc2803.

Keerthikumar, S. *et al.* (2016) 'ExoCarta: A Web-Based Compendium of Exosomal Cargo', *Journal of Molecular Biology*, 428(4), pp. 688–692. doi: 10.1016/j.jmb.2015.09.019.

Kenicer, J. *et al.* (2014) 'Molecular characterisation of isogenic taxane resistant cell lines identify novel drivers of drug resistance', *BMC Cancer*, 14(1). doi: 10.1186/1471-2407-14-762.

Khan, S. *et al.* (2014) 'Early diagnostic value of survivin and its alternative splice variants in breast cancer', *BMC Cancer*, 14(1), p. 176. doi: 10.1186/1471-2407-14-176.

Kharaziha, P. *et al.* (2012) 'Tumor cell-derived exosomes: A message in a bottle', *Biochimica et Biophysica Acta - Reviews on Cancer*. Elsevier B.V., 1826(1), pp. 103–111. doi: 10.1016/j.bbcan.2012.03.006.

Khasraw, M., Bell, R. and Dang, C. (2012) 'Epirubicin: Is it like doxorubicin in breast cancer? A clinical review', *Breast*. Elsevier Ltd, 21(2), pp. 142–149. doi: 10.1016/j.breast.2011.12.012.

Khongkow, M. *et al.* (2013) 'SIRT6 modulates paclitaxel and epirubicin resistance and survival in breast cancer', *Carcinogenesis*, 34(7), pp. 1476–1486. doi: 10.1093/carcin/bgt098.

Khvorova, A., Reynolds, A. and Jayasena, S. D. (2003) 'Functional siRNAs and miRNAs exhibit strand bias', *Cell*, 115(2), pp. 209–216. doi: 10.1016/S0092-8674(03)00801-8.

Kim, J. E. *et al.* (2018) 'Diagnostic value of microRNAs derived from exosomes in bronchoalveolar lavage fluid of early-stage lung adenocarcinoma: A pilot study', *Thoracic Cancer*, 9(8), pp. 911–915. doi: 10.1111/1759-7714.12756.

Korc, M. and Friesel, R. (2009) 'The role of fibroblast growth factors in tumor growth.', *Curr Cancer Drug Targets*, pp. 639–651. doi: 10.1007/978-1-4615-3088-6_10.

Kosaka, N. *et al.* (2013) 'Neutral sphingomyelinase 2 (nSMase2)-dependent exosomal transfer of angiogenic micrornas regulate cancer cell metastasis', *Journal of Biological Chemistry*. Â© 2013 ASBMB. Currently published by Elsevier Inc; originally published by American Society for Biochemistry and Molecular Biology., 288(15), pp. 10849–10859. doi: 10.1074/jbc.M112.446831.

Kowal, J. *et al.* (2016) 'Proteomic comparison defines novel markers to characterize heterogeneous populations of extracellular vesicle subtypes', *Proceedings of the National Academy of Sciences of the United States of America*, 113(8), pp. E968–E977. doi: 10.1073/pnas.1521230113.

Kozomara, A. and Griffiths-Jones, S. (2011) 'MiRBase: Integrating microRNA annotation and deep-sequencing data', *Nucleic Acids Research*, 39(SUPPL. 1). doi: 10.1093/nar/gkq1027.

Kozomara, A. and Griffiths-Jones, S. (2014) 'MiRBase: Annotating high confidence microRNAs using deep sequencing data', *Nucleic Acids Research*, 42(D1). doi: 10.1093/nar/gkt1181.

Kumar, S. R. *et al.* (2020) 'RNA cargos in extracellular vesicles derived from blood serum in pancreas associated conditions', *Scientific Reports*, 10(1), p. 2800. doi: 10.1038/s41598-020-59523-0.

Kwapisz, D. (2021) 'Pembrolizumab and atezolizumab in triple-negative breast cancer', *Cancer Immunology, Immunotherapy*, pp. 607–617. doi: 10.1007/s00262-020-02736-z.

Lan, J. *et al.* (2019) 'M2 macrophage-derived exosomes promote cell migration and invasion in colon cancer', *Cancer Research*, 79(1), pp. 146–158. doi: 10.1158/0008-5472.CAN-18-0014.

Lander, A. D. and Selleck, S. B. (2000) 'The elusive functions of proteoglycans: In vivo veritas', *Journal of Cell Biology*, 148(2), pp. 227–232. doi: 10.1083/jcb.148.2.227.

Laurila, P. and Leivo, I. (1993) 'Basement membrane and interstitial matrix components form separate matrices in heterokaryons of PYS-2 cells and fibroblasts', *Journal of Cell Science*, 104(1), pp. 59–68. doi: 10.1242/jcs.104.1.59.

Le, M. T. N. *et al.* (2014) 'MiR-200-containing extracellular vesicles promote breast cancer cell metastasis', *Journal of Clinical Investigation*, 124(12), pp. 5109–5128. doi: 10.1172/JCI75695.

Lee, J. K. *et al.* (2013) 'Exosomes derived from mesenchymal stem cells suppress angiogenesis by down-regulating VEGF expression in breast cancer cells', *PLoS ONE*, 8(12), p. 84256. doi: 10.1371/journal.pone.0084256.

Lee, Y. *et al.* (2004) 'MicroRNA genes are transcribed by RNA polymerase II', *EMBO Journal*, 23(20), pp. 4051–4060. doi: 10.1038/sj.emboj.7600385.

Lee, Y., El Andaloussi, S. and Wood, M. J. (2012) 'Exosomes and microvesicles: Extracellular vesicles for genetic information transfer and gene therapy', *Human Molecular*

Genetics, 21(R1). doi: 10.1093/hmg/dds317.

Lennox, K. A. and Behlke, M. A. (2010) 'A direct comparison of anti-microRNA oligonucleotide potency', *Pharmaceutical Research*, 27(9), pp. 1788–1799. doi: 10.1007/s11095-010-0156-0.

Li, C. *et al.* (2020) 'Regulatory T cells in tumor microenvironment: New mechanisms, potential therapeutic strategies and future prospects', *Molecular Cancer*. Molecular Cancer, 19(1), pp. 1–23. doi: 10.1186/s12943-020-01234-1.

Li, H. *et al.* (2018) 'MiR-519a enhances chemosensitivity and promotes autophagy in glioblastoma by targeting STAT3/Bcl2 signaling pathway', *Journal of Hematology and Oncology*, 11(1). doi: 10.1186/s13045-018-0618-0.

Li, J. *et al.* (2015) 'MiR-21 expression predicts prognosis in diffuse large B-cell lymphoma', *International Journal of Clinical and Experimental Pathology*, 8(11), pp. 15019–15024. Available at: www.ijcep.com/.

Li, L. *et al.* (2018) 'The landscape of miRNA editing in animals and its impact on miRNA biogenesis and targeting', *Genome Research*, 28(1), pp. 132–143. doi: 10.1101/gr.224386.117.

Lieberman, J. (2018) 'Tapping the RNA world for therapeutics', *Nature Structural & Molecular Biology*, 25, pp. 357–364. doi: 10.1038/s41594-018-0054-4.

Lin, S. and Gregory, R. I. (2015) 'MicroRNA biogenesis pathways in cancer', *Nature Reviews Cancer*. Nature Publishing Group, 15(6), pp. 321–333. doi: 10.1038/nrc3932.

Liu, L., Qu, W. and Zhong, Z. (2015) 'Down-regulation of miR-503 expression predicate advanced mythological features and poor prognosis in patients with NSCLC', *International Journal of Clinical and Experimental Pathology*, 8(5), pp. 5609–5613. Available at: www.ijcep.com/.

Liu, Q. *et al.* (2013) 'Malate dehydrogenase 2 confers docetaxel resistance via regulations of JNK signaling and oxidative metabolism', *Prostate*, 73(10), pp. 1028–1037. doi: 10.1002/pros.22650.

Liu, T. *et al.* (2019) 'Exosome-transmitted miR-128-3p increase chemosensitivity of oxaliplatin-resistant colorectal cancer', *Molecular Cancer*. Molecular Cancer, 18(1), pp. 1–17. doi: 10.1186/s12943-019-0981-7.

Liu, Y., Gu, Y. and Cao, X. (2015) 'The exosomes in tumor immunity', *OncoImmunology*, 4(9), pp. 1–8. doi: 10.1080/2162402X.2015.1027472.

Liu, Y. and Shi, S. L. (2021) 'The roles of hnRNP A2/B1 in RNA biology and disease', *Wiley Interdisciplinary Reviews: RNA*, 12(2), pp. 1–23. doi: 10.1002/wrna.1612.

Livraghi, L. and Garber, J. E. (2015) 'PARP inhibitors in the management of breast cancer: Current data and future prospects', *BMC Medicine*. doi: 10.1186/s12916-015-0425-1.

Llorente, A. *et al.* (2013) 'Molecular lipidomics of exosomes released by PC-3 prostate cancer cells', *Biochimica et Biophysica Acta - Molecular and Cell Biology of Lipids*, 1831(7), pp. 1302–1309. doi: 10.1016/j.bbalip.2013.04.011.

Lo, Y. W. *et al.* (2015) 'Mitochondrial proteomics with siRNA knockdown to reveal ACAT1 and MDH2 in the development of doxorubicin-resistant uterine cancer', *Journal of Cellular and Molecular Medicine*, 19(4), pp. 744–759. doi: 10.1111/jcmm.12388.

Long, J. *et al.* (2015) 'MiR-503 inhibited cell proliferation of human breast cancer cells by suppressing CCND1 expression', *Tumor Biology*, 36(11), pp. 8697–8702. doi: 10.1007/s13277-015-3623-8.

Lu, A. Y., Junk, K. W. and Coon, M. J. (1969) 'Resolution of the cytochrome P-450-containing omega-hydroxylation system of liver microsomes into three components.', *Journal of Biological Chemistry*, 244(13), pp. 3714–3721. doi: 10.1016/s0021-9258(18)83427-5.

Lu, P. *et al.* (2017) 'MEX3C interacts with adaptor-related protein complex 2 and involves in miR-451a exosomal sorting', *PLoS ONE*, 12(10). doi: 10.1371/journal.pone.0185992.

Lugano, R. *et al.* (2018) 'CD93 promotes β1 integrin activation and fibronectin fibrillogenesis during tumor angiogenesis', *Journal of Clinical Investigation*, 128(8), pp. 3280–3297. doi: 10.1172/JCI97459.

Lund, E. *et al.* (2004) 'Nuclear Export of MicroRNA Precursors', *Science*, 303(5654), pp. 95–98. doi: 10.1126/science.1090599.

Lüönd, F., Tiede, S. and Christofori, G. (2021) 'Breast cancer as an example of tumour heterogeneity and tumour cell plasticity during malignant progression', *British Journal of Cancer*. https, pp. 164–175. doi: 10.1038/s41416-021-01328-7.

Lv, M. meng *et al.* (2014) 'Exosomes mediate drug resistance transfer in MCF-7 breast cancer cells and a probable mechanism is delivery of P-glycoprotein', *Tumor Biology*, 35(11), pp. 10773–10779. doi: 10.1007/s13277-014-2377-z.

Lv, T. *et al.* (2018) 'MiR-503 is down-regulated in osteosarcoma and suppressed MG63 proliferation and invasion by targeting VEGFA/Rictor', *Cancer Biomarkers*, 23(3), pp. 315–322. doi: 10.3233/CBM-170906.

Macfarlane, L.-A. and Murphy, P. R. (2010) *MicroRNA: Biogenesis, Function and Role in Cancer, Current Genomics*. Available at: http://microrna.sanger.ac.uk.

Madhunapantula, S. V. and Robertson, G. P. (2009) 'The PTEN-AKT3 signaling cascade as a therapeutic target in melanoma', *Pigment Cell and Melanoma Research*, 22(4), pp. 400–419. doi: 10.1111/j.1755-148X.2009.00585.x.

Mahdavi, M. *et al.* (2019) 'Hereditary breast cancer; Genetic penetrance and current status with BRCA', *Journal of Cellular Physiology*, 234(5), pp. 5741–5750. doi: 10.1002/jcp.27464.

Makki, J. (2015) 'Diversity of breast carcinoma: Histological subtypes and clinical relevance', *Clinical Medicine Insights: Pathology*, 8(1), pp. 23–31. doi: 10.4137/CPath.s31563.

Maloney, S. M. *et al.* (2020) 'Mechanisms of taxane resistance', *Cancers*, pp. 1–57. doi: 10.3390/cancers12113323.

Marchbanks, P. A. *et al.* (2012) 'Oral contraceptive formulation and risk of breast cancer', *Contraception*, 85(4), pp. 342–350. doi: 10.1016/j.contraception.2011.08.007.

Marie Hardwick, J. and Soane, L. (2013) 'Multiple functions of BCL-2 family proteins', *Cold Spring Harbor Perspectives in Biology*, 5(2). doi: 10.1101/cshperspect.a008722.

Marinello, J., Delcuratolo, M. and Capranico, G. (2018) 'Anthracyclines as Topoisomerase II poisons: From early studies to new perspectives', *International Journal of Molecular Sciences*. doi: 10.3390/ijms19113480.

Marino, A. L. F. *et al.* (2014) 'MicroRNA expression as risk biomarker of breast cancer metastasis: A pilot retrospective case-cohort study', *BMC Cancer*, 14(1), pp. 1–12. doi: 10.1186/1471-2407-14-739.

Marupudi, N. I. *et al.* (2007) 'Paclitaxel: A review of adverse toxicities and novel delivery strategies', *Expert Opinion on Drug Safety*, 6(5), pp. 609–621. doi: 10.1517/14740338.6.5.609.

Marvel, D. and Gabrilovich, D. I. (2015) 'Myeloid-derived suppressor cells in the tumor microenvironment: Expect the unexpected', *Journal of Clinical Investigation*, pp. 3356–3364. doi: 10.1172/JCI80005.

Masood, S. (2016) 'Neoadjuvant chemotherapy in breast cancers', *Women's Health*, pp. 480–491. doi: 10.1177/1745505716677139.

Masoud, V. and Pagès, G. (2017) 'Targeted therapies in breast cancer: New challenges to fight against resistance', *World Journal of Clinical Oncology*, pp. 120–134. doi: 10.5306/wjco.v8.i2.120.

Van der Maten, M. *et al.* (2019) 'L1 cell adhesion molecule in cancer, a systematic review on domain-specific functions', *International Journal of Molecular Sciences*. doi: 10.3390/ijms20174180.

Matsuyama, H. and Suzuki, H. I. (2020) 'Systems and synthetic microRNA biology: From biogenesis to disease pathogenesis', *International Journal of Molecular Sciences*. doi: 10.3390/ijms21010132.

McDonald, E. S. *et al.* (2016) 'Clinical diagnosis and management of breast cancer', *Journal of Nuclear Medicine*, 57, pp. 9S-16S. doi: 10.2967/jnumed.115.157834.

Minárik, P. *et al.* (2002) 'Malate Dehydrogenases - Structure and function', *General Physiology and Biophysics*, 21(3), pp. 257–265.

Minciacchi, V. R., Freeman, M. R. and Di Vizio, D. (2015) 'Extracellular Vesicles in Cancer: Exosomes, Microvesicles and the Emerging Role of Large Oncosomes', *Seminars in Cell and Developmental Biology*, 40, pp. 41–51. doi: 10.1016/j.semcdb.2015.02.010.

Minetto, P. *et al.* (2019) 'Harnessing NK Cells for Cancer Treatment', *Frontiers in Immunology*, p. 2836. doi: 10.3389/fimmu.2019.02836.

Mishra, P. *et al.* (2020) 'Assessment of Cytokeratin Expression in Carcinoma Breast', *Journal of Evolution of Medical and Dental Sciences*, 9(35), pp. 2545–2549. doi: 10.14260/jemds/2020/553.

Mohamed, A. *et al.* (2013) 'Targeted therapy for breast cancer', *American Journal of Pathology*. American Society for Investigative Pathology, 183(4), pp. 1096–1112. doi: 10.1016/j.ajpath.2013.07.005.

Momenimovahed, Z. and Salehiniya, H. (2019) 'Epidemiological characteristics of and risk factors for breast cancer in the world', *Breast Cancer: Targets and Therapy*, pp. 151–164. doi: 10.2147/BCTT.S176070.

Montemurro, F., Nuzzolese, I. and Ponzone, R. (2020) 'Neoadjuvant or adjuvant chemotherapy in early breast cancer?', *Expert Opinion on Pharmacotherapy*. Taylor & Francis, 21(9), pp. 1071–1082. doi: 10.1080/14656566.2020.1746273.

Moon, H. J. *et al.* (2013) 'MCF-7 cells expressing nuclear associated lysyl oxidase-like

2 (LOXL2) exhibit an epithelial-to-Mesenchymal transition (EMT) phenotype and are highly invasive in Vitro', *Journal of Biological Chemistry*, 288(42), pp. 30000–30008. doi: 10.1074/jbc.C113.502310.

Moran-Jones, K. *et al.* (2005) 'hnRNP A2, a potential ssDNA/RNA molecular adapter at the telomere', *Nucleic Acids Research*, 33(2), pp. 486–496. doi: 10.1093/nar/gki203.

Mørch, L. S. *et al.* (2017) 'Contemporary Hormonal Contraception and the Risk of Breast Cancer', *New England Journal of Medicine*, 377(23), pp. 2228–2239. doi: 10.1056/nejmoa1700732.

Moreno-Bueno, G. *et al.* (2003) 'Cyclin D1 gene (CCND1) mutations in endometrial cancer', *Oncogene*, 22(38), pp. 6115–6118. doi: 10.1038/sj.onc.1206868.

Mortensen, R. D. *et al.* (2011) 'Posttranscriptional activation of gene expression in Xenopus laevis oocytes by microRNA-protein complexes (microRNPs)', *Proceedings of the National Academy of Sciences of the United States of America*, 108(20), pp. 8281–8286. doi: 10.1073/pnas.1105401108.

Munich, S. *et al.* (2012) 'Dendritic cell exosomes directly kill tumor cells and activate natural killer cells via TNF superfamily ligands', *OncoImmunology*, 1(7), pp. 1074–1083. doi: 10.4161/onci.20897.

Munro, A. F., Cameron, D. A. and Bartlett, J. M. S. (2010) 'Targeting anthracyclines in early breast cancer: New candidate predictive biomarkers emerge', *Oncogene*. Nature Publishing Group, 29(38), pp. 5231–5240. doi: 10.1038/onc.2010.286.

Nagl, L. *et al.* (2020) 'Tumor Endothelial Cells (TECs) as Potential Immune Directors of the Tumor Microenvironment – New Findings and Future Perspectives', *Frontiers in Cell and Developmental Biology*. doi: 10.3389/fcell.2020.00766.

Nagy, J. A. *et al.* (2010) 'Heterogeneity of the tumor vasculature', *Seminars in Thrombosis and Hemostasis*, pp. 321–331. doi: 10.1055/s-0030-1253454.

Nakanishi, K. (2016) 'Anatomy of RISC: how do small RNAs and chaperones activate Argonaute proteins?', *WIREs RNA*, 7, pp. 637–660. doi: 10.1002/wrna.1356.

Nascimento, R. G. do and Otoni, K. M. (2020) 'Histological and molecular classification of breast cancer: what do we know?', *Mastology*, 30, pp. 1–8. doi: 10.29289/25945394202020200024.

Nedaeinia, R. *et al.* (2016) 'Locked nucleic acid anti-miR-21 inhibits cell growth and invasive behaviors of a colorectal adenocarcinoma cell line: LNA-anti-miR as a novel approach', *Nature Publishing Group*. doi: 10.1038/cgt.2016.25.

Ngambenjawong, C., Gustafson, H. H. and Pun, S. H. (2017) 'Progress in tumor-associated macrophage (TAM)-targeted therapeutics', *Advanced Drug Delivery Reviews*, pp. 206–221. doi: 10.1016/j.addr.2017.04.010.

Niaz, S. and Hussain, M. U. (2018) 'Role of GW182 protein in the cell'. doi: 10.1016/j.biocel.2018.05.009.

Van Niel, G., D'Angelo, G. and Raposo, G. (2018) 'Shedding light on the cell biology of extracellular vesicles', *Nature Reviews Molecular Cell Biology*. Nature Publishing Group, 19(4), pp. 213–228. doi: 10.1038/nrm.2017.125.

Nolte-'t Hoen, E. N. M. *et al.* (2009) 'Activated T cells recruit exosomes secreted by

dendritic cells via LFA-1', *Blood*, 113(9), pp. 1977–1981. doi: 10.1182/blood-2008-08-174094.

O'brien, J. *et al.* (2018) 'Overview of MicroRNA Biogenesis, Mechanisms of Actions, and Circulation', *Frontiers in Endocrinology | www.frontiersin.org*, 9, p. 402. doi: 10.3389/fendo.2018.00402.

O'Brien, K. *et al.* (2020) 'RNA delivery by extracellular vesicles in mammalian cells and its applications', *Nature Reviews Molecular Cell Biology*, pp. 585–606. doi: 10.1038/s41580-020-0251-y.

O'Brien, K. M. *et al.* (2010) 'Intrinsic breast tumor subtypes, race, and long-term survival in the carolina breast cancer study', *Clinical Cancer Research*, 16(24), pp. 6100–6110. doi: 10.1158/1078-0432.CCR-10-1533.

O'Neil, N. J., Bailey, M. L. and Hieter, P. (2017) 'Synthetic lethality and cancer', *Nature Reviews Genetics*, pp. 613–623. doi: 10.1038/nrg.2017.47.

Orang, A. V., Safaralizadeh, R. and Kazemzadeh-Bavili, M. (2014) 'Mechanisms of miRNA-mediated gene regulation from common downregulation to mRNA-specific upregulation', *International Journal of Genomics*. doi: 10.1155/2014/970607.

Ørom, U. A. and Lund, A. H. (2007) 'Isolation of microRNA targets using biotinylated synthetic microRNAs', *Methods*, 43(2), pp. 162–165. doi: 10.1016/j.ymeth.2007.04.007.

Osborne, C. K., Wakeling, A. and Nicholson, R. I. (2004) 'Fulvestrant: An oestrogen receptor antagonist with a novel mechanism of action', *British Journal of Cancer*, 90, pp. S2–S6. doi: 10.1038/sj.bjc.6601629.

Oshi, M. *et al.* (2020) 'M1 Macrophage and M1/M2 ratio defined by transcriptomic signatures resemble only part of their conventional clinical characteristics in breast cancer', *Scientific Reports*, 10(1), p. 16554. doi: 10.1038/s41598-020-73624-w.

Paller, C. J. and Antonarakis, E. S. (2011) 'Cabazitaxel: A novel second-line treatment for metastatic castration-resistant prostate cancer', *Drug Design, Development and Therapy*, pp. 117–124. doi: 10.2147/DDDT.S13029.

Palucka, K. *et al.* (2010) 'Are they clinically relevant?', *Cancer Journal*, pp. 318–324. doi: 10.1097/PPO.0b013e3181eaca83.

Pan, B. T. and Johnstone, R. M. (1983) 'Fate of the transferrin receptor during maturation of sheep reticulocytes in vitro: Selective externalization of the receptor', *Cell*, 33(3), pp. 967–978. doi: 10.1016/0092-8674(83)90040-5.

Pankov, R. and Yamada, K. M. (2002) 'Fibronectin at a glance', *Journal of Cell Science*, 115(20), pp. 3861–3863. doi: 10.1242/jcs.00059.

Pasquinelli, A. E. (2012) 'MicroRNAs and their targets: Recognition, regulation and an emerging reciprocal relationship', *Nature Reviews Genetics*. Nature Publishing Group, 13(4), pp. 271–282. doi: 10.1038/nrg3162.

Patel, S. *et al.* (2018) 'Unique pattern of neutrophil migration and function during tumor progression', *Nature Immunology*, 19(11), pp. 1236–1247. doi: 10.1038/s41590-018-0229-5.

Pathan, M. *et al.* (2019) 'Vesiclepedia 2019: A compendium of RNA, proteins, lipids and metabolites in extracellular vesicles', *Nucleic Acids Research*, 47(D1), pp. D516–D519. doi: 10.1093/nar/gky1029.

Paul Launchbury, A. and Habboubi, N. (1993) 'Epirubicin and doxorubicin: a comparison of their characteristics, therapeutic activity and toxicity', *Cancer Treatment Reviews*, 19(3), pp. 197–228. doi: 10.1016/0305-7372(93)90036-Q.

Peng, D. H. *et al.* (2017) 'ZEB1 induces LOXL2-mediated collagen stabilization and deposition in the extracellular matrix to drive lung cancer invasion and metastasis', *Oncogene*, 36(14), pp. 1925–1938. doi: 10.1038/onc.2016.358.

Peng, Y. *et al.* (2014) 'MicroRNA-503 inhibits gastric cancer cell growth and epithelial-to-mesenchymal transition', *Oncology Letters*, 7(4), pp. 1233–1238. doi: 10.3892/ol.2014.1868.

Peng, Y. and Croce, C. M. (2016) 'The role of microRNAs in human cancer', *Signal Transduction and Targeted Therapy*. doi: 10.1038/sigtrans.2015.4.

Pérez-Boza, J. *et al.* (2020a) 'hnRNPA2B1 inhibits the exosomal export of miR-503 in endothelial cells', *Cellular and Molecular Life Sciences*. Springer International Publishing, 77(21), pp. 4413–4428. doi: 10.1007/s00018-019-03425-6.

Pérez-Boza, J. *et al.* (2020b) 'hnRNPA2B1 inhibits the exosomal export of miR-503 in endothelial cells', *Cellular and Molecular Life Sciences*, 77(21), pp. 4413–4428. doi: 10.1007/s00018-019-03425-6.

Pérez-Boza, J., Lion, M. and Struman, I. (2018) 'Exploring the RNA landscape of endothelial exosomes', *Rna*, 24(3), pp. 423–435. doi: 10.1261/rna.064352.117.

Perou, C. M. *et al.* (2000) 'Molecular portraits of human breast tumours', *Nature*, 406. doi: 10.1038/246170a0.

Pestell, R. G. (2013) 'New roles of cyclin D1', *American Journal of Pathology*. American Society for Investigative Pathology, 183(1), pp. 3–9. doi: 10.1016/j.ajpath.2013.03.001.

Peters, L. and Meister, G. (2007) 'Argonaute Proteins: Mediators of RNA Silencing', *Molecular Cell*, 26(5), pp. 611–623. doi: 10.1016/j.molcel.2007.05.001.

Pettersen Hessvik, N. and Llorente, A. (2018) 'Current knowledge on exosome biogenesis and release', *Cell. Mol. Life Sci*, 75, pp. 193–208. doi: 10.1007/s00018-017-2595-9.

Phukan, J. P., Sinha, A. and Deka, J. P. (2015) 'Cytological grading of breast carcinoma on fine needle aspirates and its relation with histological grading', *South Asian Journal of Cancer*, 04(01), pp. 032–034. doi: 10.4103/2278-330x.149948.

Pickup, M. W., Mouw, J. K. and Weaver, V. M. (2014) 'The extracellular matrix modulates the hallmarks of cancer', *EMBO reports*, 15(12), pp. 1243–1253. doi: 10.15252/embr.201439246.

Pietrasik, S. *et al.* (2020) 'Interplay between BRCA1 and GADD45A and its potential for nucleotide excision repair in breast cancer pathogenesis', *International Journal of Molecular Sciences*. doi: 10.3390/ijms21030870.

Plebanek, M. P. *et al.* (2017) 'Pre-metastatic cancer exosomes induce immune surveillance by patrolling monocytes at the metastatic niche', *Nature Communications*, 8(1). doi: 10.1038/s41467-017-01433-3.

Pols, M. S. and Klumperman, J. (2009) 'Trafficking and function of the tetraspanin

CD63', *Experimental Cell Research*. Elsevier Inc., 315(9), pp. 1584–1592. doi: 10.1016/j.yexcr.2008.09.020.

Popp, H. D. *et al.* (2017) 'Immunofluorescence microscopy of γH2AX and 53BP1 for analyzing the formation and repair of DNA double-strand breaks', *Journal of Visualized Experiments*, 2017(129), p. 56617. doi: 10.3791/56617.

Pula, B. *et al.* (2013) 'Podoplanin expression in cancer-associated fibroblasts correlates with VEGF-C expression in cancer cells of invasive ductal breast carcinoma', *Neoplasma*, 60(5), pp. 516–524. doi: 10.4149/neo_2013_067.

Qi, H. *et al.* (2018) 'Long noncoding RNA SNHG7 accelerates prostate cancer proliferation and cycle progression through cyclin D1 by sponging miR-503', *Biomedicine and Pharmacotherapy*. Elsevier, 102(1), pp. 326–332. doi: 10.1016/j.biopha.2018.03.011.

Qian, X. L. *et al.* (2013) 'Syndecan Binding Protein (SDCBP) Is Overexpressed in Estrogen Receptor Negative Breast Cancers, and Is a Potential Promoter for Tumor Proliferation', *PLoS ONE*, 8(3). doi: 10.1371/journal.pone.0060046.

Qiu, T. *et al.* (2013a) 'MiR-503 regulates the resistance of non-small cell lung cancer cells to cisplatin by targeting Bcl-2', *International Journal of Molecular Medicine*, 32(3), pp. 593–598. doi: 10.3892/ijmm.2013.1439.

Qiu, T. *et al.* (2013b) 'MiR-503 regulates the resistance of non-small cell lung cancer cells to cisplatin by targeting Bcl-2', *International Journal of Molecular Medicine*, 32(3), pp. 593–598. doi: 10.3892/ijmm.2013.1439.

Raiborg, C. and Stenmark, H. (2009) 'The ESCRT machinery in endosomal sorting of ubiquitylated membrane proteins', *Nature*, pp. 445–452. doi: 10.1038/nature07961.

Ramsay, R. G. and Gonda, T. J. (2008) 'MYB function in normal and cancer cells', *Nature Reviews Cancer*, 8(7), pp. 523–534. doi: 10.1038/nrc2439.

Rana, S. *et al.* (2012) 'Toward tailored exosomes: The exosomal tetraspanin web contributes to target cell selection', *International Journal of Biochemistry and Cell Biology*. Elsevier Ltd, 44(9), pp. 1574–1584. doi: 10.1016/j.biocel.2012.06.018.

Raposo, G. and Stoorvogel, W. (2013) 'Extracellular vesicles: Exosomes, microvesicles, and friends', *Journal of Cell Biology*, 200(4), pp. 373–383. doi: 10.1083/jcb.201211138.

Reddy, K. B. (2015) 'MicroRNA (miRNA) in cancer', *Cancer Cell International*. ???, 15(1), pp. 4–9. doi: 10.1186/s12935-015-0185-1.

Reynolds, D. S. *et al.* (2017) 'Breast Cancer Spheroids Reveal a Differential Cancer Stem Cell Response to Chemotherapeutic Treatment', *Scientific Reports*, 7(1). doi: 10.1038/s41598-017-10863-4.

Ribatti, D., Tamma, R. and Annese, T. (2020) 'Epithelial-Mesenchymal Transition in Cancer: A Historical Overview', *Translational Oncology*. The Authors, 13(6), p. 100773. doi: 10.1016/j.tranon.2020.100773.

Ribeiro, M. F. *et al.* (2013) 'Exosomes function in pro- and anti-angiogenesis', *Current Angiogenesis*, pp. 54–59. doi: 10.2174/2211552811302002001.

Ricard-Blum, S. (2011) 'The Collagen Family', *Cold Spring Harbor Perspectives in Biology*, 3(1), pp. 1–19. doi: 10.1101/cshperspect.a004978.

Rodriguez-barrueco, R. *et al.* (2017) 'miR-424(322)/503 is a breast cancer tumor suppressor whose loss promotes resistance to chemotherapy', *Genes & Development*, 424(322), pp. 553–566. doi: 10.1101/gad.292318.116.7.

Rodriguez-Barrueco, R. *et al.* (2017) 'miR-424(322)/503 is a breast cancer tumor suppressor whose loss promotes resistance to chemotherapy', *Genes & development*, 31(6), pp. 553–566. doi: 10.1101/gad.292318.116.

Rosenberger, L. *et al.* (2019) 'Stem cell exosomes inhibit angiogenesis and tumor growth of oral squamous cell carcinoma', *Scientific Reports*, 9(1). doi: 10.1038/s41598-018-36855-6.

Rosenkranz, K. M. *et al.* (2018) 'The Feasibility of Breast-Conserving Surgery for Multiple Ipsilateral Breast Cancer: An Initial Report from ACOSOG Z11102 (Alliance) Trial', *Annals of Surgical Oncology*, 25(10), pp. 2858–2866. doi: 10.1245/s10434-018-6583-6.

Roucourt, B. *et al.* (2015) 'Heparanase activates the syndecan-syntenin-ALIX exosome pathway', *Cell Research*, 25(4), pp. 412–428. doi: 10.1038/cr.2015.29.

Roy, R., Chun, J. and Powell, S. N. (2012) 'BRCA1 and BRCA2: Different roles in a common pathway of genome protection', *Nature Reviews Cancer*, pp. 68–78. doi: 10.1038/nrc3181.

Sabatier, R. *et al.* (2014) 'Claudin-low breast cancers: Clinical, pathological, molecular and prognostic characterization', *Molecular Cancer*, 13(1). doi: 10.1186/1476-4598-13-228.

Safaei, R. *et al.* (2005) 'Abnormal lysosomal trafficking and enhanced exosomal export of cisplatin in drug-resistant human ovarian carcinoma cells', *Molecular Cancer Therapeutics*, 4(10), pp. 1595–1604. doi: 10.1158/1535-7163.MCT-05-0102.

Sahai, E. *et al.* (2020) 'A framework for advancing our understanding of cancer-associated fibroblasts', *Nature Reviews Cancer*, pp. 174–186. doi: 10.1038/s41568-019-0238-1.

Sala, A. (2005) 'B-MYB, a transcription factor implicated in regulating cell cycle, apoptosis and cancer', *European Journal of Cancer*, 41(16), pp. 2479–2484. doi: 10.1016/j.ejca.2005.08.004.

Salim, U. *et al.* (2022) 'Biogenesis, characterization, and functions of mirtrons', *Wiley Interdisciplinary Reviews: RNA*, 13(1). doi: 10.1002/wrna.1680.

Sansone, P. *et al.* (2017) 'Packaging and transfer of mitochondrial DNA via exosomes regulate escape from dormancy in hormonal therapy-resistant breast cancer', *Proceedings of the National Academy of Sciences of the United States of America*, 114(43), pp. E9066–E9075. doi: 10.1073/pnas.1704862114.

Santangelo, L. *et al.* (2016) 'The RNA-Binding Protein SYNCRIP Is a Component of the Hepatocyte Exosomal Machinery Controlling MicroRNA Sorting', *Cell Reports*. ElsevierCompany., 17(3), pp. 799–808. doi: 10.1016/j.celrep.2016.09.031.

Savina, A., Vidal, M. and Colombo, M. I. (2002) 'The exosome pathway in K562 cells is regulated by Rab11', *Journal of Cell Science*, 115(12), pp. 2505–2515. doi: 10.1242/jcs.115.12.2505.

Scaltriti, M. *et al.* (2009) 'Lapatinib, a HER2 tyrosine kinase inhibitor, induces stabilization and accumulation of HER2 and potentiates trastuzumab-dependent cell cytotoxicity', *Oncogene*, 28(6), pp. 803–814. doi: 10.1038/onc.2008.432.

Schindler, C. *et al.* (2019) 'Exosomal delivery of doxorubicin enables rapid cell entry and enhanced in vitro potency', *PLoS ONE*, 14(3). doi: 10.1371/journal.pone.0214545.

Schmid, P. *et al.* (2020) 'Pembrolizumab for Early Triple-Negative Breast Cancer', *New England Journal of Medicine*, 382(9), pp. 810–821. doi: 10.1056/nejmoa1910549.

Schmidt, O. and Teis, D. (2012) 'The ESCRT machinery', *Current Biology*. Elsevier, 22(4), pp. R116–R120. doi: 10.1016/j.cub.2012.01.028.

Sedgwick, A. E. and D'Souza-Schorey, C. (2018) 'The biology of extracellular microvesicles', *Traffic*, 19(5), pp. 319–327. doi: 10.1111/tra.12558.

Segev, A., Nili, N. and Strauss, B. H. (2004) 'The role of perlecan in arterial injury and angiogenesis', *Cardiovascular Research*, pp. 603–610. doi: 10.1016/j.cardiores.2004.03.028.

Senkus, E. *et al.* (2015) 'Primary breast cancer: ESMO Clinical Practice Guidelines for diagnosis, treatment and follow-up', *Annals of Oncology*. Elsevier Masson SAS, 26(Supplement 5), pp. v8–v30. doi: 10.1093/annonc/mdv298.

Shalapour, S. and Karin, M. (2015) 'Immunity, inflammation, and cancer: An eternal fight between good and evil', *Journal of Clinical Investigation*, 125(9), pp. 3347–3355. doi: 10.1172/JCI80007.

Shang, N. *et al.* (2017) 'Dendritic cells based immunotherapy', *American Journal of Cancer Research*, pp. 2091–2102. Available at: www.ajcr.us/.

Sherman-Baust, C. A. *et al.* (2011) 'Gene expression and pathway analysis of ovarian cancer cells selected for resistance to cisplatin, paclitaxel, or doxorubicin', *Journal of Ovarian Research*, 4(1), p. 21. doi: 10.1186/1757-2215-4-21.

Shurtleff, M. J. *et al.* (2016) 'Y-box protein 1 is required to sort microRNAs into exosomes in cells and in a cell-free reaction', *eLife*, 5(AUGUST), pp. 1–23. doi: 10.7554/eLife.19276.

Si, W. *et al.* (2019) 'The role and mechanisms of action of microRNAs in cancer drug resistance', *Clinical Epigenetics*. Clinical Epigenetics, pp. 1–24. doi: 10.1186/s13148-018-0587-8.

Skotland, T., Sandvig, K. and Llorente, A. (2017) 'Lipids in exosomes: Current knowledge and the way forward', *Progress in Lipid Research*. The Authors, 66, pp. 30–41. doi: 10.1016/j.plipres.2017.03.001.

Skryabin, G. O. *et al.* (2020) 'Lipid Rafts in Exosome Biogenesis', *Biochemistry (Moscow)*, pp. 177–191. doi: 10.1134/S0006297920020054.

Soare, G. R. and Soare, C. A. (2019) 'Immunotherapy for Breast Cancer: First FDA Approved Regimen', *Discoveries*, 7(1), p. e91. doi: 10.15190/d.2019.4.

Sørlie, T. *et al.* (2001) 'Gene expression patterns of breast carcinomas distinguish tumor subclasses with clinical implications', *Proceedings of the National Academy of Sciences of the United States of America*, 98(19), pp. 10869–10874. doi: 10.1073/pnas.191367098.

Soto-Heredero, G., Baixauli, F. and Mittelbrunn, M. (2017) 'Interorganelle communication between mitochondria and the endolysosomal system', *Frontiers in Cell and Developmental Biology*, p. 95. doi: 10.3389/fcell.2017.00095.

Spada, S. *et al.* (2021) 'Fibronectin as a multiregulatory molecule crucial in tumor

matrisome: from structural and functional features to clinical practice in oncology', *Journal of Experimental and Clinical Cancer Research*. Journal of Experimental & Clinical Cancer Research, 40(1), pp. 1–14. doi: 10.1186/s13046-021-01908-8.

Stefanski, C. D. *et al.* (2019) 'APC loss affects DNA damage repair causing doxorubicin resistance in breast cancer cells', *Neoplasia (United States)*. Neoplasia Press, Inc., 21(12), pp. 1143–1150. doi: 10.1016/j.neo.2019.09.002.

Sterzenbach, U. *et al.* (2017) 'Engineered Exosomes as Vehicles for Biologically Active Proteins', *Molecular Therapy*. Elsevier Ltd., 25(6), pp. 1269–1278. doi: 10.1016/j.ymthe.2017.03.030.

Svensson, K. J. *et al.* (2013) 'Exosome uptake depends on ERK1/2-heat shock protein 27 signaling and lipid raft-mediated endocytosis negatively regulated by caveolin-1', *Journal of Biological Chemistry*, 288(24), pp. 17713–17724. doi: 10.1074/jbc.M112.445403.

Svoronos, A. A., Engelman, D. M. and Slack, F. J. (2016) 'OncomiR or tumor suppressor? The duplicity of MicroRNAs in cancer', *Cancer Research*, pp. 3666–3670. doi: 10.1158/0008-5472.CAN-16-0359.

Szakács, G. *et al.* (2006) 'Targeting multidrug resistance in cancer', *Nature Reviews Drug Discovery*, 5(3), pp. 219–234. doi: 10.1038/nrd1984.

Tabet, F. *et al.* (2014) 'HDL-transferred microRNA-223 regulates ICAM-1 expression in endothelial cells', *Nature Communications*, 5. doi: 10.1038/ncomms4292.

Tang, J. *et al.* (2021) 'hnRNPA2B1 Promotes Colon Cancer Progression via the MAPK Pathway', *Frontiers in Genetics*, 12(September), pp. 1–10. doi: 10.3389/fgene.2021.666451.

Tang, T. *et al.* (2021) 'Advantages of targeting the tumor immune microenvironment over blocking immune checkpoint in cancer immunotherapy', *Signal Transduction and Targeted Therapy*. doi: 10.1038/s41392-020-00449-4.

Tanzer, M. L. (2006) 'Current concepts of extracellular matrix', *Journal of Orthopaedic Science*, 11(3), pp. 326–331. doi: 10.1007/s00776-006-1012-2.

Tchurikov, N. A. *et al.* (2013) 'DNA Double-Strand Breaks Coupled with PARP1 and HNRNPA2B1 Binding Sites Flank Coordinately Expressed Domains in Human Chromosomes', *PLoS Genetics*, 9(4). doi: 10.1371/journal.pgen.1003429.

Theocharis, A. D. *et al.* (2016) 'Extracellular matrix structure', *Advanced Drug Delivery Reviews*. Elsevier B.V., 97, pp. 4–27. doi: 10.1016/j.addr.2015.11.001.

Théry, C. *et al.* (2018) 'Minimal information for studies of extracellular vesicles 2018 (MISEV2018): a position statement of the International Society for Extracellular Vesicles and update of the MISEV2014 guidelines', *Journal of Extracellular Vesicles*, 7(1). doi: 10.1080/20013078.2018.1535750.

Théry, C., Zitvogel, L. and Amigorena, S. (2002) 'Exosomes: Composition, biogenesis and function', *Nature Reviews Immunology*, 2(8), pp. 569–579. doi: 10.1038/nri855.

Tian, T. *et al.* (2014) 'Exosome uptake through clathrin-mediated endocytosis and macropinocytosis and mediating miR-21 delivery', *Journal of Biological Chemistry*. Â© 2014 ASBMB. Currently published by Elsevier Inc; originally published by American Society for Biochemistry and Molecular Biology., 289(32), pp. 22258–22267. doi: 10.1074/jbc.M114.588046.

Torreggiani, E. *et al.* (2016) 'Multimodal transfer of MDR by exosomes in human osteosarcoma', *International Journal of Oncology*, 49(1), pp. 189–196. doi: 10.3892/ijo.2016.3509.

Trajkovic, K. *et al.* (2008) 'Ceramide triggers budding of exosome vesicles into multivesicular endosomes', *Science*. Science, 319(5867), pp. 1244–1247. doi: 10.1126/science.1153124.

Trams, E. G. *et al.* (1981) 'Exfoliation of membrane ecto-enzymes in the form of micro-vesicles', *BBA - Biomembranes*, 645(1), pp. 63–70. doi: 10.1016/0005-2736(81)90512-5.

Tricarico, C., Clancy, J. and D'Souza-Schorey, C. (2017) 'Biology and biogenesis of shed microvesicles', *Small GTPases*. Taylor & Francis, 8(4), pp. 220–232. doi: 10.1080/21541248.2016.1215283.

Troughton, L. D., Zech, T. and Hamill, K. J. (2020) 'Laminin N-terminus α31 is upregulated in invasive ductal breast cancer and changes the mode of tumour invasion', *bioRxiv*, p. 2020.05.28.120964. doi: 10.1101/2020.05.28.120964.

Tutt, A. N. J. *et al.* (2021) 'Adjuvant Olaparib for Patients with BRCA1 - or BRCA2 - Mutated Breast Cancer', *New England Journal of Medicine*, 384(25), pp. 2394–2405. doi: 10.1056/nejmoa2105215.

Ushiki, T. (2002) 'Collagen fibers, reticular fibers and elastic fibers. A comprehensive understanding from a morphological viewpoint', *Arch Histol Cytol*, 109, p. 26.

Valadi, H. *et al.* (2007) 'Exosome-mediated transfer of mRNAs and microRNAs is a novel mechanism of genetic exchange between cells', *Nature Cell Biology*, 9(6), pp. 654–659. doi: 10.1038/ncb1596.

Vasudevan, S. (2012) 'Posttranscriptional Upregulation by MicroRNAs', *Wiley Interdisciplinary Reviews: RNA*, 3(3), pp. 311–330. doi: 10.1002/wrna.121.

Vasudevan, S., Tong, Y. and Steitz, J. A. (2007) 'Switching from repression to activation: MicroRNAs can up-regulate translation', *Science*, 318(5858), pp. 1931–1934. doi: 10.1126/science.1149460.

Velasco, R. and Bruna, J. (2010) 'Chemotherapy-induced peripheral neuropathy: An unresolved issue', *Neurología (English Edition)*. Elsevier, 25(2), pp. 116–131. doi: 10.1016/s2173-5808(10)70022-5.

Veronesi, U. *et al.* (2005) 'Breast cancer', *Lancet*, 365(9472), pp. 1727–1741. doi: 10.1016/S0140-6736(05)66546-4.

Verweij, J., Clavel, M. and Chevalier, B. (1994) 'Paclitaxel (Taxol™) and docetaxel (Taxotere™): Not simply two of a kind', *Annals of Oncology*, 5(6), pp. 495–505. doi: 10.1093/oxfordjournals.annonc.a058903.

Vesely, M. D. *et al.* (2011) 'Natural innate and adaptive immunity to cancer', *Annual Review of Immunology*, 29, pp. 235–271. doi: 10.1146/annurev-immunol-031210-101324.

Villarroya-Beltri, C. *et al.* (2013a) 'Sumoylated hnRNPA2B1 controls the sorting of miRNAs into exosomes through binding to specific motifs', *Nature Communications*, 4, pp. 1–10. doi: 10.1038/ncomms3980.

Villarroya-Beltri, C. *et al.* (2013b) 'Sumoylated hnRNPA2B1 controls the sorting of miRNAs into exosomes through binding to specific motifs', *Nature Communications*. doi:

10.1038/ncomms3980.

Villeneuve, D. J. *et al.* (2006) 'cDNA microarray analysis of isogenic paclitaxel- and doxorubicin-resistant breast tumor cell lines reveals distinct drug-specific genetic signatures of resistance', *Breast Cancer Research and Treatment*, 96(1), pp. 17–39. doi: 10.1007/s10549-005-9026-6.

Vindin, H., Mithieux, S. M. and Weiss, A. S. (2019) 'Elastin architecture', *Matrix Biology*. Elsevier B.V, 84, pp. 4–16. doi: 10.1016/j.matbio.2019.07.005.

Voduc, K. D. *et al.* (2010) 'Breast cancer subtypes and the risk of local and regional relapse', *Journal of Clinical Oncology*, 28(10), pp. 1684–1691. doi: 10.1200/JCO.2009.24.9284.

Vonderheide, R. H. *et al.* (2010) 'Tremelimumab in combination with exemestane in patients with advanced breast cancer and treatment-associated modulation of inducible costimulator expression on patient T cells', *Clinical Cancer Research*, 16(13), pp. 3485–3494. doi: 10.1158/1078-0432.CCR-10-0505.

Voutouri, C. *et al.* (2016) 'Hyaluronan-Derived Swelling of Solid Tumors, the Contribution of Collagen and Cancer Cells, and Implications for Cancer Therapy', *Neoplasia (United States)*. The Authors, 18(12), pp. 732–741. doi: 10.1016/j.neo.2016.10.001.

Waks, A. G. and Winer, E. P. (2019) 'Breast Cancer Treatment: A Review', *JAMA - Journal of the American Medical Association*, 321(3), pp. 288–300. doi: 10.1001/jama.2018.19323.

Walz, A. L. *et al.* (2015) 'Recurrent DGCR8, DROSHA, and SIX Homeodomain Mutations in Favorable Histology Wilms Tumors', *Cancer Cell*. Elsevier Inc., 27(2), pp. 286–297. doi: 10.1016/j.ccell.2015.01.003.

Wang, H. *et al.* (2013) 'Hypersensitivity reaction studies of a polyethoxylated castor oil-free, liposome-based alternative paclitaxel formulation', *Molecular Medicine Reports*, 7(3), pp. 947–952. doi: 10.3892/mmr.2013.1264.

Wang, L. *et al.* (2019) 'CD103-positive CSC exosome promotes EMT of clear cell renal cell carcinoma: Role of remote MiR-19b-3p', *Molecular Cancer*, 18(1). doi: 10.1186/s12943-019-0997-z.

Wang, S. *et al.* (2016) 'Annexin A2 facilitates endocytic trafficking of antisense oligonucleotides', *Nucleic Acids Research*, 44(15), pp. 7314–7330. doi: 10.1093/nar/gkw595.

Wang, Y. *et al.* (2019) 'MiR-148a-3p Suppresses the Proliferation and Invasion of Esophageal Cancer by Targeting DNMT1', *Genetic Testing and Molecular Biomarkers*, 23(2), pp. 98–104. doi: 10.1089/gtmb.2018.0285.

Wang, Y. J. *et al.* (2017) 'Pterostilbene prevents AKT-ERK axis-mediated polymerization of surface fibronectin on suspended lung cancer cells independently of apoptosis and suppresses metastasis', *Journal of Hematology and Oncology*, 10(1). doi: 10.1186/s13045-017-0441-z.

Wani, M. C. *et al.* (1971) 'Plant Antitumor Agents.VI.The Isolation and Structure of Taxol, a Novel Antileukemic and Antitumor Agent from Taxus brevifolia2', *Journal of the American Chemical Society*, 93(9), pp. 2325–2327. doi: 10.1021/ja00738a045.

Watkins, E. J. (2019) 'Overview of breast cancer', *Journal of the American Academy of Physician Assistants*, 32(10), pp. 13–17. doi: 10.1097/01.JAA.0000580524.95733.3d.

Wei, Y. *et al.* (2014) 'Exosomal miR-221/222 enhances tamoxifen resistance in recipient ER-positive breast cancer cells', *Breast Cancer Research and Treatment*, 147(2), pp. 423–431. doi: 10.1007/s10549-014-3037-0.

Wen, Y. *et al.* (2018) 'MiR-503 suppresses hypoxia-induced proliferation, migration and angiogenesis of endothelial progenitor cells by targeting Apelin', *Peptides*. Elsevier, 105(January), pp. 58–65. doi: 10.1016/j.peptides.2018.05.008.

Wieckowski, E. U. *et al.* (2009) 'Tumor-Derived Microvesicles Promote Regulatory T Cell Expansion and Induce Apoptosis in Tumor-Reactive Activated CD8 + T Lymphocytes', *The Journal of Immunology*, 183(6), pp. 3720–3730. doi: 10.4049/jimmunol.0900970.

Wight, T. N., Kinsella, M. G. and Qwarnström, E. E. (1992) 'The role of proteoglycans in cell adhesion, migration and proliferation', *Current Opinion in Cell Biology*, 4(5), pp. 793–801. doi: 10.1016/0955-0674(92)90102-I.

Wilson, R. and Doudna, J. A. (2018) 'Molecular mechanisms of RNA interference A BIOLOGICAL VIEW OF RNA INTERFERENCE • Small regulatory RNAs in cellular function and dysfunction HHS Public Access'. doi: 10.1146/annurev-biophys-083012-130404.

Winter, J. *et al.* (2009) 'Many roads to maturity: MicroRNA biogenesis pathways and their regulation', *Nature Cell Biology*, 11(3), pp. 228–234. doi: 10.1038/ncb0309-228.

Winters, S. *et al.* (2017) *Breast Cancer Epidemiology, Prevention, and Screening, Progress in Molecular Biology and Translational Science*. Elsevier Inc. doi: 10.1016/bs.pmbts.2017.07.002.

Woods, D. and Turchi, J. J. (2013) 'Chemotherapy induced DNA damage response Convergence of drugs and pathways', *Cancer Biology and Therapy*, pp. 379–389. doi: 10.4161/cbt.23761.

Wu, S. *et al.* (2018) 'Upregulation of the EMT marker vimentin is associated with poor clinical outcome in acute myeloid leukemia', *Journal of Translational Medicine*. BioMed Central, 16(1), pp. 1–9. doi: 10.1186/s12967-018-1539-y.

Xie, L. H. *et al.* (2017) 'CD123 target validation and preclinical evaluation of ADCC activity of anti-CD123 antibody CSL362 in combination with NKs from AML patients in remission', *Blood Cancer Journal*, 7(6), p. 567. doi: 10.1038/bcj.2017.52.

Xing Zhang1†, Sen Wang1†, Haixiao Wang4†, Jiacheng Cao1†, Xiaoxu Huang1, Zheng Chen2, Penghui Xu1, Guangli Sun1, Jianghao Xu1, Jialun Lv1 and Zekuan Xu1, 3* (2019) 'Circular RNA circNRIP1 acts as a microRNA- 149-5p sponge to promote gastric cancer progression via the AKT1/mTOR pathway', *Molecular Cancer*. Molecular Cancer, (1), pp. 18–20. doi: 10.1186/s13046-020-01791-9.

Xu, J. F. *et al.* (2017) 'Exosomes containing differential expression of microRNA and mRNA in osteosarcoma that can predict response to chemotherapy', *Oncotarget*, 8(44), pp. 75968–75978. doi: 10.18632/oncotarget.18373.

Xu, J., Liao, K. and Zhou, W. (2018) 'Exosomes Regulate the Transformation of Cancer Cells in Cancer Stem Cell Homeostasis'. doi: 10.1155/2018/4837370.

Xu, K. *et al.* (2017) 'miR-503-5p confers drug resistance by targeting PUMA in colorectal carcinoma', *Oncotarget*, 8(13), pp. 21719–21732. doi: 10.18632/oncotarget.15559.

Xu, W. *et al.* (2018) 'MiR-29 family inhibits resistance to methotrexate and promotes cell apoptosis by targeting COL3A1 and MCL1 in osteosarcoma', *Medical Science Monitor*,

24, pp. 8812–8821. doi: 10.12659/MSM.911972.

Yagi, T. *et al.* (2019) 'Plasma exosomal microRNA-125b as a monitoring biomarker of resistance to mFOLFOX6-based chemotherapy in advanced and recurrent colorectal cancer patients', *Molecular and Clinical Oncology*, 11(4), pp. 416–424. doi: 10.3892/mco.2019.1911.

Yamada, N. *et al.* (2013) 'Role of intracellular and extracellular microRNA-92A in colorectal cancer', *Translational Oncology*, 6(4), pp. 482–492. doi: 10.1593/tlo.13280.

Yanagishita, M. (1993) 'Function of proteoglycans in the extracellular matrix', *Pathology International*, 43(6), pp. 283–293. doi: 10.1111/j.1440-1827.1993.tb02569.x.

Yang, Juan, Li, Y., *et al.* (2020) 'Sirt6 promotes tumorigenesis and drug resistance of diffuse large B-cell lymphoma by mediating PI3K/Akt signaling', *Journal of Experimental and Clinical Cancer Research*. Journal of Experimental & Clinical Cancer Research, 39(1), pp. 1–16. doi: 10.1186/s13046-020-01623-w.

Yang, Y. (2015) 'Cancer immunotherapy: Harnessing the immune system to battle cancer', *Journal of Clinical Investigation*, pp. 3335–3337. doi: 10.1172/JCI83871.

Yang, Yu *et al.* (2020) 'Loss of hnRNPA2B1 inhibits malignant capability and promotes apoptosis via down-regulating Lin28B expression in ovarian cancer', *Cancer Letters*. Elsevier B.V., 475, pp. 43–52. doi: 10.1016/j.canlet.2020.01.029.

Yang, Yuhui *et al.* (2020) 'Myeloid-Derived Suppressor Cells in Tumors: From Mechanisms to Antigen Specificity and Microenvironmental Regulation', *Frontiers in Immunology*, p. 1371. doi: 10.3389/fimmu.2020.01371.

Yang, Zhiyong, Zhao, N., *et al.* (2020) 'Exosomes derived from cancer stem cells of gemcitabine-resistant pancreatic cancer cells enhance drug resistance by delivering miR-210', *Cellular Oncology*, 43(1), pp. 123–136. doi: 10.1007/s13402-019-00476-6.

Yersal, O. and Barutca, S. (2014) 'Biological subtypes of breast cancer: Prognostic and therapeutic implications', *World Journal of Clinical Oncology*, pp. 412–424. doi: 10.5306/wjco.v5.i3.412.

Yi, R. *et al.* (2003) 'Exportin-5 mediates the nuclear export of pre-microRNAs and short hairpin RNAs', *Genes and Development*, 17(24), pp. 3011–3016. doi: 10.1101/gad.1158803.

Yin, L. *et al.* (2020) 'Triple-negative breast cancer molecular subtyping and treatment progress', *Breast Cancer Research*. Breast Cancer Research, 22(1), pp. 1–13. doi: 10.1186/s13058-020-01296-5.

Yu, D. dan *et al.* (2015) 'Role of miR-155 in drug resistance of breast cancer', *Tumor Biology*, 36(3), pp. 1395–1401. doi: 10.1007/s13277-015-3263-z.

Yuen, G. J., Demissie, E. and Pillai, S. (2016) 'B Lymphocytes and Cancer: A Love–Hate Relationship', *Trends in Cancer*, pp. 747–757. doi: 10.1016/j.trecan.2016.10.010.

Zaborowski, M. P. *et al.* (2015) 'Extracellular Vesicles: Composition, Biological Relevance, and Methods of Study', *BioScience*, 65(8). doi: 10.1093/biosci/biv084.

Zecchin, A. *et al.* (2017) 'How endothelial cells adapt their metabolism to form vessels in tumors', *Frontiers in Immunology*, p. 1750. doi: 10.3389/fimmu.2017.01750.

Zhang, J. *et al.* (2022) 'Immunostimulatory Properties of Chemotherapy in Breast Cancer: From Immunogenic Modulation Mechanisms to Clinical Practice', *Frontiers in*

Immunology. doi: 10.3389/fimmu.2021.819405.

Zhang, Y. *et al.* (2019) 'Exosomes: Biogenesis, biologic function and clinical potential', *Cell and Bioscience*. BioMed Central, 9(1), pp. 1–18. doi: 10.1186/s13578-019-0282-2.

Zhang, Z. *et al.* (2015) 'Anthracyclines potentiate anti-tumor immunity: A new opportunity for chemoimmunotherapy', *Cancer Letters*. Elsevier Ireland Ltd, 369(2), pp. 331–335. doi: 10.1016/j.canlet.2015.10.002.

Zhao, H. *et al.* (2016) 'Tumor microenvironment derived exosomes pleiotropically modulate cancer cell metabolism', *eLife*, 5(FEBRUARY2016). doi: 10.7554/eLife.10250.

Zhao, J. J. *et al.* (2009) 'Identification of miRNAs associated with tumorigenesis of retinoblastoma by miRNA microarray analysis', *Child's Nervous System*, 25(1), pp. 13–20. doi: 10.1007/s00381-008-0701-x.

Zhu, Z. *et al.* (2017) 'Macrophage-derived apoptotic bodies promote the proliferation of the recipient cells via shuttling microRNA-221/222', *Journal of Leukocyte Biology*, 101(6), pp. 1349–1359. doi: 10.1189/jlb.3a1116-483r.

Zietzer, A. *et al.* (2020) 'The RNA-binding protein hnRNPU regulates the sorting of microRNA-30c-5p into large extracellular vesicles', *Journal of Extracellular Vesicles*, 9(1). doi: 10.1080/20013078.2020.1786967.

Zingoni, A. *et al.* (2017) 'Natural killer cell response to chemotherapy-stressed cancer cells: Role in tumor immunosurveillance', *Frontiers in Immunology*, p. 25. doi: 10.3389/fimmu.2017.01194.

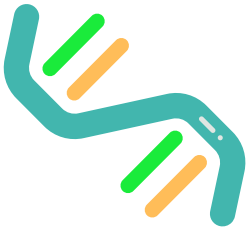


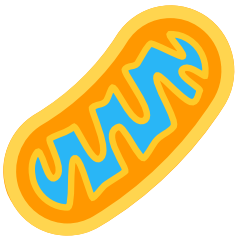
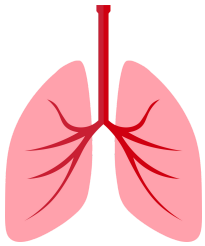

Publications

Publications

During my thesis, I participate in several publications.

In two of them, I was co-first author * (Pérez-Boza, Boeckx, et al., 2020) (Zamberlan, Boeckx, et al., 2022).

List of publications

hnRNPA2B1 inhibits the exosomal export of miR-503 in endothelial cells.

CMLS, 2020. Pérez-Boza J.*, **Boeckx A.***, ..., Struman I.

Inhibition of the mitochondrial protein Opa1 curtails breast cancer growth.

J Exp Clin Cancer Res, 2022. Zamberlan M.*, **Boeckx A.***, ..., Herkenne S.

Macrophage-derived exosomes attenuate fibrosis in airway epithelial cells through delivery of

antifibrotic miR-142-3p

Thorax, 2019. Guiot J., Cambier M., Boeckx A., ..., Struman I., Njock MS.

Extracellular vesicles mediate communication between endothelial and vascular smooth muscle cells.

Int J of Mol Sci., 2022. Fontaine M., et al.

Sorting and packaging of RNA into extracellular vesicles shape intracellular transcript levels.

BMC, 2022. O'Grady T., et al.

UNRAVELLING THE EXOSOMAL EXPORT OF MIR-503 AND ITS IMPLICATION IN TUMOR RESPONSE TO CHEMOTHERAPY

Tumors are heterogeneous systems in constant interactions with their microenvironment. The communication between cancerous and other types of cells might help in the development of new anti-cancer strategies. Extracellular vesicles (EVs), involved in cell-to-cell communication, are key players in tumor progression. Indeed, all cell types generate EVs. By transferring their bioactive content from a donor to a recipient cell, these particles can induce cellular changes. Interestingly, EVs carry microRNAs, small non-coding RNAs involved in multiple pathways. In the context of malignancies, EVs and miRNAs highly participate in tumor progression and modulate the response to treatment.

In this work, we demonstrated that epirubicin induced the export of an anti-tumoral miRNA, miR-503, into EVs released from endothelial cells. We identified four proteins involved in the sorting mechanism: ANXA2, hnRNPA2B1, TSP1, and VIM. We showed that upon epirubicin treatment, the miR-EXO complex (complex formed by miR-503 and the proteins attached to it) disrupts. hnRNPA2B1 returned to the nucleus while ANXA2 and miR-503 were exported into EVs. We performed protein knockdown and observed that hnRNPA2B1 silencing mimicked epirubicin treatment. Therefore, we concluded that hnRNPA2B1 inhibited miR-503 sorting into EVs. Then, we performed functional assays to determine the effects of this endothelial silencing on breast cancer cells. Coculture experiments revealed that the endothelial knockdown of hnRNPA2B1 indeed increased the levels of miR-503 within triple-negative breast cancer cells while the levels of its targets, CCND2 and CCND3, were downregulated. The inhibition of these pro-tumoral targets reduced the proliferative, migratory and invasive capacities of tumor cells. Moreover, we analyzed the functions of miR-503 on epirubicin and paclitaxel-resistant breast cancer cells. Interestingly, the basal levels of the miRNA were downregulated in resistant cells compared to the sensitive ones. Using several functional assays, we demonstrated that miR-503 overexpression curtailed the tumorigenicity of both responding and non-responding cells. Its targets, CCND1 and CCND3, were also downregulated. Moreover, we treated cancer cells with miR-503-loaded EVs and the same phenotype was observed. In vivo experiments showed that EVs enriched in miR-503 could reduce tumor growth drastically. Finally, clinical data revealed that the deletion of miR-503 decreased the survival of breast cancer patients.

Taken together, these results suggest that endothelial and cancer cells interact through the transfer of miRNAs via EVs. Their incorporation curtails breast cancer cell progression. Moreover, the anti-tumoral functions of miR-503 are conserved in resistant cells.

LIÈGE université GIGA institute
fnrs LA LIBERTÉ DE CHERCHER
télévie
Fondation Léon Fredericq